THE SUITABILITY OF COAL-OIL AND OTHER SLURRIES AS BLAST FURNACE TUYERE INJECTANTS

by

D.P. JENKINS C.Eng., M.Inst.E

This thesis is submitted in part fulfilment of regulations for the degree of Doctor of Philosophy of the C.N.A.A.

May 1983

Sponsoring Establishment: Polytechnic of Wales
Collaborating Establishment: British Steel Corporation
Welsh Laboratory

Supervisor: Dr. C. Davies
Department of Chemical Engineering
Polytechnic of Wales

SUMMARY

This thesis examines the combustion of coal-oil slurries in the unusual low-recirculation conditions obtaining in the blast furnace tuyere raceway.

A computer-controlled combustion rig was built which would simulate, as nearly as possible, the conditions of air velocity (typically 200 m/s) air preheat temperature (typically 1000^{o}C) and oxygen enrichment (up to 26% oxygen content by volume) obtaining on a modern blast furnace.

The results from this rig were used to calibrate a mathematical model of the mixing and combustion processes taking place. A theory of atomisation is proposed whereby the smaller coal particles are retained within the larger oil droplets, leaving the larger coal particles to combust separately. Using error analysis of the mathematical model, the size of coal particle which can remain within an oil droplet was found to have a ratio of less than 0.14.

The apparatus was not as accurate in the delivery of slurry as it was in the delivery of preheated, oxygenated air. The total accuracy was found to have a 95% probability of less than 10% error.

The mathematical model, however, was found to have a 95% probability of less than 5% error. When the work of other investigations - into the degree of recirculation obtaining in the tuyere raceway - is complete, the model will provide a satisfactory basis for prediction of maximum injection rates of coal-oil slurries into the tuyeres of a blast furnace, given the conditions of air blast obtaining.

ACKNOWLEDGEMENTS

The author would like to express his gratitude to the Management of BSC, Welsh Laboratory for the opportunity of carrying out this project, and for their support over its duration.

I am also grateful to my supervisor, Dr. Clive Davies of the Polytechnic of Wales for his good advice and encouragement. My colleagues, whose support is deeply appreciated, will forgive me for singling out "Algy" Baker for especial thanks for his refractory work, and also the Typing Services Department of Welsh Laboratory, whose patience has been sorely tried.

Finally, I am grateful for the patience and perseverance of not only my wife, Margaret, but also the family we have acquired over the duration of this project.

ABSTRACT.

A Study of the Metallic Content of an Urban Environment.

Antony Richard Baron.

Metal in roadside dust levels in St.Helens, Merseyside, have been investigated and the results statistically correlated with the incidence of perinatal deaths and congenital abnormalities in the town.

Nine areas of the town were defined, which had significantly different perinatal death and congenital abnormality rates. These areas then formed the basis of a dust sampling survey, the collection of samples being carried out over the 12 month period from September 1980.

The analysis of over 800 samples for the potentially teratogenic / fetotoxic metals arsenic, cadmium, chromium, cobalt, copper, mercury, nickel, lead and zinc were performed. Metals were extracted from dust samples with 2 mol dm^{-3} nitric acid and determined by flame atomic absorption or atomic fluorescence techniques.

Individual metals and multiple metal combinations were correlated with the distribution of perinatal deaths and congenital abnormalities using correlation and multiple regression analysis methods. Zinc, zinc / arsenic, zinc / cobalt, zinc / cadmium, zinc / lead and cadmium / copper had correlations significant at the $p = 0.05$ level.

The suprisingly large correlation factors obtained were evaluated in the light of current teratogenic and fetotoxic research. Several models have been proposed which attempt to reconcile the low correlations found here for some metals and the strong indications of their teratogenic and / or fetotoxic activity, suggested in biomedical literature.

Present and past metal sources which might explain the observed metal distribution pattern were investigated. Several likely sources were identified which may account for highly elevated local levels, other sources being thought to contribute to general urban levels.

Also studied were; dust sampling techniques: analytical treatment of samples: the possibility of sampler and / or temporal effects and inter-metal associations.

CONTENTS

CONTENTS (Continued.....) Page No.

CONTENTS (Continued .....) Page No.

CONTENTS (Continued .....) Page No.

CONTENTS (Continued.....)

1. INTRODUCTION

1.0. The Purpose of Tuyere Injection

1.0.0. Background

Since World War II, blast furnace productivity has doubled, and the specific coke consumption has been halved. This revolution in blast furnace practice has been brought about by four complementary operational techniques:

(a) Preparation of the burden by sintering or pelletising.
(b) The addition of oxygen to the air blast.
(c) The increase in temperature of the air blast.
(d) The injection of supplementary fuel at the tuyere.

More recently, the running of furnaces at high top pressure has also provided a further performance increment.

This investigation deals primarily with (d) the injection of supplementary fuel at the tuyere, but obviously (b) and (c) are inextricably linked with this practice.

1.0.1. The Tuyere Environment

The conditions encountered at the tuyere are typically: air velocity 150-260m/s, air temperature 800-1300^{o}C, air oxygen content 21% to 26%, and air pressure 1.5 to 6.0 bar absolute.

Immediately in front of the tuyere there is a free space called the "raceway" which is kept clear by the momentum of the air blast. The adiabatic combustion temperature of the air blast with the white-hot coke immediately enclosing the raceway is called the "Raceway Adiabatic Flame Temperature" (RAFT). The RAFT has a considerable influence on the furnace operating parameters.

1.0.2. Practical Limits to the Raceway Adiabatic Flame Temperature

Generally speaking, the higher the RAFT is, the more productive the blast furnace becomes, whilst the specific coke consumption drops. However, as the temperature rises, alkalis in the slag begin to distil, and the phenomena of "checks", "slips" and "hanging" occur. Higuchi et al[1] recommend an upper limit to RAFT of 2400^{o}C to avoid these problems.

There is a lower limit to RAFT which Higuchi et al[1] put at 2200°C. This temperature, however, is a minimum which is recommended for a blast furnace of very high productivity, and European and American furnaces operate at as low a temperature as 2000°C. However, 2100°C is recommended British practice, this value giving a leeway for contingencies, since a furnace "freezing" through too low a temperature is by no means unknown.

1.0.3. Influence of Blast Parameters and Tuyere Injection on RAFT

The influence of oxygen enrichment and preheating of the air blast on RAFT is, as one would expect with any other combustion situation, to increase the temperature of combustion.

Water vapour in the air will decrease the temperature, since the endothermic water gas reaction will take place. Almost all injected fuels reduce the RAFT, since the fuel usually has a finite heat requirement to decompose it. The exception to this is of course coke breeze, since that has already been subjected to destructive distillation.

If it is desired to replace some of the blast furnace coke with oil or some other injectant, then the resultant drop in flame temperature must be compensated for by either lowering the blast humidity, raising the blast temperature or increasing the amount of oxygen enrichment. Higuchi et al[1] give an indication of alterations to air blast parameters which are necessary to balance heavy fuel oil injection.

A method of determination of RAFT is given by Beck & Kyle[2] as:

$$T_F = V_T(924+576390_B+(0.0099T_B-27.74)H_B+(0.4820_B+6.269)T_B)-K_1R_I \;/\; V_T(6.968+6.8750_B+0.0167H_B)+K_2R_I$$

where: $k_1 = (1.792C_I+300.3H_D-2.026H_I-0.172N_T-6.8870_I)D_I$

and: $k_2 = (0.00162\ 0_I+0.00093N_I+0.0121H_I)D_I$

and: T_F = RAFT (°C)

V_T = Blast volume corrected for leakage (nm^3/min)

O_B = Fraction of oxygen in blast
T_B = Temperature of blast (^oC)
H_B = Humidity of blast (gH_2O/nm^3)
R_I = Volume flow rate of injectant (ℓ/hr)
C_I = Carbon content of injectant (%)
H_D = Heat of dissociation of injectant (kcal/g)
H_I = Hydrogen content of injectant (%)
N_I = Nitrogen content of injectant (%)
O_I = Oxygen content of injectant (%)
D_I = Density of injectant (kg/ℓ).

Using this equation and the relevant data for various injectants given by Kyle and Freidenfelds[3] the thermochemical maxima of oil coal and coal-oil slurry injection rates can be determined for any particular value of RAFT in terms of the injectant/oxygen ratio. This conveniently gives the maximum ratios to be investigated. It can be shown that, even for the case of a 50% 902 rank coal-oil slurry, the thermochemically acceptable maxima gives a sub-stoichiometric quantity.

1.1. Brief Survey of Fuel Injection Practice

1.1.0. Liquid Fuels

Until recently, the practice of oil injection into Blast Furnace tuyeres was so widespread as to be almost universal. A very large amount of operating experience has been accumulated, and is adequately documented in reviews and symposia, e.g.[4,5]. Apart from coal injection, which will be dealt with later and gas injection[6], which is strictly speaking outside the scope of this work, the only other common injectant of note is coke oven tar[7,8]. However, since tar is not significantly different in handling or combustion characteristics from heavy fuel oil, it will not be separately considered.

Examination of the literature shows that, as stated earlier, the limiting factor in the modern blast furnace is not RAFT, but the limitation of complete combustion of the injectant. In 1972 Coche[9], in his review of injection

practice, estimated that the maximum oil injection rate with normal atomising practice corresponds to the stoichiometric ratio of combustion to CO_2 and H_2O. Subsequent development of the "shock-wave" tuyere by Della Cassa et al[10] promised to raise the injectant level to that corresponding to the stoichiometric ratio of combustion to CO and H_2O. For a conventional steam-atomised oil injection system Quigley et al[11] recommended a maximum utilization of 80% of the available oxygen in the blast by the oil, to allow for air distribution variations between tuyeres. Exceeding this usually results in incomplete combustion, with the carry-over of soot to the blast furnace gas cleaners.

1.1.1. Solid Fuels

Although not as widespread as oil injection, the use of a solid injectant is not unknown. There are two main schools of thought in coal injection practice today. The first of these is that it is unnecessary to obtain complete combustion of the coal in the raceway. This is exemplified by Strassburger et al[12] and Dietz[13] in the USA at Weirton and by Summers et al[14] in England at Stanton and Stavely.

The second school of thought is that complete combustion is necessary. In the USA Bell et al[15] hold this view as do Andronov and Plotkin[16] and Yarmal et al[17] in the USSR.

In the "incomplete combustion" school of thought, the coal comminution is only sufficient to enable air transport to take place; typically from 1mm to 3mm maximum size. Indeed, trouble was experienced at Wierton[12] due to an excess of fines. However, at the same installation[13] shorting of the electrostatic precipitators in the gas cleaning plant was experienced due to incomplete combustion of the injected coal. This was partially corrected[12] by moving the lance position back along the axis of the blowpipe to increase the residence time of the coal particles.

In the "complete combustion" school of thought, the coal is ground to pulverised fuel size, typically 80% less than 76μ. On these installations, problems of incomplete combustion have not been encountered.

However, as Wenzel[18] points out it could well be that the very large particles, >2mm, are retained in the stack until gasified, whilst intermediate sized particles, between 100μ and 1mm, are carried over into the gas cleaning plant. Small particles, <100μ, would combust or combust and then gasify during their total furnace residence time. The operating evidence gained tends to support this view, since the "complete combustion" school of thought is virtually trouble free at injection rates of up to 115Kg coal/THM[19] whilst only some of the "incomplete combustion" school are.

1.1.2. Coal-Oil Slurries

There have been numerous attempts at coal-oil slurry injection since oil injection itself became popular during the early 1960's.

In the U.K., work was carried out at Workington Works and notably Ebbw Vale Works[20] on the injection not only of coal-oil slurries, but also lime-oil, flue dust-oil and dolomite-oil slurries. However, the injection was confined to three tuyeres at limited injection rate, and thus the information available from the trials was restricted.

In Europe after some initial preparatory work[21,22] CNRM carried out a full scale trial[23] at Seraing Works. Injection rates of up to a maximum of 68 Kg of slurry per tonne of hot metal (THM) were attained with a slurry composition of 62% coal of size range less than 12mm, with no carry-over or driving problems.

In Japan, equipment was developed by Morinaga et al[24], enabling full scale trials to be carried out on a blast furnace.

In America, the position is summed up by Craig and Holowaty[25], who state that several companies have run

small-scale trials, but the relative economics of coal, oil and capital costs resulted in no "production" systems.

Throughout the world these investigations were all carried out in the early 1960's, when the cost of oil relative to coal was declining at its' most rapid pace, thus providing the economic dis-incentive necessary for the abandonment of this line of research.

1.2. Previous Laboratory Work on Blast Furnace Injection Systems

1.2.0. Oil Systems

The British Steel Corporation (B.S.C.) is a contributor in this field, beginning with the work of Isaac et al[26] at the International Flame Research Foundation (IFRF).

In this work programme, comparative tests of oil atomising systems were carried out using prototypical blast velocity and tuyere size, and within the context of its limited objectives, was successful. There were, however, several drawbacks associated with this work:

i) A strict time deadline imposed by contractual constraints.
ii) The comparative and hence largely qualitative nature of the results.
iii) The air preheat temperature available, 600°C, was considerably below that encountered in modern blast furnace practice.

Despite these limitations, however, the programme resulted in a very successful design of oil atomisation system[27] which is now employed on all B.S.C. blast furnaces.

A most interesting programe of work was carried out by Bryce[28] in a coke-burning rig. In this apparatus the air blast was heated in a preheater to either 850°C or 1050°C and introduced into the coke-filled reaction vessel via a half-sized tuyere into which the oil injection was carried out. However, little attempt was made to relate to known oil spray combustion and aerodynamic characteristics.

1.2.1. Coal Systems

Morinaga et al[24] in the course of their work programme on coal-oil studies conducted studies on the "combustibilities" of the various coals to be used in the test programme. However, it seems as though no air preheat was used, and it is unclear whether prototypical air blast velocities were used.

Injection of coal into experimental blast furnaces has been carried out both in Japan[29] and the USA[30] with good coke replacement ratios in each case.

1.2.2. Coal-oil Slurry Systems

Considerable laboratory work has been carried out on coal-oil slurries from the point of view of rheological and sedimentation properties. In Japan, Morinaga et al[24] carried out this work, whilst Moss[31] reports work carried out by Esso Research Ltd, and Whittingham and Windsor[32] describe similar work by British Petroleum. Shell Research U.K.[33] have carried out extensive work not only on the rheology and sedimentation of coal-oil slurries but also on their wet grinding. The combustion properties have also been empirically investigated.

1.3. Other Applications of Coal-Oil Systems

There has been considerable interest in coal-oil mixtures in applications other than blast furnaces. The work being reported is largely of small scale trials[34] or full scale trials[35] for application in boiler plant. Experimental work is also being done, mostly empirical furnace tests[36,37,38] and physical properties[39] and preparation of the mixtures[40]. Coal-water-oil mixtures are also being investigated[41] with a view to increasing the coal energy contribution of the mixture, whilst improving combustibility and rheological properties. Work is also being carried out on fundamental droplet research[42,43] to which greater attention will be paid in section 2.

1.4. Formulation of Research Programme Objectives

1.4.0. General Principles

It is clear from the foregoing that the mechanisms of combustion of injectants at the blast furnace tuyeres have not been closely investigated at prototypical values of air blast preheat, velocity and oxygen level. Moreover, apart from Andronov and Plotkin[16] there has been little attempt at applying existing combustion theory to the combustion of injectants. The injection process, throughout the world has been operated until now on a largely empirical basis. As has already been noted, this has resulted in some cases in a variety of operating troubles such as slips, hanging and carbon carry over to the gas cleaning plant.

These operating problems, particularly hanging and slips, can result in a considerable amount of furnace damage and downtime, and are a hazard to the work force. If it is possible to eliminate the injection source of these problems - there are other sources - then a considerable benefit will accrue. In a more economic vein, the replacement of part of the oil injectant with considerably cheaper non-coking coal is likely to save between £1 and £1.5 million at 1981 prices for a medium sized furnace.

However, to implement this saving, an understanding of the combustion process involved in the injection of coal/oil slurries is necessary to avoid operational problems and aid economic optimisation.

The ideal objective must therefore be to aquire the ability to predict the maximum injection rate of slurry given the furnace operating circumstances and the properties of the coal and the oil available, preferably without having to carry out a time and money consuming and potentially dangerous furnace trial. In addition, of course, the optimisation of the fuel itself can be studied, for example in the optimisation of degree of grinding of the coal.

If a mathematical model of the combustion process can be produced, calibrated by laboratory trials, which predicts the quantity and size distribution analysis of the incompletely combusted coal particles remaining at the end of the tuyere raceway zone, then this can be correlated with full-scale furnace trials to determine that level of residue and its size distribution which is necessary to cause furnace operational difficulties. When a sufficient level of correlation has been achieved, other furnaces may then be commissioned with a coal/oil injection system on the basis of the model predictions, without the necessity for the potential hazard of deliberate production of "hanging" in a furnace to ascertain its economic optimum level of injection.

Thus this programme of work must set out to construct a prototype mathematical model of the mixing and combustion processes, together with the laboratory trials necessary to calibrate and verify the model.

1.4.1. Parameters to be Investigated

From the foregoing, it can be seen that the parameters which would have an effect on the combustion of an oil injectant would be:

i) Blast temperature
ii) Blast Oxygen content
iii) Blast Velocity
iv) Ratio of oil to air
v) Nature of oil atomisation, and the size distribution of droplets formed.

For a coal-oil slurry, the following parameters must be added:

vi) Proportion of coal in the slurry
vii) Coal particle size distribution
viii) Coal rank, and combustion properties of char.

The actual range of parameter values for the investigation should ideally be between the limits found in blast furnace practice throughout the world, as shown in the table below:

Parameters	Minimum value	Maximum Value
Blast temperature	800°C	1300°C
Blast Oxygen content	21%	26%
Blast Velocity	150ms^{-1}	250ms^{-1}
Oxygen combusted by injectant (percent of stoichiometric)	30%	100%
Nature of oil atomisation	No atomisation	Homogenised water-oil emulsion, oxygen atomisation etc.
Proportion of coal in slurry	30%	50%
Coal particle size	<35μ	6mm

This table calls for comment on two points: firstly, the atomisation system cannot be readily varied and so for reasons which will become apparent in the next chapter, a BSC device using steam atomisation was decided upon for the duration of the trials.

Secondly, coal particle size is normally a widely distributed range for any given "grind" so two "grinds" of varying fineness were used.

The remaining parameters in both the mathematical model and the laboratory tests must be capable of variation between the minimum and maximum values. With this concept in mind, therefore, the mathematical model and the apparatus were constructed.

2. MATHEMATICAL MODEL OF THE AERODYNAMIC AND COMBUSTION PROCESSES OF COAL-OIL SLURRIES

2.0. Objective

The objective of this mathematical model is to be able, as stated in the previous chapter, to predict either the burnout point of the slurry flame or alternatively the proportion, composition and size distribution of the fuels remaining at the end of the raceway or some other predetermined point.

With the air preheat temperatures and air velocities encountered, some considerable new ground is being covered in the practical research programme. The mathematical model, however, will only break new ground where strictly necessary, and will have numerous simplifying assumptions built in. The model will therefore be pragmatic, and will be confined for the present to a one-dimensional case in the interests of simplicity and ease of modification. Whilst two-dimensional models are becoming relatively common[44,45], it is unlikely that the assumptions made in this work programme, especially concerning temperature and chemical similarity, will allow any greater accuracy than with a one-dimensional model.

Since quantitative measurements taken during combustion of coal-oil slurries as such is scarce, the first objective in this chapter is to separate the whole process into the five distinct and well-documented processes which can be combined to describe the complete process of mixing with oxidant and subsequent combustion of a coal-oil slurry. These will be dealt with in turn, and are:

a) The formation of a cloud of droplets and particles.

b) Aerodynamic processes of turbulent mixing and recirculation.

c) The combustion of a spray of oil droplets.

d) The combustion of a cloud of coal particles.

e) The interactive effects of (c) and (d), and their concurrency or sequence, as the case may be, of combustion.

2.1. Assumptions made in the mathematical model

i. Model Type

It is assumed, as stated, that the model is that of a one-dimensional axisymmetrical flame, despite the fact that due to its jet nature there is a velocity gradient at right angles to the axis following a Gaussian curve[46]. This gradient can be partially compensated for in the flame sampling procedure, as will be shown in chapter 5.

ii) Chemical effects

In reality, there is a considerable degree of oxygen depletion in the raceway when there is no oil injection[26], and oxygen is substituted for by carbon monoxide and carbon dioxide. However, in the physical model, the composition of the entrained gases will be determined largely by the stoichiometric characteristics of the initial injectant and air, and this can be compensated for in the mathematical model. The relevant composition of entrained gas in the prototype blast furnace raceway may easily be corrected for in the mathematical model when, later, it is applied to the blast furnace. Obviously, this latter section of the work belongs with the full-scale work, and will not be dealt with here.

2.2. Aerodynamic Processes in the Mathematical Model

2.2.0. Mixing of air and fuel streams

The mixing process in the model can be adequately described in two dimensions, assuming radial symmetry. However, since this is a one-dimensional model, a reasonably accurate simulation will suffice.

Unfortunately, most of the work which has been carried out on flame length deals with the entrainment of low-velocity surrounding air by a high velocity fuel jet, which may[47,48] or may not[49,50] be swirling.

In the situation obtaining at the tuyere in a blast furnace, however, the air blast has a considerably higher momentum than the fuel stream.

The use of the Pieri[51] mixing correlation for annular concentric jets overcomes this difficulty by using the Toor[52] mixing index.

For a non-swirling jet, Pieri shows that:

$$M = \frac{A' X}{1+A'X} \qquad (1)$$

where: M is the mixing index

A' is a constant whose value is approximately 3

X is the dimensionless distance along the flame axis which is equal to $\frac{x}{D}$ for non-swirling components.

where: x is the distance from the nozzles, D is the effective diameter found from the momentum-weighted mean diameters of the nozzles.

The index M is indicative of the degree of completion of a reaction between a fuel gas and oxidant, the rate of which is controlled entirely by turbulent diffusion.

In this case, however, the combustion process is not instantaneous, and so the mixing index must be used in conjunction with the combustion rate equations developed later to produce a time - local oxygen concentration, in rather a different manner from Kattan and Adler[53] who also applied the mixing index to non-instantaneous reactions.

2.2.1. Recirculation of Combustion Products

Recirculation of the blast furnace raceway will obviously be very small due to the flow-impeding effects of the surrounding burden. However, the model tuyere to be used in the flame tunnel available, which is of 900mm diameter, results in considerable recirculation.

As will be seen later in Chapter 3, a scale model tuyere of 70mm was decided upon. With these sizes of tuyere and flame tunnel, the degree of recirculation of combustion products can be approximately calculated by using the equation developed by Ricou and Spalding[54]

$$\frac{\dot{M}_r}{\dot{M}_o} = 0.32 \left(\frac{\rho_r}{\rho_o}\right)^{\frac{1}{2}} \frac{x}{d_o} - 1 \qquad (2)$$

where $\dot{M}_r$ = mass flow of recirculated gases

$\dot{M}_o$ = mass flow of nozzle fluid

ρ_r = density of recirculated gases

ρ_o = density of nozzle fluid

x = axial distance from nozzle

d_o = diameter of nozzle

However, recirculation is assumed by Field et al[55] to reach a maximum at the point halfway between the nozzle and the point where the jet boundary reached the wall of the enclosure. An angle between the jet axis and jet boundary of 9.7^o was used.

2.3. Combustion of Oil

2.3.0. Atomisation and drop size distribution

A review of the process of atomisation of liquid fuels for combustion has been carried out by Eisenklam[56] and by Williams[57,58], whilst Simmons has produced correlations for both Drop size/volume fraction[59] and Drop size/Number Distribution[60]. Most of the data for these correlations were obtained by means of the high speed spray analyser[61], and the wax droplet method[62] of spray analysis.

The most often used method of describing the size distribution of oil droplets is, as with particle size range analyses of coal, the Bennet[63]/Rosin-Rammler[64] distribution.

This states that:

$$R = e^{-Bx^n} \qquad (3)$$

where R is the weight fraction of droplets greater in diameter than x,

B is the size constant

n is the distribution constant

However, attempts to show that combustion of a spray can be accurately described by a mean diameter of oil droplet, e.g. Probert[65] have been discounted by Dickinson and Marshall[66]. The development of a one-dimensional model by Nurazzaman, Siddal and Beer[67] confirmed this.

The model thus developed must therefore take account of distribution of droplet sizes. Sixteen ranges are used so that widely varying distribution may be studied.

The size ranges are:-
<5μ, 5-9.5, 9.5-13.1, 13.1-18.1, 18.1-25, 25-34.5, 34.5-47.7. 47.7-65.8, 65.8-90.8, 90.8-125, 125-173, 173-239, 239-329, 329-454, 454-627. It can be seen that the size range span ratio is 1.38 except for the span 5-9.5 which is 1.38^2.

2.3.1. Hydrocarbon Models of Droplet Combustion

Williams[58] has produced an exhaustive review of hydrocarbon droplet combustion. Virtually all theoretical models of droplet combustion have been derived from the original model of Godsave[68] who postulated a spherical droplet burning in a non-convecting air stream. The mode of combustion considered that the droplet was surrounded by a spherical envelope of flame, heat conduction from which evaporated the fuel droplet. The resultant vapour diffused to the flame - which was of infinitely small thickness - where it combusted stoichimetrically with oxygen diffusing from the surrounding air.

Practical verification of this model is complicated because convection currents are formed by the combustion process, so that the resultant flame envelope is distorted from the spherical.

The rate of combustion of the oil droplet is thus constrained by two considerations: (1) The rate of evaporation of the droplet and (2) The rate of diffusion of oxygen to the flame envelope. The distance of the flame envelope from the droplet is thus affected by the relative magnitude of these two processes, and knowledge of this is necessary to evaluate mass combustion rate in Godsave's original equation.

2.3.2. Evaluation of rate of combustion of a Hydrocarbon oil Droplet

A detailed theoretical model is unnecessary for the attainments of the objectives of this investigation. What is required is that the following objectives are realised:

1) The model agrees reasonably well with experimental results.

2) The model is such that the parameters which alter during the combustion process, notably ambient temperature and oxygen concentration can readily be taken into account.

3) The model must use readily available data.

These criteria are realised in the mathematical model of Long[69] who proposed that for a unit surface area:

$$\frac{dm}{dt} = \frac{k}{cd}\left\{2\ell n\left[1 + \frac{c(T_f - T_s)}{Q}\right] + \frac{\rho dc}{16\chi k}\ell n\left(1 + \frac{\chi n^{\infty}}{\Omega}\right)\right\} \quad \ldots\ldots(4)$$

where: k = mean thermal conductivity of the intra-flame space

c = mean specific heat of fuel vapour in the intra-flame space

d = droplet diameter

T_f = Flame temperature

T_s = Droplet surface temperature

ρ = mean density of oxygen beyond the flame

D = mean diffusivity of oxygen beyond the flame

χ = number of moles of combustion products derived from stoichiometric combustion of unit mass of fuel with oxygen

n^{∞} = mole fraction of oxygen in bulk surrounding gas

Ω = number of moles of oxygen required for stoichiometric combustion of unit mass of fuel with oxygen.

However, the second mass transfer term is often omitted since this involves an error of less than 10%. In the finite difference model used, the flame temperature is affected at each iteration by the ambient temperature and composition of the gases. The flame temperature is calculated from a consideration of stoichiometric combustion (by assumed model definition) of the oil with the gases at ambient temperature and composition for that iteration.

The equation used in the final model was thus the simplified heat conduction version, with values as given by Long[69].

2.3.3. Combustion of Residual Oils

It has been shown by several workers, notably Masdin[70], that the combustion of residual fuel oil does not follow the theoretical model of combustion as well as distillate fuel oils. There is consensus that the residual oil follows normal evaporation until approximately 90% of its mass has been combusted, and then a skeletal carbon "cenosphere" is formed, in a manner analogous to the devolatilisation of coal. Account could be taken of this in the mathematical model at a penalty of complication of the model. However, in the case of coal-oil slurries considerably larger quantities of devolatilised carbon are also being combusted, and since the cenosphere effect is unlikely to be detected by measurement, it is ignored. This is a reaonably safe assumption since the formation of cenospheres is heavily dependent upon size, as shown by Masdin[70], who suggested that, in the case of pitch - creosote, 100μ droplets would form 8μ cenospheres. Since the cenosphere size $\propto$ droplet size^2 (where size is in cm), then the cenosphere size in a normal spray would be very small, with consequent rapid combustion.

2.4. Combustion of Coal Particles

2.4.0. Size Distribution of Coal Particles

As with oil droplets the Rosin-Rammler distribution is utilised. For the purpose of the combustion model,

the distribution is divided into the same discrete size ranges as the oil droplets, the diameter of the particles being taken as the geometric mean of the range limits.

The use of the Rosin-Rammler distribution for coal was the deciding factor in choosing this distribution for the slurry, as against other distributions such as that proposed by Tanasawa and Tesima[71]. The size during devolatilisation is assumed to be unchanged, i.e. no swelling occurs, and the shape of the particles is assumed to be spherical throughout, even though this is actually only near the truth after devolatilisation.

2.4.1. Modes of Coal Combustion

The combustion of coal particles takes place in two distinct processes. Firstly, the coal devolatilises so that a near-spherical residual particle is left, which is almost entirely carbon and mineral matter.

The fast or "flash" devolatilisation of the coal which occurs in the combustion of fine coal powder results in a much greater evolution of volatiles than the dry, ash-free (d.a.f.) volatile matter figure would suggest. This has been borne out by laboratory studies of flash heating[72] including very rapid heating by laser pulses[73]. The evidence is thus that a greater proportion of carbon is volatilised than is normally the case with slow carbonisation.

The subsequent combustion of the coal residue is usually assumed to be the combustion of pure carbon, the rate determining step of which can be either kinetically or diffusionally controlled depending on gas temperature and composition and residue particle size.

2.4.2. The Devolatilisation Process of Coal Particles

Although there are reports of combustion of volatiles of coal behaving analogously to an oil droplet[74] in that it obeys a "d^2 law", the work by Badzioch, Sainsbury and Hawksley[75] have shown that the weight change on devolatilisation is best expressed by the empirical equation:

$$\Delta W = Vo(1-C_1)Q\ 1-\exp\ (-C_2\ \exp(-C_3/T))t \quad .....(5)$$

where: ΔW is weight loss after t milliseconds

Q is a factor converting change in volatile matter to weight loss

Vo is the original d.a.f. Volatile Matter

C_2 and C_3 are constants

and $C_1 = \exp\ -K_1(T-K_2)$ .....(5(a))

where K_1 and K_2 are constants

and T is expressed in Degrees Absolute, and t is in ms.

For Bituminous coals, C_3 = 8900K, and for non-swelling coals C_1 = 0.14. For non-swelling bituminous coals, only C_2 therefore varies.

It was reported[72] that particle size had no influence on rate of devolatilisation, up to the 60μ used in the test. Since the bulk of the coal used is below this size, it is assumed that this is true of all sizes used.

Equations 5 and 5a are in a suitableform for use in a finite difference model, and so are used unaltered. Evidence exists[76] that residue combustion begins before the final end of devolatilisation, so this point is set at 0.90 V_o $(1-C_1)Q$ to limit the lag in devolatilisation due to the exponential form of equation(5).

2.4.3. The Combustion of the Coal Residue

Early work on captive carbon spheres by Tu et al[77] showed that the rate limitation of combustion was diffusion of oxygen to the surface of the carbon, giving rise to a "d^2 law" whereby the time of combustion of the carbon sphere was given by:

$t = K_c d^2$ where K was the rate constant for the carbon; the carbon spheres were 250mm in diameter.

Later work by Essenhigh[74] on coal confirmed that diffusion controlled combustion was, in fact, the case for large particles. The diffusional differential equation of reaction rate per unit external area assuming that diffusion rate is slower than reaction rate is given by:

$$\frac{dM}{dt} = -K_d(O_g - O_s) \qquad .....(6)$$

where M is particle mass at time t, O is oxygen partial pressure (g in the ambient gas and s at the surface)(for infinite kinetics and total diffusion control, O_s = zero). K_d is the diffusional rate constant given by:

$$K_d = \frac{3\phi\ \rho_o\ D_o}{4d}\left(\frac{T}{T_o}\right)^{0.75} \qquad .....(7)$$

where: ϕ is the reaction mechanism (1 for reaction to CO_2, 2 for reaction to CO)

ρ_o is the gas density at T_o degress absolute,
D_o is the diffusion coefficient of oxygen in nitrogen at T_o (the other gases present being ignored), d is the diameter of the particle,
T_o is the reference temperature for ρ_o & D_o,
T is the mean of the gas and particle surface temperatures. (The latter has been measured practically[78,79]).

However, the work of Essenhigh[74] was conducted with particles of 300μ and over and previous work by Hottel & Stuart[80] had suggested that for typical sizes of particles associated with pulverised fuel (∿50μ) reaction kinetics could influence overall reaction rate.

If the reaction rate is slower than diffusion rate

$$\frac{dM}{dt} = -K_s.O_s \qquad .....(8)$$

(where $O_s = O_g$ if the diffusion rate is infinite)
where K_s is the surface reaction rate constant, given by the Arrhenius equation:

$$K_s = K'_s \exp(-\Delta E/RT_s) \qquad .....(9)$$

where ΔE = activation energy
K'_s = pre-exponential constant.

If the two rates are of the same order of magnitude, then a combined diffusion/kinetic equation can be formed by substituting (8) in (6) to give:

$$\frac{dM}{dt} = \frac{O_g}{\frac{1}{K_d} + \frac{1}{K_s}} \qquad .....(10)$$

Lowe et al[81] put this in terms of rate of change of mass of unburnt fraction of particle:

$$\frac{dU}{dt} = \frac{O_g . S . U}{\frac{1}{K_d} + \frac{1}{K_s}} \qquad .....(11)$$

where $S = \frac{\text{particle surface area}}{\text{mass at time t}} = \frac{6}{d\rho}$ for spherical particles .....(12)

and U = mass fraction of particle unburnt at time t.

The assumption is still made that the carbon particles burnt only at the surface, but Field[82,83] and others[84,85,86,87] proved that this was not entirely true, and that combustion also took place in the pores of the particle which were left by the evolution of volatiles.

Not only does the size of particles vary with degree of burnout, therefore, but so also does the apparent density due to combustion in the pores of the char. Field showed that the size and density of the particles varied with fractional unburnt char thus:

$$d = d_o U^{\alpha} \qquad .....(13(a))$$

$$\rho = \rho_o U^{\beta} \qquad .....(13(b))$$

where d = diameter, ρ = density
α, the size exponent = 1/3 for constant density combustion and 0 for constant size combustion, and β the density exponent = 0 for constant density combustion and 1 for constant size combustion. From geometric considerations, $3\alpha + \beta = 1$.

Substituting (13(a)) and (13(b)) into (12) we obtain:

$$S = \frac{6}{d_o U^{\alpha} \rho_o U^{\beta}} = \frac{6 U^{-\alpha-\beta}}{d_o \rho_o} \qquad .....(14)$$

Substituting (14) in (11) we obtain:

$$\frac{dU}{dt} = \frac{-O_g}{\frac{1}{K_d} + \frac{1}{K_s}} \cdot \frac{6U^{(1-\alpha-\beta)}}{d_o \rho_o} \qquad .....(15)$$

this together with equations (7) and (9) are used for evaluation of char combustion rate in the model, the implicit assumption being made that the relative velocities between particle and gas stream is small.

2.5. Likely Behaviour of Coal/Oil Slurry During Combustion

There is very little published data on the combustion of coal-oil slurries. Most investigations have been of an empirical nature either as in boiler plant trials or experimental furnace trials on a "combustibility" basis (see section 1.3). The only significant work outside this has been done by Law et al[42] and especially by Braide et al[43], where coal-oil slurries of 30% w/w coal were subjected to single droplet tests. However, the coal particle sizes were small ($\sim 3\mu$) and the resultant droplet varied little from residual fuel oil in its' combustion characteristics.

2.5.0. Atomisation of the Slurry

If the slurry is atomised in a normal twin fluid atomiser then it can reasonably be expected that the resultant size distribution arises from the fact that the smaller droplets are formed at the zone of higher shear forces in the atomiser, rather than formation on a purely random basis.

The coal is also distributed in size, and assuming homogeneous distribution of the size ranges throughout the oil, then, upon the formation of oil droplets, some larger coal particles will obviously be at the position of high shear forces in the atomiser, thus coinciding with the formation of smaller droplets.

Some of the larger coal particles will obviously now appear as "free" coal particles. In general, therefore, the smaller the droplets of slurry formed, the lower their coal content will be, and vice versa. However, since homogeneous distribution of the coal was assumed, the larger droplets of slurry cannot contain more than the original proportion of coal (indeed by the above definition it must contain somewhat less). Therefore, for distributed size ranges of the coal and distributed

size ranges of the slurry, some "free" coal must inevitably appear unless the proportion of coal is low, and the "grind" is much finer than the slurry drop size distribution.

Having established that some free coal must necessarily appear, it now remains to ascertain what quantity of coal and at what size distribution actually is free of the slurry.

2.5.1. Determination of Free Coal Quantity and Distribution

This topic is only of interest insofar as it affects the combustion of the slurry and free coal. That is, an analogue which gives the same combustion characteristics is acceptable.

Essenhigh[74] has shown that the combustion constant of coal in the "d^2 law" is approximately one order of magnitude higher than that of oil. Thus a coal particle of 1/3 the diameter of an oil droplet will have approximately the same burning time. It is uncertain whether the location of a coal particle within a droplet of three times the diameter of the particle would actually be allowed by the atomising shear forces.

It is also uncertain whether the particle would remain "part" of the droplet during the disruptive boiling undergone by residual fuel oil during combustion. It is thus initially assumed that all sizes of coal below 0.3 of the slurry droplet diameter can remain in the slurry droplet and, furthermore, do not significantly alter the combustion characteristics of the droplet, as determined by Braide et al[43].

The same size ranges are used for coal and slurry. It will be seen that, with the size range span of 1.38 used, a coal particle 4 size ranges below that of the slurry droplet is capable of remaining within the droplet since it will be $(1/1.38^4)$, i.e. 0.3 of the size of the slurry droplet.

If the size ranges are numbered 0, 1, 2--15 in order of increasing fineness, then the n^{th} slurry droplet size range will only contain coal particles of the $n+4^{th}$ size range or finer (n+5, n+6 etc.). For a complete distribution, therefore, the coal sizes 0 to 3 will be completely free from the slurry, the 4th coal fraction will be contained only in the 0th fraction of slurry, the 5th fraction will be contained only in the 0th and 1st fractions of slurry etc. The relationship between slurry and free coal is thus "four overlaps".

Consider Fn to be the proportion of free coal in fraction n relative to total coal mass supplied and Sn is the proportion of slurry in the n^{th} size range of the total of the atomised slurry (i.e. excluding free coal). If P is the relative mass of coal to oil as supplied to the atomiser and Cn is the proportion of coal in the n^{th} size range of the total coal mass, then:

Proportion of slurry which can hold the n^{th} fraction of coal $= \sum_{0}^{n-4} S_n$

It can then be assumed due to homogeneity that this proportion of the n^{th} fraction of coal has been assimilated in the slurry, the remainder being "free" coal i.e.

$$F_n = (1 - \sum_{0}^{n-4} S).Cn \cdot P \qquad .....(16)$$

expressed in terms of unit flow of oil.

The total atomised slurry mass flowrate relative to unit flowrate of oil is thus the mass of slurry supplied to burner - total free coal

i.e. $$S_T = 1+P - \sum_{0}^{15} F_n \qquad .....(17)$$

and the mass flowrate of each fraction of atomised slurry per unit oil flow is:

$$MS_n = S_n \cdot S_T \qquad .....(18)$$

Equation (14) to (16) above are thus used in the determination of the free coal and slurry flows.

2.5.2. Composition of the Atomised Slurry

Whilst the slurry droplets are assumed to burn as do residual fuel oil droplets as stated in 2.5.1. above, the composition and calorific value must be altered in proportion to their relative masses i.e., using (15) above:

$$\text{Property of slurry} = \frac{\text{Property of coal } x(S_T-1)+\text{Property of oil}}{S_T} \qquad .....(19)$$

This gives only the mean property of the slurry, as the finer the slurry fraction, the nearer to the composition of pure residual oil it becomes; it is an adequate representation of the slurry as a whole.

The exception to the above is the density, since:

$$\text{mean density of slurry} = S_T / \left(\frac{S_T-1}{\rho coal} + \frac{1}{\rho oil}\right) \qquad .....(20)$$

2.5.3. Determination of Gas Composition and Temperature

The rate of change of Oxygen composition in the gas will be given by:

$$\delta O_2 = \delta M.R_s + \delta \Delta W.R_v + \delta U.R_r \qquad .....(21)$$

where O_2 is the mass of oxygen consumed, R is the stoichiometric ratios whose subscripts: s = slurry, v = volatiles and r = residue.

Similarly

$$\delta CO_2 = \delta M.C_s.\frac{44}{12} + \delta \Delta W.C_v.\frac{44}{12} + \delta U.\frac{44}{12} \qquad .....(22)$$

where C is proportion of carbon.

and

$$\delta H_2O = \delta M.H_s.\frac{18}{2} + \delta \Delta W.H_v.\frac{18}{2} \qquad .....(23)$$

and for temperature:

$$\delta T = (\delta M.CV_s + \delta \Delta W.CV_v + \delta U.CV_r)/V.Cp. \qquad .....(24)$$

where CV is the calorific value of the combustibles and V & C_p are the volume and mean specific heat of the gases respectively,

and where $\delta \Delta W$ is the change of ΔW throughout the iteration, i.e. on the n^{th} iteration:

$$\delta\Delta W = \Delta W_n - \Delta W_{n-1}$$

and $$\delta M = \frac{dM}{dt}.\delta t, \quad \delta U = \frac{dU}{dt}.\delta t$$

where δt is the iterative step-length.

2.6. Construction of the model

2.6.0. Integration procedure

The various one-dimensional models which have been constructed have used a variety of integration procedures in their make-up, usually simple Euler integration, (for example see references 88 and 89). Since 1967, however, the development of two-dimensional models has proceeded rapidly beginning with the work of Pun and Spalding[44] which was later applied to pulverized coal combustion (for an example see reference 90) and gas combustion and radiation[91]. Analogue computers have also been successfully used[92,93]. The great advantage of using an analogue computer in this situation is its very rapid integration of differential equations. A hybrid computer, i.e. an analogue computer linked to a digital computer by Digital to Analogue and Analogue to Digital converters, would be even more satisfactory, particularly for two-dimensional models.

However, at least in this initial attempt, a one-dimensional model will be used on a digital computer. The main reason why this type of model is not very inaccurate in this situation is because of the small diameter of the model tuyere used and the high velocities ensure that mixing is very rapid in terms of time and so the well-tried equations of droplet and particle combustion will have more emphasis in the final result than is the case with the usual burner types.

Several simplifications are made in the model:

i) Particle and gas velocities assumed to be equal.

ii) Free coal particle temperature is assumed to be 400K higher than gas temperature[79].

iii) The diffusion coefficient of oxygen in pure nitrogen is used, the combustion products being ignored.

iv) The ash in the free coal is assumed to reside in separate particles from the combustible.

v) The slightly higher than atmospheric pressure in the practical system is ignored. Hedley and Guldenpfennig[94] show that this is a reasonable assumption.

Simple Euler integration is used in the model.

2.6.1. Selection of Machine

An important consideration is the machine on which the model is run. The machines available are:

(a) The "Pet" microcomputer with 32K RAM, Language: BASIC

(b) The PDP11/45 microcomputer with 16K available RAM, Language: BASIC+ (at the BSC Welsh Laboratory Building)

(c) The DEC system 20 (at the Polytechnic of Wales) with 256K available RAM, Language: FORTRAN IV, BASIC+2.

The factors influencing the choice of machine were:

i) The speed of the machine. Obviously this is of prime importance with 200 iterations (each containing up to a further 30) to be considered. However, if the machine is fitted for batch processing, this is not as important during the "production" period i.e. after debugging.

ii) Memory capacity of the machine. This question arose largely through the limited capacity due to the operating system of the PDP/11/45. However, the programme was made to fit into the 16K available.

iii) Ease of editing during the "debugging" period. Obviously many alterations had to be made to the model before it would function correctly, and with a poor editing facility this could be very time consuming.

Before writing the model, therefore, these points were considered, with the following results:

i) Whilst the Decsystem 20 had obviously both sufficient processor speed and memory for the job, it suffered from the disadvantage of distance from the experimental

location, and also a rather slow editing procedure. A batch procedure was available.

ii) The proximity of the PDP11/45 to the apparatus was less disadvantageous, but nevertheless involved a car journey. It also suffered from a slow editing procedure but, more important, the core could well be too small for the model. A batch procedure was available.

iii) The "Pet" would certainly take the model from the viewpoint of capacity, but experience with identical programmes had shown that it was 30-40 times slower than the PDP11/45 (depending on the loading of the latter). However, with its two tape decks it could be made to operate on a batch basis, and the editing facility was extremely powerful.

It was therefore, decided to initially write the programme of the model on the "Pet" so that early modifications could be made easily, and the space taken by the programme could be evaluated (by a simple command to the machine) to see whether it could later be transferred to the PDP11/45, or failing that, to the Decsystem 20. This also settled the language, since only BASIC was upwards compatible with the other two languages.

The programme was therefore written onto the "Pet" in batch form and was found to take about 14K bytes. After correction, it was found that a "run" took about 30 mins. The model was thus capable of being loaded onto the PDP11/45, with a run time of 3-4 minutes, depending on other usage. The entire 80 runs of the series could thus be executed in a single night batch operation on the PDP11/45, reducing the travel criterion.

After the model was complete and debugged, one of the new generation of 16-bit microcomputers, the "SIRIUS", became available for the duty of running the mathematical model. This machine had 128k bytes of RAM, with 1.2Mbytes of floppy disc memory. The 16-bit processor was considerably faster than the "PET", and the availability of a compiler meant that yet greater speed could be achieved. All the final optimisation was carried out on this machine.

2.6.2. Simplified Flowchart of Slurry Combustion Model

This version of the model is for anthracite/oil slurry, and does not include a volatiles combustion section.

The operations below refer to the Flowchart in Fig. 1.

Operation	Description
A	Have all the variable condition runs been carried out?
B	Read in parameters of run to be conducted.
C	i) Calculate slurry mass in each fraction, and the free coal in each fraction (equations 16-20). ii) Calculate number of drops, mass of drop and surface area of each fraction. iii) Calculate number of free coal particles, mass of free coal particles and surface area for each fraction.
D	Let M = 1
E	Advance time by selected time step.
F	Calculate mixing index (equation 1).
G	Has recirculation eddy been reached?
H	Calculate entrainment into the jet (equation 2).
I	Calculate disentrainment (pro-rata for distance).
J	Calculate new gas composition.
K	Calculate new velocity of jet, new width of jet and new axial position of section under consideration.
L	Has the x-axis position X(M) just been passed?
M	Store results of gas composition obtaining at X(M).
N	IS M = 5?
O	Let N = O
P	IS N^{th} slurry fraction burnt out?
Q	Calculate mass of slurry burnt in N^{th} fraction in t step (equation 4).
R	IS N^{th} coal fraction burnt out?
S	Calculate mass of coal burnt in N^{th} coal fraction. (equation 15).
T	Calculate changes in gas composition (equations 21-24).

U Let N = N + 1

V IS N = 15?

W Let M = M + 1

X Are all fractions of coal burnt out?

Y Store results as being true for the rest of the sample positions.

3. DESIGN OF APPARATUS

3.0. Design Criteria

The reasonable simulation of blast furnace tuyere raceway combustion conditions requires the emulation of the prototypical air blast and injectant condition in the experimental apparatus.

3.0.0. Air Blast Conditions

The simulated air blast must achieve propotypical values of velocity, temperature and oxygen content.

In normal World-wide blast furnace practice, tuyere velocities normally encountered vary from 160 to 250m/s. The temperature of the blast ranges between 800 and 1300°C, whilst the oxygen content of the blast varies between 21% (natural air) or may be enriched up to 26%.

3.0.1. Injectant Conditions

Assuming that the injectant is heavy fuel oil based coal slurry, then for realistic combustion simulation the injectant must follow real practice in the following aspects:

(i) Composition for the heavy fuel oil. This must be similar in terms of viscosity, surface tension and chemical analysis, as will be used in practice and in the case of coal, the material should preferably be from the same mine, with the same range of size distribution.

(ii) The fuel-air stoichometric ratio available in the apparatus should cover the range experienced in blast furnace practice. In the case of oil injection, this can vary from 30% of the available oxygen to approximately 100% of the available oxygen.

(iii) The method of atomisation must produce a similar atomising effect in the apparatus as in real practice. In the case of a back-atomised burner system, where a cloud of fuel droplets is transported to the injection point suspended in a jet of steam then the steam/fuel mixture in the model should have a similar velocity in the model as in practice.

In the case of fuel/water emulsions, then the emulsion should have the same quantity of water present, and it must also have a similar water droplet size distribution in the experimental apparatus as in the prototype.

3.1. Design of Hot Air Blast Supply System

3.1.0. Principle of Operation

It is very difficult to simulate precisely the very exacting conditions of temperature, velocity and oxygen concentration obtaining in the blast furnace tuyere.

Originally, it was intended to produce the necessary conditions of temperature in a pebble-bed air heater. However, investigations into this method of hot air production with its cyclic mode of operation, physical bulk and difficulty of construction, were discontinued at an early stage.

A rotary regenerator to heat the air was next considered. However, the pressures necessary for attainment of the velocity criterion would have caused very high leakage in such a device.

Finally it was decided to use direct combustion heating of the air. Since perfect chemical similarity to tuyere raceway combustion conditions cannot be obtained in the experimental apparatus, (due to the absence of coke, iron ore, limestone and iron particles) the imposition of further dissimilarity in the form of vitiation of the combustion air with carbon dioxide and water is unlikely to greatly increase inaccuracies in the results, providing the oxygen concentration similarity criterion is met.

3.1.1. Constraints Upon Design

With the method of hot air production established, the constraints imposed by the available equipment were examined.

The production of simulated "air" would require air proper, fuel and also oxygen supply both to make up the deficiency caused by the fuel and also to enrich the final product up to a maximum of 26% oxygen by volume.

(a) Air

At the laboratory the available equipment consisted of two fans, each capable of delivering air at the rate of $1.5m^3.s^{-1}$ at a pressure of 3.5 $kN.m^{-2}$ gauge. The available air was thus either $3.0m^3.s^{-1}$ at $3.5kN.m^{-2}$ gauge (fans in parallel) or $1.5m^3.s^{-1}$ at $7.0kN.m^{-2}$ gauge (fans in series).

(b) Oxygen

A pipeline leg of nominal 50.8mm (2") bore conducts oxygen to the laboratory from the works mains at a pressure of 13.8 bar gauge. The oxygen is at a purity of better than 99.9%. The constraint in operation here is one of velocity in the 50.8mm leg of the main.

Since the main is of mild steel, a velocity limit of $8m.s^{-1}$ (plug flow) is enforced. This, coupled with the pressure drop along the leg, limits the oxygen flow to the laboratory.

The heat liberated by combustion varies with different fuels but is generally proportional to the oxygen used in combustion. The average energy release is approximately 12.5 MJ per kg of oxygen. With a 2 MW thermal loading on the flame tunnel, a maximum total system oxygen load (oxygen for combustion plus enrichment and oxygen in air) can be no greater than $2/12.5 = 0.16kg.s^{-1}$.

3.1.2. Evaluation of Design Parameters

(a) Combustion of Propane-Oxygen-Air

The complete combustion of propane takes place as follows:

$$C_3H_8 + 5O_2 \rightarrow 3CO_2 + 4H_2O \qquad (25)$$

therefore, to combust propane and oxygen such that the wet waste products will contain 21% oxygen:

$$0.21 = \frac{V}{V + 3 + 4}$$ where V is the volume of excess oxygen required.

$\therefore$ V = 1.861

therefore, for a wet waste gas analysis of 21% oxygen, 1 volume of propane should be combusted in 6.861 volumes of oxygen, giving three volumes of CO_2, four of H_2O and 1.861 of oxygen. This forms the basis for the simulated "air" to be used in the work programme, the quantity of diluent air proper governing the temperature. This volume of oxygen represents the minimum flow necessary.

Therefore, if V_1 is the propane flow and V_2 is the oxygen flow,

$$V_{2(min)} = 6.861\ V_1 \qquad \ldots\ldots(26)$$

If V_n is the total volume flow, V_1 is the propane flow, V_2 is the oxygen flow and V_3 is the air flow, then when any oxygen concentration,

Po, is required:

from equ. (25) above,

Total volume of products = 2 x propane flow + oxygen flow + air flow

i.e. volume flow, $V_n = 2V_1 + V_2 + V_3$ ....(27)

then, for an oxygen concentration of Po in the product gases:

$$Po = \frac{V_2 + 0.21V_3 - 5V_1}{V_n} \qquad \ldots\ldots(28)$$

$$\therefore\ PoV_n = V_2 + 0.21\ V_3 - 5V_1$$

$$\therefore\ V_2 = PoV_3 - 0.21V_3 + 5V_1$$

but, from (27), $V_3 = V_n - 2V_1 - V_2$

$$\therefore\ V_2 = PoV_3 - 0.21\ (V_n - 2V_1 - V_2) + 5V_1$$

$$\therefore\ V_2 = \frac{(Po-0.21).V_n + 5.42V_1}{0.79} \qquad \ldots\ldots(29)$$

Therefore, since the maximum oxygen proportion required is 26%,

$$V_{2(max)} = \frac{0.05V_n + 5.42V_1}{0.79} \qquad \ldots\ldots(30)$$

For any given required volume flowrate, therefore, the maximum air requirement will be:

$$V_{3(max)} = V_n - 2V_1 - V_{2(min)} \quad \ldots\ldots(31)$$

and the minimum air requirement will be:

$$V_{3(min)} = V_n - 2V_1 - V_{2(max)} \quad \ldots\ldots(32)$$

V_n, the NTP flow, is a function of required velocity and temperature obtaining in the combustion chamber and tuyere system:

$$V_n = \frac{273}{T} \times C \times \left(\frac{D}{1000}\right)^2 \times \frac{\pi}{4} \quad \ldots\ldots(33)$$

where:

C = Blast Velocity (m/s)

T = Absolute combustion chamber temperature (K)

D = Diameter of tuyere (mm)

(b) Pressure Drop

The pressure drops encountered in the entire rig are:

(1) Velocity head pressure drop at the model tuyere exit.

(2) Pressure drop along the model tuyere.

(3) Pressure drop encountered at the cross sectional area change between the combustion chamber trunking and the model tuyere.

(4) Pressure drop in the burners.

The first three may be calculated together using the "practical flow formula" from Spiers[95], which, with the additional factor of 6.575×10^{12}, allows the use of Sl units throughout.

(c) Measurement and Control Considerations

The "turndown" of a differential pressure flowrate measuring device is of the order of 20% of maximum value. Taking the flowrate below this level results in the occurrence of unacceptable inaccuracies. The minimum flowrates normally encountered in each of the supply gases to the apparatus must not therefore fall below this value.

The control valves must be sized so as to accommodate the maximum flow encountered with the correct pressure drop.

3.1.3. Evaluation of Flowrate Requirements

The upper limits to flowrates have thus been shown to be important in the design of the apparatus. Therefore, to achieve the required velocities within these constraints, the most influential single variable in the design will be the diameter of the model tuyere itself, that is, the selection of an appropriate scale ratio.

To calculate individually all the permutations of tuyere diameter, tuyere velocity and temperature together with calculations of all the various flowrates, would be very tedious. A simple computer programme was written to speed up the decision making.

The pressure drop formula already referred to was incorporated into the programme. The velocity assumption was increased in steps of10 $m.s^{-1}$ from its original level of 160 $m.s^{-1}$ until the pressure either exceeded that supplied by the fans, or else attained the maximum velocity to be encountered (250$m.s^{-1}$). When either of these criteria was achieved, the tuyere size, velocity, pressure and propane, oxygen and air flows were printed out.

This process is carried out for tuyere diameters of 68-90mm in 2mm increments, and for temperatures between 800 and 1300°C inclusive in 100°C increments, and for oxygen contents of 21-26%.

It was rapidly established that the existing fan system was quite unequal to the task. Velocities of only 170$ms.^{-1}$ were achieved at 800°C with the available maximum pressure of 7.0 $kN.m^{-2}$.

A pair of high pressure fans were obtained, each capable of supplying 0.7$m^3.s^{-1}$ of air at a pressure of 8.7$kN.m^{-2}$. The air supply situation was thus now altered to either 1.4$m^3.s.^{-1}$ at 8.7$kN.m^{-2}$ (fans in parallel) or 0.7m^3s^{-1} at 17.4$kN.m^{-2}$. When the value of 17.4$kN.m^{-2}$ for

pressure and $0.7m^3.s^{-1}$ for volume was substituted in the programme, it was established that the maximum required velocity, $250m.s.^{-1}$, was achievable.

Data also provided by the programme are:

(1) The maximum flows encountered or any given diameter of tuyere.
(2) The average flows encountered for any given diameter of tuyere.
(3) If a contingency of 20% is added to the maximum flows encountered, and these are divided into the relevant minimum flows encountered a working turndown ratio for each orifice plate is given. If it is worse than 25%, a warning is given.

Also taken into account are the other contraints in section 3.1.1.:

(1) Fuel rate too high
(2) Oxygen flow too high
(3) The potential energy release is too large for the flame tunnel.

If any of these constraints are transgressed, the programme prints out the tuyere size and the relevant fault, and continues with the next tuyere size without printing out any other information.

It was found that these results showed that at 78mm and above, thermal overload of the flame tunnel can take place. The mean flows, particularly of propane, give an excellent indication of the quantity of gas storage needed together with an estimate of running cost.

A tuyere size of 70mm was initially chosen as being sufficiently far from the thermal overload situation whilst still allowing a scale ratio of approximately 0.45.

The final design parameters were thus finalized as follows. The flows including the 20% contingency previously mentioned:

Tuyere size: 70 mm
Max. propane flow: 5.06 $l.s^{-1}$ (35.8Kg/hr)

Max. oxygen flow: $56.20\ l.s^{-1}$

Max. air flow: $0.336 m^3.s.^{-1}$

3.2. Design of Hot Blast Air Supply Combustion Chamber

The combustion chamber design has four limiting factors:

(i) The high temperature within the chamber (up to 1350°C).

(ii) The high oxygen content in the gases (21-26%).

(iii) The low shell temperature allowable (<200°C)

(iv) Relatively large heat release (approx. 0.56MW max.)

It was decided to use a stack-bonded fibre lining (Kerlane 60) which, with a thermal conductivity of $0.45 Wm^{-1}K^{-1}$ would give a shell temperature of approximately 160°C when the inside face temperature was 1350°C.

The burners used were five Eddy Ray 1/20 nozzle-mix burners each rated at 120 kW. At this rating, their total normal rate of air flow would be $0.15 m^3 s^{-1}$, so that for this duty, the volumetric flowrate of air and oxygen to the burners would be approximately double that normally encountered.

At this flowrate, it was found that the air pressure drop was $2 kNm^{-2}$ and the flame length 0.6 m. The flame length, however, would obviously be shorter in the duty envisaged since the incoming air would have an oxygen content of 35% or greater.

The length of the combustion chamber was set at 1.7m to allow adequate mixing, and breadth and height at 0.9m was found to give adequate room for mounting the burners in the back plate.

The final arrangement is shown in Fig.2, which also shows the trunking (also lined as above) which conducts the product gas mixture to the model tuyere. It will be noted that there are three right angled bends in the movement of the gas mixture. This is partly from convenience and partly to ensure satisfactory mixing. The entire structure was fabricated from 6mm mild steel plates.

3.3. Design of Model Tuyere and Injection Lance

In practice, tuyeres are constructed from high-purity

copper and are water cooled. However, in the model no splashing by molten metal of slag would occur, and so the tuyere was constructed in a mild steel casing, lined down to the appropriate diameter with Morgan Super Armourcrete castable refractory using a circular former (see Fig.3a).

The injection lance (Fig.3b) follows previous practice[27] in having an adjustable clearance in the oil/steam mixing chamber. This allows a constant steam/oil ratio for varying oil flowrates, whilst maintining identical pressure at those varying flowrates. The result is that the shear forces occurring in expanding the steam result in a similar droplet size distribution in the oil.

3.4. Design of Slurry Mixing/Supply System

3.4.0. Slurry Parameters

(a) Composition and Viscosity

To supply a coal/oil slurry to the combustion chamber it must first be prepared.
Some initial work showed that the highest concentration of coal in oil which is feasible is about 50% by weight. The highest apparent viscosity likely to be encountered would only occur when the temperature of the slurry is likely to be lower than normal, i.e. less than 70°C. This viscosity was found to be about 10 poise. In normal running, a maximum of 40% coal would be used, resulting in an apparent viscosity of about 1-2 poise at 90°C.

(b) Flowrate

The maximum oil flowrate can be calculated from the oxygen content of the air subsequent to propane combustion:

The maximum oxygen loading (from 3.1.3) will be:

$336 \times 0.21 + 56.2 - 5 \times 5.6 = 101.46$ litres/sec.

The combustion of 1kg of heavy fuel oil requires $2.28 m^3$ of oxygen.

Thus, for the stoichiometric combustion of oil, the oil mass flowrate at maximum conditions should be 0.0445 $kg.s^{-1}$.

If the density of the oil is 950$kg.m^{-3}$, the maximum volumetric flowrate would be 0.0468 litres per second.

The specification of the pump is thus:

(a) Capable of pumping a 50% solid slurry, with 1mm anthracite as the largest most abrasive solid.

(b) Capable of pumping this composition of slurry at a viscosity of 10poise at a pressure of 650kNm^{-2} absolute, and a flowrate of at least 5 x 10^{-2} ℓs^{-1}.

A "Mono" type pump was obtained which could meet these criteria for the recirculating leg of system, and a metering gear pump for the accurate delivery of the required flowrate.

3.4.1. Construction of Mixing and Pumping Rig

Since continuous slurry mixing would be very difficult to carry out without sophisticated handling equipment, it was decided to produce the slurry on a batch basis; the capability of continuous pumping whilst a batch was being prepared was retained.

A final design of apparatus is shown in Fig.4. It consists of a three-tank system. Tank 1 is the tank in which the actual mixing of the components takes place, Tank 2 is the tank from which the pumping is done and Tank 3 is the purge tank, containing gas oil, with which the system is filled after every series of tests.

Tanks 1 and 3 are pivotable so as each to be able to pour into tank 2. This is accomplished by means of the overhead crane. All tanks are surrounded by steam jackets for heating purposes.

3.4.2. Operation of the System

(1) The steam supply to all tanks is turned on, and an appropriate volume of the fuel oil under test is passed to tank 1 through a nutating disc oil meter. The volume is corrected to mass, (the appropriate temperature and thus specific volume being known) and the mass of coal to be used is weighed out. The stirrer is started in the oil, and the coal is steadily added to the vortex until the entire quantity has been added.

(2) When the slurry has reached the appropriate temperature it is poured into Tank 2, and pumping commences. If a further batch is to be tested, preparation can commence without disturbing the first batch.

(3) When the system is shut down at the end of the day's work, gas oil is poured from the purge Tank 3 into tank 2 and the entire oil system is filled with gas oil prior to shut down.

3.5. Adaption of the Flame Tunnel

The flame tunnel is shown in Fig.5; the main dimensions are 0.914m diameter by 3.5m long. Sampling ports are distributed at 0.9m and thereafter at 0.457m intervals along its length. As stated previously the maximum thermal input is 2MW.

3.6. Design of Sampling Apparatus

3.6.0. Construction

Since the flame is to be subjected to gas and solids sampling an apparatus which would enable these measurements to be taken in a reproducible position in the X (axial) and Y (radial) axes is essential.

In addition, the capability of varying the position of the sampling points along both axes would allow the correction of positions with experience.

A rig was thus constructed which could sample at virtually any co-ordinate (given the availability of a sample port) along 2-metres of the length of the flame tunnel (X-axis) or across 60% of the width of the tunnel (Y-axis). Each axis of the sampling rig (Fig.6) consists

of a movable platform sitting on a sliding track propelled by the rotation of a threaded rod as with a lathe. The rod is rotated by a reversible, variable speed D.C. motor. Obviously, the platform, sliding track and motor of the Y-axis is carried upon the X-axis platform.

3.6.1. Operation

Positioning of the sampling probe is executed by cutting-off the current to the motor. Each platform has beneath it an arm which operates a series of single pole double throw microswitches which are positioned along the track at points which correspond to the co-ordinates at which samples are to be taken.

A logic chain is set up by means of the microswitches such that a pulse of current along a pair of wires will send the probe to its next position. This entails:

(a) A pulse is sent to the X-axis motor of the rig resulting in movement of the probe along the X-axis from the 'rest' position to the first sampling port in the side of the flame tunnel.

(b) A pulse is sent to the Y-axis motor which inserts the probe into the first port and as far as the first sampling position in the tunnel. Subsequent pulses to the Y axis motor send the probe to the remaining sampling points in the first port, after the readings taken at each point have stabilized.

(c) On reaching the last sampling point of the Y-axis, the pulse this time reverses the motor and returns it to the 'rest position'.

(d) When the Y-axis motor has reached the retracted rest position the X-axis motor is activated until the next position on the X-axis is reached. The sequence then returns to (b).

(e) When the final position on the X-axis has been reached, the motor is reversed until the "rest" position on the X-axis is reached. The rig is then ready to repeat the entire sequence.

The wiring circuitry is shown in Figure 7.

4. INSTRUMENTATION AND CONTROL HARDWARE

The overall layout of the measurement and control features is shown in Fig.8.

4.0. Instrumentation of Apparatus

4.0.0. Flow Control Section

The gases supplied to the combustion chamber (propane, oxygen and air) are monitored for volumetric flowrate, absolute pressure and temperature, so that a mass flow for each may be obtained and hence accurate calculations of final velocity made.

(a) Flow Measurement

From considerations of ease of operation the orifice plate has a great deal to commend it compared with the difficulties of construction involved in the use of nozzles or venturis. It was decided to use the orifice plate as the standard measuring device.

The Kent tables[96] were used in the sizing of the orifice plates The simplified flow formula used was:-

$$Q = C.K. \sqrt{\frac{H.P}{S.T}} \qquad \ldots\ldots\ldots(34)$$

where Q = Gas flow, $l.s^{-1}$
C = Orifice plate constant
K = Conversion Factor (S.I./Imperial)
H = Differential Pressure ($kN.m^{-2}$)
P = Absolute Pressure ($kN.m^{-2}$)
S = Specific Gravity (Air = 1)
T = Absolute Temperature (K)

Since the Kent tables used were in Imperial units the conversion factor K was calculated so that direct substitution of the S.I. values could be carried out. These tables were used in preference to the British Standards method for the reason that the pipe runs necessary for conformity with B.S. were simply unobtainable, and the inaccuracies caused by this and by measurement errors are likely to outweigh

the very small difference in the value of orifice plate constant which was noted between the two methods of calculation. A D/d ratio of less than 0.6 was aimed for. The results are shown in the table below.

Pipe runs of not less than 20 diameters upstream of the orifice plate and not less than 10 diameters downstream were settled on as the realistic lengths attainable.

Orifice Plate Constants

	Propane	Oxygen	Air
Differential Pressure Across Orifice Plate ($kN.m^{-2}$)	4.90	4.90	4.90
Maximum Flowrate ($\ell.s^{-1}$)	5.06	51.00	336.00
Absolute Pressure ($kN.m^{-2}$)	237.9	1330.5	125.8
Temperature (^{o}C)	0	15	45
Specific Gravity	1.5225	1.1073	1.0
Calculated Value of C	11.15	46.34	930.5
Nominal Pipe Bore, D, mm (inches)	50.8 (2.0)	50.8 (2.0)	203.2 (8.0)
Orifice Size d(mm)	10	21.0	90
Nominal Actual Value of C	11.38	50.9	950
Value of C Corrected for pipe bore variations and pressure tapping positions	11.38	50.88	948.9

(b) Instruments Used

With the orifice plates constants known, information must be supplied on the temperature and absolute pressure of the supply of the gases, as well as the differential pressure across the orifice plate itself.

(1) Temperature

In all cases of fluid flow, the temperature measurement of the fluids was achieved by the insertion of an iron-constantan thermocouple into the respective pipelines. Iron-constantan was used for reasons of high output voltage relative to temperature differential.

(2) Absolute Pressure

The pressure of the gas supplies was measured using C.E.L. Transducers, with outputs of 9-12mV for maximum range values.

The range values used were:

Propane 0-207 kN/m^2 (0-30psig)
Oxygen 0-1379kN/m^2 (0-200psig)
Air 0-69 kN/m^2 (0-10psig)

The air pressure obtaining at the time was then added to the above values to calculate the absolute pressures.

(3) Differential Pressure

The instruments used here were one Kent "Deltapi" differential pressure transducer, measuring a range span of 0-4.9kN/m^2, (0-500mm water gauge) across the orifice plates and giving a signal of 0-10ma, and three Furness Controls differential pressure transducers giving an output of 0-1V over the same range.

4.0.1. Model Tuyere Section

Ideally, the measurements at the tuyere should comprise: gas composition, temperature and velocity. Regretably, the latter is very difficult to accomplish at the conditions of temperature and velocity used. However, with accurate final temperature and pressure readings, together with the supply volume flowrate readings, an accuracy of at least 2.5% could reasonably be expected in a final calculated value of velocity. This

is as accurate as any method which could be devised for pitot or constriction-acceleration type of measurements.

(a) Composition of Gases Supplied to Tuyere

The composition of gases supplied to the tuyere is found from equation (28) in section 3.1.2:

Concentration of oxygen in gases

$$= \frac{V_2 + 0.21V_3 - 5V_1}{V_n}$$

$$\text{i.e. } PO_2 = \frac{V_2 + 0.21\,V_3 - 5V_1}{2V_1 + V_2 + V_3}$$

(b) Air Temperature at Tuyere

Measurement of temperature takes place in the later section of the trunking connecting the combustion chamber and the tuyere. A platinum/platinum-rhodium thermocouple was used.

It was originally intended to use a suction pyrometer to obtain this reading, but the use of a wall material which has a low thermal conductivity together with a low thermal capacity ensures that the surface which is viewed radiatively by the thermocouples is virtually at the same temperature as the thermocouples. This, together with the high velocity which provides high convective heat transfer to both walls and thermocouples, ensures that the readings are sufficiently accurate.

4.0.2. Slurry Mixing and Supply System

This can be split into two main sections. The measurement of the oil or slurry temperature and flowrate, and the measurement of the variables associated with the steam atomising agent.

(1) The slurry mass flowrate was measured and controlled by means of a metering pump. This pump is of the gear type, and its speed is infinitely variable

(between 0 and 1.7kg/min) by means of a Phase Frequency converter which controls the rotor speed. The Phase Frequency converter is controlled by a 0-5V signal from a Digital to Analog converter channel. Calibration was by "bucket and stop watch".

(2) Measurements on Atomising Steam

The current standard method of oil atomisation for tuyere oil injection as practiced in the British Steel Corporation is by forming an emulsion of 5-10% by weight of water, by condensing steam in the oil. However, the use of a back-atomising technique could require steam/oil ratios as high as 0.6, and so it was decided to size orifice plates and valves to this value.

For a maximum oil mass flowrate encountered of 4.44×10^{-2} Kgs^{-1}, the maximum steam flowrate, required would thus be $2.665 \times 10^{-2} Kgs^{-1}$. The steam was available at a pressure of 1300 $kN.m^{-2}$ and a temperature of $245^{o}C$.

For measurement of mass flow, an orifice plate was again used, the dimensions being calculated from the equation given in the "Kent" booklet[96]:

$$Q = C.K. \sqrt{H.W.} \quad \ldots\ldots\ldots (35)$$

Where

H = Pressure differential across orifice, mm water gauge

W = Density in g/cc, Q = flow in kg hr

from the tables the resultant orifice plate sizes are:

Orifice diameter = 17mm

Pipe diameter = 50.8mm

Corrected value of C = 66.7

4.0.3. Flame Tunnel Section

(a) Temperature

The flame tunnel itself is instrumented with twelve Platinum/Platinum Rhodium thermocouples,

which have their tips just protruding from the walls. Their function was to warn of overheating of the refractory brickwork, and for approximate calculation of radiation interchange with the flame.

(b) Gas Analysis

Samples were taken from the flame by a water cooled probe. The gas was filtered, cooled and dried and passed to a Hartmann and Braun rapid analyser bank, consisting of:

(i) A carbon monoxide analyser

(ii) A carbon dioxide analyser

(iii) A methane analyser

(iv) A hydrogen analyser

(v) An oxygen analyser

(i) to (iii) operate on the infra-red absorbtion principle, (iv) operates by thermal conductivity (v) operates on the paramagnetic principle.

The output signals were 0-10ma from minimum to maximum range.

4.1. Flow Control of Apparatus

The control valves which control gaseous volume flowrates to the apparatus were sized according to the formula given by manufacturers:

$$CV = \frac{20.76\ Q\ \sqrt{\ G}}{\sqrt{\ (P_1-P_2)(P_1+P_2)}}$$

where CV = Valve constant

Q = NTP flowrate (ls^{-1})

G = Specific gravity of gas (air = 1)

P_1 = Upstream pressure (kNm^{-2})

P_2 = Downstream pressure (kNm^{-2})

Gas	Flowrate (ls^{-1})	Upstream Pressure (kNm^{-2})	Downstream Pressure (kNm^{-2})	Calculated CV
Air	336	124	122.0	314.5
Oxygen	56.2	1330.5	122.0	0.927
Propane	5.06	238	122.0	0.634

The valve initially selected for controlling oil or slurries was a 19mm Saunders Diaphragm valve. However, this was unsuccessful and control was imposed by variation of pump rotor speed.

Since it was decided that the apparatus was to be automatically controlled (see Section 4.2) the valves are all operated by a pneumatic motor, actuated by air at a gauge pressure of $500kNm^{-2}$.

The signal required by the valves consists of an air supply of gauge pressure 20 to $100kN/m^{-2}$ (3-15psig). Since the control signals are, however, electrical, the signal is first passed to an electrical-to-pneumatic converter which gives an output pressure of 20 to $100kNm^{-2}$ proportionally from an original electrical signal of 0-10ma. All valves failed in the "closed" position.

4.2. Data Collection & Computer Hardware System

Since there are five flows to be controlled as a result of data collected from 18 inputs of temperature, pressure and differential pressure it was evident that manual control of the apparatus would be very difficult, with poor repeatability. Indeed, recording and display of the 12 control readings would be difficult let alone allow any meaningful readings on the flames themselves. It was therefore decided to take advantage of the recent advances in microelectronics and computing to collect, correlate and act upon the data to control the apparatus in a repeatable fashion.

If the conditions of temperature, velocity and oxygen content of the blast are to be controlled, together with the fuel/oxidant and fuel/atomising agent ratios, then it is only a small step to also automate the collection of gas samples.

This automation is made possible by the contruction of the sampling rig, referred to in 3.5 above. With this apparatus, the positioning of the gas sampling probe is closely repeatable.

Therefore, a modern microcomputer system was obtained which could be interfaced with the necessary inputs. Fig.9 shows the schematic complete system which consists of:

(a) An electromechanical multiplexer system which scans each input in turn, driven by a 16-channel relay unit. This had to be constructed:

Fig.10 shows the wiring diagram.

(b) An operational amplifier which amplifies the signals from 0-20mV to 0-5V.

(c) A proprietary 8-bit analog-to-digital converter, which converts the voltage inputs to the digital signal necessary for input to the microcomputer; it had 16 channels.

(d) The microcomputer itself, which consists of a Commodore "Pet" with 16K bytes of RAM, with the software contained in 16K of ROM. Visual display is by VDU, with a tractor printer interfaced to give "hard copy". A cassette tape deck acted as a mass-storage device.

(e) A proprietary digital-to-analog converter, which gives a steady dc output of 0 to 5V. This has eight output channels, the voltage output in each case being "latched", i.e. remaining steady when not being addressed by the computer. These outputs have a maximum output current of about 1ma which is inadequate to operate the electrical-to pneumatic converters which control valve opening.

(f) Five booster amplifiers which have a voltage gain of unity, but can supply a current of 100ma. These are placed in the line between the D-to-A and the E-to-P converters to supply the requisite current. Fig.11 shows the wiring diagram of two channels of the amplifier.

4.3. Physical Layout of the Apparatus

Fig.12 is the overall layout of the system showing the relative position of each piece of apparatus mentioned.

5. MEASUREMENT & CONTROL SOFTWARE

5.0. Derivation of Atomising Steam Mass Flow and Pressure Control Subroutine

5.0.0. Sequence of Events

As stated in section 3.3., itwas essential to maintain both the steam/oil mass ratio and the atomiser steam supply pressure constant. With a variable oil mass flowrate the steam flowrate and hence the supply pressure must alter.

Both the control valve position and the atomiser clearance must alter to maintain both the mass flowrate and pressure criteria. The following routine was thus developed:

a) The computer scans the relevant channels (see 5.3.7.) and interprets the data into steam mass flowrate (see 5.2.2.). The pressure at the atomiser is entered through the keyboard.

b) The computer calculates an intermediate figure of pressure, and displays it on the screen. The atomiser is then adjusted to this pressure. The computer then scans and calculates mass flow again, and moves the control valve so that the correct steam mass flow and, by implication,the correct steam pressure result.

c) The computer then scans, interprets and alters the control valve until the mass flow is correct. If the pressure is now incorrect the process is repeated from (a).

5.0.1. Calculation of Intermediate Pressure

If M and P are mass flows and absolute pressures, and subscripts o, r, s, a and i refer to initial, required, supply,atmospheric and intermediate respectively, and K and A are the flow constants for the control valves and atomiser respectively then initially:

$$M_o = K_o\sqrt{(P_s^2 - P_o^2)} \qquad .....(36)$$

and

$$M_o = A_o\sqrt{(P_o^2 - P_a^2)} \qquad .....(37)$$

After adjustment of the atomiser until the intermediate pressure is reached, the following would obtain:

$$M_i = K_o\sqrt{(P_s^2 - P_i^2)} \qquad \ldots\ldots(38)$$

and: $$M_i = A_r\sqrt{(P_i^2 - P_a^2)} \qquad \ldots\ldots(39)$$

After computer adjustment of the control valve, the following should obtain, assuming no inaccuracy:

$$M_r = K_r\sqrt{(P_s^2 - P_r^2)} \qquad \ldots\ldots(40)$$

and: $$M_r = A_R\sqrt{(P_r^2 - P_a^2)} \qquad \ldots\ldots(41)$$

now from (36):

$$M_o^2 = K_o^2(P_s^2 - P_s^2) \qquad \ldots\ldots(42)$$

and from (41)

$$M_r^2 = A_r^2(P_r^2 - P_a^2) \qquad \ldots\ldots(43)$$

dividing (43) by (42) and rearranging, the expression

$$\frac{K_o^2}{A_r^2} = \frac{M_o^2(P_r^2 - P_a^2)}{M_r^2(P_s^2 - P_o^2)} \quad \text{is obtained.} \qquad \ldots\ldots(44)$$

It can be seen that all values on the RHS of (44) are known

$$\text{Let} \quad F = \frac{K_o^2}{A_r^2} \qquad \ldots\ldots(45)$$

Equating (38) and (39) and squaring:

$$K_o^2\,(P_s^2 - P_i^2) = A_r^2\,(P_i^2 - P_a^2)$$

$$\therefore \quad \frac{K_o^2}{A_r^2} = \frac{(P_i^2 - P_a^2)}{(P_s^2 - P_i^2)} \quad \text{i.e. from (45)} \quad F = \frac{(P_i^2 - P_a^2)}{(P_s^2 - P_i^2)} \qquad ..(46)$$

Making P_i the subject of equation 46,

$$P_i = \sqrt{[(F.P_s^2 + P_a^2)/(1 + F)]} \qquad \ldots\ldots(47)$$

Since F is known from equations (45) and (44) all the RHS of equation (47) is known, and thus the intermediate pressure, which must be achieved by adjustment to the atomiser, can be calculated.

5.1. Derivation of the Volumetric Flow Proportional Control Subroutines

(a) Calculation of approximate volumetric flow requirements.

From 3.2.3., the NTP "air" volume flowrate required for the model tuyere is:

$$V_n = \frac{273}{T} \cdot C \cdot \frac{D^2}{1000} \cdot \frac{\pi}{4} \qquad \text{.....(33)}$$

From any particular values of PO_2, C and D will be constant.

Collecting the constants, then:

$$K = 273 \cdot \frac{D^2}{1000} \cdot \frac{\pi}{4}$$

$$\therefore V_n = \frac{C.K.}{T} \qquad \text{.....(48)}$$

(i) The propane volume flowrate may be found from an energy balance:

$$S.V_1 = V_n.(T-To).Cp.$$

$$\therefore V_1 = \frac{C.K.}{T}.(T-T_o).\frac{Cp}{S} \qquad \text{.....(49)}$$

(ii) The volumetric flow requirement of oxygen and air can be found from a concentration balance and a volumetric balance:

(a) Oxygen balance:

from 3.2.3.,

$$V_2 = \frac{(Po - 0.21).Vn + 5.42V_1}{0.79} \qquad \text{...(29)}$$

$$\therefore V_2 = \frac{(Po - 0.21)\ C.K.T^{-1} + 5.42V_1}{0.79} \qquad (50)$$

(b) Volumetric Balance

$$V_3 = V_n - 2V_1 - V_2 \qquad \text{.....(31/32)}$$

$$V_3 = \frac{C.K}{T} - V_2 - 2V_1 \qquad \text{.....(51)}$$

In the start-up or resetting routines, therefore, the above flow equations are used.

Due to radiation and convection losses from the apparatus, the imperfect linearity of control valve response and the inaccuracies inherent in orifice plate systems, these flow values, even as set, will be incorrect.

Proportional control will therefore be necessary to "fine-tune" the system, and continuously correct it as the experiments proceed and conditions gradually alter. (Propane tank temperature, oxygen supply pressure variations etc).

Proportional Control Subroutine

Overall, from equation 49, 50 and 51 above, it may be seen that the three necessary volume flowrates are functions of velocity, temperature and oxygen concentration required:

i.e. $V_r = f(C,T,Po)$

Then the general corrections to the volumetric flowrates δV_r, would be:

$$\delta V_r \simeq \delta C.\frac{\partial V_r}{\partial C} + \delta T.\frac{\partial V_r}{\partial T} + \delta Po.\frac{\partial V_r}{\partial Po}$$

where δ variable = discrepancy between measured value and required value of variable

(i) The corrective increment for the propane flow would thus be:

$$\delta V_1 \simeq \delta C.\frac{\partial V_1}{\partial C} + \delta T.\frac{\partial V_1}{\partial T} + \delta Po.\frac{\partial V_1}{\partial Po}$$

partial differentiation of equation (49) gives:

$$\frac{\partial V_1}{\partial C} = \frac{K.Cp}{S}.\left(1 - \frac{T_o}{T}\right) \qquad .....(52)$$

$$\frac{\partial V_1}{\partial T} = \frac{K.C.Cp.To}{S.\ T^2} \qquad .....(53)$$

$$\frac{\partial V_1}{\partial Po} = 0 \qquad .....(54)$$

(ii) For the oxygen flow, the corrective increment to be applied would be:

$$\delta V_2 \simeq \delta C.\frac{\partial V_2}{\partial C} + \delta T.\frac{\partial V_2}{\partial T} + \delta Po.\frac{\partial V_2}{\partial Po}$$

which, by partial differentiation of equation (50) gives:

$$\frac{\partial V_2}{\partial C} = \frac{K}{0.79T}(Po - 0.21) + 6.8608.\frac{\partial V_1}{\partial C} \quad .....(55)$$

$$\frac{\partial V_2}{\partial T} = \frac{C.K.}{0.79T^2}(Po-0.21) + 6.8608.\frac{\partial V_1}{\partial T} \quad .....(56)$$

$$\frac{\partial V_2}{\partial Po} = \frac{C.K.}{0.79T} + 6.8608.\frac{\partial V_1}{\partial Po}$$

but $\frac{\partial V_1}{\partial Po} = 0,$

$$\therefore \frac{\partial V_2}{\partial Po} = \frac{C.K.}{0.79T} \quad .....(57)$$

(iii) For the air flow, the corrective incremental flow would be:

$$\delta V_3 \simeq \delta C.\frac{\partial V_3}{\partial C} + \delta T.\frac{\partial V_3}{\partial T} + \delta O.\frac{\partial V_3}{\partial O}$$

which, by partial differentiation of equation (51) gives:

$$\frac{\partial V_3}{\partial C} = \frac{K}{T} - \frac{\partial V_2}{\partial C} - \frac{2\partial V_1}{\partial C} \quad .....(58)$$

$$\frac{\partial V_3}{\partial T} = -\frac{C.K.}{T^2} - \frac{\partial V_2}{\partial T} - \frac{2\partial V_1}{\partial T} \quad .....(59)$$

$$\frac{\partial V_3}{\partial Po} = 0 - \frac{\partial V_2}{\partial Po} - \frac{2\partial V_1}{\partial Po}$$

but $\frac{\partial V_1}{\partial Po} = 0,$

$$\therefore \quad \frac{\partial V_3}{\partial Po} = -\frac{\partial V_2}{\partial Po} \qquad \text{.....(60)}$$

Equations 52 to 60 inclusive were then incorporated in a computer test programme to verify the efficency of the equations. The programme operates as follows:

A set of values for velocity, temperature and oxygen concentration are entered to represent the required values, and another set of values are entered to simulate the values which would in practice, be measured during a data collection scan. This second set of values is substituted in equation 49 to 51 to obtain "actual" volumetric flowrates.

If the two sets of values are within pre-determined limits (velocity $<3ms^{-1}$, temperature $<5^{o}C$, oxygen concentration pre-determined $<0.01\%$) the control algorithm is bypassed. If it is not, then the appropriate differences are multiplied by the appropriate differential coefficients and the three incremental volume changes are calculated. The new "actual" volumetric flowrates are thus altered to $V_{new} = V_{old} + \delta V_{new}$.

From the new volumes the new expected temperature, velocity and oxygen concentration are calculated, and are again examined to see whether they are within the limits. If they are not the process is repeated. If they are, the programme prints out the new results for temperature, velocity and oxygen concentration, together with the number of passes through the programme which were necessary to achieve the required values to within the tolerance limits.

The programme was found to correct all parameters to within 2.5% tolerance limits in two passes even when all the maximum step

changes likely to be encountered (250°C in temperature, 40m/s in velocity, and 5% in oxygen concentration) were made simultaneously.

However, it was clear that the precision of the data collection and control hardware (particularly the control valves themselves) was not as high as the corrective algorithms within the programme, and so, for a step change at least, the first pass of the corrective algorithm was to be followed by a time lag to allow near steady state conditions to settle in.

To make sure that no false readings were acted upon, the control algorithm did not execute until a delay has elapsed such that the transducers with slowest response (the sheathed thermocouples in the blast air supply system) will have reached 98% of the new steady-state value. This time lag was calculated from the usual exponential thermocouple response.

5.2. Development of Data Interpretation Subroutine

5.2.0. Temperature Measurements

There are two types of thermocouple on the apparatus, platinum/rhodium and iron/constantan. The response from these, as with all thermocouples, is of the form:

$$E = a + bT + cT^2$$

where E is the EMF output and T is the temperature differential between that measured and the ambient.

Data was obtained from temperature/EMF tables to establish values for a and b, assuming a second order polynominal i.e. quadratic.

This was carried out for the ranges 0-200°C and 200-400°C for the Fe/Constantan thermocouples, and for the ranges 0 - 300°C, 300-600°C, 600-900°C, 900-1200°C, 1200-1500°C - for the Pt/PtPh thermocouples.

Cold junction compensation was carried out by calculating the relevant EMF for the ambient temperature and adding to

it the measured EMF. This EMF is then sent to the appropriate range and then used in the above equation to determine the actual temperature.

5.2.1. Pressure Measurements

Both differential and absolute pressure transducers give a linear voltage output with increasing pressure.

This pressure is given by:

$$P = (R - R_o).\ K$$

where P is the pressure, R is the reading at P, R_o is the reading at zero (or atmospheric) pressure, and K_t is the transducer constant.

5.2.2. Flowrates

The appropriate temperatures pressures and differential pressures obtained in 5.2.0 and 5.2.1. are used in equations (34) and (35) to obtain the relevant flowrates in N.T.P. terms of the various gases and steam.

5.2.3. Gas Analyses

Each gas analyser has the response:

$$A = (R - R_o)K_a$$

where A is the gas analysis at reading R, and R_o is the reading with pure nitrogen. K_a is the analyser constant, found from using a span gas.

5.3. Flowcharts of Apparatus Measurement and Control Programme

5.3.0. Flowchart of Main Programme

The operations below are shown in Fig.13.

Operation	Description
A	Start-up routine (see 5.3.1.)
B	Keyboard entry of conditions of blast temperature, velocity etc.
C	Measurement and control routine (see 5.3.2.).
D	Send correct level signal to phase frequency converter for required oil flow.
E	Routine to correct steam pressure and mass flowrate (see 5.0.).
F	Is the analyser to be calibrated?
G	Analyser calibration routine (see 5.3.3.).
H	Check conditions of flame tunnel temperature using scanning routine (see 5.3.5.) and data interpretation routine (see 5.2.).
I	Is wall temperature high enough?
J	Has one minute elapsed since H?
K	Is the probe at the x-axis rest position?
L	Send signal to move probe to next x-axis position.
M	Is the probe moving to the first x-axis position?
N	As C.
O	Has the probe arrived at the next x-axis position?
P	Send signal to move probe to next y-axis position.

Operation	Description
Q	Has probe arrived at next y-axis position?
R	Carry out gas analyses routine (see 5.3.4.).
S	Is probe at last y-axis position?
T	Send signal to reverse y-axis.
U	Print out results for all analyses at that x position.
V	Is y-axis at rest position?
W	Is probe at last x-axis position?
X	Send signal to reverse x-axis.

5.3.1. First Level Subroutine for Start-up

The operations below are shown in Fig.14.

Operation	Description
A	Entry to Routine from GOSUB statement in Main Programme.
B	Read in constants and dimension all arrays and subscripted variables.
C	Keyboard input of ambient temperature and pressure.
D	Scan all multiplexer channels (see 5.3.5.).
E	Assign zero value to op amp from short-circuit voltage reading.
F	Assign zero values to all transducers.
G	Display "start recirculating pump and Phase Frequency converter".
H	Keyboard input to verify G.
I	Send maximum signal to fuel valve.
J	Keyboard input of weight of receiver.
K	Let N = N + 1
L	Send signal level L (N) to Phase Frequency Converter.
M	Has T(N) seconds passed since step L?
N	Send zero signal level to Phase Frequency Converter.
O	Keyboard input of new weight of receiver.
P	Calculate mass of fuel passed.
Q	Is N = 4?
R	Calculate signal/mass flowrate characteristics of Phase Frequency Converter.

Operation	Description
S	Send predetermined signal levels to air, oxygen, propane and steam valves.
T	Display instructions to start fans and open supply valves.
U	Keyboard input to verify T.
V	Display instructions to light air preheater using spark and manual valve.
W	Keyboard input to verify light-up.
X	Return to main programme to statement after GOSUB.

5.3.2. First Level Subroutine for Measurement of Variables and Valve Control

The operations below are shown in Fig.15.

Operation	Description
A	Entry to subroutine form GOSUB statement in main programme.
B	Scan all channels (see 5.3.5.).
C	Interpret data (see 5.2.).
D	Calculate errors between actual values and required values of temperature, velocity etc.
E	Are all errors within acceptable limits?
F	Return to programme to statement after GOSUB.
G	Calculate increments in flows required to correct temp. velocity etc. (see 5.1.).
H	Calculate signal increment required and send new signals to the control valves (see 5.3.6.).
I	Has 30 seconds elapsed since executing H?
J	As B.
K	As C.
L	Calculate errors between flows required and flows measured.
M	Are the flow errors acceptable?

5.3.3. First Level Subroutine for Calibration of Gas Analyser

The operations below are shown in Fig.16.

Operation	Description
A	Entry to subroutine from GOSUB statement in Main Programme.
B	Display "Turn on zero gas to analyser".
C	Keyboard entry to confirm instruction B.
D	Has delay of one minute occurred since keyboard entry?
E	Let N = 29
F	Let N = N+1
G	Read channel N (see 5.3.7.).
H	Is N = 35?
I	Let analyser zeros = readings obtained.
J	Let N = 29
K	Let N = N+1
L	Display "Turn on span gas N".
M	Keyboard entry to confirm instruction L.
N	Has one minute elapsed since keyboard instruction?
O	As G
P	Let voltage (reading - zero) = span.
Q	Calculate % gas per unit voltage.
R	Display "Turn off gas N".
S	Keyboard entry to confirm instruction R.
T	Is N = 35?
U	Has 30 seconds elapsed since keyboard entry S?
V	Return to main programme to statement after GOSUB.

5.3.4. First Level Subroutine for sample gas analysis

The operations below refer to Fig.17.

Operation	Description
A	Entry to subroutine from main program.
B	Has 30 seconds elapsed since A?
C	Let M = M+1
D	Let N = 29
E	Let N = N+1
F	SCAN CHANNEL N (see 5.3.7.) then put R(M,N) = Reading.
G	Is N = 35?
H	Is M = 2?
I	Let N = 29
J	Let N = N+1
K	IS R(2,N) within 2% of R(1,N)?
L	Let M = 0
M	Is N = 35?
N	Calculate gas analyses from R(2,N)
O	Return to main program to statement after GOSUB.

5.3.5. Second Level Subroutine for Scanning all Channels on Multiplexer

The operations below refer to Fig.18.

Operation	Description
A	From GOSUB in main program or higher subroutine.
B	Let M = 7
C	Let M = M+1
D	Close relay M
E	Let N = 1
F	Let N = N+1
G	Close relay N
H	GO TO ADC sampling routine on ADC channel 0 (see 5.3.8.)
I	Calculate millivoltage on multiplexer channel.
J	Open relay N
K	Is N = 7?
L	Open relay M
M	Is M = 12?
N	Return to statement after GOSUB in main programme or higher level subroutine.

5.3.6. Second Level Subroutine for Control Valve Actuation

The operations below refer to Fig.19.

Operation	Description
A	From GOSUB statement in high routine.
B	Calculate voltage increment for steam and oxygen.
C	Is Propane flow less than $3.451.s^{-1}$?
D	Assign propane value constant
E	IS Propane flow less than $3.01.s^{-1}$?
F	As D
G	As D
H	Let M = 0
I	Let M = M+1
J	Let Air flow = Air flow + 0.5 x valve correction.
K	Is air flow less than $0.228m^3.s^{-1}$?
L	Assign air valve constant K(M)
M	Is air flow less than $0.19m^3.s^{-1}$?
N	As L
O	Is air flow less than $0.15m^3.s^{-1}$?
P	As L
Q	As L
R	Is M = 3?
S	Let K air value = (K(1)+4K(2)+K(3))/6 : Let N = 0
T	N = N+1
U	Let signal (N) = old signal (N) + valve constant x volume flow change
V	Turn signal (N) to nearest integer value, and send to channel N on DAC.
W	Is N = 5?
X	Return to higher routine.

5.3.7. Third Level Subroutine for Scanning Single Multiplexer Channel

The operations below refer to Figure 20.

Operation	Description
A	From GOSUB in higher level routine.
B	Calculate the number of the two relays to be activated for the relevant multiplexer channel number.
C	Close 1st relay
D	Has 0.05 seconds elapsed since C?
E	Close 2nd relay.
F	AS D
G	GO TO ADC sampling routine on ADC channel 0 (see 5.3.8.).
H	Calculate millivoltage on multiplexer channel.
I	Open 2nd relay.
J	Open 1st relay.
K	Return to higher routine.

5.3.8. Fourth Level Subroutine for Scanning Analog-to-Digital Converter

The operations below refer to Figure 21.

Operation	Description
A	From GOSUB statement in higher routine.
B	Has 0.05 seconds elapsed since entering routine?
C	Open ADC channel required.
D	Let PD = 0: N = 0
E	Let N = N + 1
F	Dummy statements to achieve correct reading rate.
G	Get integer value from ADC representative of voltage.
H	Let PD = PD + integer value.
I	Is N + 12?
J	Close ADC channel.
K	Let PD = (PD/12) x (5/255) volts.
L	Return to higher routine.

6. DISCUSSION OF RESULTS

6.0. Commissioning and Modification of Apparatus

6.0.0. Measurement Systems

6.0.0.0. Instrumentation

Initially, reliable operation of the multiplexer, operational amplifier and ADC were established. Since the Analog to Digital Converter (ADC) did not recognise negative signals, it was found that it was necessary to run the operational amplifier at positive offset so that marginally negative signals could be accommodated.

6.0.0.1. Differential Pressure Transducers

Each transducer was subjected to the following procedure:

(a) The zero was adjusted until the output of the transducer amplifier was approximately zero, that is, until the output from the operational amplifier was approximately the same as that offset resulting from a short circuit across the input of the operational amplifier.

(b) A differential pressure of 500 mm water gauge was applied to the transducer and the span adjustment of the transducer amplifier was adjusted to give an output just within the maximum measured by the ADC.

(c) The applied pressure to the transducer was varied in four steps from 0 to 500 mm water gauge, and the results graphed. A

linear factor was thus obtained in terms of mm water gauge per mv measured at the operational amplifier input.

6.0.0.2. Absolute Pressure Transducers

The transducers are in the form of a Wheatstone bridge, which imbalances with applied pressure. The output from these transducers were determined at the factory, in terms of mv output per applied bridge volt at the nominal maximum pressure, the output relationship being linear. Thus it should only be necessary to know the zero error of each transducer, and the applied bridge voltage. This latter value was set accurately at 10.0 volts on the power supply (which supplies all the absolute pressure transducers) using a digital voltmeter.

In practice it was found that transducers had to be calibrated against calibrated pressure gauges.

6.0.0.3. System Initialisation

Since there are four differential and four absolute pressure transducers,each with their own zero error, it was found to be too time consuming to zero each one. Therefore, at the commencement of the day's work, all supply valves were shut and all control valves were opened, thus applying atmospheric pressure to every transducer. The outputs were then scanned and these values stored as offset voltages to be deducted from subsequent readings.

6.0.1. Control Systems

6.0.1.0. Linear Trim Control Valves

These comprise the valves controlling the flow of oxygen, propane and steam to the rig. They are so constructed that at the design values of input and output pressures the flow of fluid through them will be directly proportional to degree of opening.

The procedure was as follows:

(a) The zero of each electrical to pneumatic converter was adjusted until the valve in question was at the point of opening at zero electrical signal. The internal resistance of the E to P converters was determined to be approximately 500Ω. Thus a signal of 0-5 v applied to these machines results in the 0-10 ma necessary for a 3-15 psig signal air output to the valves. The throughput of fluid was measured at 0-5 volts in 1 volt increments and the valve characteristics were graphed in terms of volts applied per m^3 per second of flow.

The maximum flows required were determined by running at the various system maxima and a value of ballast resistor was calculated which, when put in series with the E to P transducer resulted in a flowrate 20% over the maximum requirement at an applied voltage of 5 volts. The overall valve characteristics were then re-evaluated and a final figure of voltage per unit flow was obtained to be placed in the control programme.

6.0.1.1. Butterfly Valve

The procedure outlined in 6.0.1.0. above was adhered to, except that the throughputs were measured at applied voltage 0 to 5 volts in 0.5 volt increments because of the marked non-linearity of this type of valve. The necessary ballast resistors were added and the valve characteristics re-evaluated at 0.25 volt increments. The characteristic was then divided into five linear sections the limits of each being determined by the flowrate and this was found to give adequate accuracy.

6.0.1.2. Slurry Pump Control

The failure to control the slurry flow by means of a control valve resulted in motor speed control by means of a phase frequency converter. This machine is controlled by either a 4-20 ma or a 0-10 v signal. It was found that the 0-5v output from the digital to analogue converter resulted in a slurry flow of 0-1.7 kg per minute, which was ideal for the apparatus requirements. However, whilst the reproducibility of results was excellent as could be measured by the existing scales, the characteristic of the machine was not linear.

However, the division of the applied voltage against slurry output characteristic into four linear sections provided a slurry output which was predictable to within 1%. This calibration is carried out at the start of each day's work.

6.0.2.0. Initial Running

The levels of air and propane valve opening for reliable ignition in the combustion chamber were

found by trial and error, and then built in to the control programme.

The delays between valve adjustment and the steadying out of the subsequent transducer reading variations were determined and built into the control subroutines.

Similarly, the delay between these alterations and response of the air preheat measurement thermocouple was determined and again built into the relevant subroutine.

6.0.2.1. Modifications after Initial Running

After some time of running at flame tunnel wall temperatures of greater than 1500°C it was found that the automatic sampling rig would not insert the probes at the appropriate sampling ports. This was found to be due to expansion of the steel shells. As a result it was decided to pass air between the steel shells (see Fig. 5) using an available fan.

During these high temperature runs it was found that the model tuyere refractory had melted. This was because of the oxidation of the steel surrounding the refractory which protruded slightly into the furnace. The resultant iron oxides formed a low temperature melting eutectic with the highly refractory cement used for tuyere construction, which then melted.

The solution in this case was to cool the protruding steelwork by a coil of copper 6 mm O.D. tube carrying cooling water.

6.0.2.2. Modifications after Initial Results

It was rapidly established during these runs that considerable gas recirculation took place. This was theoretically predicted in equation (2) by Ricou and Spalding [54].

The decision was made to constrain the jet by relining the flame tunnel such that the combustion space so formed followed the outlines of the theoretical jet boundary shown in Fig. 5.

This reline was implemented by constructing a wooden conical former, inserting it in the flame tunnel and ramming the surrounding space with mouldable high-alumina refractory.

The result was that no back-flow nor any anomalous flow patterns could be detected.

6.0.2.3. Modifications to Sampling System

As a result of the new tunnel lining the velocity profile occurring across the combustion space (see Section 6.1.1.following) deviated considerably from the Gaussian form to be expected from the normal recirculatory flow pattern. As a result, the original radial sampling positions chosen were incorrectly positioned to representative samples of the gases.

It became obvious that more radial sampling points than the original five were necessary, because of the considerable change in cross-sectional distance occurring at each successive axial sampling port.

Some "runs" were carried out with the new lining to ascertain where the steepest concentration gradients were. These were found to be in the first port, between approximately 100 mm and 150 mm from the axis. Three sampling points were set aside to monitor this gradient, and another four were disposed such that one was positioned at the periphery of the combustion space in each of the first, second, third and fourth ports (the combustion space radius at the fifth port is nearly the same as the fourth).

A further position was retained at the flame axis.

However, it was clear that the radial sampling positions which barely penetrate the later ports were unusable in the first port. Further, the concentration of radial sampling positions occurring near the axis of the tunnel (necessary for accuracy in port 1) sampled only unrepresentatively small portions of the total gas flow along the combustion space.

It was thus decided that sampling should actually take place at only five of the eight radial sampling points, the points selected varying along the tunnel. Originally, the distribution was in order of sampling: 216 mm, 162 mm, 0 mm, 54 mm and 108 mm from the axis, and it can be seen that there were two sampling positions on either side of the combustion space axis. However, this desirable feature had to be abandoned in the interests of collecting more representative samples, since the hardware configuration could not be readily adapted nor could too much insertion length of probes be tolerated. The positions are, in order of sampling:

Radial Position No.	Distance from axis	Axial ports using the position
1	390 mm	4, 5
2	310 mm	3, 4, 5
3	230 mm	2, 3, 4, 5
4	190 mm	1, 2, 3
5	162 mm	1, 2, 4, 5
6	135 mm	1, 3
7	0 mm	All
8	108 mm	1, 2

These radial positions were arrived at after the consideration of the proportion of the area of the combustion space which was represented by the annulus whose edges are two selected radial sampling positions. The results of these calculations are shown in Appendix 1. The positions were chosen such that the areas were split into as near to four equal areas as possible. The selection also retained a sampling position as near the wall as possible so that unsampled area was minimised, and retaining somewhat closer grouping at the points of steeper concentration gradient.

For the runs with heavy fuel oil only, position 3 was 270 mm, 2 was 350 mm and 1 was 430 mm from the flame axis, so as to fulfill the objective of minimising unsampled area. However, it was found after analysing the results of oil-only firing that cooling air was leaking into the flame tunnel around the edges of the sampling port tube. The large expansion and contraction of the lining upon

cyclical heating and cooling made permanent repairs impossible, and so it was decided to move Nos. 1, 2 and 3 sampling positions 40mm further into the flame tunnel to minimise the effects of this inleakage, resulting in the final sampling positions shown above. The programme on heavy fuel oil was then to be repeated.

6.0.2.4. Modifications Caused by Mechanical Wear

It was found that, after only 3-4 hours of running on coal-oil slurries, that the results showed that the fuel-oxidant mixture was too lean. By a process of elimination, the fault was traced to the gear metering pumps suffering excessive wear.

It was found that, in contrast to when new, the output of the pumps at fixed speeds varied with back-pressure.

These pumps were therefore calibrated as outlined in 6.0.1.2. but were calibrated at three back-pressures. A back-pressure feedback facility was then inserted into the subroutine which calculated the pump speed, and reasonable accuracy was partially restored.

It was found that full restoration of accuracy required checking of the calibration of slurry flow between runs with recalibration of the pump taking place where necessary.

Even with the above measures, it was found necessary to increase the range on the Phase Frequency computer from 0-50 Hz to 0-100 Hz. When this limit was reached it was necessary to replace the gears to achieve the desired flowrate.

The replacement gears were made in the Welsh Laboratory workshop, and were constructed as spur gears (instead of the original helical) and were case-hardened after grinding. These gears showed an improvement in that some 4-5 hours running could be obtained from them.

Since appreciable wear took place during runs it was decided that the results obtained were too inaccurate. The results obtained to date (some 31 runs) were discarded.

The final solution to the problem was to use an over-capacity peristaltic pump, geared down to give the requisite flowrates. An air reservoir was added downstream of the pump together with a length of copper tube downstream of the reservoir. This combination reduced the fluctuations of output associated with this type of pump. The work programme was then restarted.

6.0.2.5. Procedural Alterations Caused by Adoption of Peristaltic Pumping

It was found that the peristaltic pump gave a flowrate accuracy of only approximately ±5% on the basis of pre-calibration. However, it was found that, whatever volume flowrate was being passed, this flowrate did remain constant.

The cause of this variation was found to be temporary stalling of the drive motor when run at the low speed necessary because of the pump's overcapacity. This stalling was particularly prevalent on slurries of coal No. 4, presumably due to higher viscosity due to smaller coal particle size

giving higher back pressure. This temporary stalling occurred when the shoe of the pump remade contact with the hose. Unfortunately, it was impossible to eliminate this fault because of the inherently low torque available from the phase frequency converter at the lower frequencies.

The result of this was that after conditions had "settled down" at the commencement of a new run, the flowrates resulting at the lower flow requirements were too low.

6.1. Form and Treatment of Data from the Apparatus

6.1.0. Readings Taken

Ideally, readings of flame tunnel gas velocity, gas temperature particulate loading of the gas and analysis of the gas should be taken.

However, the actual programme fell a long way short of this ideal, because of the non-availability of suitable equipment and the non-availability of funding to develop such equipment.

The primary problem was to obtain velocity measuring equipment to withstand the high temperature and high particulate loading of the gas. The secondary problem was that the manufacturers of venturi pyrometer would give no guarantees of the accuracy of their instruments at the encountered conditions of particulate loadings, temperatures and velocities at right angles to the instrument axis.

The utility of particulate sampling as a technique is limited without the gas velocity (corrected for density

and hence temperature) being known,as non-isokinetic sampling results in unrepresentative particulate loading of the sampled gas.

Attempts were made to obtain particulates with a view to analysis by ash tracer techniques. However, as shown in Fig.22, the "Land" type sampling probe was unequal to the task at the high temperatures obtaining.

This was not surprising as the design maximum gas temperatures for this is 2000°C.

The final result was that the only really reliable readings which can be taken on the flames is that of gas analysis.

6.1.1. Treatment of the Gas Analysis Readings in The Control Programme

6.1.1.0. Gas Composition Corrections

(a) Hydrogen analysis

The hydrogen present in the gas was analysed by means of thermal conductivity. Any gas having a significantly different conductivity from carrier nitrogen will thus affect the reading, and account must be taken of this in evaluating the level of hydrogen present.

The relative conductivities of the relevant gases are:

Nitrogen = 1.0, oxygen = 1.03, carbon monoxide = 0.98, carbon dioxide = 0.687, methane = 1.515, hydrogen = 7.424.

Since the meter reading is zero on pure nitrogen, then the offset incurred for any of the above gases when pure is equal to: relative conductivity -1.

The carbon dioxide deviation is so large that there is a corrective signal fed from the carbon dioxide meter. It should only be necessary to compensate for the remaining gases, but, in practice, it was found that the corrective signal was not entirely accurate, and software compensation had to be introduced.

Assuming that the chemical symbols represent readings of percentage by volume of that species in the gas sampled, and that the meters are reading accurately, then:

$$6.424\ H_2 = 6.424 \times \text{true}\ \%H_2 + 0.03\ O_2 - 0.02\ CO + 0.515\ CH_4$$

$$\therefore \text{true}\ \%\ H_2 = H_2 - 0.0047\ O_2 + 0.0031\ CO - 0.08\ CH_4 + K.CO_2 \quad ...(64)$$

where K is the correction factor for CO_2.

(b) Correction of gas analysis readings to mathematical model form

The output from the mathematical model is in terms of dry gas analysis, but all methane, carbon monoxide and hydrogen are presumed to have been fully combusted to carbon dioxide and water vapour (which is chilled out). The readings of gas sampled must thus be corrected to this form for comparability with the model. Notional combustion is thus carried out on the readings as follows:

O_c = oxygen consumed = 0.5 CO + 0.5 H_2 + 2 CH_4 ..... (65)

N_2 = nitrogen present = 100 - O_2 - CO_2 - H_2 - CO - CH_4 .... (66)

Ce = CO_2 liberated = CO + CH_4 .....(67)

The corrected carbon dioxide percentage, taking into account carbon dioxide liberated and oxygen and hydrogen consumed, is given by:

$$\text{corrected \% } CO_2 = \frac{CO_2 + Ce}{CO_2 + Ce + N_2 + O_2 - O_c} \times 100 \quad \ldots\ldots(68)$$

and the corrected oxygen percentage will be:

$$\text{corrected \% } O_2 = \frac{O_2 - O_c}{CO_2 + Ce + N_2 + O_2 - O_c} \times 100 \quad \ldots\ldots(69)$$

The equations (65) to (69) assume that the hydrogen percentage has been corrected as in equation (64).

6.1.1.1. Gas Velocity and Geometric Corrections

The results obtained from the mathematical model are for single points along the flame, since the model is one-dimensional. However, real flames exhibit radial velocity concentration and temperature gradients. To produce a mean value for any parameter at a given axial distance, it is therefore necessary to take readings at several radial sampling positions at that axial distance, and then produce a velocity weighted mean from these readings.

The velocity profile [46] followed by a free submerged jet is of the Gaussian form:

$$C = C_{max} \cdot \exp\left[-k \left\{\frac{y}{x}\right\}^2\right]$$

where: C is velocity at radial distance y from the axis and axial distance x along the axis

k is a constant

However, this does not necessarily occur with a confined jet, and so it was necessary to carry out an investigation on the velocity profiles obtaining in the flame tunnel. No measurement device was forthcoming from any manufacturers which was capable of operation at the gas temperature and solids loading encountered in these experiments, and so measurements were, perforce, carried out with maximum cold air flow. The velocity gradients must thus be assumed to follow the same profile when "hot". The results of the Pitot tube traverses are shown in Appendix 2. It is clear that the slightly humped profile existing in Port 1 had vanished by the time Port 2 is reached, and plug flow obtained. Readings were attempted in Port 3, but were inaccurate due to low velocity. However, the profile appeared flat, as expected from the results at Port 2.

Taking the results and averaging the figures obtained at equal distances from the axis (i.e. the mean of the +50 and -50 mm figures etc.). The following is obtained:

Distance from axis (mm)	Mean velocity ($m.s^{-1}$)
0	3.20
50	3.20
100	3.00
150	2.85
200	2.65

It can be seen that this profile does not resemble the Gaussian form, but is more a plug flow profile.

The volume flow pattern obtaining at Port 1 is now represented by the volume of the solid of revolution described by the velocity profile around the velocity axis. However, the velocity profile is quite flat, and errors are obviously occurring at the greater distances from the axis due to the flow being decreasingly parallel to the pitot axis. (A 5-hole pitot could not be used due to the geometrical configuration of the long first sampling port). The profile is therefore assumed to be flat in actuality.

After the gas analyses have been taken at the radial positions appropriate to that particular axial port, the axis motor is reversed and during the probe's extraction, the following procedure is carried out by the computer for each of the gas species measured, the procedure starting with the flame tunnel axis being the nth sampling position:

(i) The distance between the nth and the next radial sampling portion on the way to the wall [the (n + 1)th] is divided into 5 equal parts. The resultant distance increment is DL and the distance from the

flame axis to the beginning of the increment is termed L. The number of divisions, 5, was found by increasing the number of divisions from 1 until convergence of results of the overall procedure occurred to four significant figures.

(ii) Proceeding from the nth point to the (n + 1)th point in steps of dL. The area of the the described slice of annulus is now:

$$S = \pi .V \left[(L + DL)^2 - L^2\right]$$

where V is the velocity obtaining at L + DL/2. This is unity since a flat velocity profile is assumed.

(iii) The values of the gas species are interpolated between the two sampling positions, and the value obtained at L + DL/2 is found, and termed G.

(iv) The values ΣS and $\Sigma S.G$ are stored and the procedures repeated from step (ii) until the $(n + 1)^{th}$ sampling point has been reached. The $(n + 1)^{th}$ sampling point is now termed the n^{th}, and the procedure repeated from step (i).

(v) When the final sampling point has been reached, the procedure is repeated from that point to the wall, but using the gas analyses values obtained at the last point since values are impossible to obtain at the wall due to air infiltration through and around the sampling port.

(vi) The final gas analysis value for each species is now:

$$G_{mean} = \frac{\Sigma S.G}{\Sigma S}$$

6.1.1.2. Determination of Individual Burn-outs of Coal and Oil

(i) Determination of Oil and Coal Burn-outs on an Individual Basis

It is possible to calculate the quantities of oil and coal burnt out by means of the quantities of corrected oxygen and carbon dioxide present in the sampled gas.

Assuming that:

B_s = Coal mass burnt ($Kg.s^{-1}$)
B_L = Oil mass burnt ($Kg.s^{-1}$)
D_s = Oxygen demand of coal ($m^3\ Kg^{-1}$)
D_L = Oxygen demand of oil ($m^3\ kg^{-1}$)
S_s = Carbon dioxide production of coal ($m^3\ kg^{-1}$)
N_s = Nitrogen production of coal ($m^3\ kg^{-1}$)
S_L = Carbon dioxide production of oil ($m^3\ kg^{-1}$)
N_L = Nitrogen production of oil ($m^3 Kg^{-1}$)

a = Volumetric time proportion of carbon dioxide at point of analysis (dry basis)
b = Volumetric time proportion of oxygen at point of analysis (dry basis)
C = Volume flowrate of carbon dioxide ($m^3\ sec^{-1}$)
N = Volume flowrate of nitrogen ($m^3\ sec^{-1}$)
O = Volume flowrate of oxygen ($m^3\ sec^{-1}$)
z = C + N + O

Then, flowrate of carbon dioxide at sampling point

$= B_L.S_L + B_s.S_s + C$

and flowrate of oxygen

$= O - B_L.D_L - B_s.D_s$

and flowrate of nitrogen

$= N + B_L N_L + B_s.N_s$

The total volume is thus:

$B_L.S_L + B_s.S_s + C + 0 - B_L.D_L - B_s.D_s + N + B_L.N_L + B_s.N_s$

but $C + 0 + N = z$

$\therefore$ Total volume $= B_L(S_L-D_L+N_L) + B_s(S_s-D_s+N_s) + z$

putting $y = S_L-D_L+N_L$ and $x = S_s-D_s+N_s$

Then:

$$a = \frac{B_L.S_L + B_s.S_s + C}{z + y.B_L + xB_s}$$

making B_s the subject, we obtain:

$$B_s = \frac{a.z - C - B_L(S_L - a.y)}{S_s - a.x} \qquad \text{.....(70)}$$

similarly,

$$d = \frac{0 - B_L.De - B_s.D_s}{z + y.B_L + x.B_s}$$

rearranging:

$$b-z - 0 = B_s(-b.x-D_s) + (B_L(-b.y-D_L) \qquad \text{.....(71)}$$

Substituting (70) in (71) and making B_L the subject:

$$B_L = \frac{(a.z - C + (0 - b.z)}{(S_s - a.x.)\ (-b.x-Ds)} \Big/ \frac{(b.y + D_L) + (S_L - a.y)}{(-b.x - D_s)\ \ (S_s - a.x)} \qquad \text{.....(72)}$$

This value can then be used in (70) to obtain B_s. Expressing B_S and B_L as fractions of the coal and oil flowrates thus gives the fraction burn out of each combustant at the sampling point.

To test these equations, they were inserted into the mathematical model with a series of "dummy" but representative values of gas flows, coal composition etc. The theoretical gas analysis was "hand" calculated for a 0.8 oil burnout and a 0.5 coal burnout, and used in the above equations.

The effect of inaccurate gas analyses was studied, by deviating the oxygen and carbon dioxide volumetric proportions by 0.2% by volume, which is, as previously stated, the accuracy of the apparatus. The results are shown in the following table, where the calculated values for gas analysis used in the equations was 10.66% oxygen and 19.82% carbon dioxide for the aforementioned 0.8 oil burnout and 0.5 coal burnout:

ACCURACY OF CALCULATION OF BURNOUTS

% Oxygen	% CO_2	Calculated Oil Burnout	Calculated Coal Burnout
10.66	19.82	0.788	0.513
10.66	20.02	0.732	0.644
10.66	19.62	0.844	0.417
10.86	19.82	0.733	0.619
10.86	20.02	0.676	0.733
10.86	19.62	0.788	0.505
10.46	19.82	0.843	0.440
10.46	20.02	0.788	0.555
10.46	19.62	0.899	0.330

It can clearly be seen that even the base case is not entirely accurate due to the "rounding" of gas flows to three significant figures. Obviously such sensitivity to such a small error as 0.2% by volume of measurement is quite unacceptable, and so an alternative measure of "burnout" had to be devised.

6.1.1.3. Derivation of Combined Burnout of Slurry

Since the method of separating the burnout of coal and oil outlined in 6.1.1.2 was too inaccurate, a more satisfactory method of expressing fractional burnout had to be derived.

The final method decided upon was to treat the slurry as a homogenous fuel, and calculated the fractional burnout both in terms of oxygen analysis and carbon dioxide analysis.i.e.

$$F(\text{oxygen}) = \frac{O_s - O_a}{O_s - O_f}$$

$$F(\text{carbon dioxide}) = \frac{C_a - C_s}{C_f - C_s}$$

where F is fractional burnout, O is dry gas oxygen content C is dry gas carbon dioxide content. The subscript s is the theoretical value before combustion of the slurry (calculated from the relevant propane, oxygen and air flows), f is the final theoretical value given the gas flows and slurry flow, and a is the actual measured value.

The overall fractional burnout is then found as the mean of the above fractional burnouts.

There is naturally a noticeable difference in these values at the earlier ports since in general the oil-rich sections of the slurry burn first, taking more than its "share" of the oxygen due to the high hydrogen content of the oil compared with the solid fuels.

However the values coincide more closely as burnout continues.

The value of this method is that the "burnout" from the model can readily be expressed in the same way, utilizing the same data of flows of gases and slurry.

It was quickly established that the progressively converging values of carbon dioxide and oxygen based data occurred with the mathematical model also, as expected.

A further value of this method is that any errors in standard gas composition or drift in zeros and spans of the instrument are minimised.

6.2. Design of Experimental Programme

6.2.0. Limitations Imposed by Flame Measurement Techniques and Control System

As stated in 6.1.0 above, particulate sampling was rendered impossible by the failure of the sampling probe at high temperatures, thus limiting measurement techniques to gas analysis only.

The following points must therefore be considered:

(i) The variability of gas analysis with time is well known when sampling in flame.

(ii) The lags of the sampling system and the variation in speed of response of the gas analyses.

(iii) The pulsations of the peristaltic pump, whilst limited by an air-filled smoothing chamber, still exist.

(iv) Because of the smoothing chamber, considerable delays occur before an altered level of output is realised after a change in speed of the pump.

(v) "Drift" in the gas measurement transducers.

As a result of these sources of inaccuracy, individual "runs" are unlikely to be accurate enough for individual analysis.

It is desirable, therefore, to carry out the work programme on a parametric basis, investigating at the highest and lowest value of the variable to be changed. Equal numbers of "runs" at each level of parameter are thus desirable.

The following values of the parameters were decided upon by actually running the rig:

Parameter	High Value	Low Value
Blast temperature	1000°C	750°C
Oxygen content of blast	26%	21%
Blast velocity	240 $m.s^{-1}$	200 $m.s^{-1}$
Injection level (proportion of Stoichiometric)	0.9	0.8
Atomisation pressure	50 psig	40 psig

It can be seen that the differences in the high and low value are not as large as is ideally desirable. The reason for this is the cumulative effects of the alteration of the parameters. For example, the flow of pure oxygen at the conditions 750°C, 26% oxygen and 240 m/s is three times the flow obtained at 1000°C, 21% oxygen and 200 m/s. The selection is limited on the one hand by supply limitations and on the other by orifice plate accuracy. The even larger variation of the level of injectant resulted in a constant ratio of steam to injectant being adopted to retain the steam flow within measurable limits. The result is that only the pressure of supply can be varied in the "high" and "low" levels of atomisation. In practice, even this small allowable variation is subject to such inaccuracies of setting that pressure variations due to mass flow corrections can span this range.

It was therefore decided to fix the steam atomisation pressure at 40 psig and a mass flow of 0.4 times the slurry mass flow. This results, for each slurry type, in four variable parameters.

Each slurry has thus a set of 2^4=16 "runs" which are to be carried out on it.

The five injectants to be investigated are:

(i) Heavy fuel oil (HFO)
(ii) 60% HFO + 40% coarse coke breeze
(iii) 60% HFO + 40% fine coke breeze
(iv) 60% HFO + 40% coarse anthracite
(v) 60% HFO + 40% fine anthractie

The characteristics of which are in Appendix 3.

It can thus be seen that the total work programme consists of a maximum of 80 runs.

The original intention was to investigate lower coal concentrations in addition to the runs above, but the "coal effect" of the slurry is lessened, and the economics of the process depend upon using the maximum feasible coal concentration. The use of a concentration between 0% (HFO) and 40% is thus spurious.

6.2.1. Running of the mathematical model

The mathematical model is run using the actual conditions of slurry flow, steam flow, blast temperature, air flow, propane flow and oxygen flow outputed from the apparatus.

The burnout calculated from carbon dioxide and oxygen levels predicted by the model at each port along the flame axis are then compared with the corrected values obtained by the methods outlined in 6.1.1.3. above.

It was found that, in the case of Heavy Fuel Oil, combustion was virtually complete by the first port in all circumstances. It was thus difficult to draw conclusions regarding the droplet sizes achieved.

However, this was not the case in respect of the slurry flames, and the programme was carried out.

The predicted gas analysis readings from the mathematical model are compared with the corrected actual gas analysis readings using the following:

$$\frac{1}{n}\sum_{1}^{n}\frac{(F_p - F_a)}{F_a} \qquad \text{.....(72)}$$

and

$$\frac{1}{n}\sum_{1}^{n}\left|\frac{F_p - F_a}{F_a}\right| \qquad \text{.....(73)}$$

Where F is the fractional burnout, the subscripts p and a are predicted and actual, and n is the number of data samples.

The results for each port are calculated separately. Equation (72) gives an indication of the overall error (whether positive or negative) and equation (73) gives an indication of the degree of spread of the readings.

The total data set of 80 runs (each with analysis values at five ports) can now be divided into six sub sets:

(i) High and low stoichiometric ratios
(ii) High and low oxygen concentrations in the blast
(iii) High and low blast temperatures

(iv) High and low blast velocities

(v) Slurry type

(vi) Port of sampling.

By applying equations (72) and (73) to these subsets, it was possible to evaluate the assumptions made in the mathematical model which were affected by the parameters (i) to (vi) above. This is examined in greater detail in 6.5.

6.3. Results Obtained From Rig

6.3.0. Identification of Work Programme

Appendices 4.0.N.identify the individual runs of the work where N is the coal number in the slurry. The run number in brackets is the original number of a run which was found to be unsatisfactory and the run was repeated by the unbracketed number.

It was originally intended to repeat all of the runs in Appendix 4.0.0. However, refractory failure occurred after repeating only four of the sixteen runs.

Most of the runs with coal were satisfactory. As can be seen from Appendices 4.0.1.to 4.0.4. inclusive, only two runs had to be repeated on Coal No.2. These were due to breakdowns in the apparatus preventing the completion of the runs.

6.3.1. Presentation of Individual Results of each Run

The complete results of a run are shown in Appendix 4.1.0. It can be seen that it would be extremely space consuming to display the entire 80 runs in this fashion.

The parts of this data which are used are, for each port: "Air" temperature, propane, oxygen and air flows and

the area weighted means of the gas analyses (whose method of derivation was described in 6.1.1.).

These data were then corrected to the oxygen and carbon dioxide form shown in 6.1.1.1.(b). Finally, with this corrected form and using the relevant flows of "air" components and slurry, a "burnout" for that port was calculated as shown in 6.1.1.3.

The complete set of results for every run is thus shown in this "burnout" form - for simplicity and space saving - in Appendices 4.2.N.

6.3.2. Initial Parametric Analysis of the Results

Appendix 4.3.0. shows the mean results obtained for each of the slurry types, and this is demonstrated graphically in Fig.23.

Several points become immediately clear:

(i) The oil is completely gasified before the first port, confirming visual observation.

(ii) The slurries are either completely gasified or almost completely gasified by the time Port 4 is reached.

(iii) The slight decline in burnout from Port 4 to Port 5 indicates that the steps taken to reduce the effects of air infiltration to the flame tunnel were only partially successful beyond Port 4.

(iv) The slurry produced from coal No.4 suffered more from the aforementioned stalling of the peristaltic pump than others, as expected due to its higher viscosity. However, earlier burnout is expected due to its very high degree of

fineness of grind. Both these views are verified by the results.

(v) It will be recalled that most of the "stalling" occurred at lower flowrates of slurry and so analysis of the results by input parameter is valuable.

In Appendices 4.3.1. and 4.3.2. and their graphical representations Figs. 24-27, the following may be seen:

(i) Lower preheat temperatures - higher average slurry flowrates - lower average burnout.

(ii) Higher velocities - higher average slurry flowrates - higher average burnout.

(iii) Higher air oxygen content - higher average slurry flowrates - higher average burnout.

(iv) Higher stoichiometric ratios - higher average slurry flowrates - higher average burnout.

Examining these parameters, it can be seen that point (i) is as may be expected, due to longer ignition lag and less rapid vapourisation of oil. Point (ii) is the reverse of expected, which is lower burnout due to shorter residence time. Point (iii) is as expected but Point (iv) is the reverse of expectation which is lower average burnout due to both higher oxygen availability and longer residence times (lower final gas temperatures) expected of lower stoichiometric ratio.

From the foregoing it is clear that, on average, lower flowrates of slurry should, on balance, result in higher average burnouts. However,it is clear from Fig. 28 that this is not so. Assuming therefore that complete burnout has essentially occurred by Port 4 in the case of

slurries, it may be seen that, ignoring Port 5:

(i) Coals (1), (2) and (3) are 2% deficient in slurry flow at low flowrates.

(ii) Coal (4) is 3.4% deficient at low flows and 3.2% deficient at large flowrates.

(iii) Oil is approximately 3.5% deficient at low flows.

It is therefore necessary to ascertain whether or not these errors are random or due to systematic errors in slurry delivery.

For Coals 1,2 and 3, the results may be summarised.

	Mean Burnout at Port 4	Number of Observations	Standard Deviation
Lowest Flow	0.9801	24	0.052848
Highest Flow	1.0023	24	0.030564

The standard deviations of the two means are:

$$\frac{0.052848}{\sqrt{24}} = 0.0107876 \text{ and } \frac{0.030564}{\sqrt{24}} = 0.0062389$$

Therefore the standard deviation of the difference of mean is:

$$\sigma_d = \sqrt{[0.0107876^2 + 0.0062389^2]}$$

$$= 0.01246$$

The significance of the difference of the mean is thus:

$$\frac{1.0023 - 0.9801}{0.01246} = 1.781$$

Using this value in tables of area under the normal curve, the probability of being within the area is 0.4626.

The probability of the differences of the mean burnout being due to random errors is thus 0.5-0.4626 = 0.0374.

It can thus be confidently concluded that these differences are not caused by random errors, but are caused by one or more systematic errors, related to the flowrate.

Similarly, in the case of the highest flow of coal 4, the results may be summarised:

	Mean Burnout Port 4	Number of Observations	Standard Deviation
Highest flows, coals 1,2 & 3	1.0023	24	0.030564
Highest flows coal 4	0.9680	8	0.052292
Lowest flows coal 4	0.9661	8	0.058763

Using the same procedure as previously the probability of the discrepancy between the highest 8

flowrates and lowest 8 flowrates of coal 4 being due to random errors are 0.0394 and 0.0476 respectively. It can therefore be concluded that systematic errors are affecting the results rather than random errors.

In view of these results, it was decided to modify the data set as follows:

(i) Multiply the lowest 8 nominal oil flows (printed out by the rig control computer and used in the calculation of burnout) by 0.966.

(ii) Multiply the lowest flows in each of slurries 1, 2 and 3 by 0.98

(iii) Multiply all the flows of slurry number 4 by 0.967. The resulting data set was analysed by slurry flow and the results are shown in Appendix 4.3.4 and Fig. 29.

The results are now presented individually in Appendices 4.4.0 to 4.4.4, by slurry type in Appendix 4.5.0 and Fig. 30, and by input variables in Appendices 4.5.1.and 4.5.2, and Figs.31 to 34.

6.3.3. Confidence Limits of the Experimental Results

Due to the unfortunately early termination of the practical work programme, it was impossible to complete the results for oil runs at the new radial positions, let alone replicate the data set so as to fix confidence limits on the results obtained. However, again making the assumption of complete combustion at Port No. 4, the standard deviations of the burnouts for each coal are, from analysis of the data in Appendices 4.4.1.to 4.4.4. :

Coal 1, 4.49%; Coal 2, 4.34%; Coal 3, 4.31%;Coal 4, 5.77%

The corresponding t-test for 16 readings gives the following probabilities within the 95% confidence limits:

Coal 1 : 0.904; Coal 2: 0.908; Coal 3: 0.908; Coal 4: 0.877.

6.4 Initial Optimisation of Mathematical Model

6.4.0. Initial Optimisation of Slurry Parameters

Unfortunately, it is difficult to measure the drop-size distributions of sprays [97], and accuracy is particularly low in the case of solid conical sprays such as are encountered in this investigation. Assumptions therefore had to be made in the first instance. The basic assumptions of fractions overlap and slurry droplet size distribution were altered until the model predicted average errors of less than 5% for each coal. These errors were the average of the first four ports for the sixteen runs of each core, i.e. 48 data points. The conditions assumed were: overlap 5 fractions, mean droplet size: 100μ, distribution constant :1.2.

6.4.1. Optimisation of Efficiency

6.4.1.0. Methods of Integration Investigated

When this procedure was carried out with the step length being controlled such that approximately 1% of the total energy available in the slurry was released, then the "nominal" number of iterations is said to be 100.

When the model gave results reasonably close to those found in practice, convergence of the model was analysed.

It was found that, with Euler integration and a step length controlled to equal burnout, convergence occurred at 1000 nominal iterations i.e.controlling

burnout to 0.1% of the combustibles for each iteration.

However, since the apparatus is so programmed to accept gas analysis readings to within 0.2% by volume, this criterion was also applied to the model.

The number of iterations required was still found to be 400 to give this level of accuracy, and it was therefore decided to investigate other methods of integration to improve the model efficiency.

The methods of integration investigated are explained below, and the results of each method is shown in Appendix 5.

(1) Euler, "constant" step length. This means that the actual time increment is varied to keep the percentage of the burnout occurring in each time increment approximately constant.

(2) As (1) above, but using predicted values of the mean oxygen content and temperature which should occur throughout the iteration.i.e.at the end of iteration n, the assumed oxygen value used for iteration n + 1 is not that obtained at n, but is calculated by:

$$O_{n+1} = O_n - (O_{n-1} - O_n)/2$$

and similarly for temperature:

$$T_{n+1} = T_n + (T_n - T_{n-1})/2$$

The assumed oxygen and temperature values are thus assumed to have progressed halfway beyond the values obtained across the previous iteration.

(3) In the later stages of the burnout the "constant" quantity of burnout means that the quantity being combusted represents a growing proportion of the unburnt droplets and particles. It was thus decided to lower the proportion of burnout at each iteration as the total burnout progressed.

Several methods and values were tried, but the most effective found (in the time allotted for this section of the investigation) was found to be:

when B_t >0.5 then $B_i = B_{in}.(1-B_t+0.2)$
when B_t >0.7 then $B_i = B_{in}.(1-B_t+0.15)$
when B_t >0.8 then $B_i = B_{in}.(1-B_t+0.1)$
when B_t >0.9 then $B_i = B_{in}.(1-B_t+0.05)$

where B_t = proportion of cumulative slurry and particulate burnout
B_i = proportion of burnout per iteration
B_{in} = original nominal proportion of burnout per iteration

(4) This method uses Runge-Kutta integration, but is otherwise identical to (1) above. Since three differential coefficients must be obtained for each fraction in this method, the time taken is almost exactly doubled, but much higher accuracy occurs per nominal interaction.

(5) This method uses Runge-Kutta integration together with the method of predicted gas values as outlined in (2) above.

(6) This method is as (3) above, but using Runge-Kutta integration.

6.4.1.1. Results of Integration Efficiency Investigations

These are shown in Appendix 5 for the various methods of integration and approximate relative run time is also shown.

It can be clearly seen that the most efficient means of achieving the requisite accuracy of within approximately 0.2% oxygen differential from the 1000 iteration standard is by means of using 200 iterations with integration method (3). This method and this number of nominal iterations was subsequently used.

6.4.1.2. Elimination of Extreme Size Ranges

Once mathematically acceptable convergence was obtained, the results obtained from the model was closely examined for modification to the "physical" parameters.

Of particular note was the very small quantities of coal particles and slurry droplets which were predicted for some of the extreme size ranges by the Rosin-Rammler distribution.

This phenomenon had the effect of considerably slowing the model's operation, since the larger size ranges would be (proportionally) more unburnt and much computer time wasted in calculating minute mass transfers from them.

A modification was thus made which reduced the number of size ranges. This operated by examining the size ranges of slurry droplets in turn starting at the largest size range. If the mass of droplets in the largest size range was less than 1% of the total mass

of slurry droplets and coal particles, it was amalgamated with the next smallest size range. This size range was then examined and if the amalgamated size was less than 1% of the total, it was amalgamated with the next smallest size range. This continued until the size range whose amalgamated mass was greater than 1% of the whole was found.

The program then repeats the procedure from the smallest end of the size range, amalgamating with the next largest in this case until the 1% level is passed.

The whole procedure is then repeated for the coal fractions.

It was found that this procedure marginally enhanced the accuracy of the program and speeded up the running by 10-30% depending on slurry.

6.5. Final Optimisation of Mathematical Model

6.5.0. Criteria of Measurement of Model Accuracy

Any final measurement of model accuracy must contain a component not only of the overall accuracy of prediction, but also of the accuracy variation along the ports and the accuracy variation between high and low values of the preheat temperatures, blast velocity, oxygen content and stoichiometric ratio.

Given, for each coal slurry species:-

$$\bar{x}_n = \frac{\sum_{1st\ Run}^{16th\ Run} \frac{F_p - F_a}{F_a}_n}{16} \quad \ldots\ldots\ldots\ldots\ldots\ldots (74a)$$

where: F is Fractional Burnout and the subscripts: n refers to port number, p refers to predicted model value and a refers to actual experimental value.

and

$$\bar{x}_m = \frac{\sum_{1st\ Run}^{16th\ Run} \frac{F_p - F_a}{F_a}_m}{16} \quad \ldots\ldots\ldots\ldots\ldots\ldots (74b)$$

where: m refers to the eight conditions of low and high levels of:
temperature, velocity, oxygen and stoichiometric ratio

Then for the entire set of results for the species:

$$\bar{x} = \frac{\sum_{Port\ 1}^{Port\ 4} \bar{x}_n}{4} \quad \ldots\ldots\ldots\ldots\ldots\ldots (75a)$$

or

$$\bar{\bar{x}} = \frac{\sum_{\text{Condition 1}}^{\text{Condition 8}} \bar{x}_m}{8} \qquad \text{.....(75b)}$$

$\bar{\bar{x}}$ thus gives the mean error for the entire coal species.

The mean deviation between the ports can be found from:-

$$\delta_n = \frac{\sum_{n=1}^{n=4} \bar{x}_n - \bar{\bar{x}}}{4} \qquad \text{.....(76a)}$$

and the mean deviation between the errors of each input condition can be found from:

$$\delta_m = \frac{\sum_{m=1}^{m=8} \bar{x}_m - \bar{\bar{x}}}{8} \qquad \text{.....(76b)}$$

An "overall error" can now be defined as:

$$\delta = {}^1/_3 \left[\bar{\bar{x}} + \delta_n + \delta_m \right] \qquad \text{.....(77)}$$

These criteria of distribution were chosen since the errors are of the same order as x, unlike standard deviation (root mean square error) which would, relatively speaking, exaggerate the worse deviations from the mean. A short programme was written to evaluate these errors on a coalwise basis using the above equations.

6.5.1. Slurry Variables to be Optimised

There are several input variables which must be taken into account:-

(i) Number of size fractions "overlap" of slurry and contained coal.

(ii) The mean droplet size of the slurry formed.

(iii) The distribution of the droplet size around the mean size of droplet.

(iv) The degree of internal burning of the coal char particles.

(v) The area of the char particles given the particle size.

i.e. Area of particle $= \{\frac{d}{2}\}^2 . A_f$ .....(78)

where A_f, the area factor is equal to 4.Π for spheres, 16 for cubes.

6.5.2. Optimisation Procedure

6.5.2.0. Idealized Procedure

Optimisation is obviously not amenable to precise mathematical correction when there are five unknown variables in the input data to the model. A method of successive approximation was thus decided upon.

Ideally, the best solution would be to take a five dimensional, fine-meshed matrix (say of tenth order) and find the point of lowest error. However, since this would require 10^5 data sets each of 64 runs, this is clearly not feasible at a run time of approximately 8.5 minutes for the "standard" 200 iteration model programme.

Clearly, some economies must be found both in terms of run time and in terms of compromise in the ideal five dimensional matrix.

6.5.2.1. Run Time Economies

The most obvious economy is to cut down on the 200 iterations of the model which are necessary only to meet the stringent standards of the fully optimised model.

For comparison purposes a 2 x 2 matrix altering Rosin-Rammler size distribution exponent was run for fixed values of slurry fraction overlap, coal particle area factor and internal burning exponent. This matrix was carried out for all 64 slurry runs at 200, 50, 30 and 20 iterations. The overall error programme mentioned in 6.5.0. was then used to analyse the overall error between the model and the rig results on a coal-wise basis.

The results of this work are shown in Appendix 6.0. It can be seen that sufficient accuracy to identify the optimum is retained using a 20 iteration model, but a 30 iteration model was used in the optimisation procedure since the speed was only insignificantly slower.

6.5.2.2. Procedural Economies

It can be seen from Appendices 4.2.1. and 4.2.4.,and also from stopping the model at the first port, that nearly complete combustion of the slurry fraction has occurred by Port 1, whilst only 60-70% of the free coal has combusted by this point.

It is reasonable to consider, therefore, that the major effect on the results obtaining at the first port will be the assumption of droplet size distribution and Rosin-Rammler index of the slurry,

together with the number of fractions overlap of slurry droplets and free coal particles.

Since the distribution of both free coal particles and slurry droplets depend on these three factors, it is impossible to differentiate between them: One is therefore left with optimisation in a three-dimensional matrix.

After the first port, assuming that the slurry factors in the model have been thus far optimised, the largest influences on model accuracy will be the coal's internal burning exponent and the surface area factor.

The optimisation using the criteria outlined in 6.5.0. rather than first port accuracy is thus carried out on a two-dimensional matrix, varying both the internal burning exponent of the coal and the surface area factor. The internal burning exponent and surface area factor thus found may be re-inserted into the three dimensional matrix and the whole process repeated.

6.5.2.3. Matrix Span and Mesh Size Economies

The matrix span must be more than large enough to cover all likely possibilities. For example, the Rosin-Rammler exponent does not normally lie outside the range 0.8-1.3.

However, if the optimum value should lie at one of these extremes, it will not be possible to provide a reasonably accurate pin-point of the optimum by examination of the error profile.

Similarly, the mesh size of the matrix must not be so coarse that the lowest error point is missed beween widely separated elements of the matrix.

Finally, the generation of the error matrix must not be too time consuming, and this factor tends to be very influential in terms of mesh size selection.

6.5.2.4. Optimisation Technique

The optimisation is carried out in phases:

(i) A three-dimensional matrix is produced by the mathematical model of percentage error difference between predicted and actual values at the first port. The spans of the matrix more than cover the ranges of slurry droplet size and distribution, and slurry coal fractions overlap likely to be encountered. The mesh of this matrix is as fine as is technically feasible.

The model uses thirty iterations, and the criterion of first-port accuracy is used.

(ii) The most obvious point of low error in set A is taken as the aiming point of the second phase. This point is not necessarily the point of lowest error - which could be the result of a compounding of random errors - but a low error point which is surrounded by other low error points on all sides - the twenty seven nearest points. The point whose twenty seven surrounding points have the lowest standard deviation is taken as the lowest error point in the largest volume of low error, and is therefore likely to be the point of lowest actual error.

The process so far is taken as the first phase of the procedure.

(iii) The technique is repeated with a finer mesh size centring on the lowest error point found in the first phase. The analysis of this matrix is as in the first phase; this second phase is essentially a refinement of the first phase values. The extra computer time involved in producing this second phase is offset by the fact that this phase is an analysis of a two dimensional matrix due to the selection of one fixed overlap at each coal. Interpolation of overlaps is impossible, since overlap number is an integer.

(iv) Using the optimum values for slurry characteristics from the second phase, the model is now run to produce a two-dimensional error matrix by varying the internal burning index and the surface area factor for each coal, using the overall error concept. This is termed the third phase.

(v) The fourth to sixth phases inclusive are repeats of the first to third using the previous best values found for the various parameters, but using the overall error concept throughout.

6.5.3. Results of the Optimisation Procedure

6.5.3.0 Results of the First Phase of the Optimisation Procedure

The values chosen as the matrix boundaries were:-

Mean droplet size:	50μ - 150μ
Rosin - Rammler exponent:	0.7 - 1.4
Number of Fractions Overlap:	3 - 8

The matrix laid down was of the maximum feasible mesh size, to minimise the possibility of missing the optimum within the matrix. The finest mesh size decided upon, however, was limited by the feasible computer time. This was a 6 x 6 x 6 matrix requiring approximately 300 hours of computer time for the "Sirius" microcomputer to execute in compiled BASIC.

The values are thus:

Mean droplet size:	50, 70, 90, 110, 130 and 150μ
Rosin-Rammler Exponent	0.7, 0.84, 0.98, 1.12, 1.26, 1.40
Number of Fractions Overlap:	3, 4, 5, 6, 7, 8.

For each coal the errors between the sixteen practical runs and the theoretical predictions of the model at the first port were taken and an average error produced for the coal. This was repeated for the 216 permutations of slurry assumptions. The results are shown in Appendices 6.1.0 to 6.1.3 for each coal.

A programme was then set up to examine the 4 x 4 x 4 matrix which was completely encased within the larger 6 x 6 x 6 matrix of set A, i.e. every point, in the new subset is surrounded from the outside of the matrix by one "layer" of data points.

Taking the data point ℓ, m, n where ℓ, m and n have values between 2 and 5 for the original matrix of 1 to 6 then the mean error of the "shell" around point ℓ, m, n is defined as:-

$$\frac{1}{27}\sum_{\ell+1}^{\ell+1}\sum_{m+1}^{m+1}\sum_{n+1}^{n+1} \quad \text{(error at } \ell^* \ m^* \ n^*) \qquad (79)$$

where $\ell^* = \ell+1, \ell, \ell-1$ in turn

The standard deviation of the twenty seven points around this mean then gives an indication of the slope around the central point.

The results are shown in Appendices 6.2.0 to 6.2.3.

It can be seen in Appendices 6.1 that there is no single point of lowest error. In fact, taking the three-deminsional matrix of each coal, a two-dimensional flat surface of zero error penetrates through each. The appropriate positions of standard deviation in Appendices 6.2.2. show no particular point, along the zero error flat surface, at which the points surrounding a zero error point could be said to form a less steep "trough" around one near-zero error point than another.

The most likely conclusion that may be drawn from these results is that there exists a band of conditions of mean slurry droplet size and distribution and number of fractions overlap which gives rise to a certain quantity and distribution of both free coal and slurry. The combustion of these fractions is such that, at the first port, there is an almost equal quantity - though not necessarily similar distributions - remaining unburnt, thus giving similar burnouts at that port.

However, if the distributions are in fact similar, by the time the first port is reached, then almost any point on the zero error surface within the matrix may be taken for further investigation. An investigation

was therefore carried out on coal 1, taking two widely separated low error points.

Referring to Appendix 6.2.0, the two distributions chosen for comparison were:-

(a) No. of overlaps = 3, mean droplet size 90μ distribution index 0.84 where the error is 0.16%.

(b) No. of overlaps = 7, mean droplet size 130μ distribution index 1.4 where the error is -0.16%.

The results of these runs are shown in Appendix 6.3.0 for the original distribution at atomisation and in Appendix 6.3.1. for the predicted distribution existing at the first port.

Considering the original difference in error at the first port and also the very large differences in slurry creation parameters and upon first atomisation, the differences at the first port are relatively small.

It is therefore concluded that it does not make a great difference at this stage whichever distribution on the zero error but is chosen, so the points giving the lowest mean error in equation (79) are used which are:-

	Coal 1	Coal 2	Coal 3	Coal 4
Fractions Overlap	4	7	7	5
Mean slurry droplet size (μ)	110	130	70	90
Rosin Rammler exponent	1.12	1.12	0.98	0.98

6.5.3.1. Results of the Second Phase of the Optimisation Procedure

The lowest mean error points in 6.5.3.0. above were made the centres of new matrices as follows:-

Coal 1

Mean droplet size (μ): 95, 100, 105, 110, 115, 120
Rosin-Rammler index: 1.0, 1.04, 1.08, 1.12, 1.16, 1.20, 1.24
Number of fractions overlap: 4

Coal 2

Mean droplet size (μ): 115, 120, 125, 130, 135, 140, 145.
Rosin-Rammler index: 1.00, 1.04, 1.08, 1.12, 1.16, 1.20, 1.24
Number of fractions overlap: 7

Coal 3

Mean droplet size (μ): 55, 60, 65, 70, 75, 80, 85
Rosin-Rammler index: 0.86, 0.90, 0.94, 0.98, 1.02, 1.06, 1.10
Number of fractions overlap: 7

Coal 4

Mean droplet size (μ): 75, 80, 85, 90, 95, 100, 105.
Rosin-Rammler index: 0.86, 0.90, 0.94, 0.98, 1.02, 1.06, 1.10
Number of fractions overlap: 5

The results of this phase are shown in Appendices 6.4.0 to 6.4.3. These results are basically a "close-up" of the lowest error point. The values chosen were:

Coal 1: Fractions overlap = 4, R.R. index = 1.20, mean droplet size = 115μ

Coal 2: Fractions overlap = 7, R.R. index = 1.08, mean droplet size = 125μ

Coal 3: Fractions overlap = 7, R.R. index = 0.90, mean droplet size = 65μ

Coal 4: Fractions overlap = 5, R.R. index = 0.98, mean droplet size = 90μ

6.5.3.2. Results of the Third Phase of the Optimisation Procedure

The values for slurry parameters decided upon in 6.5.3.1. above were used, varying the assumption of area factor from 4Π (a sphere) through 16 (a cube) up to more irregular shapes with a factor of 28.

The internal burning index was varied from 0.05 which respresents almost totally internal combustion to 0.33, which represents almost entirely surface combustion.

The results are shown in Appendices 6.5.0 to 6.5.3. for coals 1 to 4 respectively.

It is clear the the internal burning factor has played a negligible part in the process. This is due to either: (i) the coals studied are not internally combusting or: (ii) the combustion of the particules has been almost entirely diffusion controlled, so that oxygen only reaches the surface of the particle.

To resolve the alternatives the programme was run in interpreted BASIC and interrupted at various stages during the burnout. The values of the diffusion and surface reaction rate coefficients for all extant size fractions were then examined.

It was found that, except at the very last stages of burnout when negligible masses of coal remained unburnt, Ks was greater than Kd so confirming diffusion controlled reactions. This is not surprising considering that:-

(i) The smaller particles are contained in the slurry droplets.
(ii) The relatively high gas temperatures due to high air preheat.

The internal burning index was thus fixed at 0.33 for all coals, and the surface area factor is set at 16 for coal 1, 19 for coal 2, 22 for coal 3 and 19 for coal 4.

6.5.3.3. Results of the Fourth Phase of Optimisation

The assumptions made are for the slurry parameters are identical to those made in the first phase, (see 6.5.3.0) except that the overall error criterion was used instead of first port error.

This was decided upon since: (i) Appendix 6.2.1. demonstrates that there is, in fact, a not inconsiderable quantity of slurry unburnt at the first port, and (ii) an approximate value for surface area factor had been obtained and internal burning eliminated for each coal, so that the coal fractions would not incur too great an inaccuracy between ports.

The results are shown in Appendices 6.6.0 to 6.6.3.respectively. It is notable that definite low points exist in the matrix with discernable slopes leading down to them. However, some of the results are equivocal and so the procedure of taking the

standard deviation around each point was carried out, the results being shown in Appendices 6.7.0 to 6.7.3. for coals 1 to 4 respectively.

The results for coal 1 are unequivocal (see Appendix 6.6.0) with a definite low point at droplet size 90μ, from Rosin Rammler Index 0.98 and overlap number 6. In Appendix 6.7.0. it can be seen that this point also corresponds to a low value of standard deviation, signifying a low-error volume surrounding it.

The results for coal 2 (see Appendix 6.6.1.) show low points at: (i) 110μ, RR index 0.84 and five fractions overlap, and (ii) at 110μ, RR index 0.98 and six fractions overlap.

Referring to Appendix 6.7.1. it can be seen that (i) has the lowest SD of the surrounding points, and this option is therfore chosen.

The result for coal 3 (Appendix 6.6.2) show low points at: (i) 70μ, RR index 0.98 and five overlaps, and (ii) 90μ, RR index 1.26 and six overlaps.

Appendix 6.7.2. shows that the latter point has the lowest SD of the surrounding points, and this option is chosen.

The results for coal 4 (Appendix 6.6.3.) show low points at: (i) 90μ, R.R. index 0.98 and five overlaps, and (ii) 110μ, R.R. index 1.26 and six overlaps.

Appendix 6.7.3. shows that the latter point has the lowest S.D. and this option is chosen.

6.5.3.4. Results of the Fifth Phase of Optimisation

Using the results from 6.5.3.3. as the appropriate centre point, the model was run using the following conditions:-

Coal No.1, 6 fractions overlap,

Mean droplet sizes: 75, 80, 85, 90, 95, 100, 105

Rosin Rammler Indices: 0.875, 0.910, 0.945, 0.980, 1.015, 1.050, 1.085

Coal No.2, 5 fractions overlap,

Mean droplet sizes: 95, 100, 105, 110, 115, 120, 125

Rosin Rammler Indices 0.735, 0.770, 0.805, 0.840, 0.875, 0.910, 0.945

Coal No.3, 6 fractions overlap,

Mean droplet sizes: 75, 80, 85, 90, 95, 100, 105

Rosin Rammler Indices: 1.155, 1.190, 1.225, 1.260, 1.295, 1.330, 1.365

Coal No.4, 6 fractions overlap,

Mean droplet sizes: 95, 100, 105, 110, 115, 120, 125

Rosin Rammler Indices: 1.155, 1.190, 1.225, 1.260, 1.295, 1.330, 1.365

The results of these model runs are shown in Appendices 6.8.0 to 6.8.3. for coals 1-4 respectively. It can be seen that there are clear low error points, and the final results for the slurry distribution are:-

Coal 1, 6 fractions overlap, mean droplet size 85μ, Rosin Rammler index 0.910

Coal 2, 5 fractions overlap, mean droplet size 110μ, Rosin Rammler index 0.875.

Coal 3, 6 fractions overlap, mean droplet size 90m, Rosin Rammler index 1.225.

Coal 4, 6 fractions overlap, mean droplet size 105μ, Rosin Rammler index 1.155.

These values are then used in the final model.

6.5.3.5. Results of the Sixth Phase of Optimisation

The droplet parameters found in 6.5.3.4. were used in the final optimisation of coal characteristics. The internal burning index was set at 0.333 (i.e., no internal burning) and the values of surface area factor found in the third stage of the optimisation were used as the centre point of this investigation, giving the following values of surface area factors be investigated.

Coal No. 1: 13, 14, 15, 16, 17, 18, 19.
Coal No. 2: 16, 17, 18, 19, 20, 21, 22.
Coal No. 3: 19, 20, 21, 22, 23, 24, 25.
Coal No. 4: 16, 17, 18, 19, 20, 21, 22.

The results of these are shown in Appendix 6.9. and the surface area factors selected are:

Coal 1: 16, Coal 2: 20, Coal 3: 22 Coal 4: 20.

6.5.4. Significance of Final Slurry and Coal Parameters Chosen

Reiterating the final fuel parameters:

Parameter	Coal 1	Coal 2	Coal 3	Coal 4
No. of overlaps	6	5	6	6
Mean droplet size (μ)	85	110	90	105
Rosin-Rammler index	0.910	0.875	1.225	1.155
Coal surface area factor	16	20	22	20

The following points emerge:-

(i) There is good agreement on the number of fractions overlap. The proposition that slurry droplet retain coal particles only below some factor of the droplet size therefore seems to have some foundation. At six fractions overlap and a 1.38 size ratio between fractions, this factor is $1/(1.38)^6 = 0.14$, smaller than originally speculated.

(ii) The finer grinds of coal, 2 and 4, produce larger mean droplet sizes of the slurries. This is to be expected, since finer grinds produce higher viscosity slurries, and higher viscosity liquids produce larger droplet sizes on atomisation.

(iii) The anthracitic coals, 3 and 4, produce a wider slurry droplet size distribution (higher Rosin-Rammler index) than the coke based slurries. Presumably this is either a particle shape or a coal density effect.

(iv) There is no clearly unequivocal result that can be inferred from the coal surface area factors, other than to state that coal 3 may be anomalous due to the breeze content of this nominally anthracitic coal.

6.6. Results from the Finalised Mathematical Model

6.6.0. Model Errors

The errors between the model burnout predictions and the burnouts actually measured were compared. An error analysis for each coal is shown in Appendices 7.0 to 7.3 respectively.

The average percentage error is the mean of all four ports and all sixteen runs of each coal and is thus based on a data set of 64 points. The analysis of the input parameters of temperature, velocity etc. are thus based on 32 points and the analysis of the port errors is based on 16 points.

Also shown are the relevant standard deviations to supply an estimate of the confidence limits of the model.

6.6.1. Individual Results

For completeness the whole set of results, for each coal, is shown in appendices 8.0 to 8.3. However, due to the variations in pump speed etc. it would be unwise to attach too much significance to each individual result. This is confirmed by the high standard deviations in Appendices 7.0 to 7.3.

Taking the results at the fourth port (where burnout has been assumed to be virtually complete) we obtained the following interesting results:

Coal Number	S.D. of Model and experimental results (%)	S.D. of experimental results (%)
1	5.18	4.49
2	4.35	4.34
3	4.91	4.31
4	6.11	5.77

It is evident that the majority of the deviation of the model from the practical results is due to the deviation of the practical results themselves.

6.6.2. Confidence Limits of the Model

Taking the results from 6.6.1. and subtracting the variances of the practical results from the model results, the standard deviation of the model results alone become:

Coal 1: Model S.D. = $\sqrt{[5.18^2 - 4.49^2]}$ = 2.63%

Coal 2: Model S.D. = $\sqrt{[4.35^2 - 4.34^2]}$ = 0.29%

Coal 3: Model S.D. = $\sqrt{[4.91^2 - 4.31^2]}$ = 2.35%

Coal 4: Model S.D. = $\sqrt{[6.11^2 - 5.77^2]}$ = 2.01%

Applying the t-test, the 95% confidence limits for the 16 runs of each coal is found to give the following probabilities:

Coal 1: 0.944
Coal 2: 0.994
Coal 3: 0.950
Coal 4: 0.957

It can thus be seen that the model's accuracy is approximately 95% for 95% of cases.

6.6.3. History of a Model Run

A temperature slurry burnout, coal burnout, and time elapsed history are shown in fig. 35 for run number 75. This demonstrates the necessity for an extra port between the tuyere and the present port 1, and for temperature and velocity measurements to further refine the model.

7. CONCLUSIONS AND RECOMMENDATIONS

7.0. Conclusions

7.0.0. Apparatus

7.0.0.0. Flame Measurement Techniques

The combination of "cold" pitot measurements and "hot" gas analysis seems to be acceptable. However, if plug flow had not been found the validity of this system would have been questionable. The system's capability of automated gas sampling and the subsequent ability to process the large quantities of data, necessary for calculation of an area-weighted mean reading of gas analysis, contributed greatly to the acceptability of these techniques. Again, if the system had been recirculatory, the results would have been questionable.

However, the aquisition of other data by alternative measurement techniques would be advantageous in terms of further verification of the mathematical model. Data such as gas temperature, gas velocity, particle analysis and particle size distribution would be of great benefit. Recommendations to these effects are made in section 7.1. later.

Gas temperature, in particular, would be valuable since the assumption of radiative losses from the flame in the mathematical model could be verified. At present, the simple assumption of 10% energy loss by radiation is made, as is commonly used in the calculation of flame temperature.

7.0.0.1. Air Preheating Methods

The principle of producing preheated "air" by

combustion of fuel-oxygen- air is cheaper and more readily controllable than a pebble bed pre-heater. Attempting to run too near the temperature limit of the fibre lining together with control "overshoot" combined to badly damage the lining. The damage was, however, fairly easily repaired.

7.0.0.2. Performance of Flame Tunnel Lining

The lining failure which occurred, causing an untimely end to the practical investigation, was due to the melting of the plastic pipe conveying cooling air to the steel annulus of the flame tunnel.

This melting was caused by hot exhaust gases emanating from a too-short waste gas flue. The melted pipe "folded", causing total blockage.

The waste gas flue has already been built up at the critical part.

However, it is concluded that the refractory carried out its duty adequately until this failure in air supply.

7.0.0.3. Sampling Rig Performance

As previously stated, this machine failed halfway through the work programme due to failure of the motor.

This failure was the last of several which occurred with this machine; all were mechanical.

The last failure was caused by a thread stripping from the x-axis threaded rod, jamming the machine and causing the motor to burn out.

It is concluded that this method of probe motion is unreliable without a sufficiently well machined threaded rod.

It is also concluded that the method of port location using optical methods is a more reliable technique than relying upon microswitches which invariably became incorrect in their positioning as the flame tunnel expanded during usage.

7.0.0.4. Control Computer and Instrumentation and Control Hardware

The control computer failed on two occasions, both of which were attributable to ingress of dust. It is thus concluded that the computer hardware should be isolated from potentially harmful atmosphere, preferrably having a separate filtered air supply. The machine is adequate for its' purpose, since no great speed is required due to the slow system responses.

The electro-mechanical multiplexer failed on several occasions, some of which were attributable to the relay unit, some attributable to the inherent vulnerability of electromechanical devices and some attributable to unprofessional construction. Even when working properly (as it did for the majority of the time), the eight-bit resolution of the original ADC was clearly inadequate when accuracy was required at the "low" end of orifice plate flows due to the signal being proportional to the square root of the flow.

Fortunately the aquisition of two 12 bit 16 channel ADC's overcame this problem and it is concluded that they are satisfactory, giving very few problems.

The 8-bit digital to analog converter was of adequate resolution providing the 0-5v span coincided with the full span of the device being controlled. This necessitated considerable adjustments and alterations to ballast resistors. It is thus concluded that a 12-bit analog to digital converter is very desirable.

The relay unit gave some difficulties as stated above. These difficulties were mainly due to the machine responding on occasion to the IEEE-488 signals to the D to A converter, and were therefore confined to channels 1-8 on the relay unit. Since the probe moving routine utilized channels 14-16 on the relay unit and was thus unaffected, this problem became unimportant after the aquisition of the 12-bit ADC's. It is thus concluded that this unit is adequate, providing not more than eight channels are required.

The unity gain amplifiers gave no difficulties, and it is concluded that they are satisfactory.

The electrical to pneumatic converters performed satisfactorily, except that the silicone oil was lost from one machine due to poor gasketting. This was quickly rectified, and it is concluded that these machines are satisfactory.

The pneumatically operated valves performed satisfactorily at all times, and are concluded to be satisfactory.

The differential pressure transducer which measured the combustion air flow across the orifice plate had a square root extractor fitted whilst 8-bit analogue to digital conversion was still being used. However, it is concluded that this addition is now unnecessary

since 12-bit conversion provides adequate resolution even at the lowest turndown conditions.

7.0.0.5. Computer Control Software

As mentioned in 7.0.0.1. above, control "overshoot" of air preheat temperature on start-up was partly responsible for damage to the combustion chamber fibre lining, and it is concluded that this defect must be rectified before further work is undertaken.

Back-purging of the measurement probes is needed so as to minimise blockage when sampling near the root of the flame, and the software for carrying this out must be implimented, together with the software necessary for gas temperature and velocity measurements.

With the above reservations, it is concluded that the software is satisfactory.

7.0.0.6. Slurry Supply System

This was responsible for the majority of the inaccuracies in the measurements taken on the rig.

Although, on an average of the sixteen runs for each coal, the supply was accurate the standard deviations were considerable (see 7.0.2.0. later)

There is no particular pattern discernable in the results obtained at Port 4 (see Appendices 4.2.0. to 4.2.4.) which could lead to a firm conclusion as to the variations in flow.

However, the very indirectness of the pumping circuit with its large reservoir results in long response times between DAC signal to the peristaltic pump and response in terms of steady-state flowrate.

Adding the previously mentioned stalling of the pumps at the lower speeds, the result is a distribution of flows around the nominal mean.

It can only be concluded that it is essential to know the flowrate of the slurry at the time of sampling as the flows of propane, oxygen and air are currently known.

The burnout can then be calculated using the known slurry flow as well as gas flows and analyser response time can be built in, so that the readings represent the actual stoichiometry obtaining.

This would be preferable to the present systems which is a stoichiometry based on actual gas flows obtaining at the beginning of the traversing of the port and a slurry flow which is assumed to be the calculated requirement.

However, it can also be concluded that the peristaltic pump set-up is by far the most suitable from the point of view of abrasion by the slurry.

7.0.0.7. Accuracy of the Apparatus

The results in Section 6.3.3. show that there is approximately a 0.9 probability of being with the 95% confidence limits. Since the results are used for calibration of a mathematic model, this low accuracy is not as serious as if the results were to be used individually.

However, it must be concluded that a major objective must be to improve the accuracy of slurry flow measurement in the apparatus.

7.0.1. Mathematical Model

7.0.1.0. Dimensionality of the Model

In view of the fact that there is little recirculation in the combustion space, and that the flow pattern - at least by the first port - is virtually plug flow, then it is concluded that a one-dimensional model is perfectly adequate for the study of tuyere raceway conditions.

7.0.1.1. Adequacy of Available Hardware

The actual running of the full set of the mathematical model is an easy task for almost any microcomputer. It is the very large number of runs carried out during the optimisation procedure which presents problems with the adequacy of the hardware.

It is unlikely that there will be a great increase in the centralised computing power in the near future.

However, the use of the "Sirius" microcomputer has been successful for this type of work. The overnight availability of a number of these machines, normally used as word processors rendered the optimisation procedure possible.

The travel necessary between the laboratory and the Research Centre is, however, inconvenient.

It is well known that analog computers[92] are far more suitable than digital machines for long integration procedures, and it is concluded that a machine of this type, hybridized with a microcomputer, is worth investigation.

7.0.1.2. Adequacy of the Optimisation Process

It is concluded that, with the present hardware, the optimisation process is adequate but extremely inconvenient. The most cost-effective method of improving the technique is outlined in 7.1.2.2.

7.0.1.3. Results from the Mathematical Model

As pointed out in 6.6.1. the results at Port 4, where complete burnout is assumed, shows that the standard deviations of the model results is only slightly higher than the standard deviations of the experimental results, which implies that it is the vagaries of the experimental results which is at fault.

Since the criteria of judgement of the model was aginast the mean of the results for each coal, and the means of the experimental results show good agreement of burnout at port 4, it can be concluded that, for any individual set of circumstances the model gives a more accurate result than any individual experimental run.

7.0.1.4. Confidence Limits of the Mathematical Model

As shown in 6.6.2. the probability of correctly

estimating burnout is approximately 0.95 at the 95% confidence level.

It is concluded that, for the technological rather than scientific purposes for which this model was devised, the accuracy of the model is adequate.

7.0.2. Conclusions on the Combustion of Coal-Oil Mixtures

7.0.2.0. Atmomisation and Mixing

For a coal-oil slurry of 40% coal by weight, some 20-30% appears as free coal particles on atomisation, i.e.0.5 - 0.75 of the coal content.

This quantity of free coal varies according to both the mean droplet size distribution of the slurry, and the mean particle size and distribution of the coal. The criterion of six "overlaps" means that particles of greater than 0.14 of the size of the corresponding droplet cannot stay with that droplet on atomisation.

The net results is that the smaller coal fractions are almost entirely remain within the oil droplets upon atomisation.

The Toor mixing index was adequate for this non-recirculating system.

7.0.2.1. Combustion of Slurry

It appears that the model of Braide[43] et al is substantially correct. This is where the slurry droplets-with fine coal particles enclosed - burns very much like heavy fuel oil.

The more recent work of Jenkins[98] et al propose a "plum pudding" model of slurry combustion for high volatile coals, but a separate combustion for anthracitic coals, paralleling this work.

7.0.2.2. Combustion of Coal Particles

This work programme has only investigated low volatile anthracite and coke breeze, and the provision for volatile matter evolution was unnecessary. Combustion of these materials took place under conditions of diffusion limited combustion and thus internal burning was not in evidence. Clearly the diffusion limitation was due to both:

(i) The smaller size fractions of coal combusting in the slurry droplets.

(ii) The very high values of gas temperature making the value of the surface reaction rate coefficient very high.

It might be expected that, with such high velocities encountered, microturbulence might make a notable contribution to the combustion processes. However, no readily discernable systematic errors can be noticed between 200 and 240ms^{-1} blast velocities. It might well be that microturbulence does exist in the earlier stages of combustion, and is reflected in incorrect results for droplet size distribution of the slurry. It is thus concluded that an earlier port is needed to verify this phenomenon, and the rate constants of the mathematical model may then be modified as suggested by Spalding[99].

7.1 Recommendations For Future Work

7.1.0. Other Technique of Coal Injection

7.1.0.0. Background

The two other processes which are being considered for the injection of coal into the blast furnace tuyere are: (i) a modification of standard pulverised fuel practice, with allowance made for the higher working pressures temperatures etc., (ii) coal slurried with additives in water.

The two process each have their advantages and disadvantages. These may be summarised as follows:-

	Air Transport	Water Transport
Advantages	(i) Massive injection rates are possible due to small RAFT depression. (ii) Existing systems are available "off the shelf".	(i) Extremely safe medium in a hazardous environment. (ii) Very low cost of installation. (iii) Relatively low running costs.
Disadvantages	(i) Very high first cost. (ii) Relatively high running costs. (iii) P.F. Constitutes a potential hazard.	(i) Only low injection rates are possible due to large RAFT depression. (ii) Not available "off the shelf"

Both systems are being tried on a pilot plant basis within the British Steel Corporation but optimisation of the system requires further research, amongst which is the

combustion properties of the coals for each system.

7.1.0.1. Coal Injection Combustion Research Programme

A recommendation as such is not being made here with regard to research into coal injection systems.

A programme of work has already been proposed for research into combustion in the tuyere raceways utilizing the practical and mathematical modelling techniques expounded above. The proposal has been accepted by the British Steel Corporation and the European Coal and Steel Community has also decided to contribute to the funding of the project.

The attraction of coal-water slurries lie in the elimination of the large proportion of oil-based slurry energy and, at least conceptually, the cost of such a slurry can approach that for pulverised fuel.

However, considerable difficulties exist in the optimisation of such a process, and the aims of the research programme will be as follows:-

(i) The optimisation of coal "grind".

(ii) Optimisation of atomisation of coal-water slurry, including the study of production of free coal particles.

(iii) Evaporation of the slurry droplets, and the subsequent combustion of the residual coal particles.

(iv) The effects of injection level, oxygen enrichment, air preheat temperatures and air velocities on the

combustion processes.

It can be seen that the programme is an extension of the coal-oil slurry programme, but will be considerably longer in terms of the number and degree of grinding of the coals to be studied.

The work programme will be repeated, except in the case of point (ii) above, for air-carried pulverised coal.

The mathematical modelling of the combustion of air-carried coal will be very simple; a modification of the existing coal oil programme will suffice.

However, the modelling of the coal-water slurries offers an interesting challenge in terms of droplet evaporation and the subsequent burnout of the residues. Optimisation of an "agglomerated residue" model is foreseen, as well as on a separate model involving the separation of the particulates on evaporation of the droplet. The better model will be developed in more detail.

7.1.1. Recommended Modification to Apparatus and Controlling Software

7.1.1.0. Flame Measurement Modifications

This is the greatest weakness inherent in the work programme on coal-oil mixtures.

A new probe-combining both gas sampling and pitot measurement at a single point-is currently under construction. It will be of considerably stouter construction than the rebuilt "Land" type probe used in this work and will be used in conjunction with a

micromanometer, which will be interfaced to the computer resulting in integrated velocity measurement over the time of gas sampling.

Additionally, an experimental temperature measurement probe is planned. This will consist of a low thermal mass ceramic - shrouded precious metal thermocouple which can be suddenly thrust from a cooled probe to the point in the gas which is to be measured. The transient response will be measured up to the safe temperature limit of the thermocouple. Since this will take a relatively short time, a machine-code scanning programme must be prepared to take several hundred samples in the few seconds available.

The response will be of the exponential form:-

$$T_t = T_f \left[1 - \exp(kt)\right]$$

where T is temperature, k is the time constant of the system and t is the elapsed time. The subscript t refers to the value obtaining at time t, and subscript f refers to final value.

The data must then be selected to eliminate initial lag of the curve, and the remaining points used to put a "best fit" of the exponential equation to the data. The final temperature may thus be found without exceeding the working temperature of the thermocouple.

The result of this is that with velocity known from the pitot readings, temperature known from the transient probe and gas analysis known, a mass flow gradient across the flame can be accurately constructed, and the "burnout" measurements treated accordingly.

7.1.1.1. Modifications to Combustion Chamber

The differential of recommended temperature maximum (1160°C) and the actual maximum running temperature (1000°C, but 1100°C was attempted) proved to be too small. Future work (see 7.1.0.1.) requires a preheat of 1200°C, and so a material capable of withstanding 1450°C is recommended.

7.1.1.2. Modifications to Flame Tunnel

The refractory damage referred to previously occurred due to cooling air failure, and inleakage of cooling air was also responsible for distortion of gas analysis readings close to the tunnel wall.

It is therefore recomended that the air cooling be changed to an induced draught system with the provision of warning of cooling air failure.

With a self-purging sampling probe, a new port should be inserted between the model tuyere and port 1, so that the model may be optimised at the earlier stages of combustion.

7.1.1.3. Modifications to Sampling Rig

The threaded rod type of probe movement was relatively unsuccessful, resulting in unreliability due to wearing threaded surfaces and slow movement giving low productivity. It is recommended that this system of propulsion be replaced by toothed-belt drive, but retaining the successful optical system of port location.

7.1.1.4. Modifications to Control Computer and Instrumentation Hardware

(i) Instrumentation

Since the future work programme will require air preheat temperatures of 1200° and 800°C, the resultant air flows will be lower than at present at constant velocity. In order to retain adequate control at these lower flow rates, the air orifice plate must be altered.

(ii) Wiring Systems

The wiring was carried out on a very low budget and consists entirely of "twisted pair" cabling and screw block connectors. It is recommended that this be replaced by multicore screened cabling with D-plug connectors for rapid alteration.

(iii) Computer Hardware

Analog-to-Digital converters of 12-bit resolution have already been substituted for the original 8-bit ADC and multiplexer. However, to take full advantage of the greater accuracy bestowed by these machines, it is recommended that a 12-bit Digital to Analog converter of at least 16 channels is added to the apparatus. Another recommended modification is to provide a hermetrically sealed cabinet or office provided with filtered air. It is remarkable that the computer hardware and the interfacing did not suffer more from environmental problems.

The third recommendation - currently being implemented - is to link the "PET" control microcomputer

with the "SIRIUS" mathematical modelling microcomputer via the IEEE-488 bus.

This results in faster data transfer, eliminating the requirement for hard copy of results from the "PET" and subsequent tedious keyboard entry of the data to the "SIRIUS".

7.1.1.5. Modifications to Control Computer Software

Modifications need to be used to the software to limit the temerature overshoot which occurs on start-up of the air preheat routine. This overshoot was largely responsible for the damage to the fibre lining of the combustion chamber.

7.1.1.6. Modifications to Slurry Supply System

There are now instruments available for accurate measurements (better than 1%) of fluid flow by electromagnetic induction in the liquid. This is only applicable to electrically conductive liquids such as water slurries. It is therefore recommended that such an instrument be obtained for the imminent work programme on coal-water slurry combustion.

7.1.2. Recommended Modifications to Mathematical Modelling Technique

7.1.2.0. Model Dimensionality

There is good agreement obtained between the area-weighted mean readings of the rig and the one-dimensional mathematical model, as concluded in 6.6. It is thus recommended that, in the regimes of low-or no-recirculation encountered in the tuyere environment, the one-dimensional mathematical model is perfectly

adequate. Two dimensional models are thus deemed unnecessary at this stage.

7.1.2.1. Model Optimisation

If a hybrid computer were used in the mathematical modelling process, the model optimisation would be extremely rapid. The limiting factors of speed would purely be the I/O time of the disks and interfaces, probably of the order of 3 seconds per run. In this set of circumstances a three dimensional matrix of mesh size 10 and a set of 64 runs could be executed in some 55 hours. Optimisation clearly becomes very rapid and such a hybrid computer is clearly a very powerful tool, particularly if the input variables can be maximised, for flexibility, up to the maximum of 32 channels available on two DAC units.

7.1.2.2. Hardware Alterations for Model Execution

As previously mentioned a minicomputer (time -sharing) or 16-bit microcomputer running on compiled BASIC take about 9 minutes per "run" of the model. The majority of this time is utilized in the long numerical integration routines.

In Russia[92] analog computers have been used in speeding up the integration routines, but a modern hybrid computer is a particularly attractive proposition. The hybrid computer would consist to:-

(i) A SIRIUS 16-bit microcomputer with 256K bytes of memory.
(ii) A Digital-to-Analog 12-bit resolution converter to programme the analog computer accurately.
(iii) Analog-to-Digital 12 bit resolution converters to read the answers from the analog computer (iv) The

analog computer proper constructed from operational amplifiers and other standard components.
(v) Line printer.

The cost of implimentation of the scheme would be relatively low, only one extra DAC being required in addition to the existing and recommended equipment used by the "PET" for rig control.

A notional scheme, using the existing "PET" related hardware and the recommended linking of the IEEE-488 buses of the "PET" and the "SIRIUS" is shown in fig. 36.

It can be seen that the rig could not be run simultaneously with the analog computer, but this is no great disadvantage given the speed of the hybrid. The "switch" selecting hybrid computer or rig is purely notional, taking the form of the "D" plugs mentioned earlier.

7.1.3. Application of the Mathematical Model to a Full-Size Tuyere

It is recommended that the results of Taggart et al[100] in respect of the degree of gas recirculation in the tuyere raceway be awaited. This will allow a modified model of considerable accuracy.

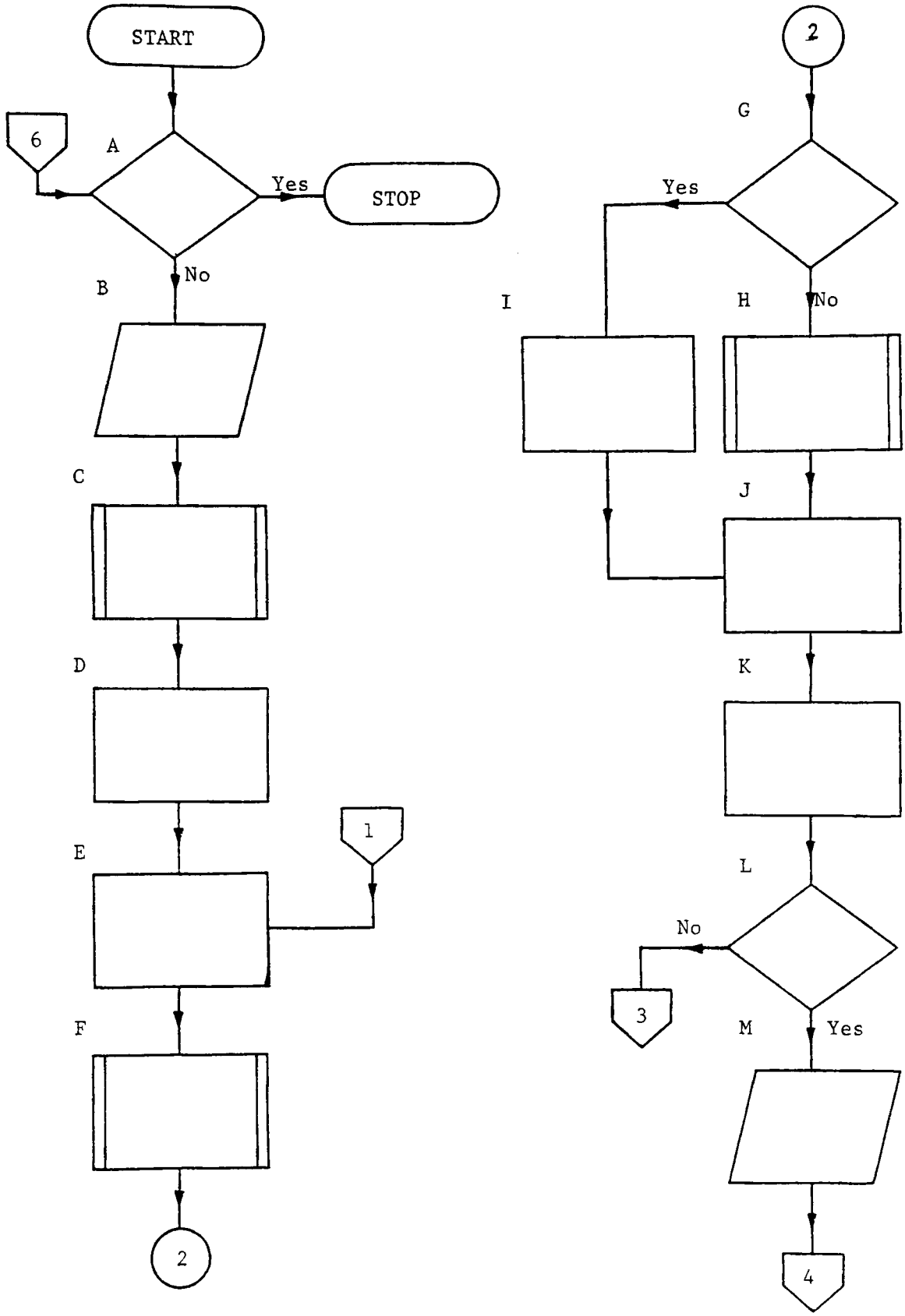

SIMPLIFIED FLOW CHART OF SLURRY COMBUSTION MODEL

FIG.1

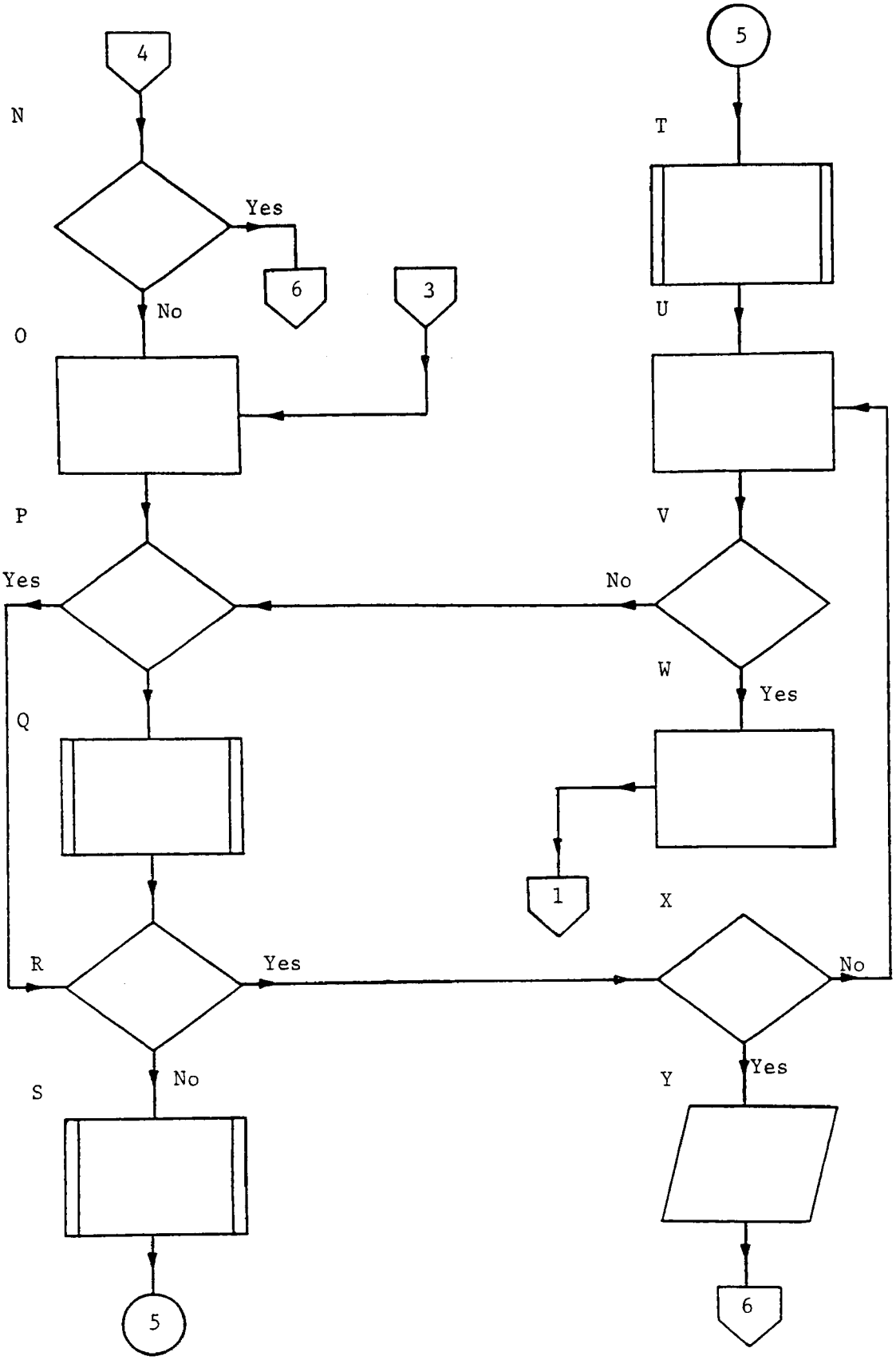

FIG.1
(Continued)

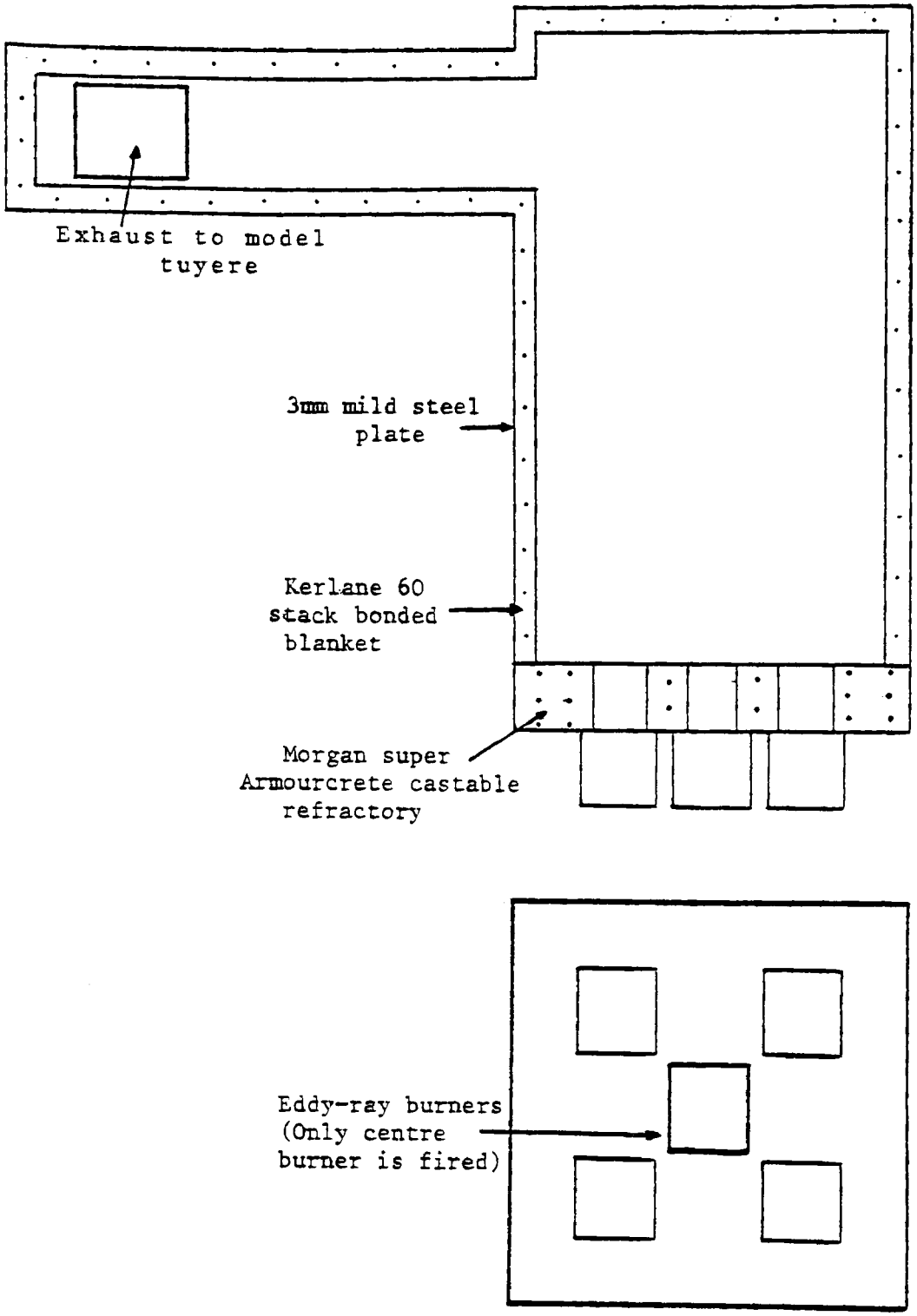

GENERAL ARRANGEMENT OF AIR PREHEATING COMBUSTION CHAMBER

(Approximate scale 15:1)

FIG.2

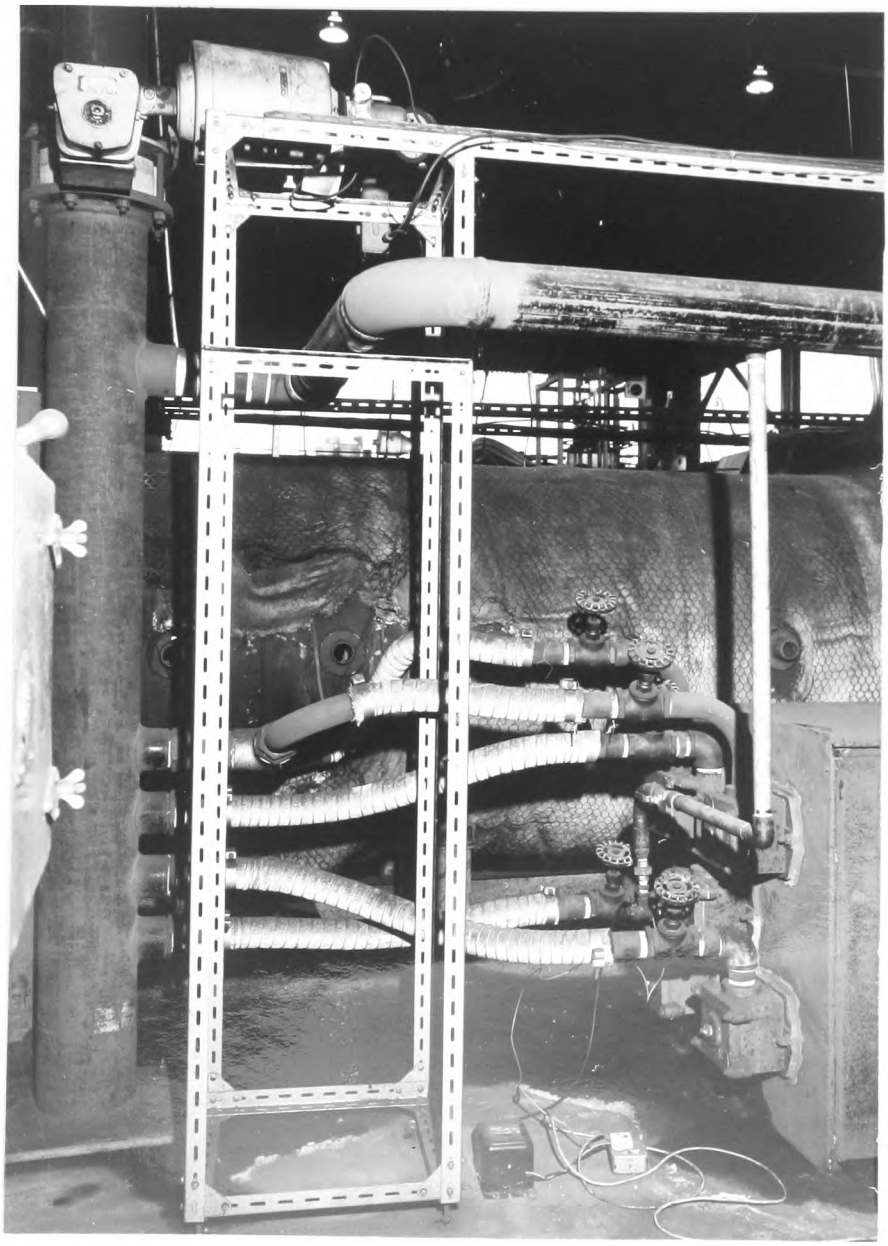

View Of Burners Of Combustion Chamber Showing Air And Oxygen Mixing Points **Fig 2(b)**

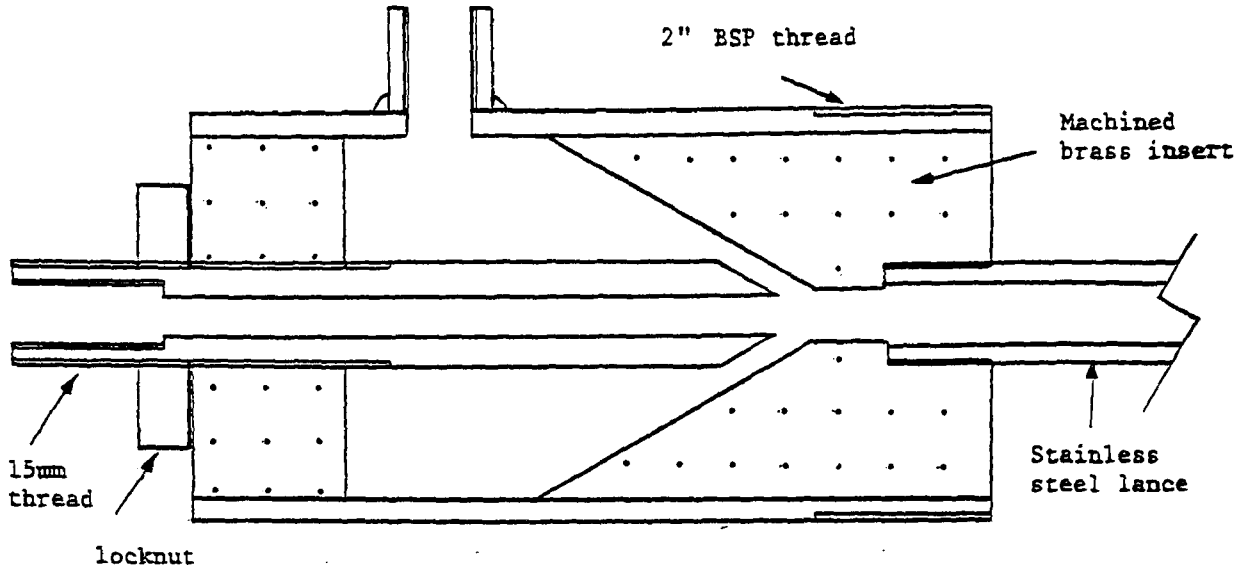

(b) ATOMISER HEAD (Approximately life size)

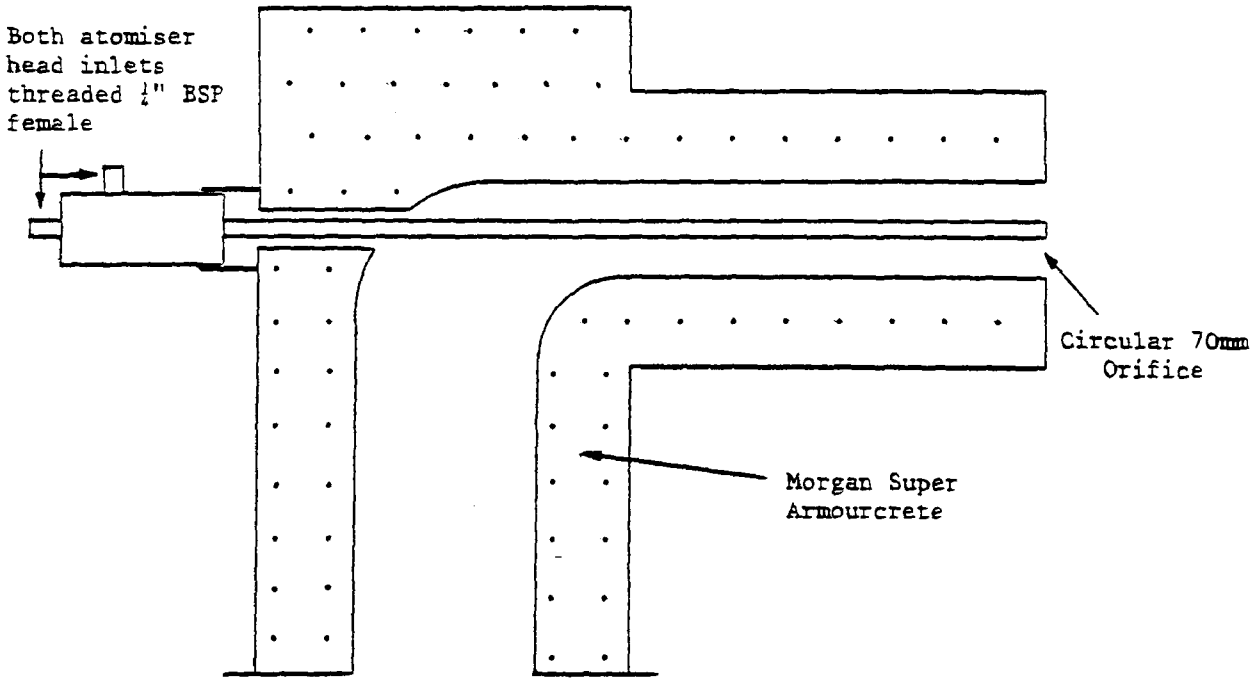

(a) REFRACTORY TUYERE AND LANCE (Approximately 1/5 scale)

FIG.3

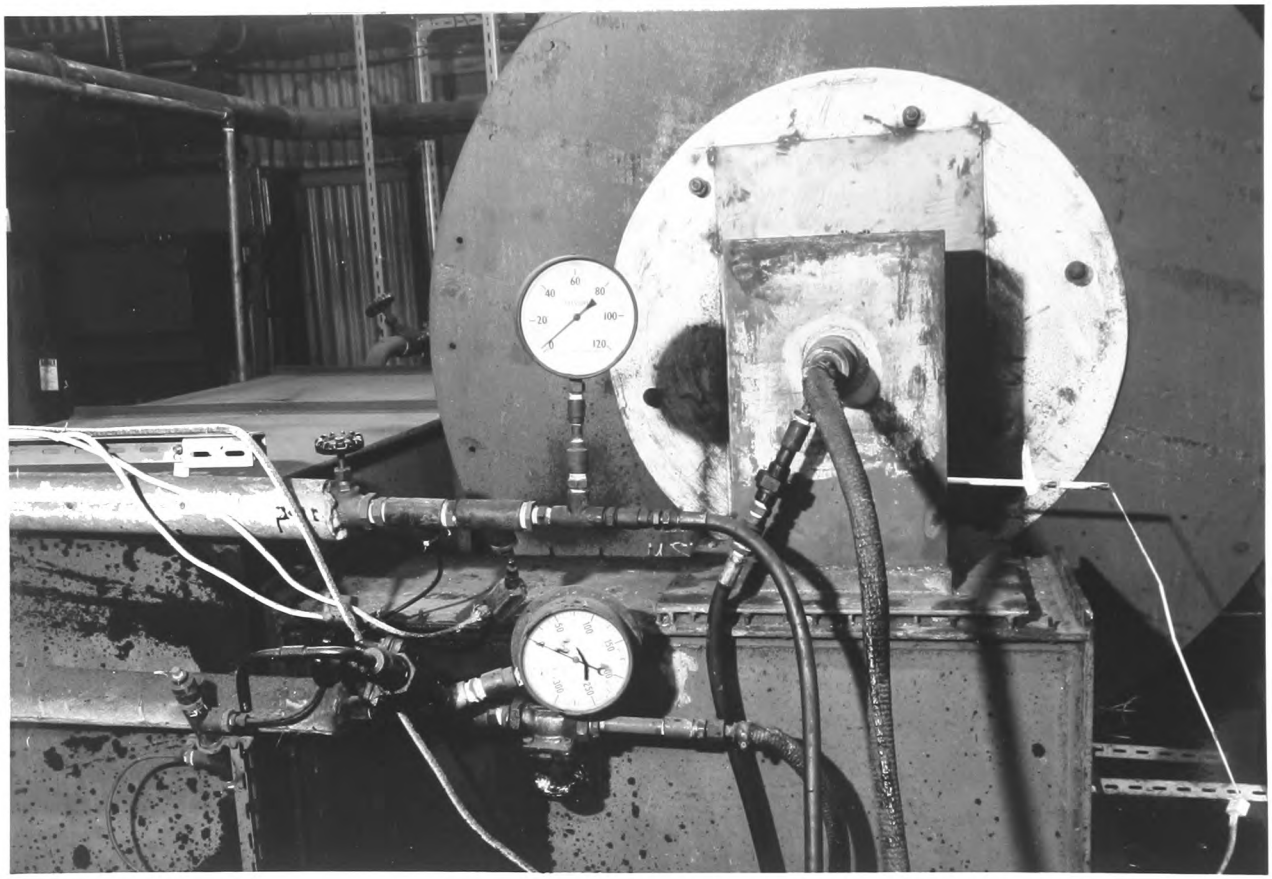

View Of Tuyere And Atomising Head **Fig 3(b)**

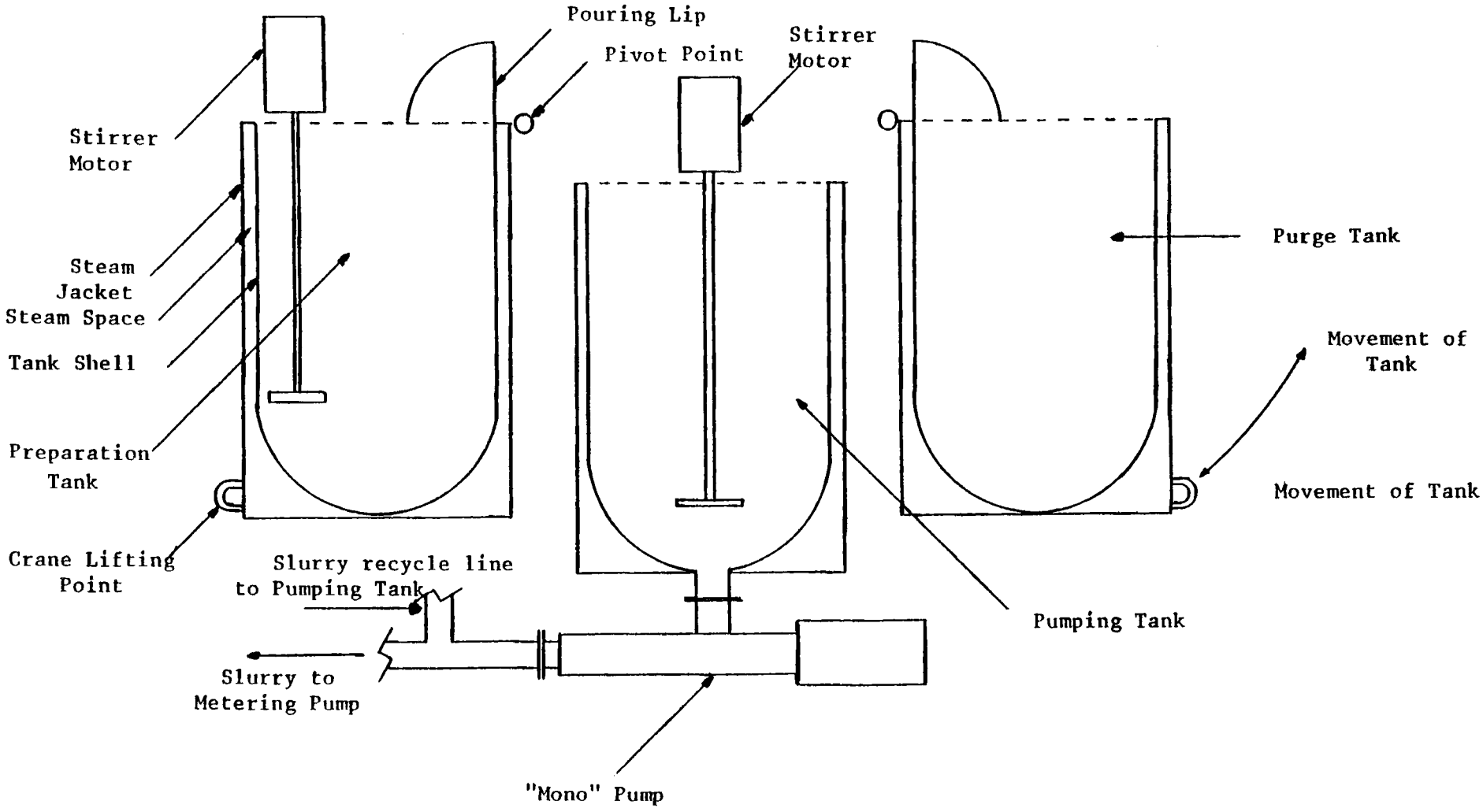

FIG. 4

MIXING AND PUMPING RIG

(Tank support details ommitted for clarity)

Scale 20:1

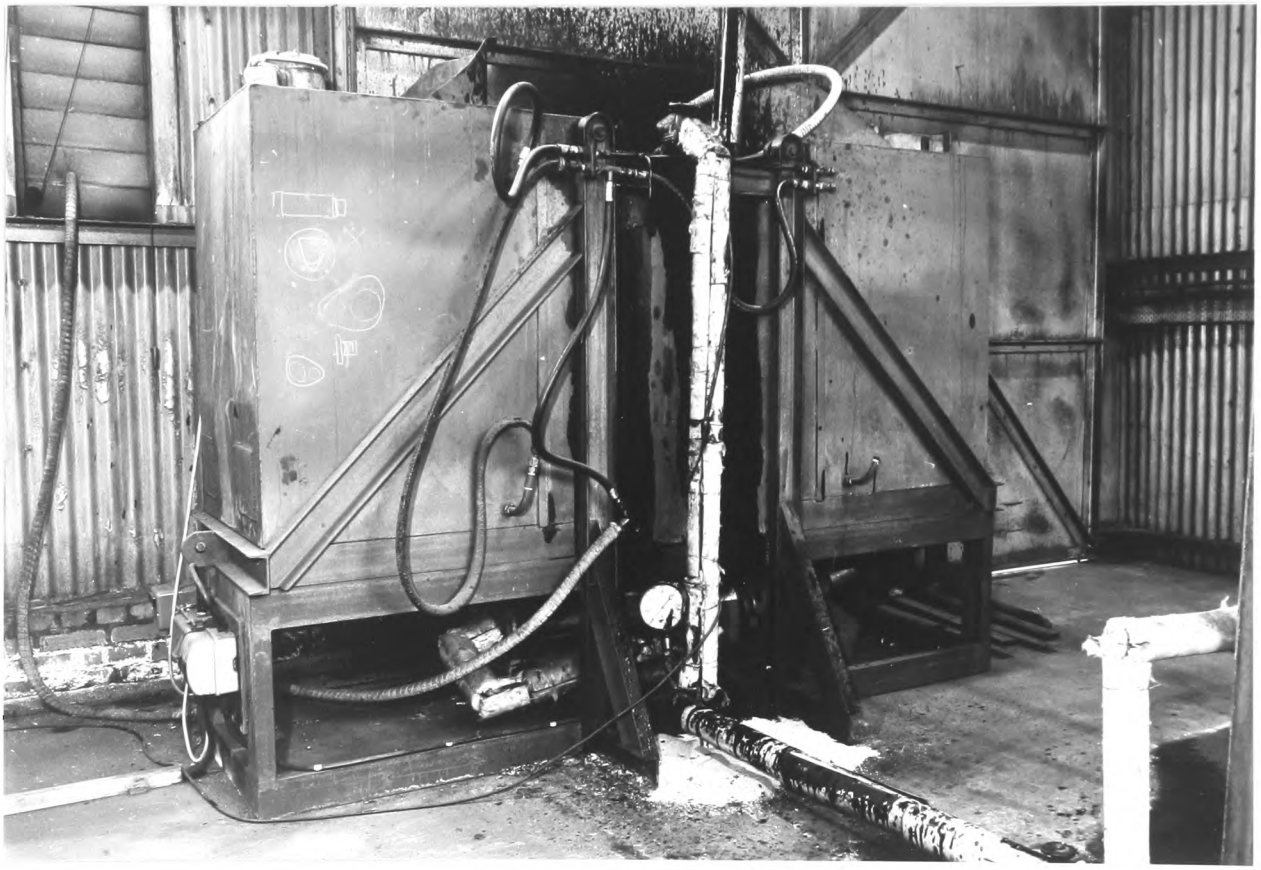

General View Of Mixing And Pumping Rig **Fig 4(b)**

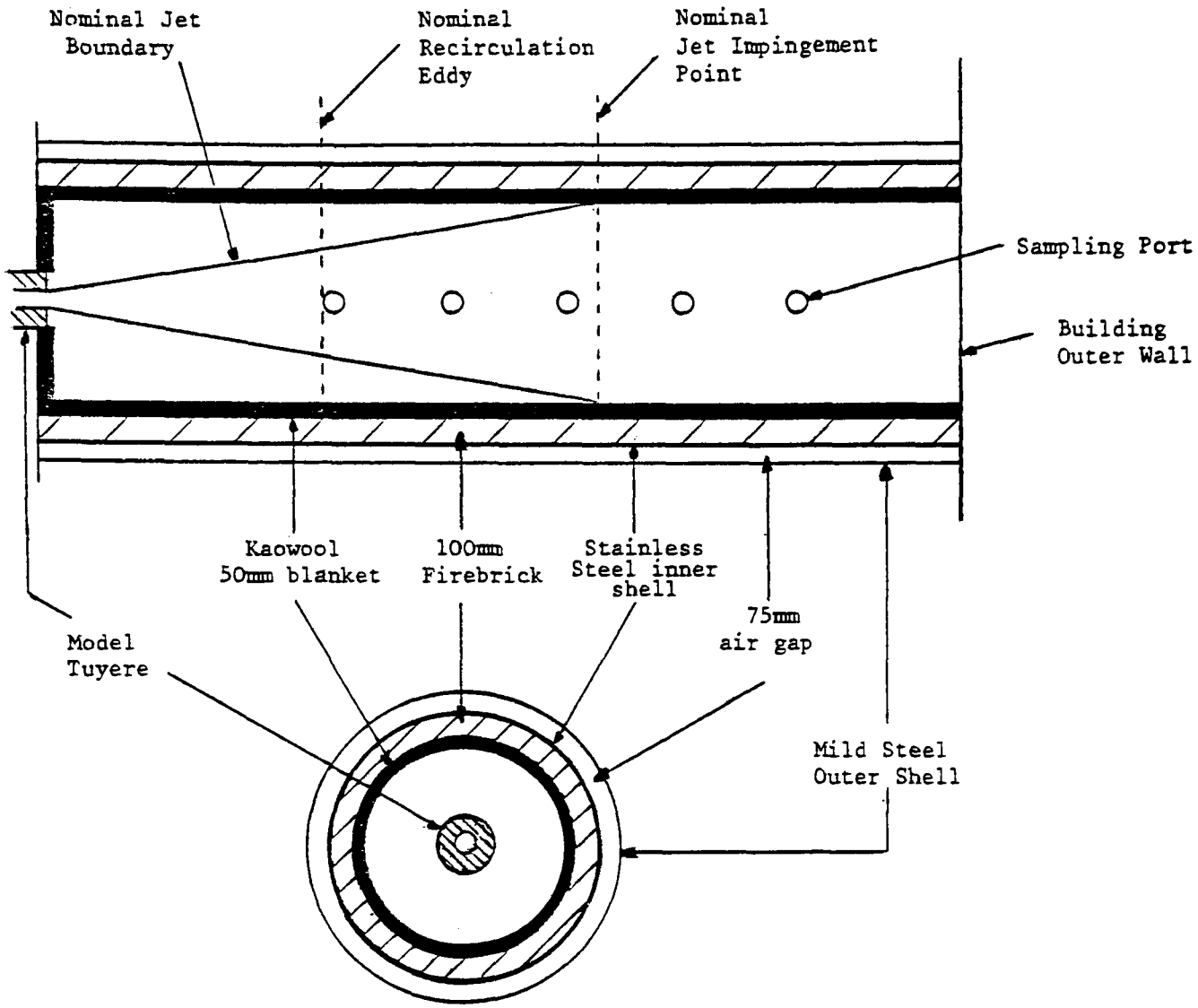

SECTION OF FLAME TUNNEL

(Scale approx. 25:1)

FIG.5.

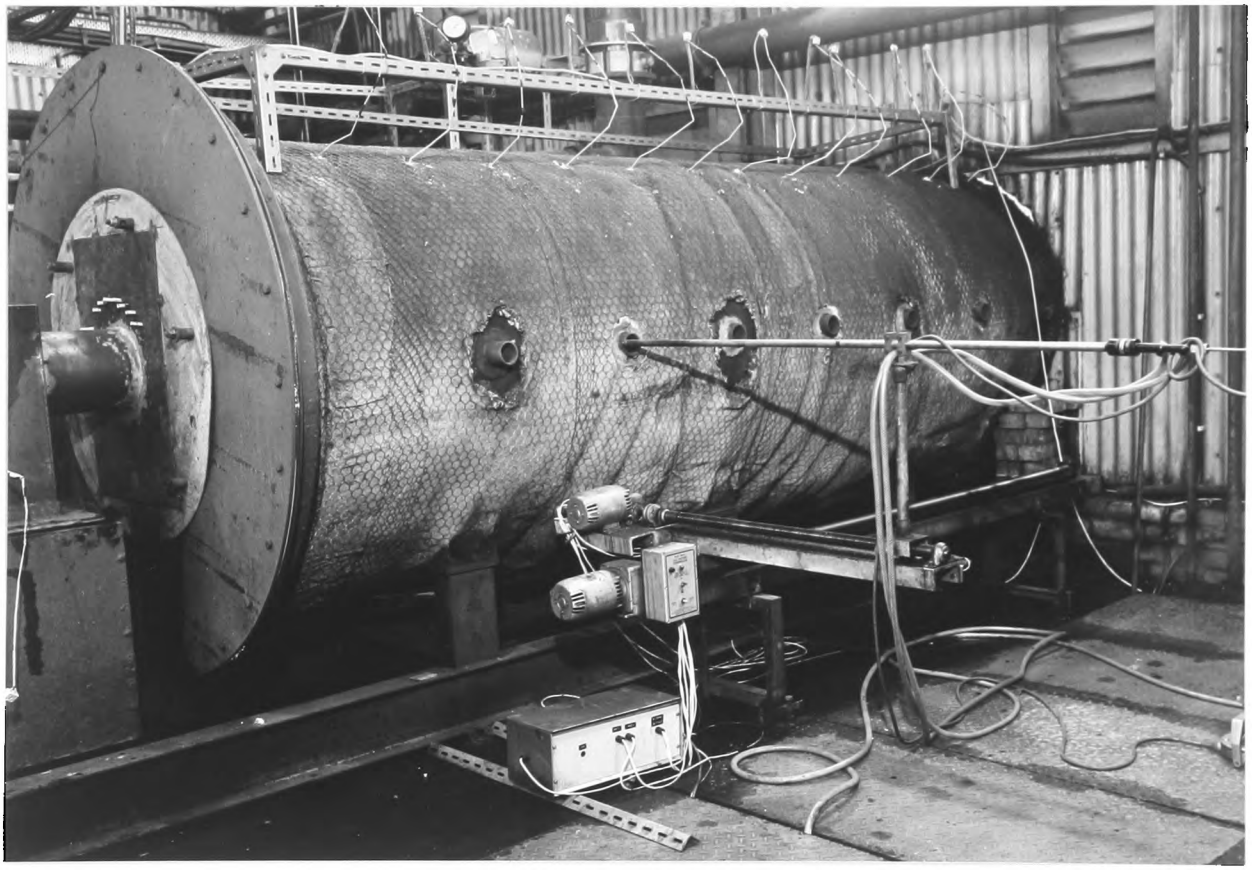

Sampling Rig Fig 6

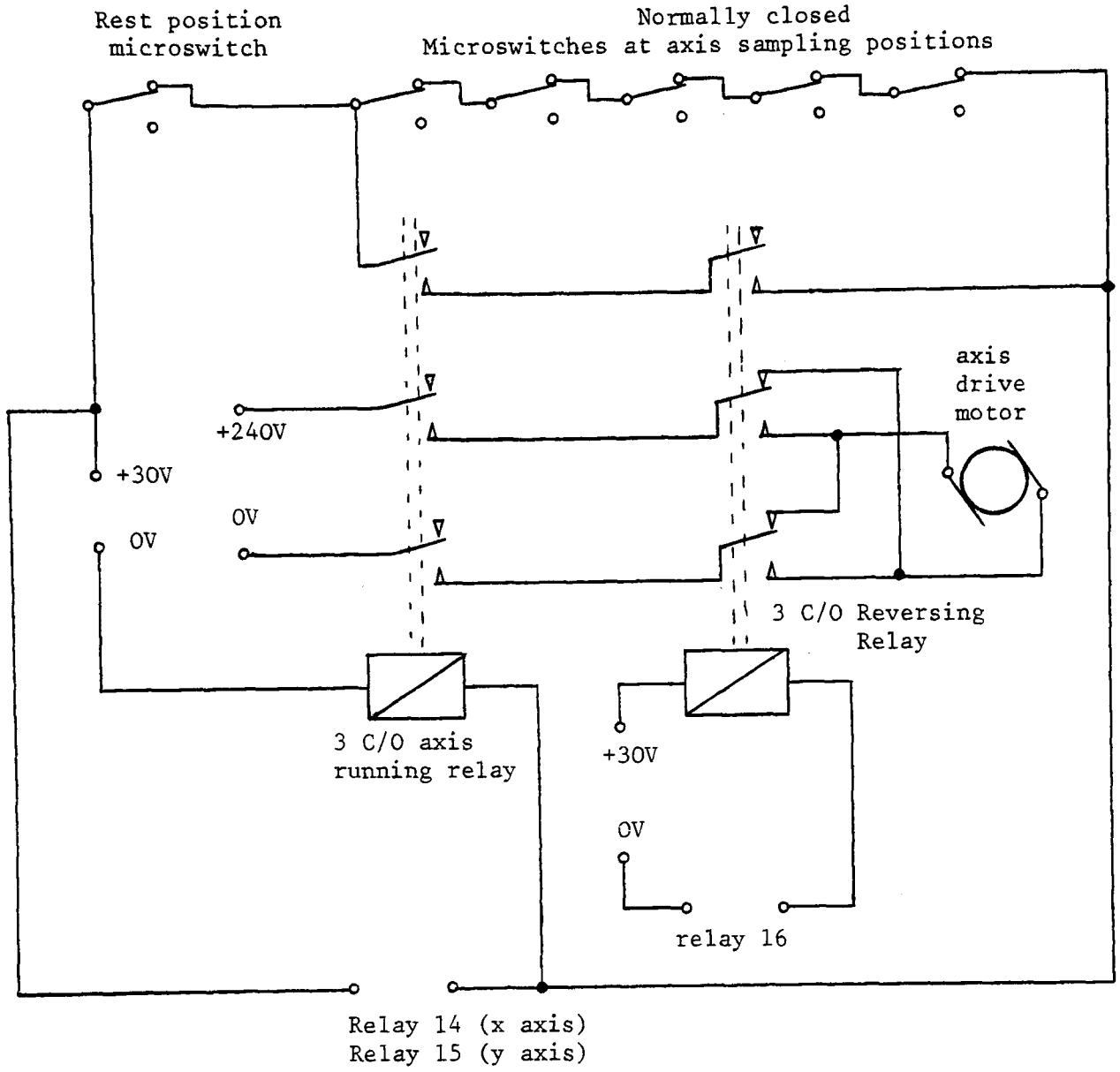

WIRING DIAGRAM FOR ONE AXIS OF SAMPLING RIG

FIG.7.

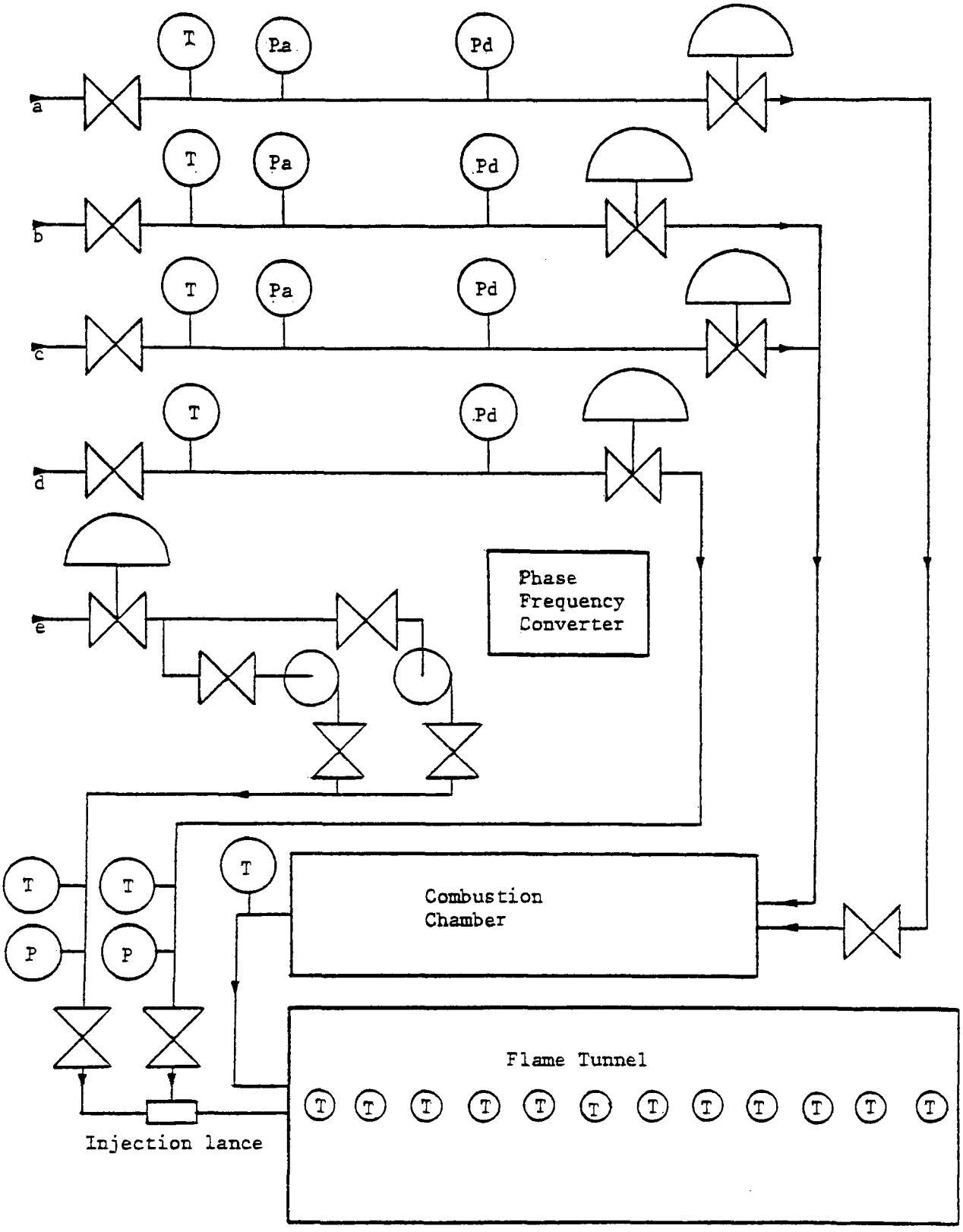

SCHEMATIC DIAGRAM OF MEASUREMENT AND CONTROL SYSTEM

a - from Propane tanks
b - from Air fans
c - from oxygen main
d - from steam main
e - from mixing and pumping rig

FIG.8.

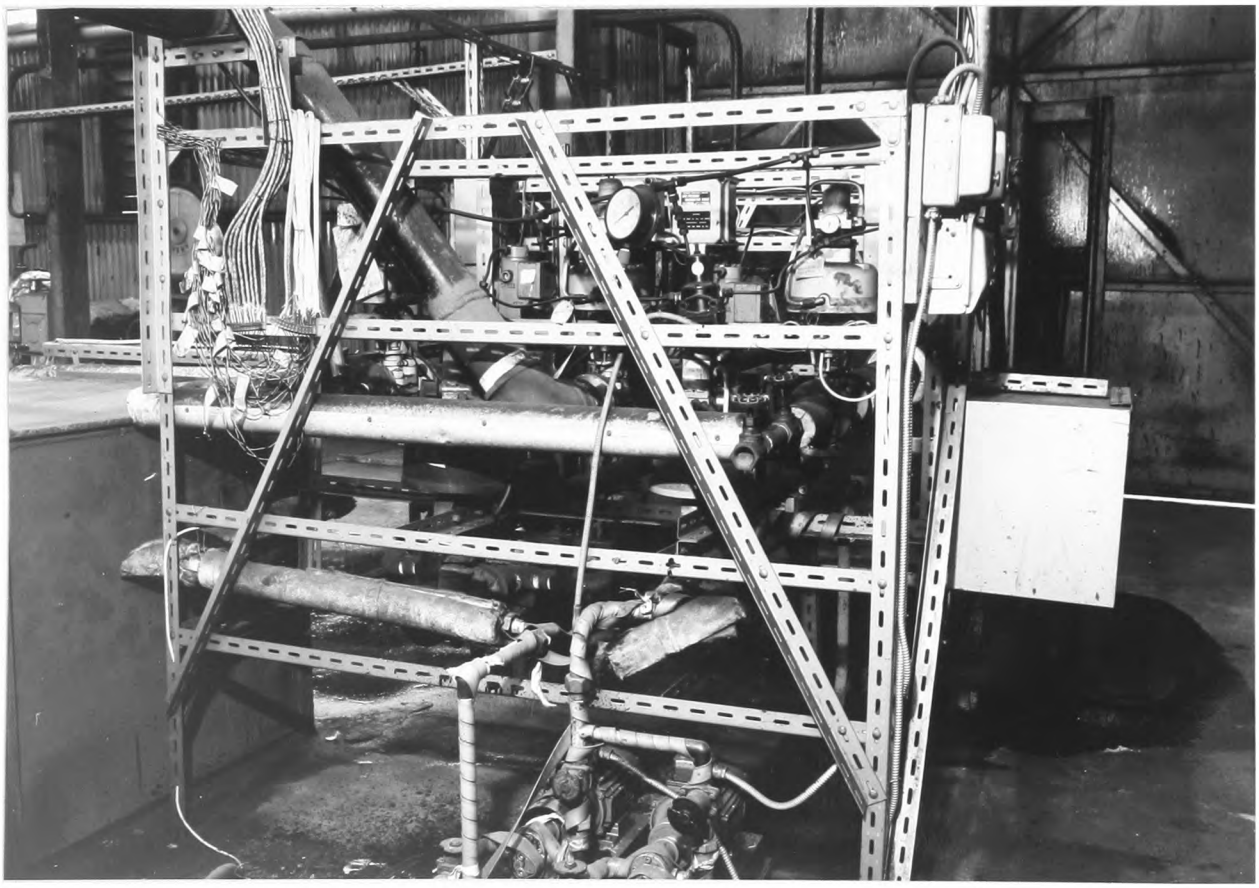

Measurement And Control Rig **Fig 8(b)**

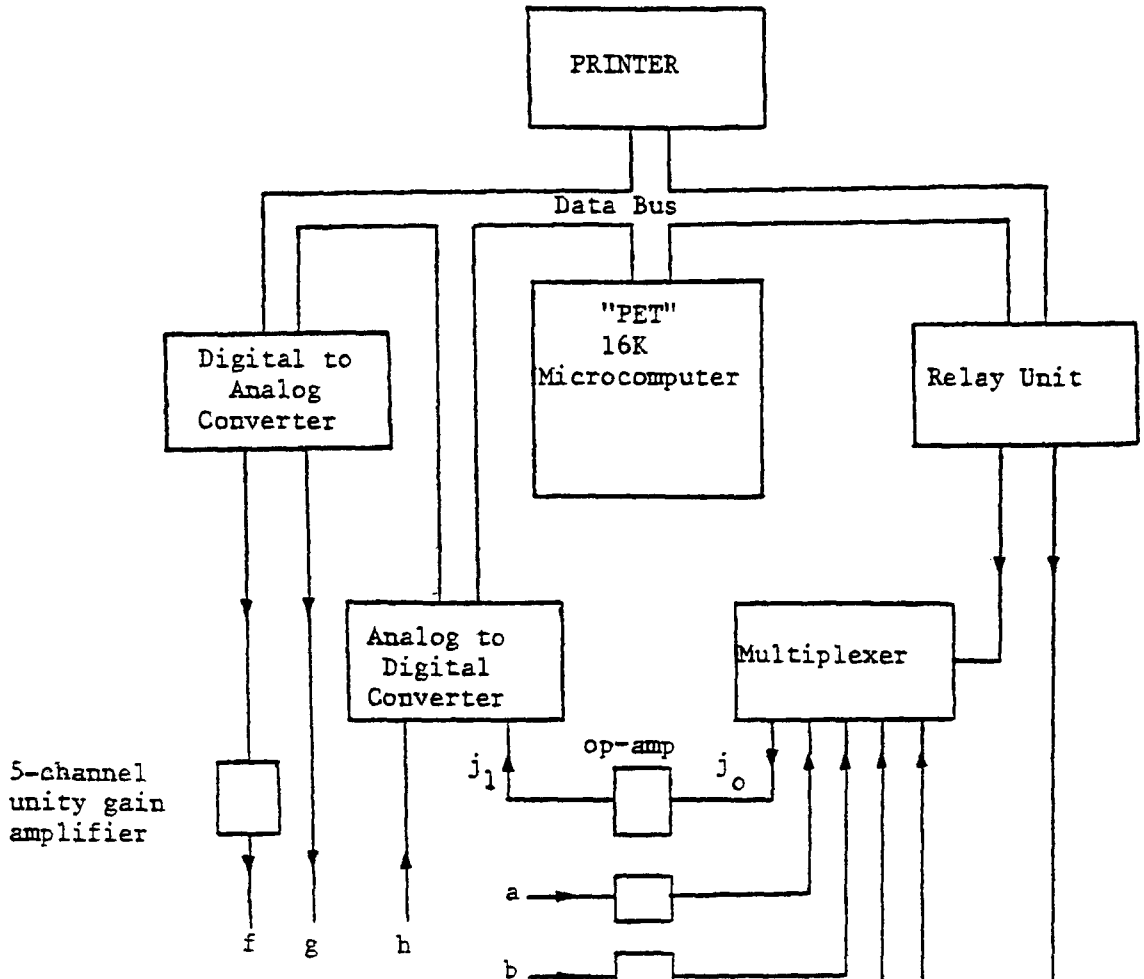

Key

a - signals from analysers (5)

b - signals from D.P. transducers (4)

c - signals from A.P. transducers (3)

d - signals from thermocouples (18)

e - control signals to sampling rig (3)

f - control signals to valves (5)

g - control signal to phase frequency converter (1)

h - status signals from sampling rig (2)

j_o, j_i - Multiplexed signals

SIMPLIFIED WIRING DIAGRAM OF DATA COLLECTION AND COMPUTER CONTROL SYSTEM

FIG. 9

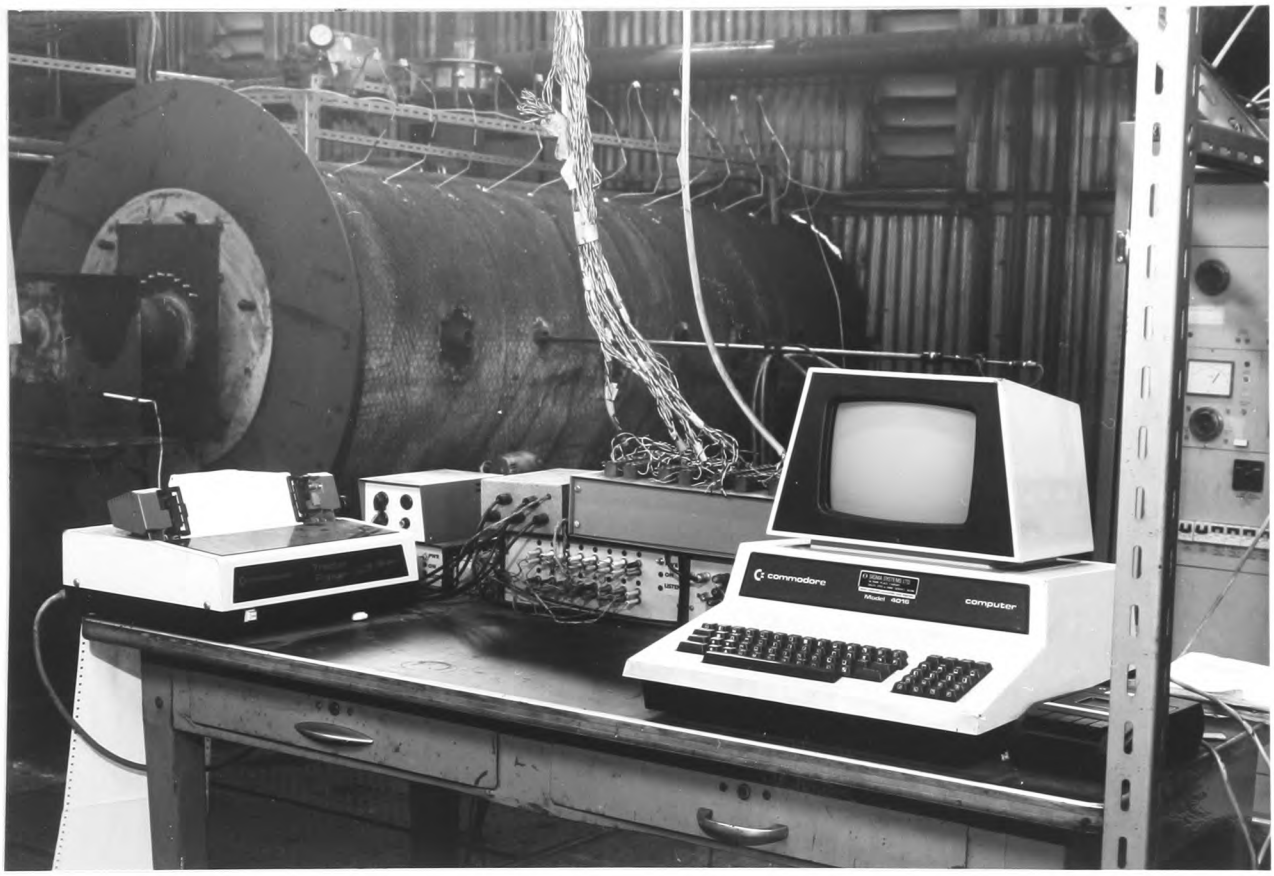

View Of Data Collection And Computer Control System

Fig 9(b)

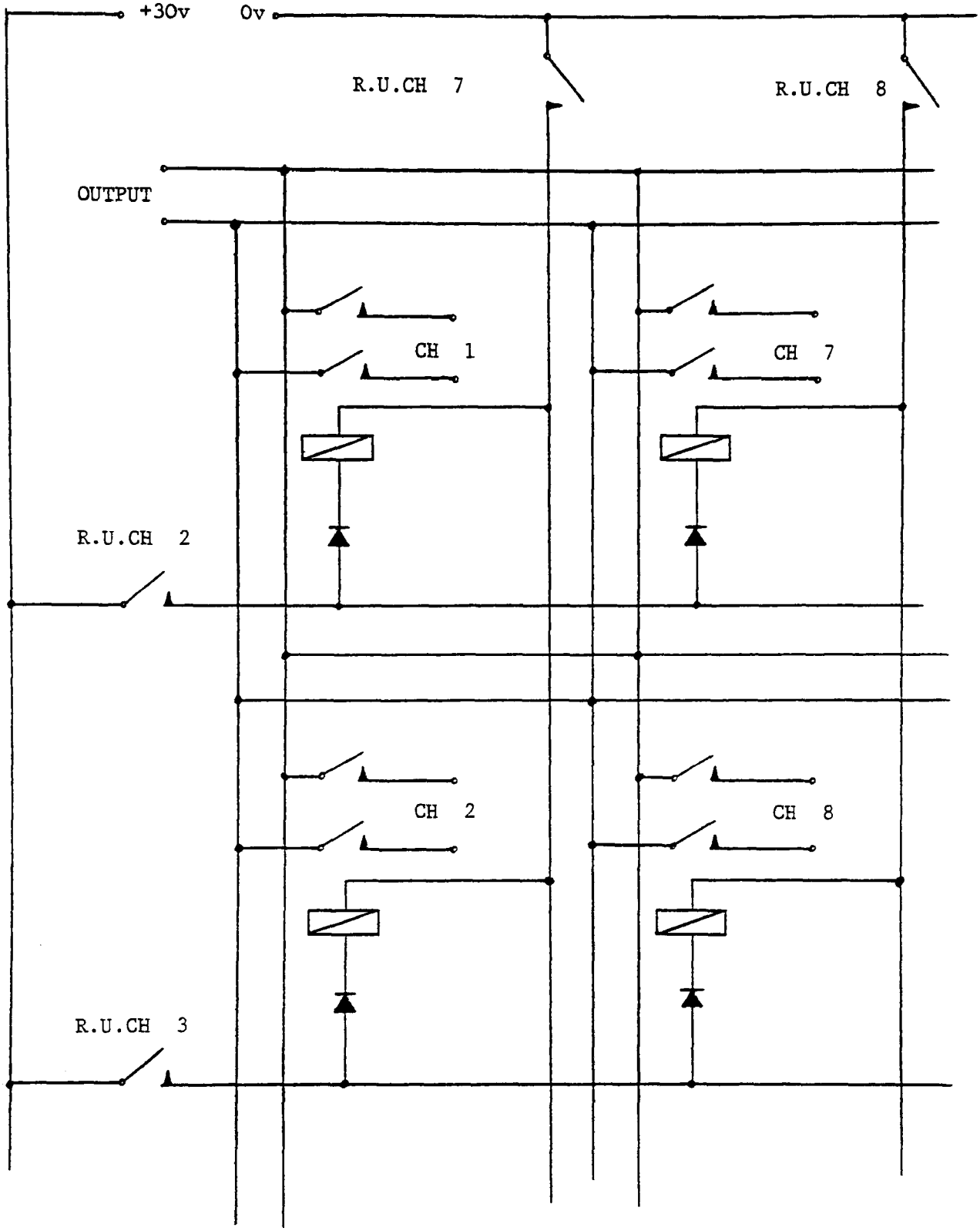

MULTIPLEXER WIRING SYSTEM

Showing 2x2 section of 6x6 matrix

R.U. = RELAY UNIT

FIG.10

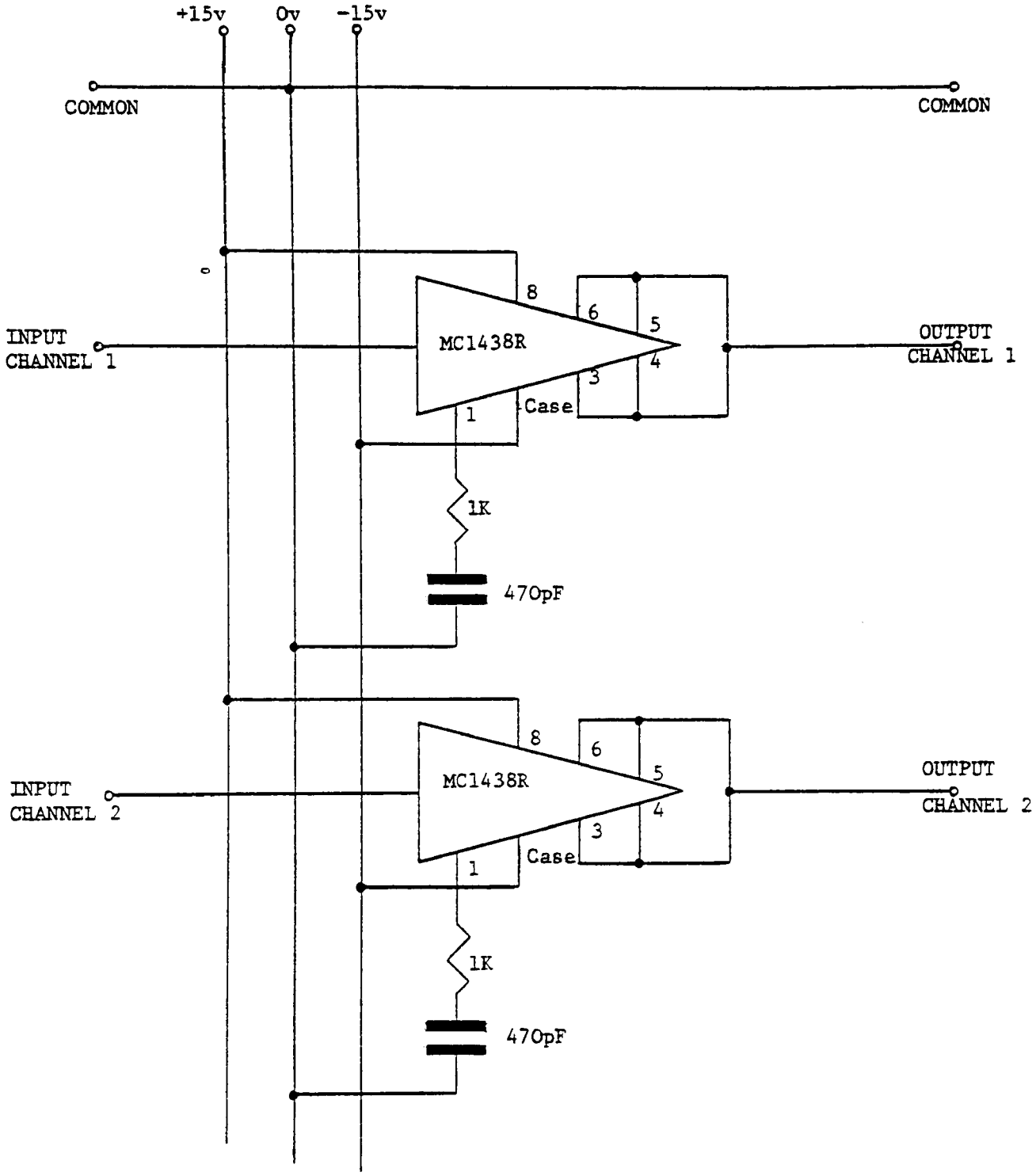

WIRING DIAGRAM OF UNITY GAIN CURRENT AMPLIFIERS

(2 channels shown out of 5)

FIG.11

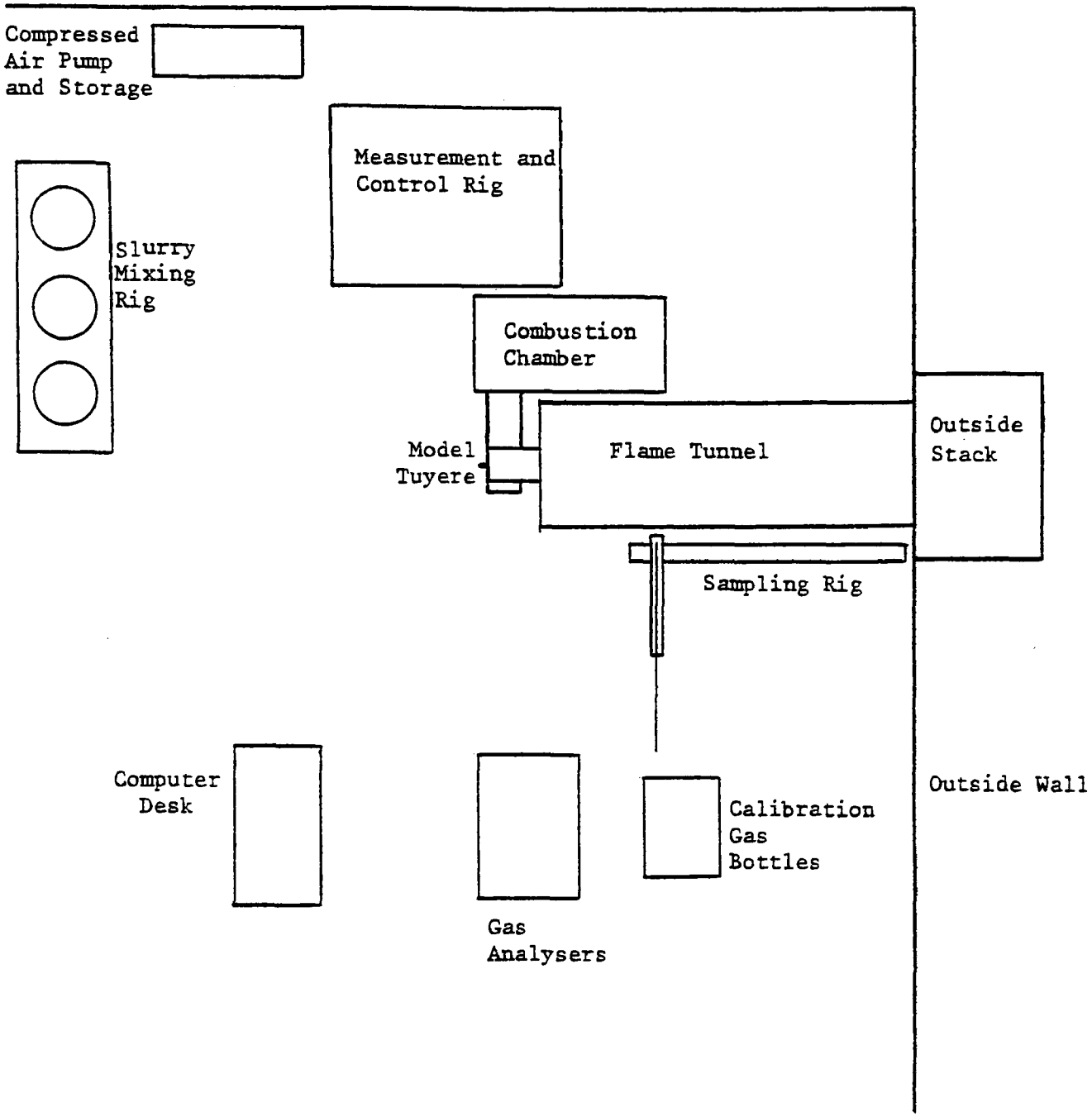

GENERAL ARANGEMENT OF APPARATUS

(Scale approx. 60:1)

FIG.12

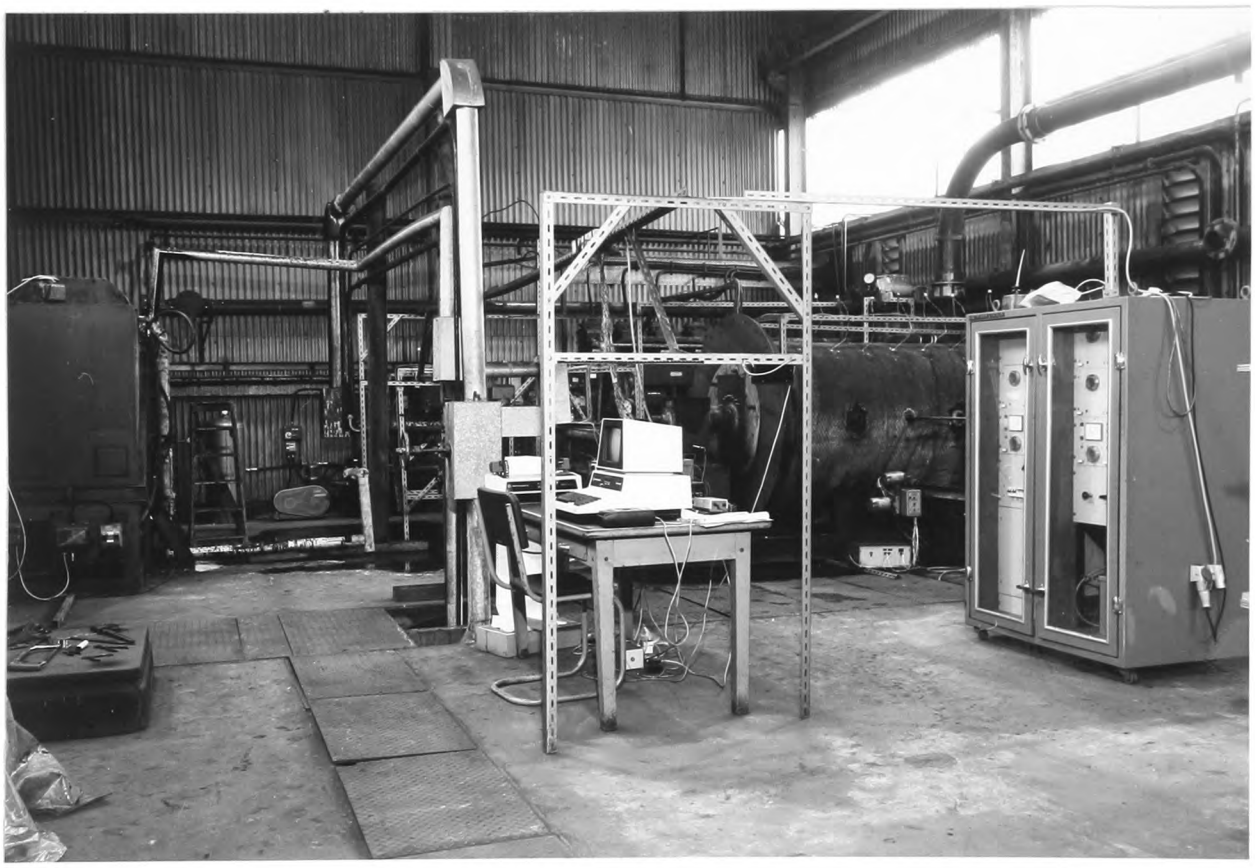

General View Of Apparatus **Fig 12(b)**

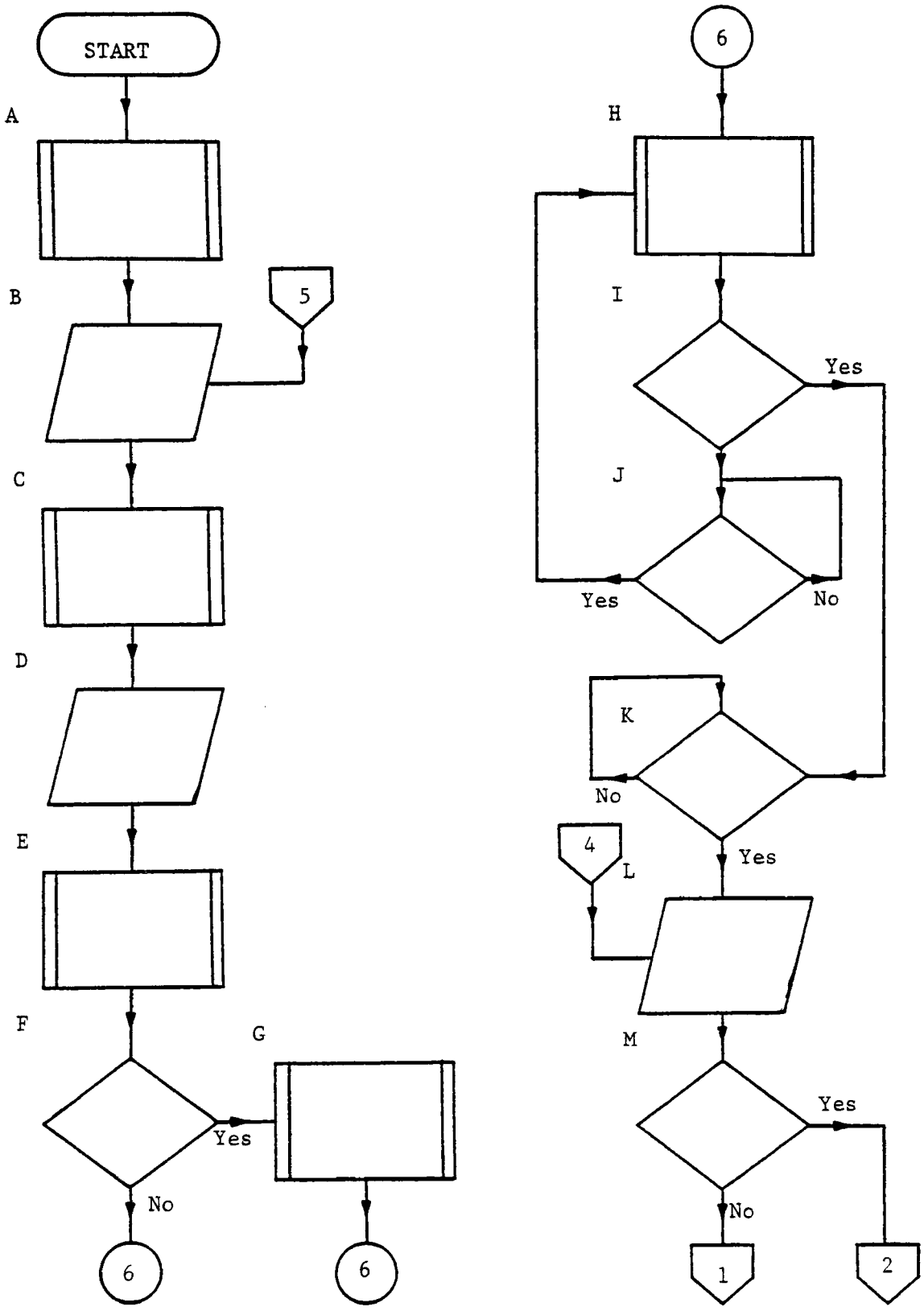

MAIN FLOWCHART OF APPARATUS CONTROL PROGRAM

FIG.13

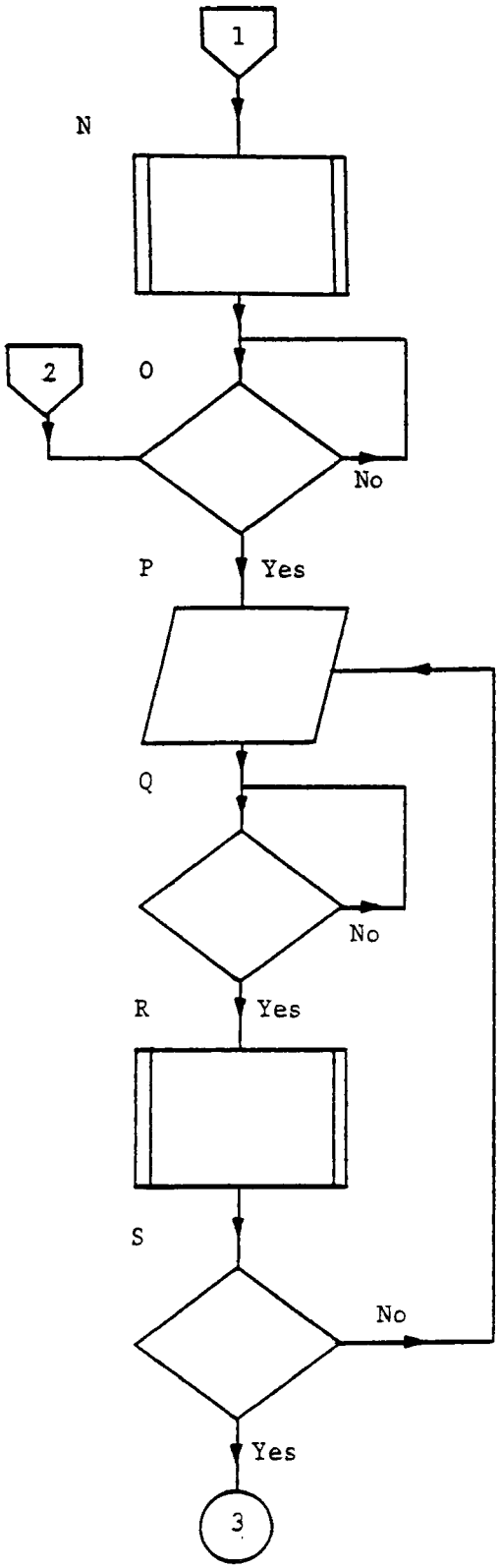

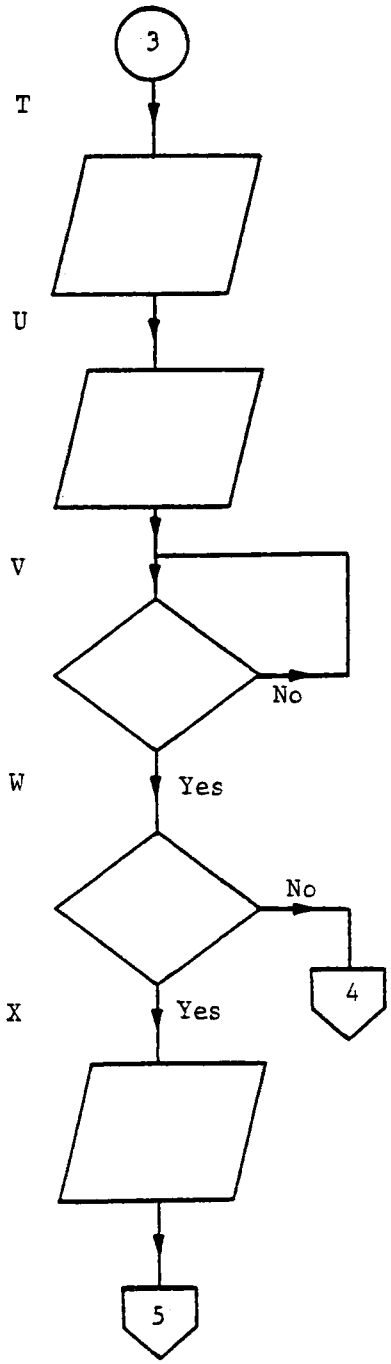

FIG.13
(continued)

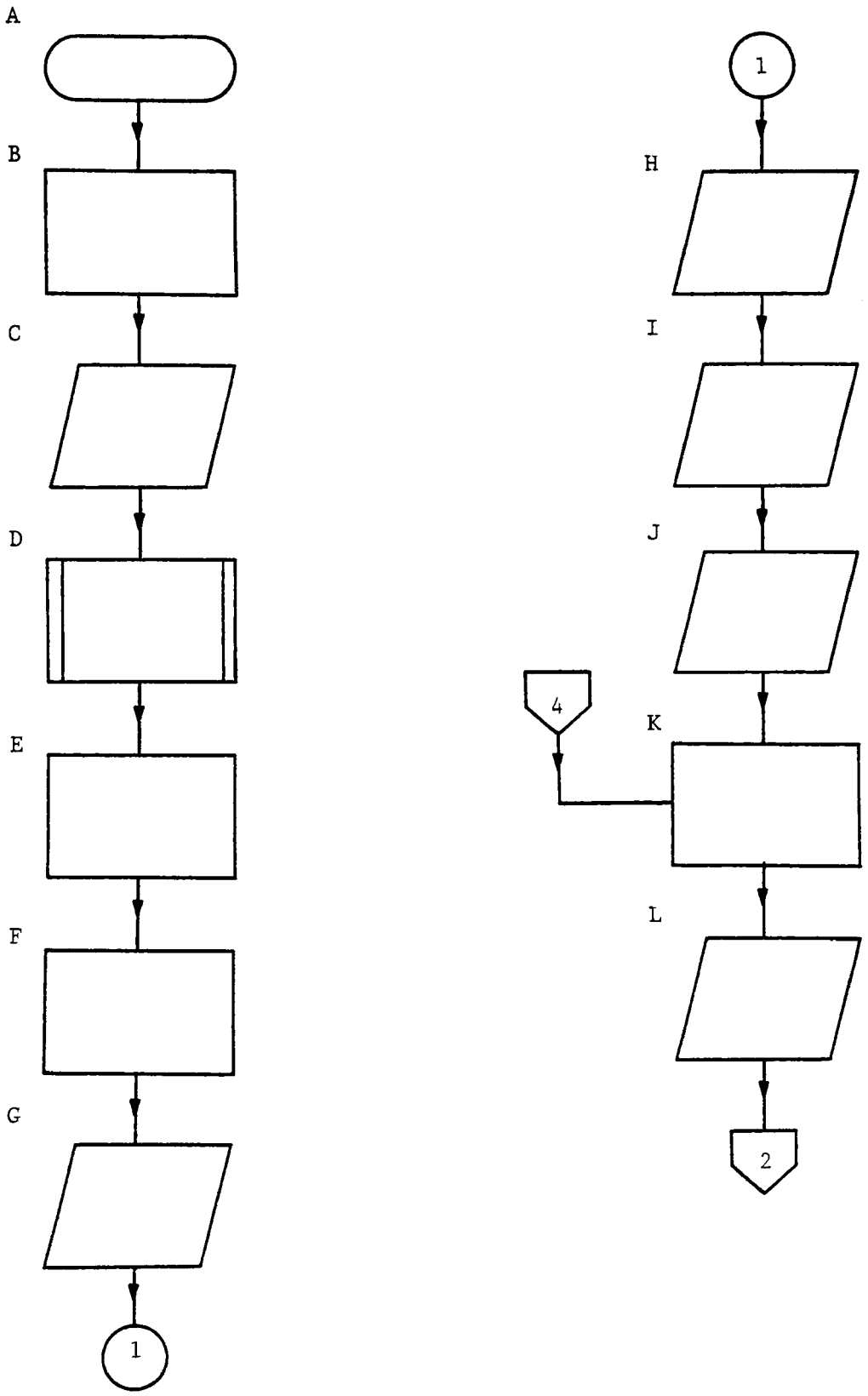

FIRST LEVEL START-UP SUBROUTINE

FIG.14

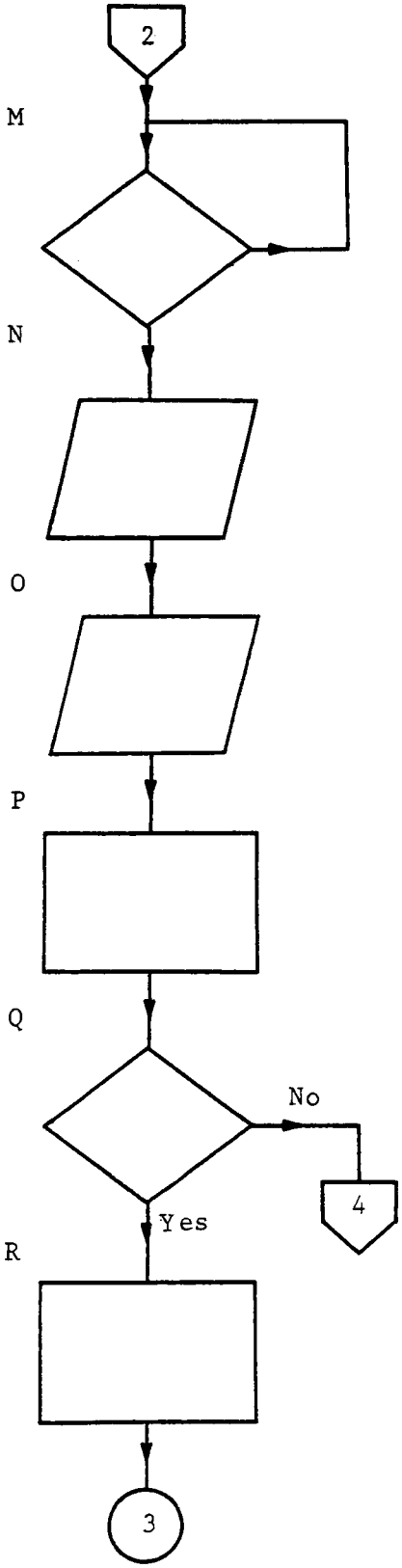

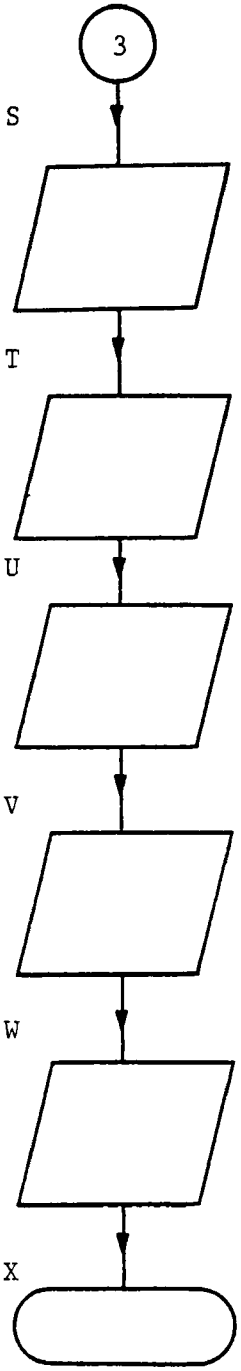

FIG.14
(continued)

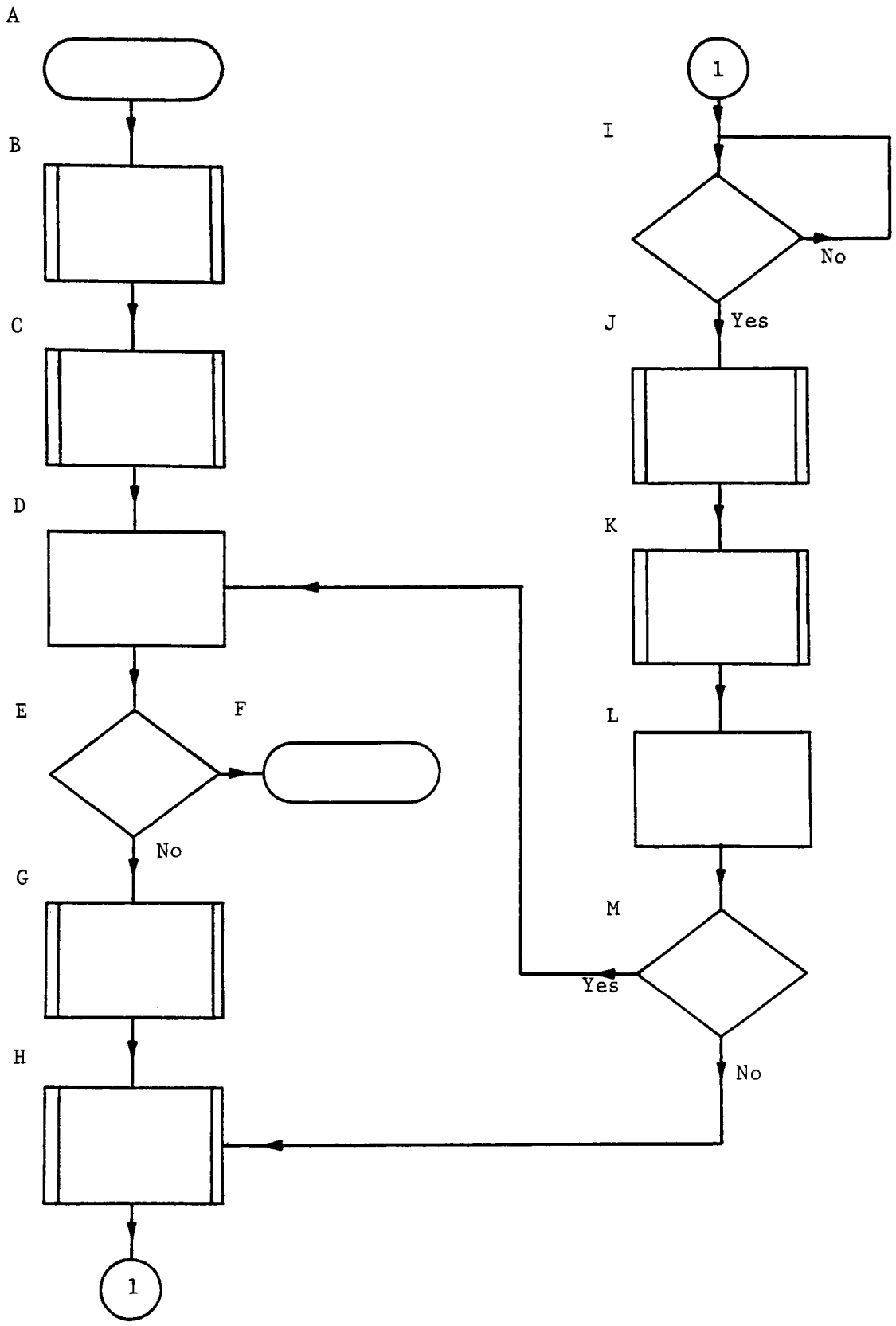

FIRST LEVEL SUBROUTINE FOR MEASUREMENT AND CONTROL

FIG.15

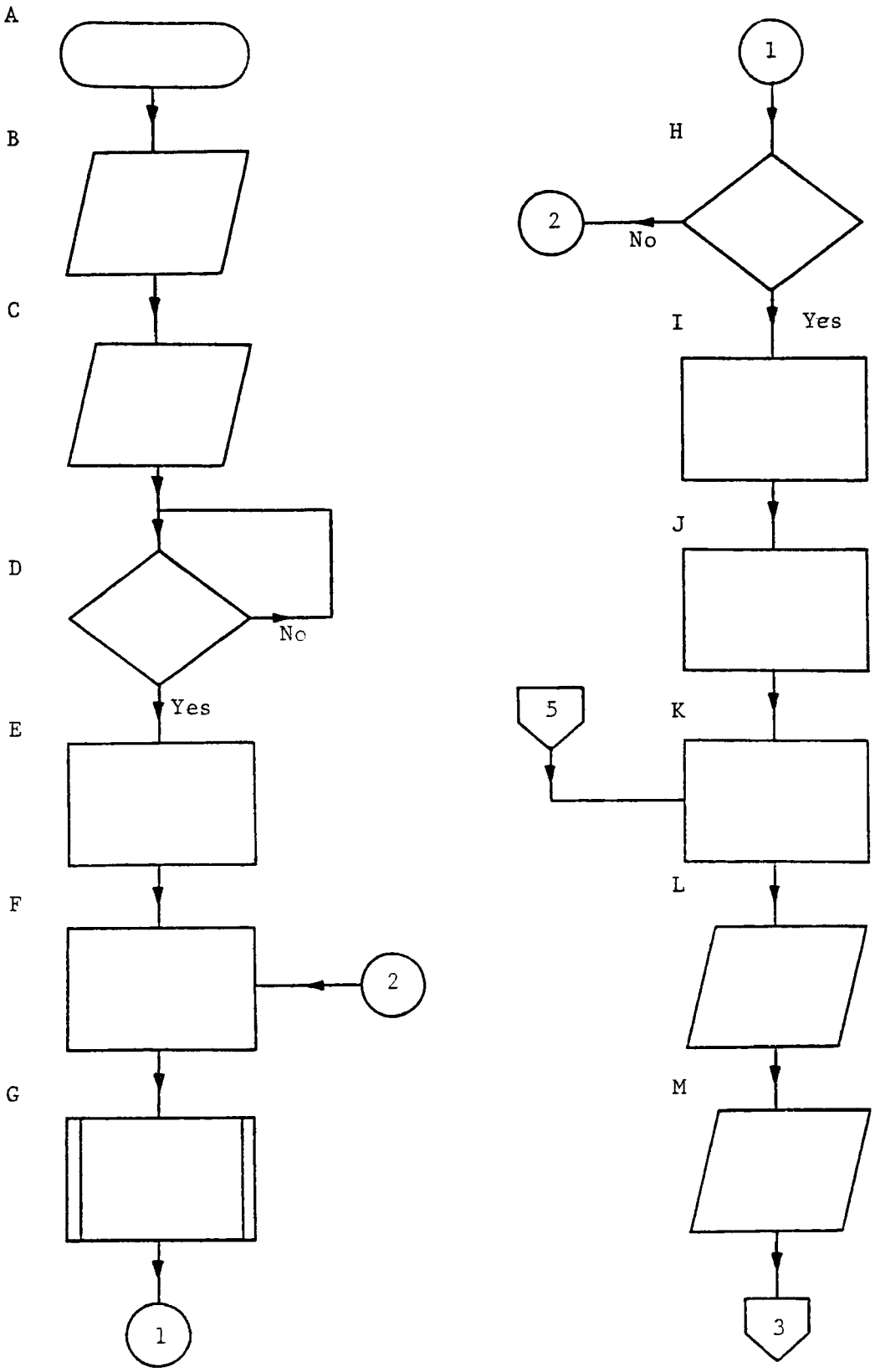

FIRST LEVEL SUBROUTINE FOR CALIBRATION OF GAS ANALYSER

FIG.16

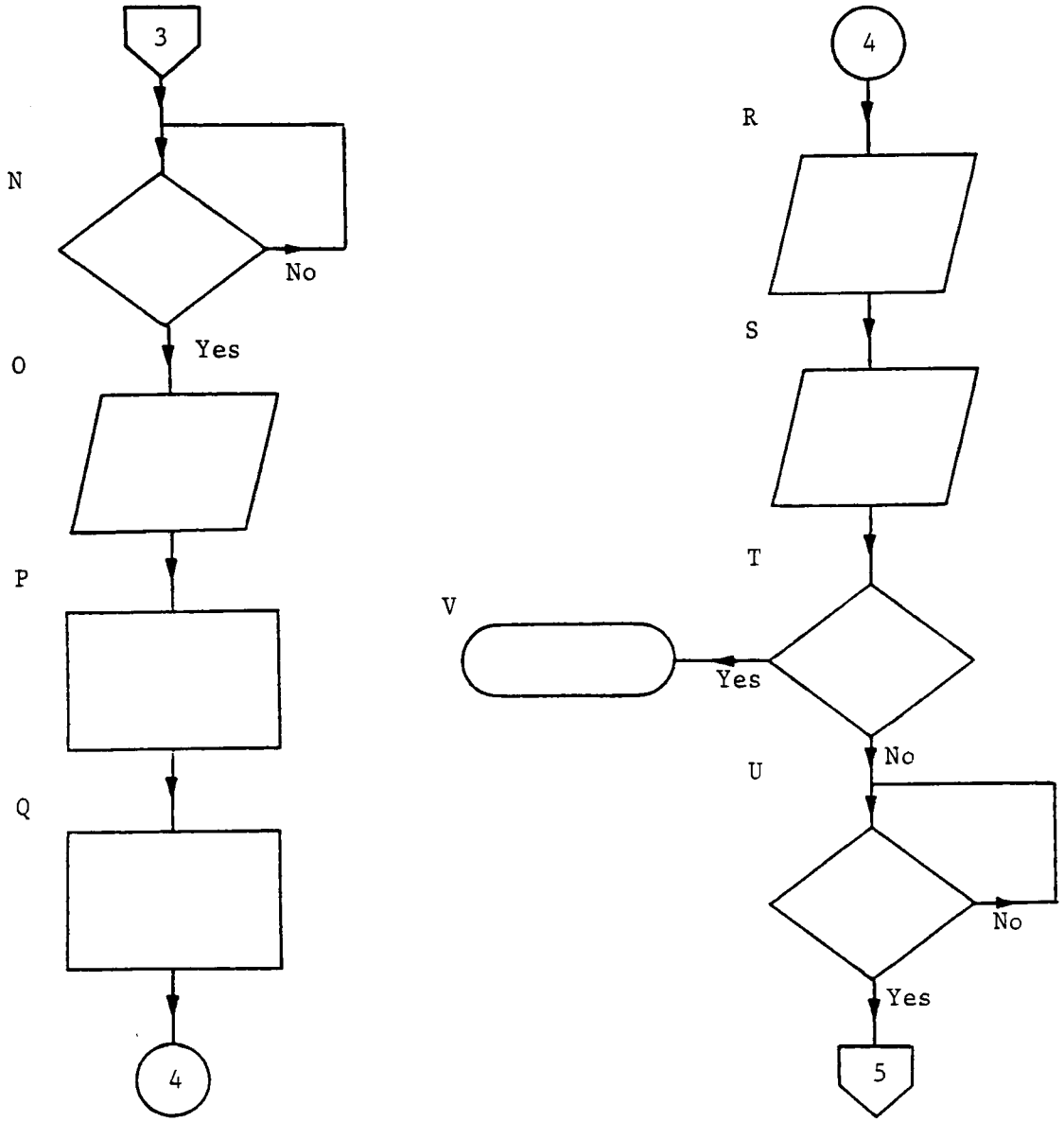

FIG.16
(continued)

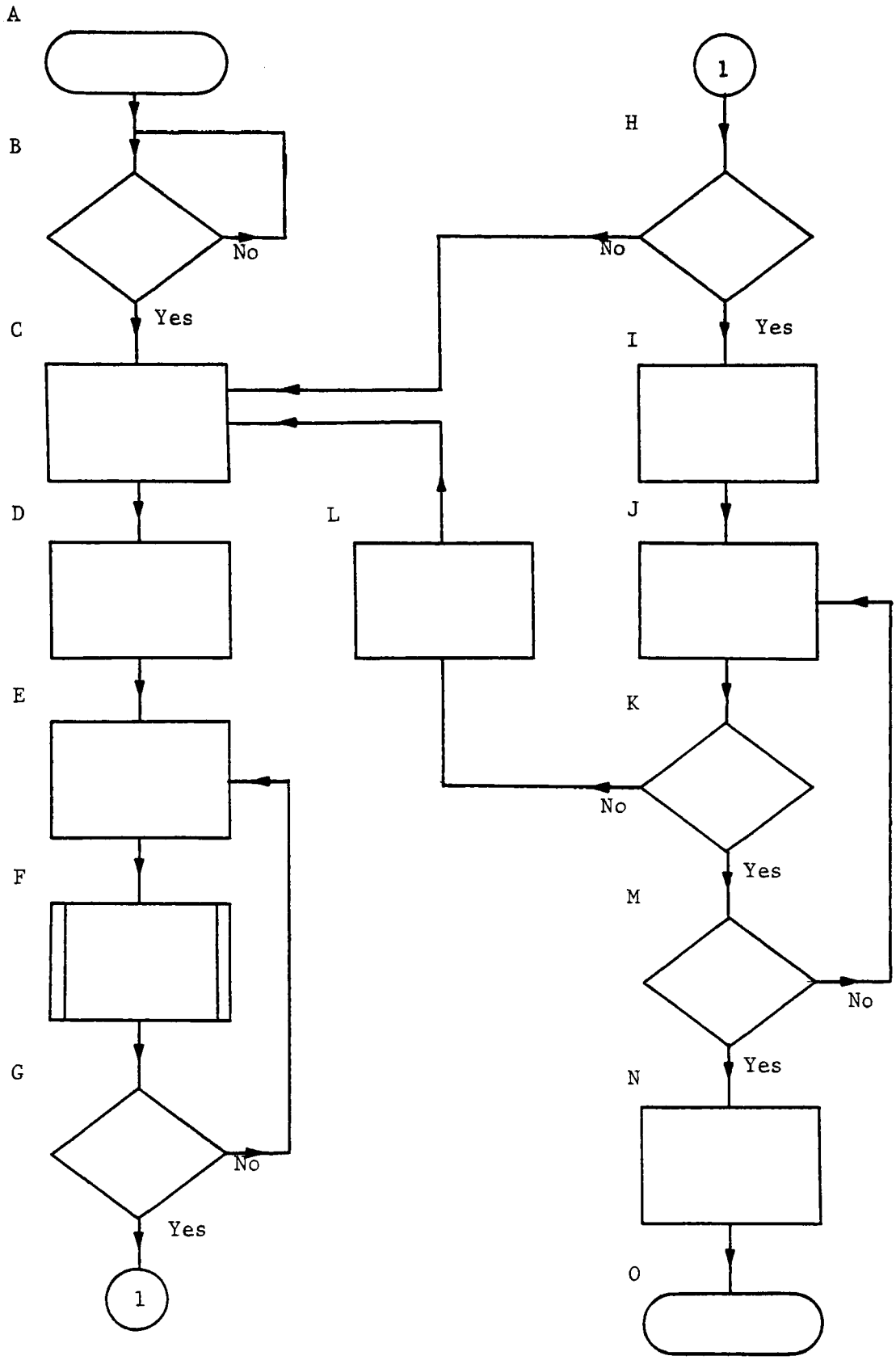

FIRST LEVEL SUBROUTINE FOR ANALYSIS OF SAMPLED GAS

FIG.17

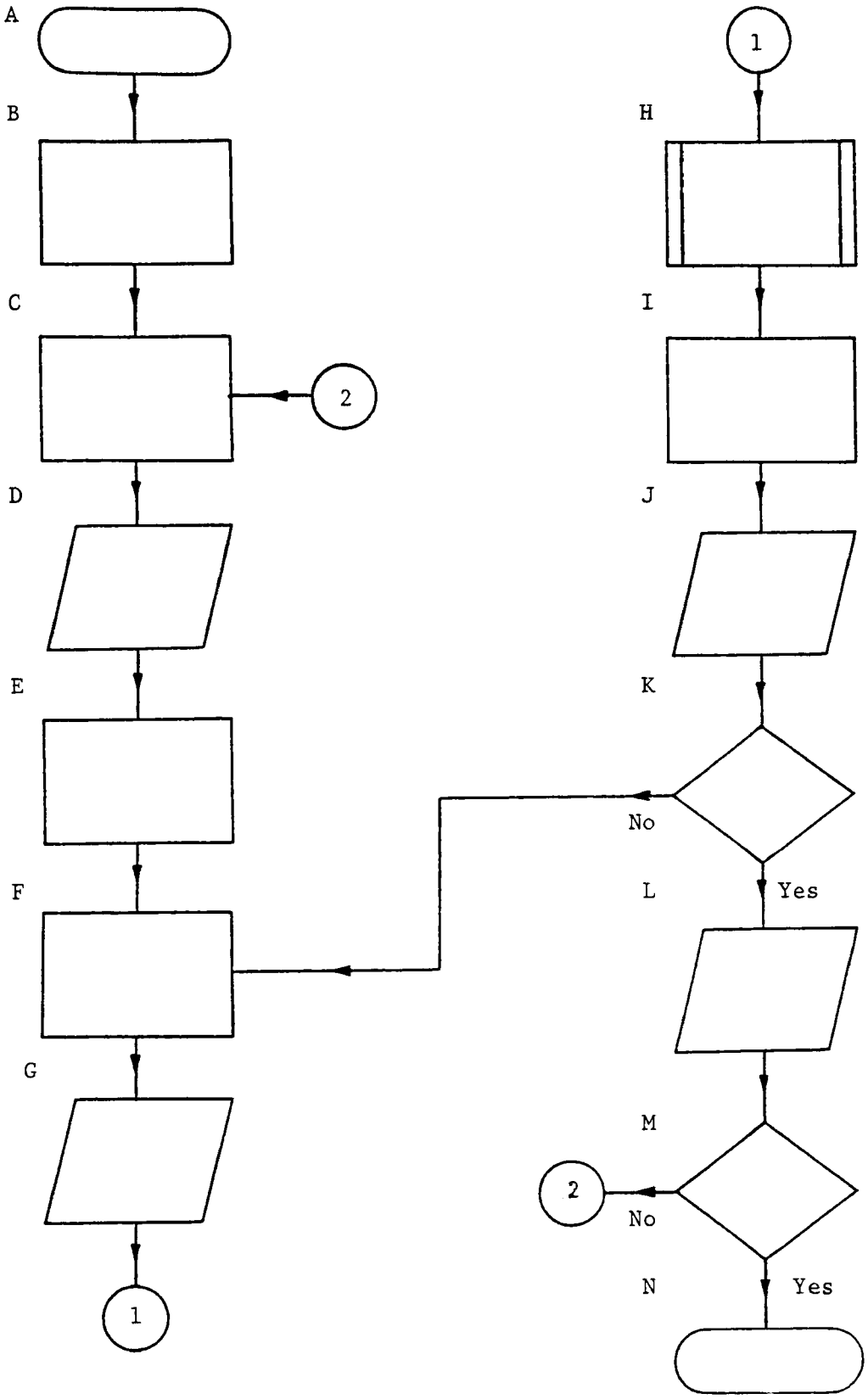

SECOND LEVEL SUBROUTINE FOR SCANNING ALL MULTIPLEXER CHANNELS

FIG.18.

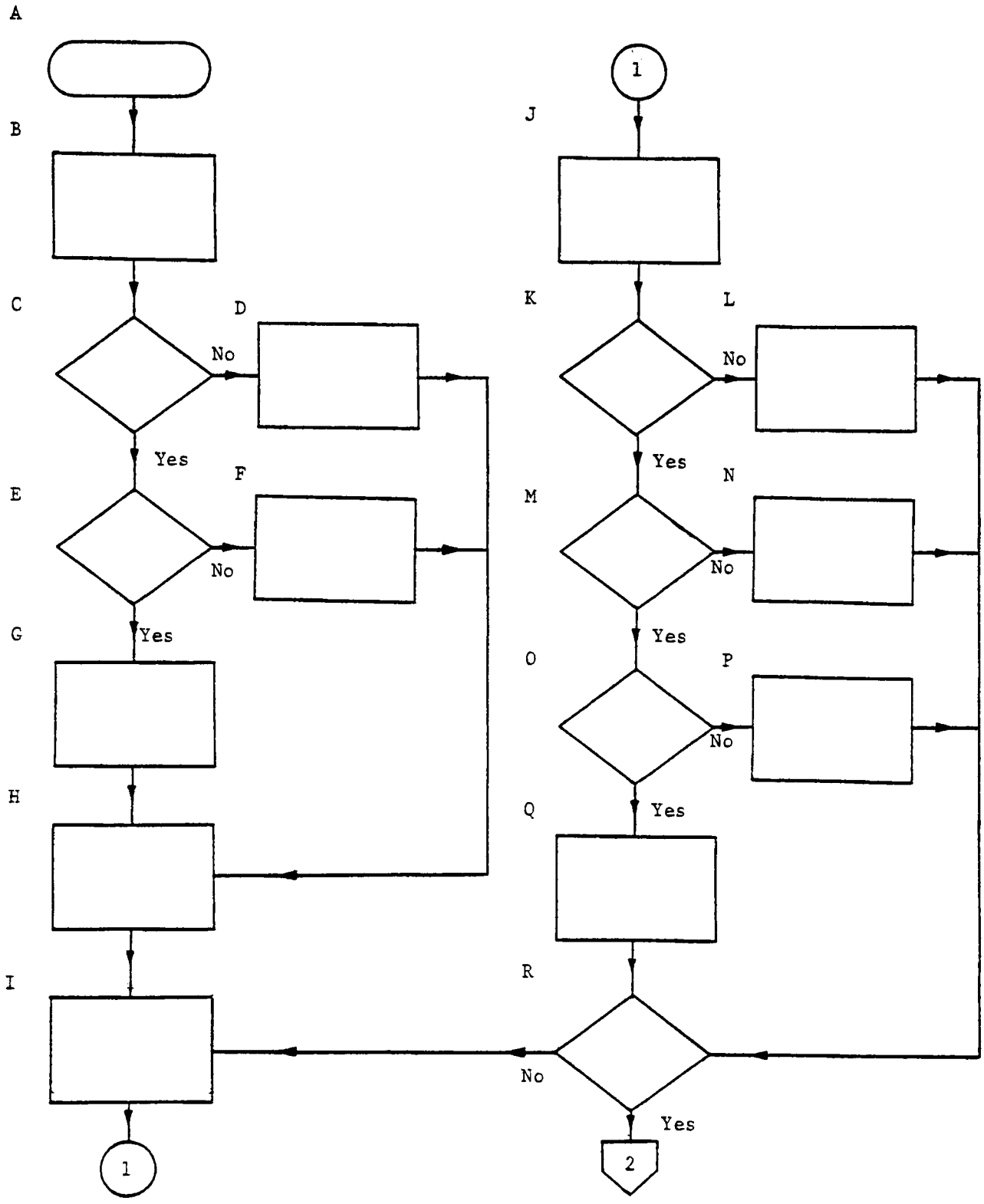

SECOND LEVEL SUBROUTINE FOR CONTROL VALVE ACTUATION

FIG.19

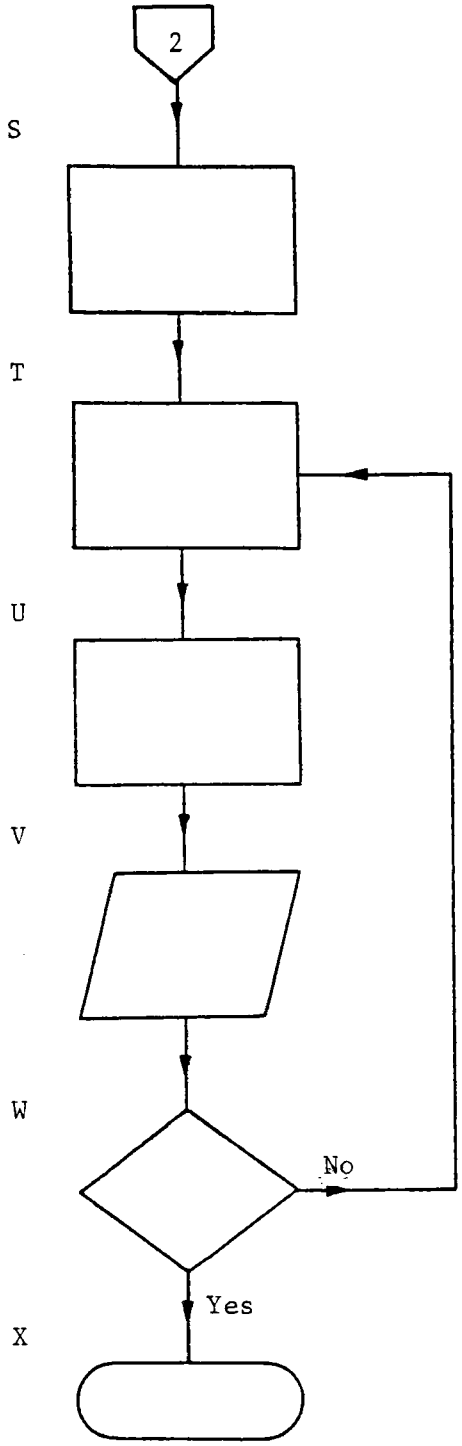

FIG.19
(continued)

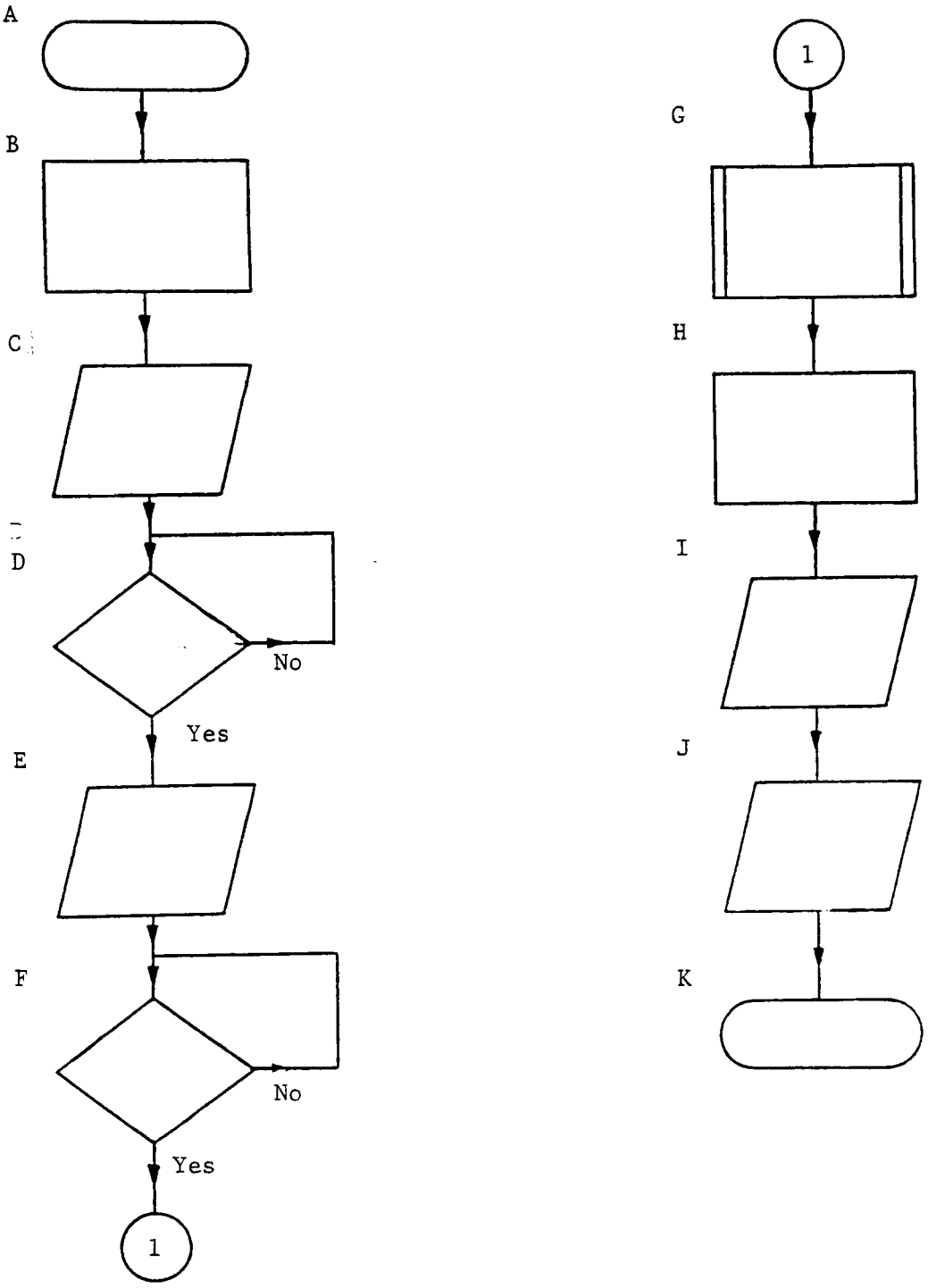

THIRD LEVEL SUBROUTINE FOR SCANNING A SINGLE MULTIPLEXER CHANNEL

FIG.20

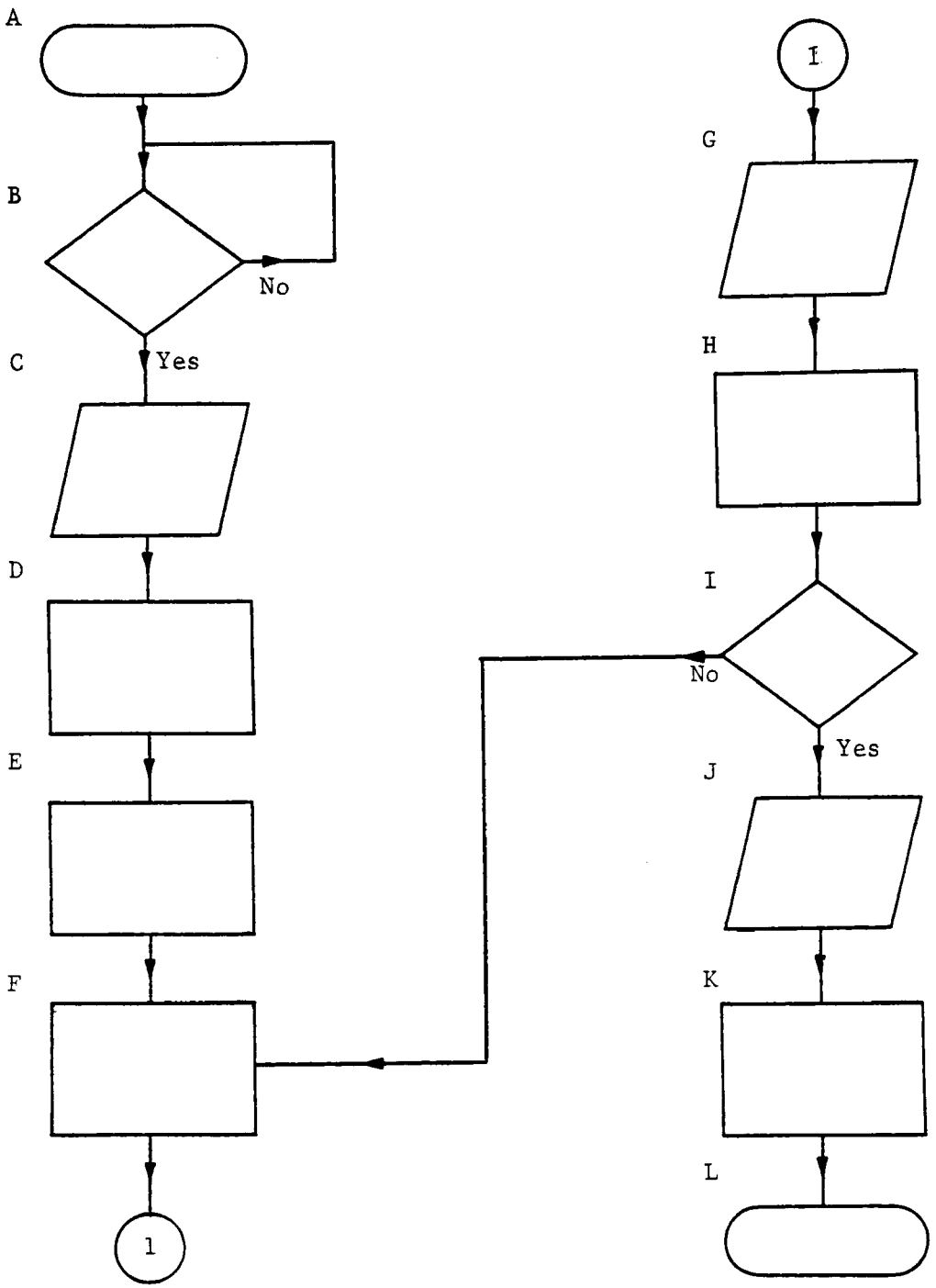

FOURTH LEVEL SUBROUTINE FOR SCANNING A SINGLE DIGITAL-TO-ANALOG CONVERTER CHANNEL

FIG.21

Failure Of Gas And Solids Sampling Probe **Fig 22**

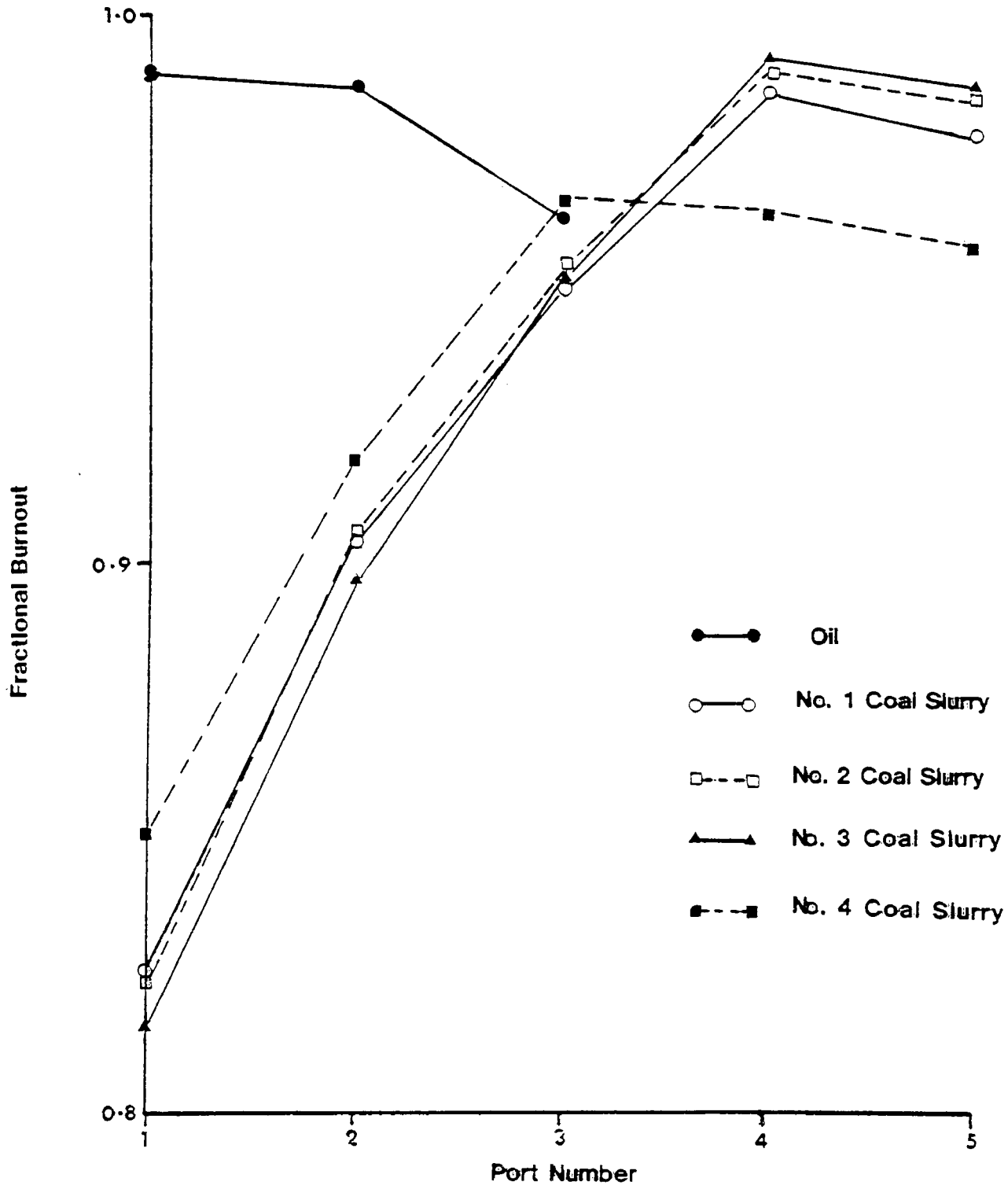

Fractional Burnout Of Slurries By Species
(Original Data Set)

Fig. 23

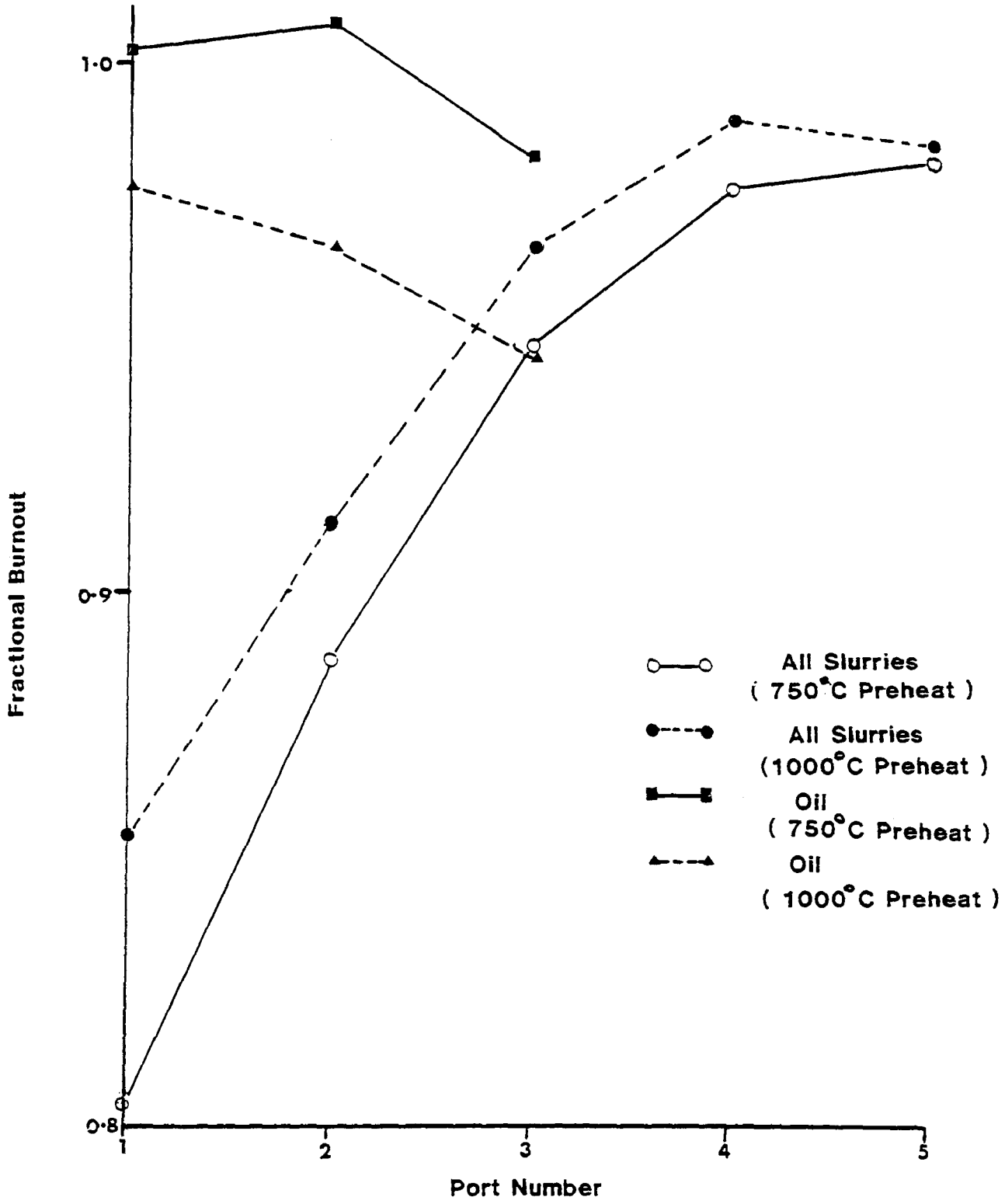

Effect Of Air Preheat Temperature On Burnout .
(Original Data Set)

Fig. 24

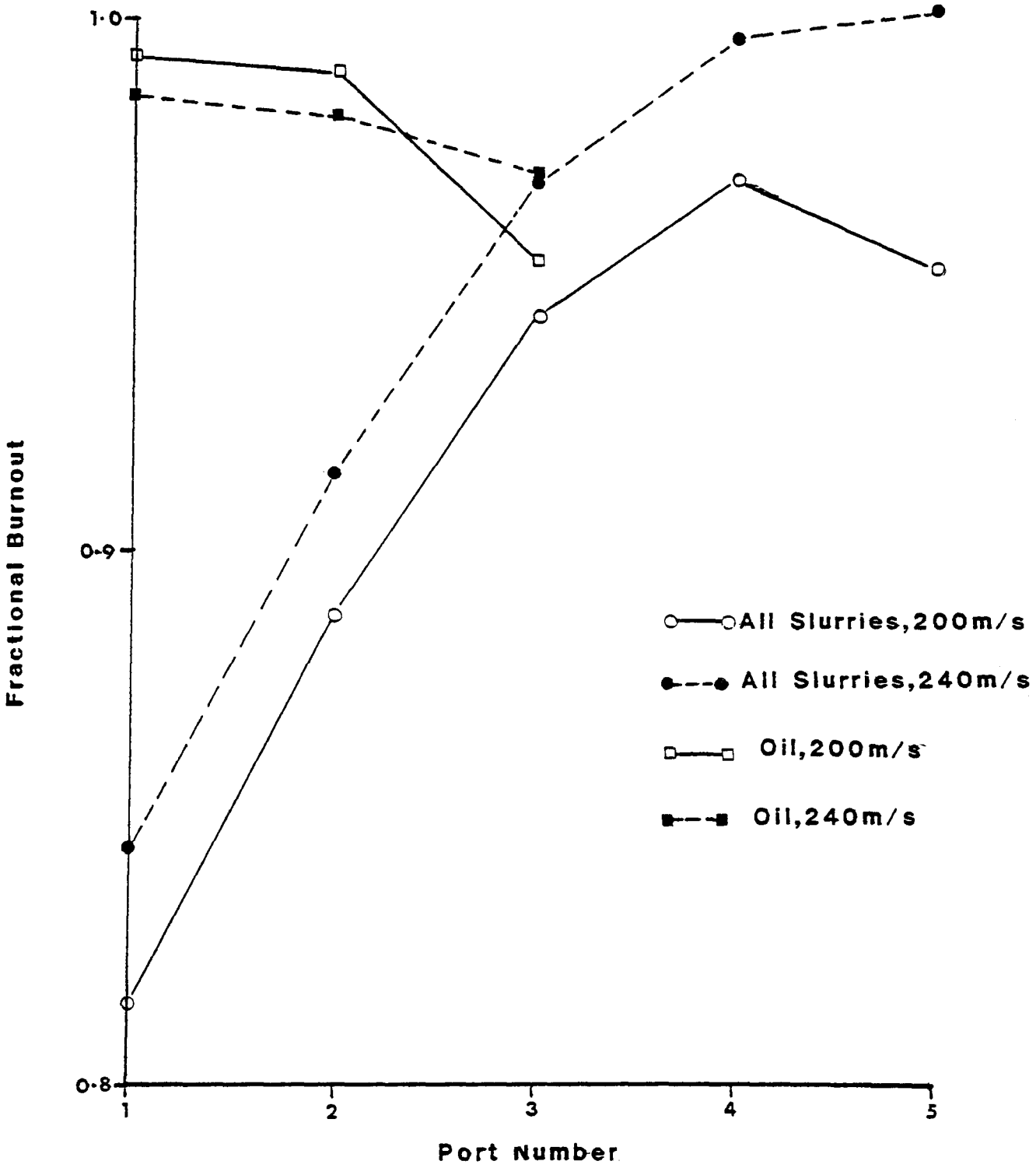

Effect Of Velocity On Burnout
(Original Dataset)

Fig 25

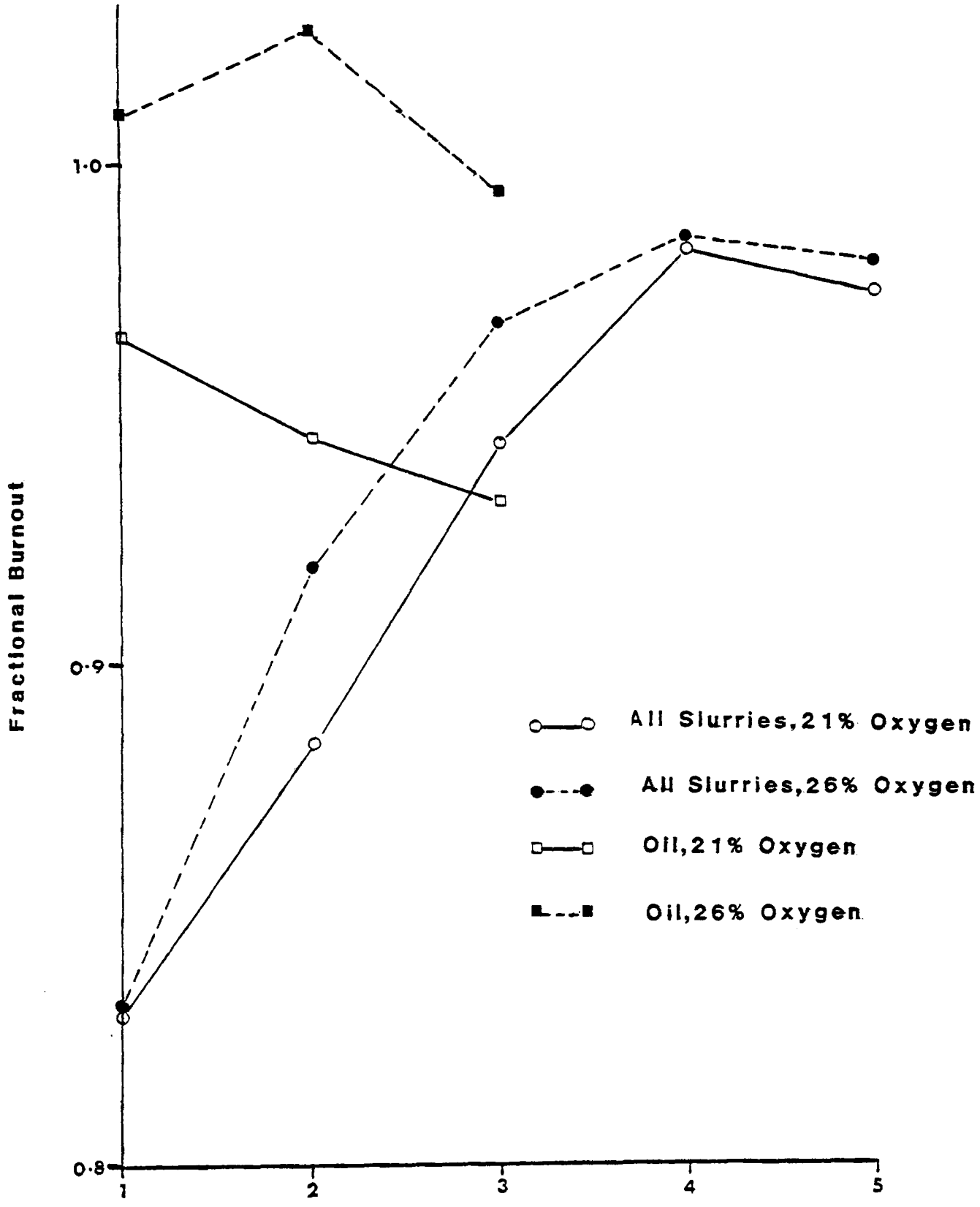

Effect Of Oxygen Enrichment
On Fractional Burnout
(Original Dataset)

Fig 26

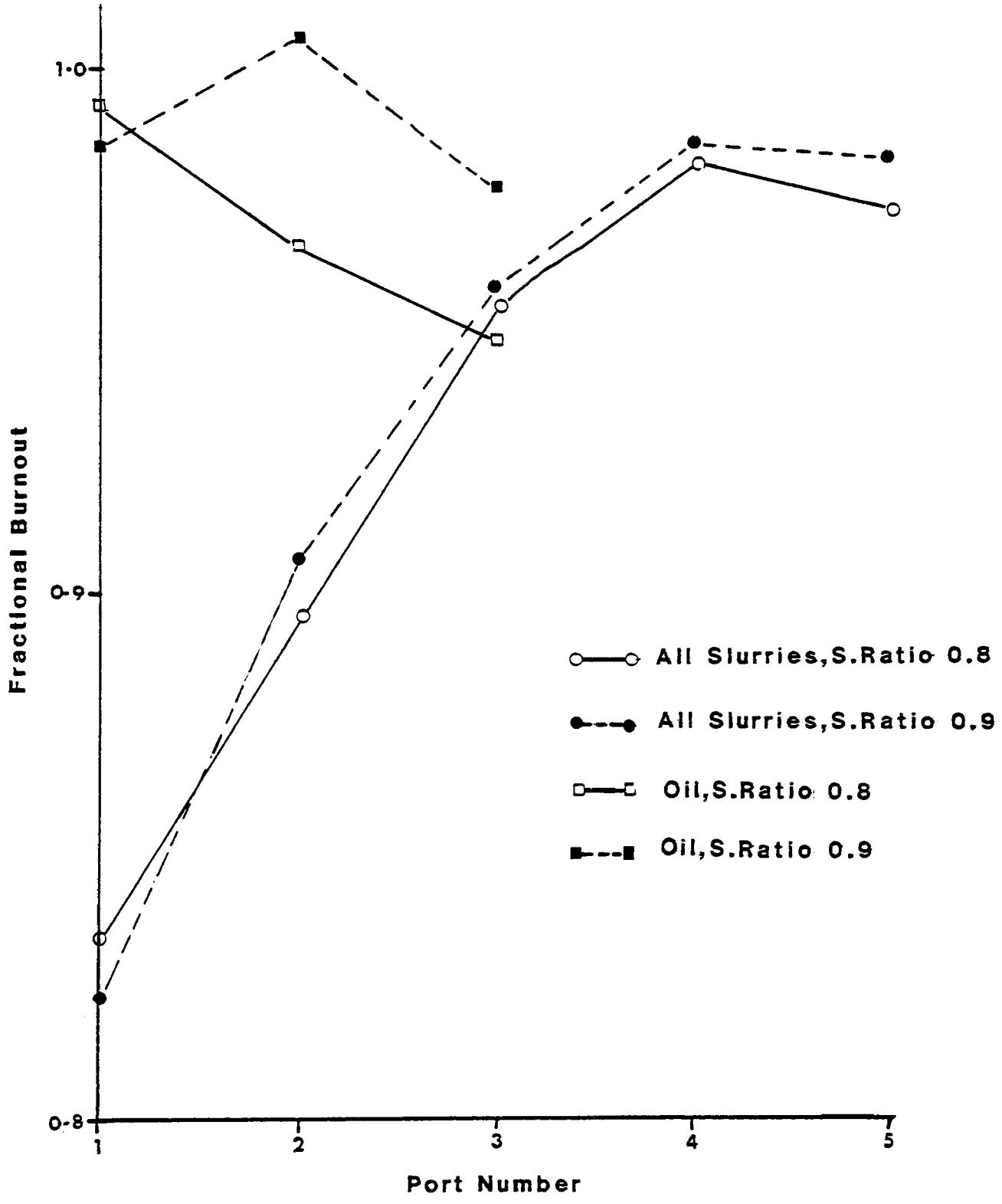

Effect Of Stoichiometric Ratio
On Fractional Burnout
(Original Dataset)

Fig 27

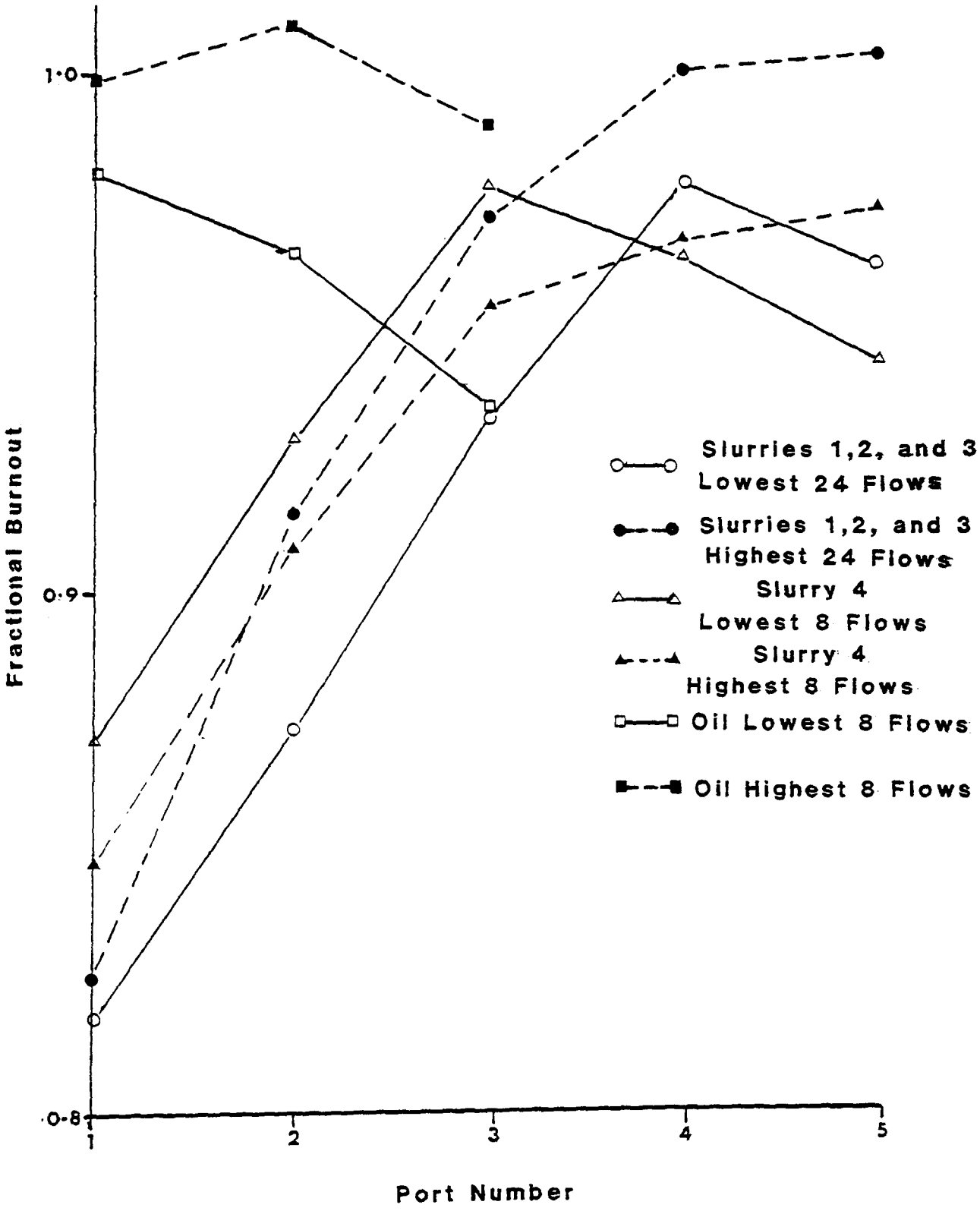

Effect Of Slurry Flow
On Burnout (Original Dataset)

Fig 28

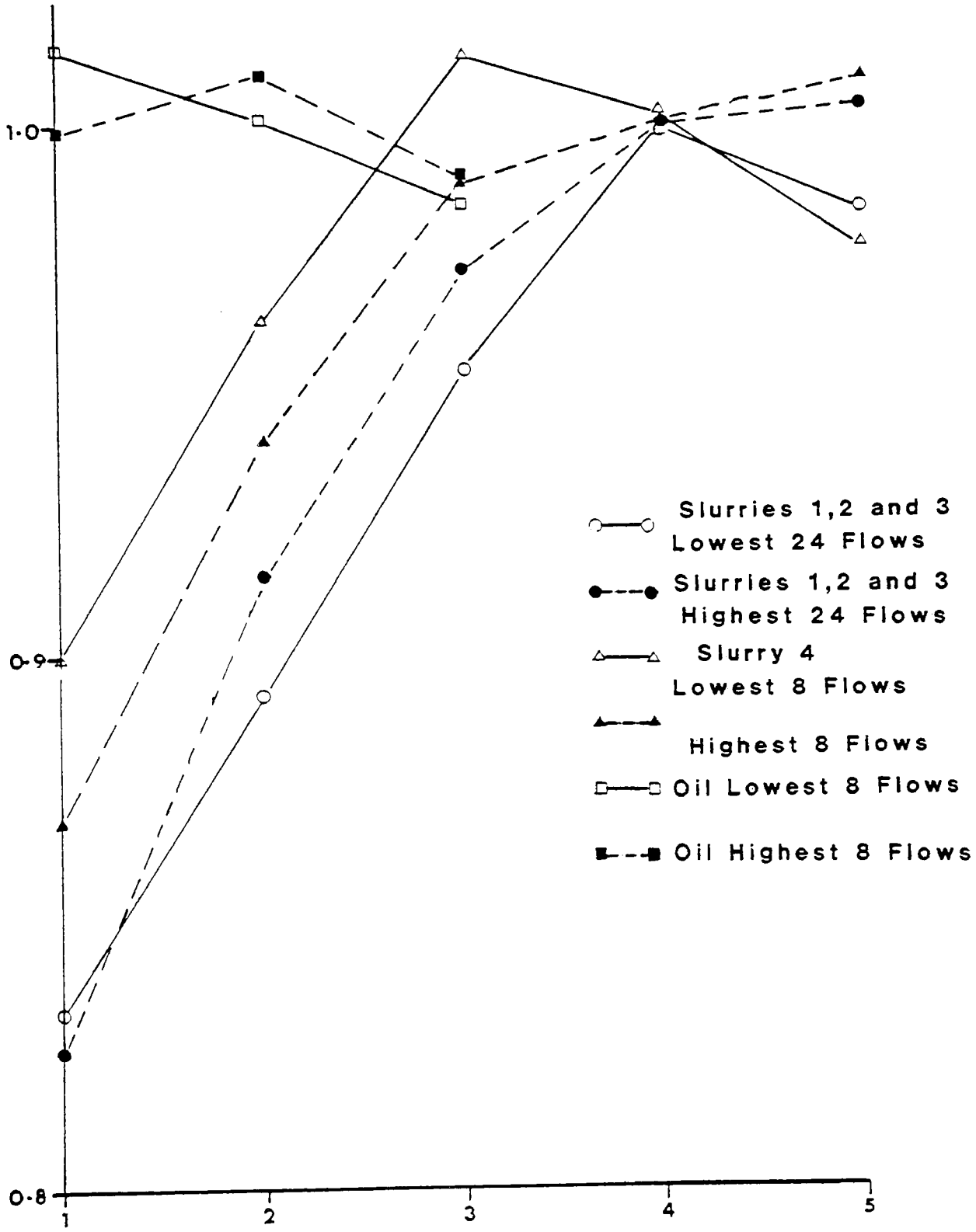

Effect Of Slurry On Burnout
(Modified Dataset)

Fig 29

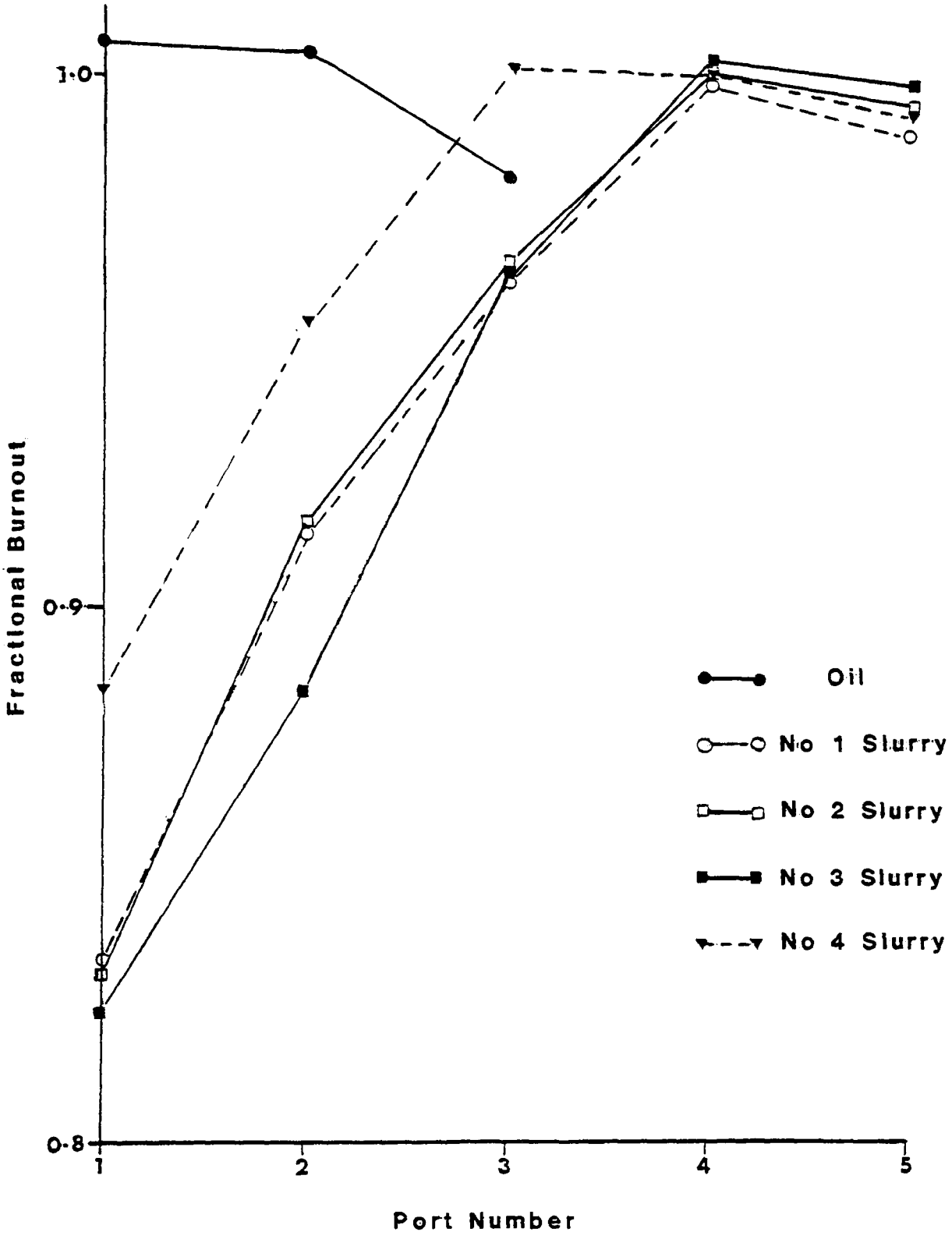

Fractional Burnout Of Slurry By Species
(Modified Dataset)

Fig 30

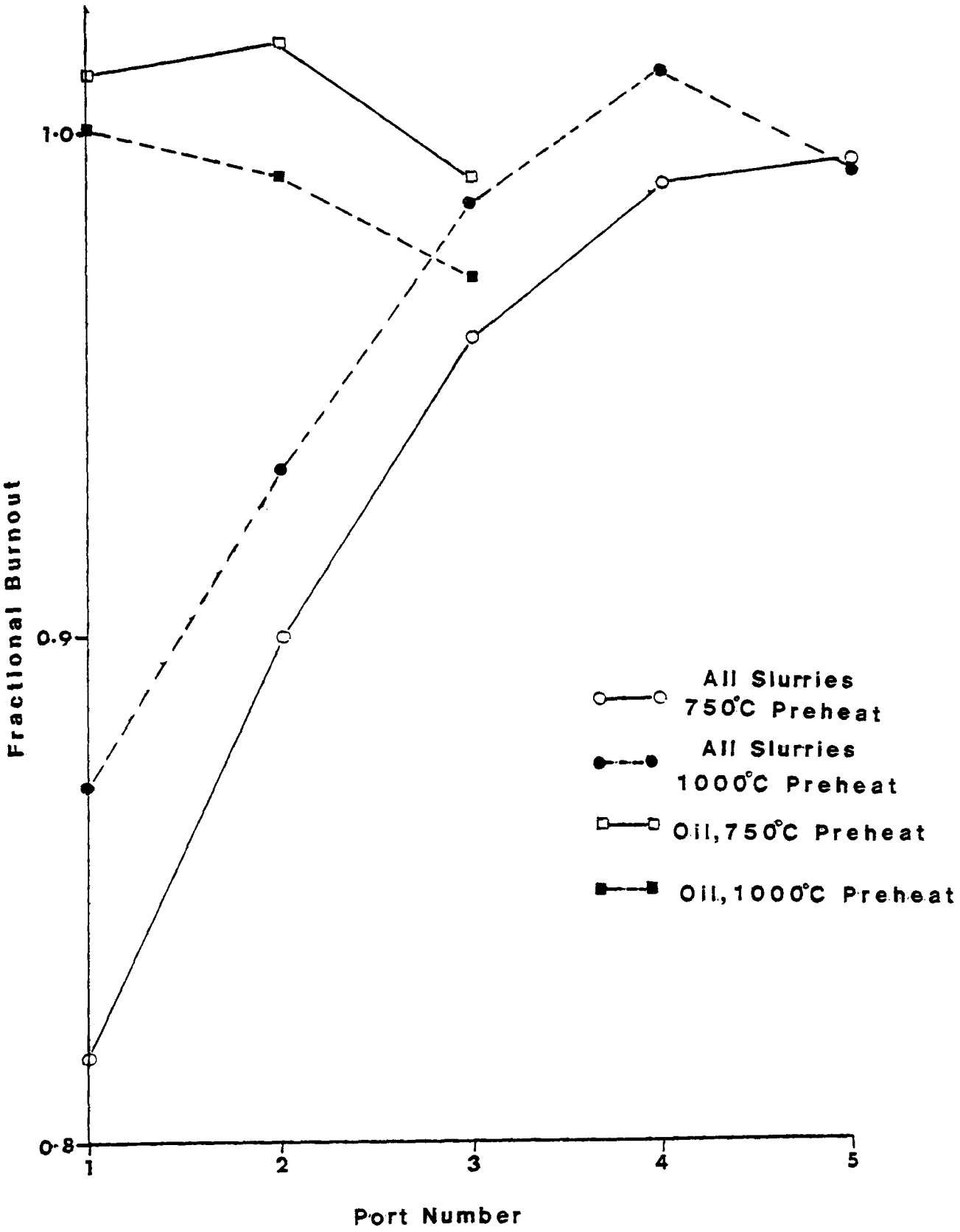

Effect Of Temperature On Burnout
(Modified Dataset)

Fig 31

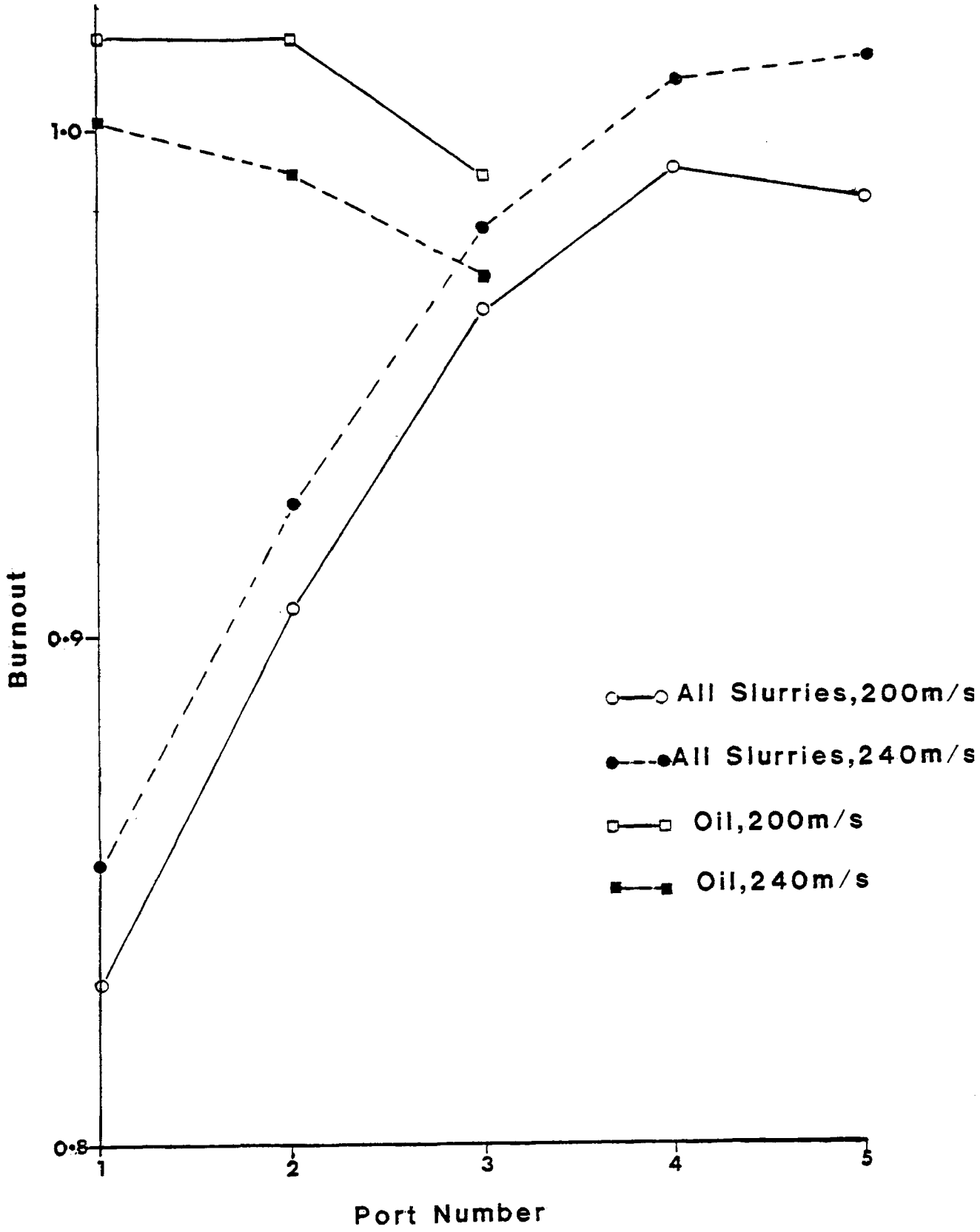

Effect Of Velocity On Burnout
(Modified Dataset)

Fig 32

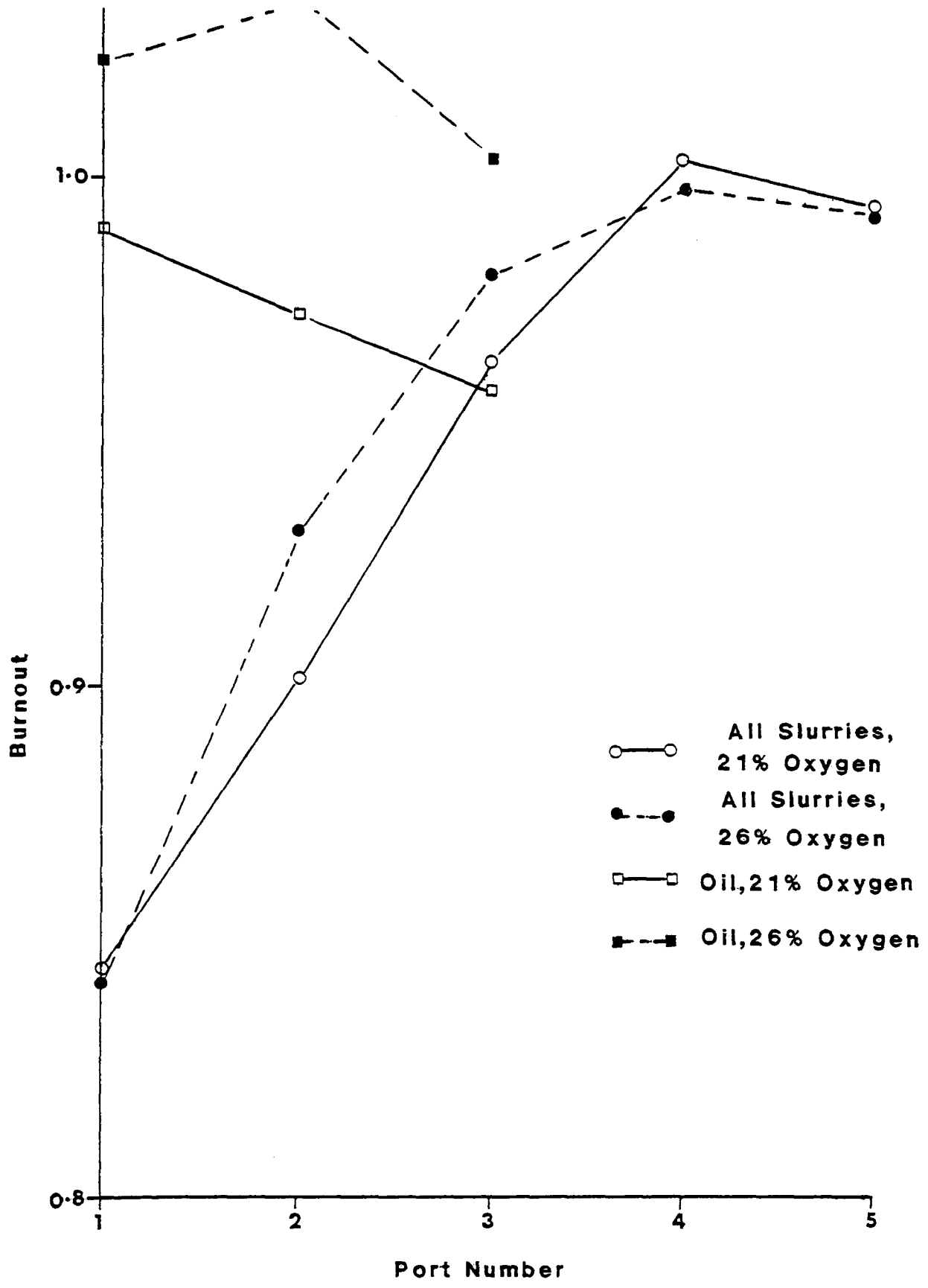

Effect Of Oxygen Enrichment
On Burnout
(Modified Dataset)

Fig 33

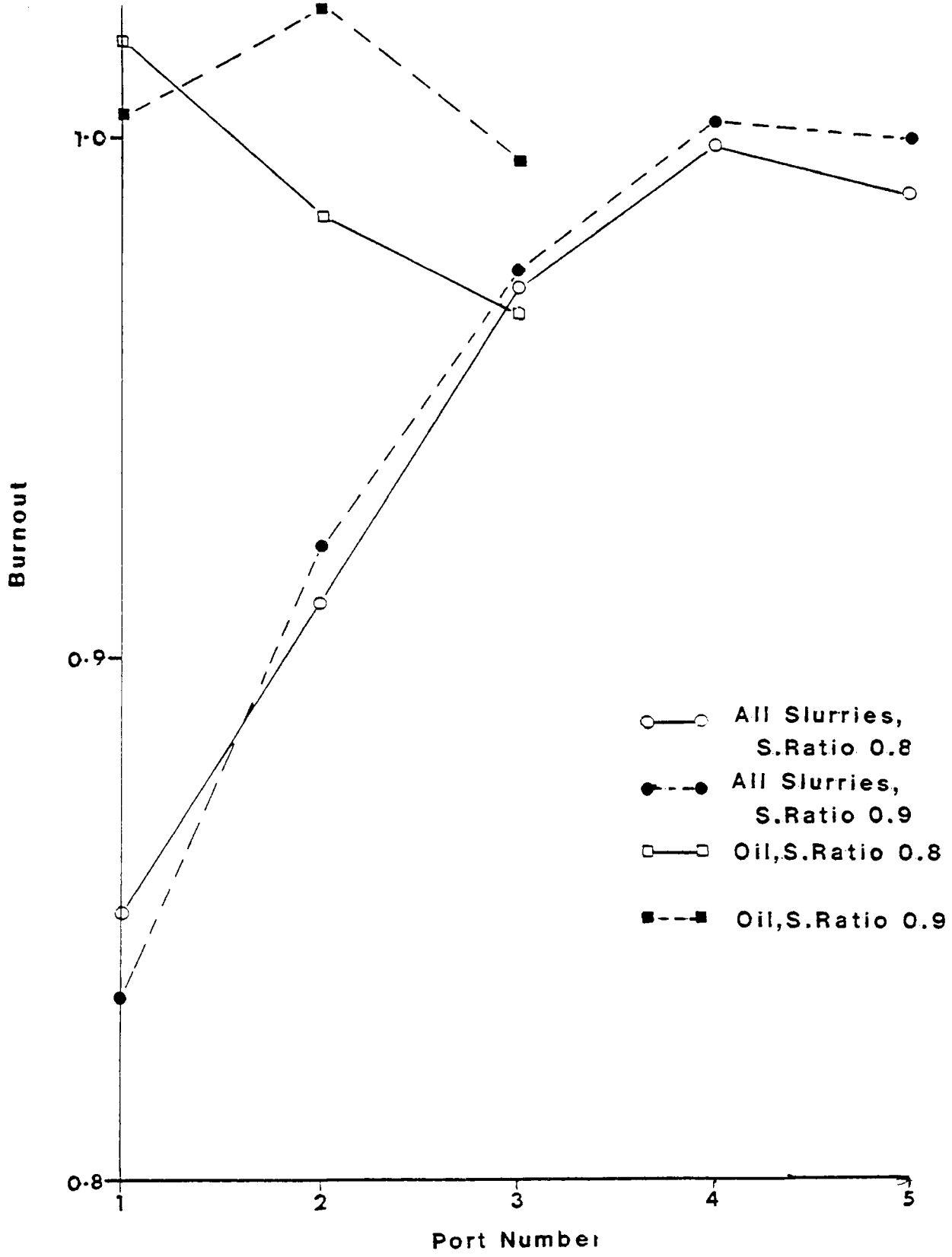

Effect Of Stoichiometric Ratio On Fractional Burnout (Modified Dataset)

Fig 34

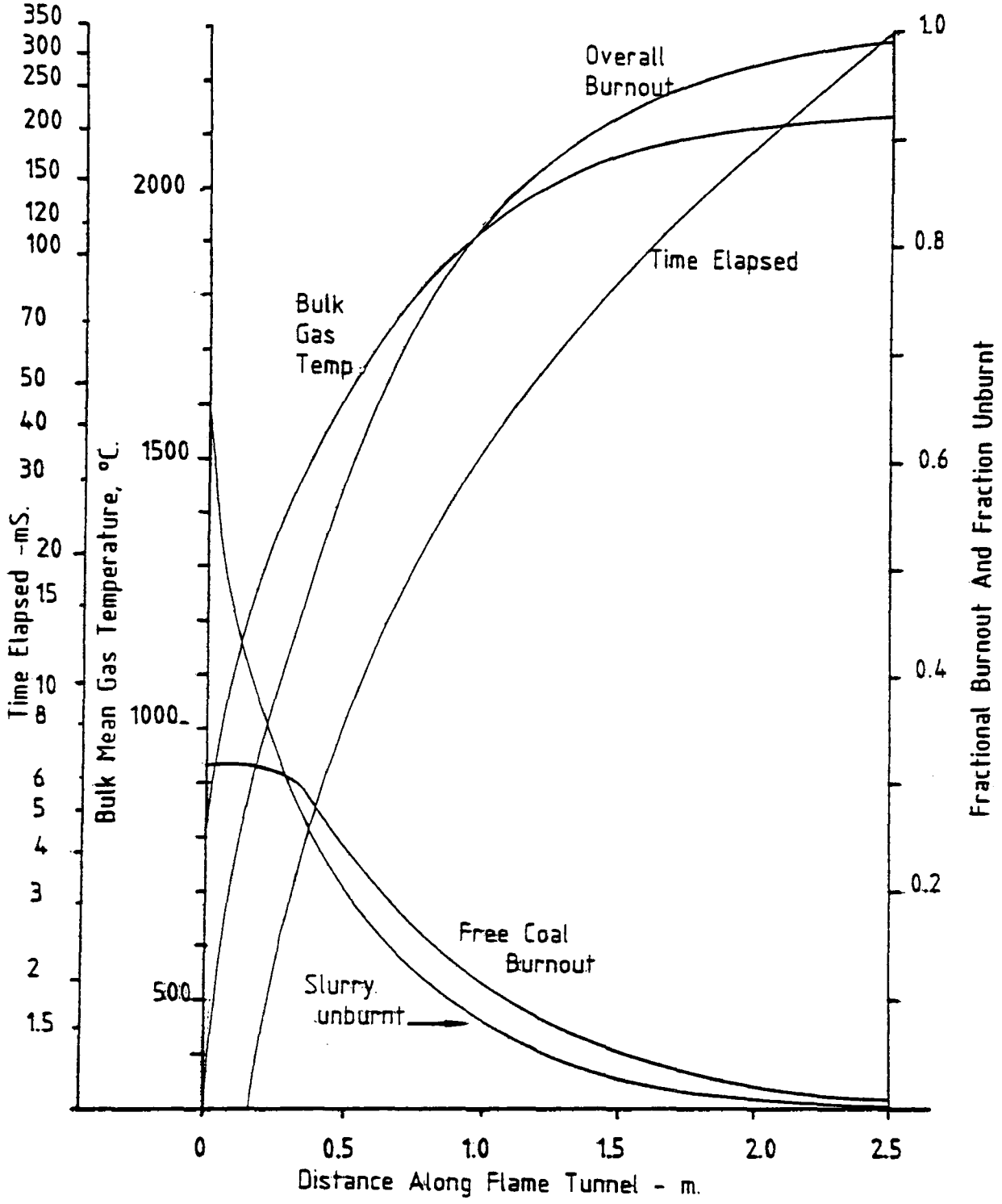

MODEL BURNOUT HISTORY OF RUN 75

FIG 35.

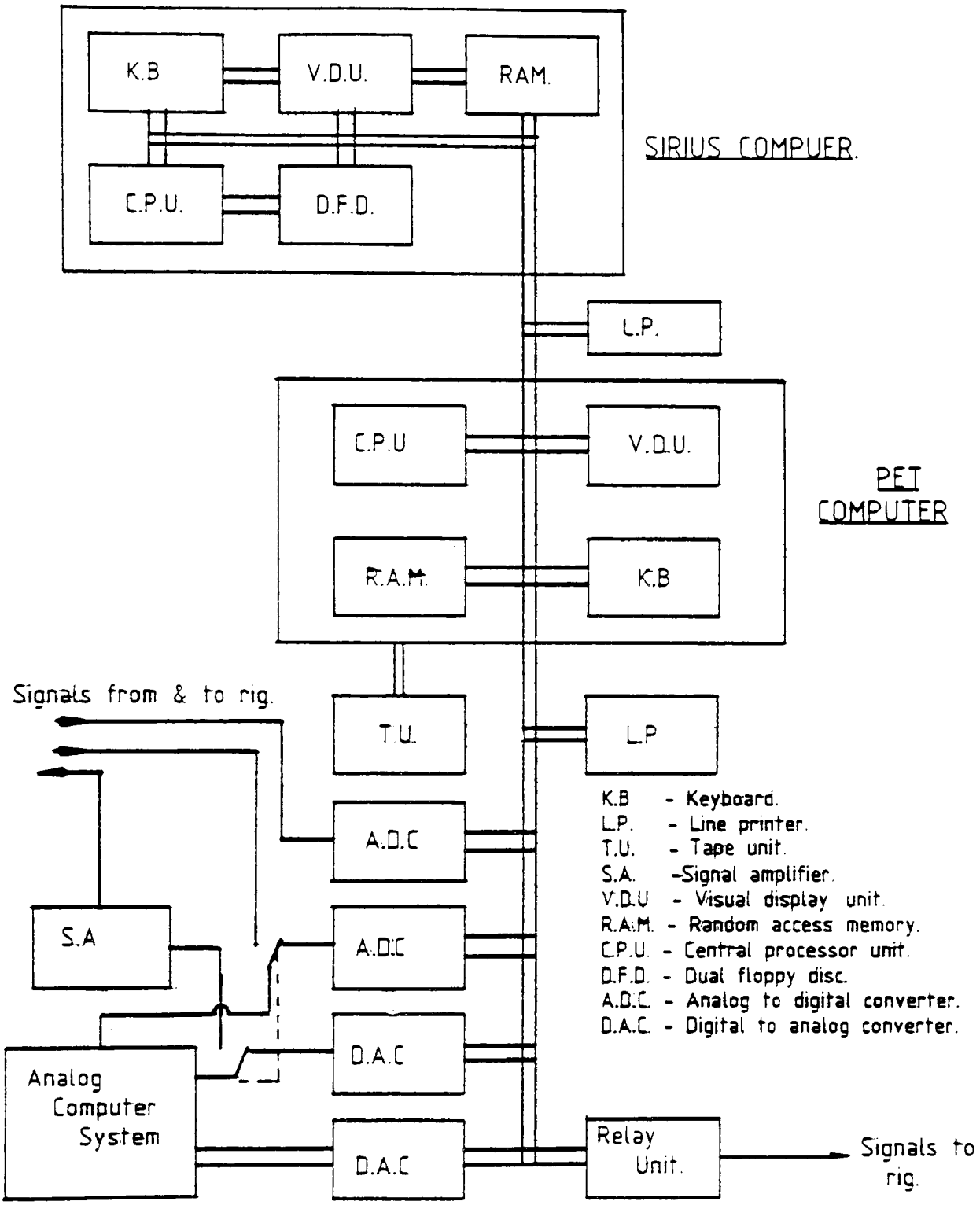

PROJECTED HYBRED COMPUTER SCHEME. FIG 36.

REFERENCES

1. "Appropriate Operational Range for Simultaneous injection of Oxygen and Oil in Large Quantity of the Blast Furnace".
   M. Higuchi, M. Iizuka, K. Kuroda, T. Sumigama.
   Tetsu-to-Hagané 60(1974), 1078.
2. "Calculation of Blast Furnace Flame Temperature".
   K. Beck and J. Kyle.
   BSC Technical Note B/2285, 1976.
3. "Economics of Injection at Blast Furnace Tuyeres".
   J. Kyle and V. Freidenfelds.
   BSC Report No. 714/13, 1974.
4. "Fuel Oil Injection into Blast Furnaces - A Literature Review".
   H.G. Lumm and G.W. Waterhouse.
   BP Trading Ltd and BP Research Centre, 1975.
5. Proc. of the Symposium on Blast Furnace Injection, Wollongong University, February 1972.
6. "Coke Oven Gas Injection into No.2 Blast Furnace at Italsider Tieste".
   A. Ghiglione, M. Giulu, E. Filippore, G. Sironi, R. Sacerdote, L. Tofful.
   Proc. Symp. on Blast Furnace injection, Wollongong University 1972.
7. "Tar Injection at the Rhodesian Iron and Steel Company".
   P.L. Daniel and E.W.D. Penard.
   (ibid).
8. "Injection of Coal Tar Pitch into the Blast Furnace".
   H. Schmuch.
   Stahl und Eisen 91 (1971) Nr.15.
9. "Why Injection - some facts and figures".
   L. Coche.
   Proc. Symp. on Blast Furnace Injection, Wollongong University 1972.
10. "Essais de Combustion D'Hydrocarbones Avec Defaut d'Air En Vue De Leur Injection Massive Daus Les Hauts Fourneaux".
    Della Casa et al.
    Journel d'Etudes sur les Flammes Apr.1972.
11. "Blast Furnace Operating Experience with High Oil Injection rates and Oxygen Enrichment".
    J.J. Quigley, R.L. Tramp and G.H. Craig.
    Report of Inland Steel Company, East Chicago, Indiana. 1973.

12. "Solid Fuel Injection at the Hanna Furnace Corporation".
J.H. Strassburger, E.J. Ostrowski and J.R. Dietz.
Proc. 21st Conference on Blast Furnaces, Coke Ovens and Raw Materials 1962.

13. "Solid Fuel Injection at Weirton".
J.R. Dietz.
Journal of Metals July 1963-499.

14. "Coal Injection into No.5 Blast Furnace at Stanton and Staveley Ltd".
E.M. Summers, L. MacNaughton and J.R. Monson.
Iron and Steel 22nd May 1963.

15. "Armco Coal Injection".
S.A. Bell, J.L. Pugh and J.R. Sexton.
Iron and Steel Magazine, August 1975.

16. "Combustion of coal dust in the Blast Furnace hearth".
V.N. Andronov, Z.S. Plotkin.
Stal', 1974, (7) 587-589

17. "Coal dust injection into the Blast Furnace hearth.
A.A. Yarmal, S.L. Yaroshevskii, L.R. Ruzhinskii, L.Z. Suplin and A.I. Ryabenko.

18. "Injection of Fuels into the Blast Furnace".
W. Wenzel.
Klepzig Fachberichte vol.72, 1964,#10 pp379-385. (translation).

19. "Coal for Blast Furnace Injection".
L.N. Fletcher and A.K. Garbee.
Presented at the 104th AIME Meeting, New York, February 1975.

20. "Blast Furnace Fuel Oil Injection Practice and Results at Ebbw Vale".
W.C.K. Pentry and J. Catlow.
ISI Special Report 72, 1962, pp38-46.

21. Revue CNRM No.1 October 1964 pp13-14.
R. Limpach.

22. Revue CNRM No.4 July 1965 pp3-6.
R. Limpach et al.

23. "Slurry Injection in the C.O.P. Society's Blast Furnace No.5 at Seraing".
CNRM D/1970/0124/8. (translation).

24. "Research into the Injection of a coal-oil slurry into the blast furnace".
K. Morinaga et al.
Tetsu-to-Hagane vol.52 1966 #2, pp107-113.

25. "Some thoughts on Hydrocarbon injection into Blast Furnaces".
G.H. Craig and M.O. Holowaty.
Future of the World Steel Industry 5th Furnas Memorial Conference 1974.

26. "An Investigation into Blast Furnace Oil Injection Techniques carried out at IFRF".
J.G. Isaac, I.H. John, J.M. Powell, T.D. Jones.
BSC Report No. 597/B. 1973.

27. "The Design of Experimental Oil Injections for use on the Blast Furnaces, Port Talbot".
T.D. Jones and K. Bowmer.
BSC Technical Note B/1046. 1971.

28. "Injection of Heavy Oil in a Half Size Blast Furnace Tuyere on a Pilot Plant Rig".
BSC Report No. CAPL/IM/21/75. 1975.

29. "Experiments on Powdered Coal Injection into 0.5m Blast Furnace".
M. Tate et al.
Tetsu-to-Hagane, 50(1964), 13, 2157-2166.

30. "Injecting Solid Fuels into Smelting Zone of an Experimental Blast Furnace".
E.J. Ostsowski et al.
USA Bureau of Mines Report 5648. 1960.

31. "Discussion on Coal Injection".
Journal Iron Steel Institute August 1963 pp 686-688. Contribution by Dr. G. Moss.

32. "Development of a Fuel Oil Slurry Injection System for Blast Furnaces".
G. Wittingham and J. Windsor.
Institute of Fuel Conference, Brussels, Sept 1961.

33. Confidential Report, Shell Research U.K. 1979.

34. "Combustion of Coal-Oil Slurry on a 100 HP Firetube Boiler".
J.J. Demeter, C.R. McCann, G.T. Bellas, J.M. Ekmann, D. Bienstock.
Pittsburgh Energy Research Centre Report PERC/R1-77/8. 1977.

35. "A demonstration of coal-oil mixture combustion in an industrial scale boiler".
A.B. Shimitzu and T.C. Derbridge.
Proc. First International Symposium on Coil Oil mixture combustion, 1978.

36. "Parametric studies of combustion".
M. Ekmann et al (ibid).

37. "Parametric studies of coal oil mixture combustion".
C.F. Busch and R.A. Brown (ibid).

38. "Thermal Efficiency of a Hot Wall Furnace fired with coal oil mixtures at low coal concentrations".
R.H. Essenhigh et al (ibid).

39. "The Determination of coal oil mixture stability".
R.W. Kugel (ibid).

40. "On the Grinding of Coal in Oil".
P.T. Luckie and G.N. Fletcher (ibid).

41. "The Feasibility of using coal-water-oil as a clean liquid fuel".
J. Dooher et al (ibid).

42. "Disruptive combustion of coal-oil mixture droplets".
C.K. Law, C.H. Lee, N. Simirasam (ibid).

43. "The Combustion of single droplets of some fuel oils and alternative liquid fuel combustions".
K.M. Braide, R.G. Isles, J.B. Jordan, A. Williams.
J. Inst. E.(115) September 1979 pp115-124.

44. "A Procedure for predicting the velocity and temperature distributions in a confined, steady, turbulent gaseous diffusion flame".
W.M. Pun and D.B. Spalding.
Report No. SF/TN/11, 1967 Mech. Engng. Dept. Imperial College.

45. "A Novel finite difference formulation for differential equations involving both first and second derivatives".
D.B. Spalding.
Int. J. Num. Meth. Eng. 4, 551-9, 1972.

46. "Combustion Aerodynamics".
J.M. Beer, N.A. Chigier.
Applied Science Publishers, London. 1967.

47. "The Length of Turbulent Swirling Flames burning in Free Surroundings".
P. Maier.
J. Inst. F (419) November 1978.

48. "The Swirling Turbulent Jet".
B.D. Pratte, J.F. Keffer.
Transastions of the ASME, J. Basic Engineering Dec. 1972 pp739-748.

49. "Determination of Flame Lengths for Freely Burning Laminar and Turbulent Flames".
P.D. Sunavala.
Chemical Age of India April/June 1960 pp 217-227.

50. "Combustion Length of Enclosed Turbulent Flames".
M.W.Thring and M.P. Newby.
Proc. 4th Symp. on Combustion, Sept.1952 pp 789-796.

51. "A mixing correlation for annular concentric jets".
G. Pieri.
J. Inst F., Dec. 1973 pp384-388.

52. "Mass Transfer in Dilute Turbulent and Non-Turbulent Systems with Rapid Irreversible Reactions and Equal Diffusivities".
H.L. Toor.
J.A.I.Ch.E. March 1962 pp70-78.

53. "A Stochastic Mixing Model for Homogeneous, Turbulent, Tubular Reactors".
A. Kattan and R.J. Adler.
J.AICH.E May 1967 pp580-585.

54. "Measurements of entrainment by axi-symmetrical turbulent jets".
F.P. Ricou and D.B. Spalding.
J. Fluid Mechanics 1961, II, 1, pp21-32.

55. "Combustion of Pulverised Coal".
M.A. Field, D.W. Gill, B.B. Morgan and P.G.W. Hawksley.
1967 BCURA Leatherhead.

56. "Atomisation of Liquid Fuel for Combustion".
P. Eisenklam.
J. Inst. F April 1961 pp130-143.

57. "The Mechanism of Combustion of Droplets and Sprays of Liquid Fuels".
A. Williams.
Oxidation and Combustion Revs. 3(1968)1-45.

58. "Combustion of Droplets of Liquid Fuels: A Review".
A. Williams.
Combustion and Flame 21, 1-31(1973).

59. "The Correlation of Drop-size Distributions in Fuel Nozzle Sprays" Part I.
H.C. Simmons.
J. Eng. Power, Trans ASME July 1977.

60. "The Correlation of Drop-size Distributions in Fuel Nozzle Sprays" Part II.
H.C. Simmons.
J. Eng. Power, Trans ASME, July 1977.

61. "A High Speed Spray Analyser for Gas Turbine Fuel Nozzles".
H.C. Simmons and D.L. Lapera.
ASME Gas Turbine Conf. Cleveland, Ohio, March 1969.

62. "Statistical Methods in the Process Industries".
M.H. Belz.
Wiley, N. York, 1973 pp103-104.

63. J. Inst. F. Correspondence Dec. 1933, pp109-111.
J.G. Bennett.

64. "The Laws Governing the Fineness of Powdered Coal".
P. Rosin and E. Rammler.
J. Inst. F Oct.1933, pp29-36.

65. "The Influence of Spray Particle Size and Distribution in the Combustion of oil droplets".
R.P. Probert.
Phil. Mag. 1946 (37).

66. "The Rates of Evaporation of Sprays".
D.R. Dickenson and W.R. Marshall.
J. AICH.E (14) 1968.

67. "The use of a simplified mathematical model for prediction of burn out of non-uniform sprays".
A.S.M. Nuruzzaman, R. Siddall and J.M. Beer.
Chem. Engng. Science 1971 vol.26. pp1635-1649.

68. "Studies of the Combustion of Drops in a fuel spray - The burning of single drops of fuel".
G.A.E. Godsave.
4th Symposium (International) on Combustion
M.I.T. September 1952, pp818-830.

69. "A simple Theoretical Model of Droplet Combustion".
V.D. Long.
J. Inst.F December 1964, pp522-525.

70. "Combustion of Single Droplets of Liquid Fuel".
E.G. Masdin PhD thesis; Sheffield University. 1960.

71. "On the Theory of Combustion Rate of Liquid Fuels".
Y. Tanasawa and T. Tesima.
Bulletin J.S.M.E. 1958, 1, 36-41.

72. "Heating of Coal with Light Pulses".
E. Rau and L. Seglin.
Meeting Amercian Chem, Soc. 7, 154, N. York (Sept. 1963).

73. "Gases from Flash and Laser Irradiation of Coal".
A.G. Sharkey, J.L. Shultz and R.A. Friedel.
Nature, 6 June 1964, pp988-989.

74. "Burning Times of Single Coal Particles".
R.H. Essenhigh PhD thesis, 1959, Sheffield University.

75. "Thermal decomposition of pulverised fuel particles".
S. Badzioch, R.B. Sainsbury and P.G.W. Hawksley.
BCURA Circular No.340, 1968.

76. "Changes in the Release of Volatiles during the Combustion of Natural Fuels".
E. Ya. Sergeera and Y.A. Yavorskii.
Therm. Engng. 16, 9, pp147-152 (1969).

77. C.M. Tu, H. Davis and H.C. Hottel.
Industr. Engng. Chem. 23, 277-285 (1934).

78. "The Temperature of Coal Particles during Combustion".
V.I. Babii and I.P. Ivanova.
Teploenergetika 1968, 15,(12),34-37.

79. "Measured Temperatures of Burning Pulverized Fuel Particles, and the Nature of the Primary Reaction Product.
A.B. Ayling and I.W. Smith.
Combustion and Flame 18, 173-184, (1972).

80. H.C. Hottell and I. Stuart.
Industr. Engng. Chem. 1940, 32, 719.

81. "Combustion Kinetics in the Modelling of Large, Pulverized Fuel Furnaces: A Numerical Experiment in Sensitivity.
A. Lowe, T.F. Wall and I. Mc.C. Stewart.
A.I.Ch.E. Journal (Vol.23 No.4 p440).

82. "Rate of Combustion of Size-graded Fractions of Char from a Lew Rank coal between 1200°K and 2000°K.
M.A. Field
Combustion and Flame 13(3), 237-252 (1969).

83. "Measurements of the Effect of Rank on Combustion Rates of Pulverized Coal".
M.A. Field.
Combustion and Flame, 14, 237-248 (1970).

84. "Microscopic Examination of Heat Treated Pulverized Coal Particles".
P. Lightman and P.J. Street.
Fuel, Lond. 47, 7-28 (1968).

85. "Structure and Surface Area of Pulverized Coal During Combustion".
D. Anson, F.D. Moles and P.J. Street.
Combustion and Flame, 16, 265-274 (1971).

86. "The Kinetics of Combustion of Pulverized Semi-Anthracite in the Temperature range 1400-2200°K".
I.W. Smith.
Combustion and Flame, 17, 421-428 (1971).

87. "Internal Burning of Pulverised Semi-anthracite: The relation between particle structure and reactivity".
I.W. Smith and R.J. Tyler.
Fuel, 1972, Vol.51, October (312-321).

88. "A Mathematical Model of the Combustion of Coal in a Cylindrical Combustion Chamber".
M.A. Field and D.W. Gill.
BCURA Circular 318.

89. "Extensions to a One-dimensional Mathematical Model of a Pulverized Coal Flame"
D.W. Gill.
BCURA Research Report 356. 1969.

90. "Mathematical Model of Combustion of solid particles in a turbulent stream with recirculation".
M.M. Gibson and B.B. Morgan.
J. Inst.F, Dec.1970 pp517-523.

91. "Towards a finite difference solution coupled with the zone method for radiative transfer for a cylindrical combustion chamber".
E.R. Steward and K.N. Tennankore.
J. Inst.F, Sept. 1979, 107-114.

92. "The extent to which the reaction intensity of pulverized fuel particles depends on their size".
T.V. Vilenskii, E.A. Parsegov, D.H. Khzmalyan.
Teploenergetika 1969, 16,(2), 72-76.

93. "Predicting the combustion of coal particles".
M.M. Baum and P.J. Street.
Combustion Science and Technology, 1971, Vol.3, pp 241-243.

94. "Theoretical Considerations of the Effect of Pressure on the combustion rate of a cloud of spherical coal particles of a non-uniform size distribution".
A.B. Hedley and F.W. Guldenpfenning.
Journal of the University of Sheffield Fuel Soc. 1969, Vol.20, pp18-29.

95. "Technical Data on Fuel".
H.M. Spiers.
6th Edition.

96. "Flow Measurement".
Kent Instruments Ltd. publication.

97. "A Review of Oil Droplet Size Measurement".
A.R. Jones.
C.E.G.B. Report R/M/N920, Dec. 1976.

98. "The effect of Coal Rank on the Heat Release From Coal/Oil Dispersions".
B.G. Jenkins, J.S. Alabaf, M.C. Patterson and F.D. Moles.
Proc. 64th C.I.C. Coal Symposium, Ottawa 1982.

99. Proc. Inst. Mech. Eng. 1954, 168, 545.

100. "Replacement of Premium Fuels at the Blast Furnace".
I.J. Taggart, M.J. McCarthy and J.M. Burgess.
B.H.P. Tech. Bull., 1982, 26(1), 76.

APPENDIX 1

PROPORTIONAL CROSS SECTIONAL AREA OF COMBUSTION SPACE DESCRIBED BY ANNULI BETWEEN RADIAL SAMPLING POSITIONS

Axial Port Number	Radial Sampling Position Numbers	Distance from Axis (mm)	Proportion Area of Combustion Space Described by Annulus
1	7-8	0-108	0.25
1	8-6	108-135	0.14
1	6-5	135-162	0.17
1	5-4	162-190	0.21
1	4-wall	190-215	0.23
2	7-8	0-108	0.14
2	8-5	108-162	0.17
2	5-4	162-190	0.12
2	4-3	190-230	0.20
2	3-wall	230-290	0.37
3	7-6	0-135	0.13
3	6-4	135-190	0.13
3	4-3	190-230	0.12
3	3-2	230-310	0.32
3	2-wall	310-370	0.30
4	7-5	0-162	0.13
4	5-3	162-230	0.13
4	3-2	230-310	0.21
4	2-1	310-390	0.27
4	1-wall	390-452	0.26
5	7-5	0-162	0.13
5	5-3	162-230	0.13
5	3-2	230-310	0.20
5	2-1	310-390	0.27
5	1-wall	390-457	0.27

APPENDIX 2

PITOT TUBE TRAVERSES

PORT 1 Diameter of Combustion Space: 430mm approx.

Distance from Axis (mm)	Velocity Measured (m/s)				Mean Velocity (m/s)
	Run 1	Run 2	Run 3	Run 4	
-200	2.6	2.6	2.8	2.8	2.7
-150	2.8	2.8	2.8	2.8	2.8
-100	3.0	3.0	3.0	3.0	3.0
- 50	3.0	3.1	3.1	3.2	3.1
0	3.2	3.0	3.5	3.1	3.2
50	3.2	3.4	3.4	3.2	3.3
100	3.0	3.0	3.0	3.0	3.0
150	3.0	2.8	2.9	2.9	2.9
200	2.5	2.8	2.4	2.7	2.6

PORT 2 Diameter of Combustion Space: 610mm approx.

Distance from Axis (mm)	Velocity Measured (m/s)				Mean Velocity (m/s)
	Run 1	Run 2	Run 3	Run 4	
-300	1.5	1.5	1.5	1.2	1.4
-225	1.5	1.5	1.5	1.5	1.5
-150	1.8	1.5	1.5	1.5	1.6
- 75	1.5	1.7	1.5	1.5	1.5
0	1.8	1.7	1.5	1.5	1.6
75	1.8	1.5	1.5	1.7	1.6
150	1.5	1.5	1.5	1.5	1.5
225	1.5	1.5	1.5	1.5	1.5
300	1.5	1.5	1.5	1.5	1.5

APPENDIX 3

PROPERTIES OF FUELS USED

Slurry Component		Coal 1	Coal 2	Coal 3	Coal 4	Oil
Description		Coarsely Ground Coke Breeze	Finely Ground Coke Breeze	Coarsely Ground* Anthracite	Finely Ground Anthracite	Residual Class G
Proximate Analysis daf.	% ASH	7.2	9.9	6.5	3.9	-
	% H_2O	8.9	1.3	7.3	4.8	-
	% V.M.	1.0	1.1	2.9	4.9	-
Ultimate Analysis (As Fired)	% C	83.1	86.8	84.2	86.9	85.2
	% H	0.4	0.4	1.2	2.7	11.9
	% S	0.9	0.9	0.8	0.6	2.9
	% N	0.8	0.8	0.8	1.0	neg
	% O	0.9	1.0	0.9	0.8	neg
	% ASH	6.2	8.9	5.7	3.6	neg
	% H_2O	7.7	1.2	6.4	4.4	neg
Net C.V. (MJ/Kg)		28,950	30,250	30,100	32,900	39,700
Size Distribution	<125μ	94.5	98.6	83.7	99.6	-
	<106μ	93.3	97.7	78.8	99.2	-
	< 90μ	89.4	95.7	71.5	98.5	-
	< 75μ	82.8	91.4	61.4	96.1	-
	< 63μ	76.3	86.3	52.7	92.7	-
	< 53μ	69.6	79.4	44.8	87.9	-
Rosin-Rammler Analysis	Constant (b)	77.3	68.5	329.9	42.1	-
	Exponent (n)	1.140	1.186	1.332	1.137	-
Mean particle size (μ)		45.3	35.3	77.6	27.1	-

* Found to be contaminated with coke breeze

APPENDIX 4.0.0

IDENTIFICATION OF WORK PROGRAMME ON OIL

Air Preheat Temperature (°C)	Air Velocity (m/s)	Air Oxygen Content (Partial Pressure)	Stoichiometric Ratio	Run Number
750	200	0.21	0.8	86(1)
750	200	0.21	0.9	85(2)
750	200	0.26	0.8	3
750	200	0.26	0.9	4
750	240	0.21	0.8	5
750	240	0.21	0.9	10
750	240	0.26	0.8	11
750	240	0.26	0.9	84(16)
1000	200	0.21	0.8	6
1000	200	0.21	0.9	7
1000	200	0.26	0.8	8
1000	200	0.26	0.9	9
1000	240	0.21	0.8	12
1000	240	0.21	0.9	13
1000	240	0.26	0.8	14
1000	240	0.26	0.9	83(15)

APPENDIX 4.0.1.

IDENTIFICATION OF WORK PROGRAMME OF SLURRY 1

Air Preheat Temperature (°C)	Air Velocity (m/s)	Air Oxygen Content (Partial Pressure)	Stoichiometric Ratio	Run Number
750	200	0.21	0.8	75
750	200	0.21	0.9	74
750	200	0.26	0.8	73
750	200	0.26	0.9	72
750	240	0.21	0.8	55
750	240	0.21	0.9	54
750	240	0.26	0.8	56
750	240	0.26	0.9	71
1000	200	0.21	0.8	46
1000	200	0.21	0.9	47
1000	200	0.26	0.8	48
1000	200	0.26	0.9	49
1000	240	0.21	0.8	51
1000	240	0.21	0.9	50
1000	240	0.26	0.8	52
1000	240	0.26	0.9	53

APPENDIX 4.0.2

IDENTIFICATION OF WORK PROGRAMME ON SLURRY 2

Air Preheat Temperature (°C)	Air Velocity (m/s)	Air Oxygen Content (Partial Pressure)	Stoichiometric Ratio	Run Number
750	200	0.21	0.8	20
750	200	0.21	0.9	21
750	200	0.26	0.8	22
750	200	0.26	0.9	26
750	240	0.21	0.8	27
750	240	0.21	0.9	28
750	240	0.26	0.8	29
750	240	0.26	0.9	30
1000	200	0.21	0.8	18
1000	200	0.21	0.9	17
1000	200	0.26	0.8	19
1000	200	0.26	0.9	23
1000	240	0.21	0.8	24
1000	240	0.21	0.9	82(25)
1000	240	0.26	0.8	31
1000	240	0.26	0.9	81(32)

APPENDIX 4.0.3.

IDENTIFICATION OF WORK PROGRAMME ON SLURRY 3

Air Preheat Temperature (°C)	Air Velocity (m/s)	Air Oxygen Content (Partial Pressure)	Stoichiometric Ratio	Run Number
750	200	0.21	0.8	64
750	200	0.21	0.9	63
750	200	0.26	0.8	66
750	200	0.26	0.9	65
750	240	0.21	0.8	67
750	240	0.21	0.9	68
750	240	0.26	0.8	69
750	240	0.26	0.9	70
1000	200	0.21	0.8	58
1000	200	0.21	0.9	57
1000	200	0.26	0.8	60
1000	200	0.26	0.9	59
1000	240	0.21	0.8	62
1000	240	0.21	0.9	61
1000	240	0.26	0.8	79
1000	240	0.26	0.9	80

APPENDIX 4.0.4.

IDENTIFICATION OF WORK PROGRAMME ON SLURRY 4

Air Preheat Temperature (°C)	Air Velocity (m/s)	Air Oxygen Content (Partial Pressure)	Stoichiometric Ratio	Run Number
750	200	0.21	0.8	35
750	200	0.21	0.9	36
750	200	0.26	0.8	37
750	200	0.26	0.9	38
750	240	0.21	0.8	40
750	240	0.21	0.9	39
750	240	0.26	0.8	41
750	240	0.26	0.9	42
1000	200	0.21	0.8	34
1000	200	0.21	0.9	33
1000	200	0.26	0.8	78
1000	200	0.26	0.9	77
1000	240	0.21	0.8	45
1000	240	0.21	0.9	76
1000	240	0.26	0.8	44
1000	240	0.26	0.9	43

APPENDIX 4.1.0

TYPICAL FULL SET OF RESULTS FROM RIG

Run 71
Coal No.1

Nominal Conditions: Air Preheat 750°C, Air Velocity 240 m/s, Oxygen Partial Pressure of Air 0.26, Stoichiometric Ratio 0.9, Slurry Mass Flow 1.65 Kg/min.

PORT 1
Actual Conditions

Air Temp. (°C)	Air Velocity (m/s)	Air Oxygen Content (P.Pressure)	Propane Flow (ℓ/s)	Oxygen Flow (ℓ/s)	Air Flow (ℓ/s)
740	241	0.257	2.54	31.3	199

Gas Analysis

Radial Position	% Oxygen	% Carbon Dioxide	% Carbon Monoxide	% Hydrogen	% Methane
1	3.83	21.06	0.45	0.07	0.10
2	4.33	20.41	0.36	0.04	0.10
3	6.71	19.31	0.14	0.00	0.10
4	8.54	17.98	0.06	0.00	0.08
5	9.25	14.31	0.19	0.03	0.07
Area Weighted Mean	7.09	17.81	0.21	0.02	0.08

PORT No.2
Actual Conditions

Air Temp. (°C)	Air Velocity (m/s)	Air Oxygen Content (P.Pressure)	Propane Flow (ℓ/s)	Oxygen Flow (ℓ/s)	Air Flow (ℓ/s)
740	240	0.259	2.49	32.1	198

Gas Analysis

Radial Position	% Oxygen	% Carbon Dioxide	% Carbon Monoxide	% Hydrogen	% Methane
1	3.75	21.59	0.14	0.01	0.09
2	3.76	21.40	0.15	0.02	0.09
3	3.78	21.28	0.15	0.01	0.08
4	3.91	21.67	0.07	0.03	0.09
5	4.05	21.46	0.08	0.04	0.09
Area Weighted Mean	3.92	21.46	0.10	0.02	0.08

PORT NO.3
Actual Conditions

Air Temp. (°C)	Air Velocity (m/s)	Air Oxygen Content (P.Pressure)	Propane Flow (ℓ/s)	Oxygen Flow (ℓ/s)	Air Flow (ℓ/s)
736	246	0.257	2.46	31.6	204

Gas Analysis

Radial Position	% Oxygen	% Carbon Dioxide	% Carbon Monoxide	% Hydrogen	% Methane
1	2.49	22.76	0.11	0.05	0.10
2	2.61	22.52	0.11	0.05	0.10
3	2.72	22.42	0.10	0.05	0.09
4	2.95	22.11	0.10	0.05	0.09
5	2.97	21.96	0.10	0.04	0.09
Area Weighted Mean	2.85	22.17	0.10	0.04	0.09

PORT 4
Actual Conditions

Air Temp. (°C)	Air Velocity (m/s)	Air Oxygen Content (P.Pressure)	Propane Flow (ℓ/s)	Oxygen Flow (ℓ/s)	Air Flow (ℓ/s)
738	242	0.256	2.54	31.6	200

Gas Analysis

Radial Position	% Oxygen	% Carbon Dioxide	% Carbon Monoxide	% Hydrogen	% Methane
1	1.61	23.57	0.11	0.06	0.10
2	1.91	23.17	0.11	0.06	0.10
3	2.00	23.13	0.11	0.06	0.10
4	2.02	23.08	0.10	0.06	0.09
5	2.09	23.00	0.10	0.05	0.10
Area Weighted Mean	2.01	23.09	0.10	0.05	0.09

PORT 5
Actual Conditions

Air Temp. (°C)	Air Velocity (m/s)	Air Oxygen Content (P.Pressure)	Propane Flow (ℓ/s)	Oxygen Flow (ℓ/s)	Air Flow (ℓ/s)

Gas Analysis

Radial Position	% Oxygen	% Carbon Dioxide	% Carbon Monoxide	% Hydrogen	% Methane
1	1.74	23.43	0.10	0.08	0.10
2	1.76	23.35	0.11	0.08	0.10
3	1.80	23.35	0.10	0.08	0.10
4	1.83	23.31	0.10	0.08	0.10
5	1.84	23.27	0.10	0.09	0.10
Area Weighted Mean	1.81	23.35	0.10	0.08	0.10

APPENDIX 4.2.0

INDIVIDUAL RESULTS OF FRACTIONAL BURNOUT

OIL ONLY

Run Number	Port 1	Port 2	Port 3	Port 4	Port 5
86	1.008	0.939	0.913	0.914	0.915
85	0.987	1.021	0.973	1.018	0.984
3	0.941	0.920	0.921		
4	0.981	1.071	1.023		
5	0.975	0.989	0.992		
10	1.041	1.020	1.025		
11	1.117	1.117	1.048		
84	0.976	0.997	0.968	0.960	0.981
6	0.857	0.814	0.863		
7	1.036	0.990	0.909		
8	1.110	1.074	0.993		
9	1.028	1.097	1.056		
12	0.945	0.925	0.912		
13	0.880	0.870	0.878		
14	0.991	0.961	0.955		
83	0.968	0.988	0.994	1.007	1.013

APPENDIX 4.2.1.

INDIVIDUAL RESULTS OF FRACTIONAL BURNOUT

COAL 1

Run Number	Port 1	Port 2	Port 3	Port 4	Port 5
75	0.802	0.814	0.865	0.921	0.917
74	0.814	0.871	0.871	0.936	0.958
73	0.798	0.906	0.967	1.006	1.031
72	0.841	0.897	0.958	1.008	1.018
55	0.924	0.909	0.945	1.007	1.004
54	0.815	0.920	0.949	1.046	1.082
56	0.831	0.949	1.010	1.010	1.010
71	0.796	0.933	0.997	1.013	1.026
46	0.783	0.930	0.943	1.037	0.938
47	0.813	0.884	0.960	0.993	0.935
48	0.789	0.837	0.845	0.861	0.796
49	0.846	0.968	1.022	1.003	0.977
51	0.842	0.862	0.960	0.981	0.984
50	0.825	0.894	0.953	1.028	1.071
52	0.891	0.953	1.012	1.013	1.017
53	0.815	0.939	0.983	0.948	0.919

APPENDIX 4.2.2.

INDIVIDUAL RESULTS OF FRACTIONAL BURNOUT

COAL 2

Run Number	Port 1	Port 2	Port 3	Port 4	Port 5
20	0.806	0.839	0.928	0.987	0.952
21	0.775	0.884	0.915	0.946	0.960
22	0.717	0.794	0.969	1.026	0.929
26	0.800	0.906	0.926	0.954	0.976
27	0.797	0.887	0.956	0.934	0.962
28	0.819	0.911	0.979	1.020	1.026
29	0.816	0.932	0.992	0.999	1.023
30	0.775	0.889	0.970	0.994	1.024
18	0.908	0.925	0.999	1.058	1.016
17	0.837	0.937	0.944	1.007	1.007
19	0.840	0.880	0.902	0.938	0.901
23	0.842	1.000	1.037	1.025	1.008
24	0.915	0.971	1.011	1.014	1.040
82	0.751	0.777	0.787	0.898	0.889
31	0.903	0.997	1.001	1.038	1.056
81	0.875	0.976	0.979	1.026	1.005

APPENDIX 4.2.3.

INDIVIDUAL RESULTS OF FRACTIONAL BURNOUT

COAL 3

Run Number	Port 1	Port 2	Port 3	Port 4	Port 5
64	0.809	0.832	0.947	1.006	1.051
63	0.813	0.867	0.961	1.000	0.996
66	0.779	0.964	0.967	0.995	0.991
65	0.761	0.845	0.930	0.971	0.967
67	0.856	0.897	0.986	1.043	1.040
68	0.805	0.892	0.932	0.965	0.990
69	0.812	0.907	0.993	1.018	1.028
70	0.795	0.893	0.966	0.966	0.914
58	0.801	0.783	0.908	0.962	0.909
57	0.855	0.916	1.023	1.089	1.065
60	0.828	0.880	0.964	1.020	0.992
59	0.780	0.835	0.909	0.910	0.927
62	0.780	0.795	0.881	0.946	0.946
61	0.768	0.794	0.897	0.956	0.941
79	0.909	0.922	0.966	1.013	1.015
80	0.904	0.976	1.028	1.043	1.057

APPENDIX 4.2.4.

INDIVIDUAL RESULTS OF FRACTIONAL BURNOUT

COAL 4

Run Number	Port 1	Port 2	Port 3	Port 4	Port 5
35	0.829	0.875	0.871	0.886	0.857
36	0.749	0.858	0.917	0.910	0.920
37	0.737	0.818	0.855	0.849	0.855
38	0.810	0.891	0.925	0.936	0.963
40	0.840	0.878	0.967	1.003	1.005
39	0.801	0.853	0.924	0.949	0.968
41	0.828	0.971	1.004	1.016	1.025
42	0.872	0.945	0.993	0.987	1.000
34	0.936	0.932	0.948	0.904	0.902
33	0.846	0.947	1.066	1.000	0.857
78	0.903	0.951	0.986	0.976	0.984
77	0.879	0.935	0.984	1.000	1.006
45	0.896	0.926	0.996	0.979	0.979
76	0.940	1.019	1.028	1.074	1.057
44	0.938	0.956	1.001	1.010	1.007
43	0.901	0.960	0.979	0.994	0.980

APPENDIX 4.3.0

MEAN RESULTS OF FRACTIONAL BURNOUT BY SLURRY TYPE

Port	Fractional Burnout				
	Oil Only	Slurry 1	Slurry 2	Slurry 3	Slurry 4
1	0.990	0.826	0.826	0.816	0.851
2	0.987	0.904	0.906	0.875	0.920
3	0.964	0.952	0.956	0.954	0.968
4		0.988	0.992	0.994	0.967
5		0.980	0.986	0.989	0.960

APPENDIX 4.3.1.

MEAN RESULT OF FRACTIONAL BURNOUT BY INPUT VARIABLE

OIL ONLY, TOTAL POPULATION 16 RUNS

Port	Air Preheat	
	750°C	1000°C
1	1.003	0.977
2	1.009	0.965
3	0.983	0.945
4		
5		

Port	Air Velocity	
	200m/s	240m/s
1	0.993	0.986
2	0.991	0.983
3	0.956	0.972
4		
5		

Port	Air Oxygen Content	
	21%	26%
1	0.966	1.01
2	0.946	1.03
3	0.933	0.995
4		
5		

Port	Stoichiometric Ratio	
	0.8	0.9
1	0.993	0.986
2	0.967	1.007
3	0.950	0.978
4		
5		

APPENDIX 4.3.2.

MEAN RESULT OF FRACTIONAL BURNOUT BY IMPUT VARIABLE

ALL SLURRIES TOTAL POPULATION 64 RUNS

Port	Air Preheat	
	750°C	1000°C
1	0.806	0.854
2	0.888	0.914
3	0.948	0.967
4	0.978	0.992
5	0.983	0.974

Port	Air Velocity	
	200m/s	240m/s
1	0.816	0.844
2	0.888	0.915
3	0.945	0.970
4	0.972	0.998
5	0.955	1.003

Port	Air Oxygen Content	
	21%	26%
1	0.830	0.831
2	0.884	0.919
3	0.945	0.969
4	0.984	0.987
5	0.976	0.982

Port	Stoichiometric Ratio	
	0.8	0.9
1	0.834	0.822
2	0.896	0.907
3	0.956	0.959
4	0.983	0.987
5	0.974	0.984

APPENDIX 4.3.3.

MEAN RESULTS OF FRACTIONAL BURNOUT, EFFECT OF SLURRY FLOW

Oil Only

Port	Lowest 8 Oil Flows	Highest 8 Oil Flows
1	0.981	0.999
2	0.966	1.010
3	0.937	0.991
4		
5		

Coal 4

Port	Lowest 8 Slurry Flows	Highest 8 Slurry Flows
1	0.872	0.848
2	0.930	0.909
3	0.979	0.956
4	0.966	0.968
5	0.945	0.975

Coals 1, 2 and 3

Port	Lowest 24 Slurry Flows	Highest 24 Slurry Flows
1	0.818	0.826
2	9.874	0.916
3	0.935	0.973
4	0.980	1.002
5	0.965	1.005

APPENDIX 4.3.4.

MODIFIED DATA SET

MEAN RESULTS OF FRACTIONAL BURNOUT, EFFECT OF SLURRY FLOW

Oil Only

Port	Lowest 8 Oil Flows	Highest 8 Oil Flows
1	1.014	0.999
2	1.002	1.008
3	0.973	0.991
4		
5		

Coal 4

Port	Lowest 8 Slurry Flows	Highest 8 Slurry Flows
1	0.900	0.869
2	0.964	0.941
3	1.014	0.990
4	1.000	1.003
5	0.979	1.010

Coals 1, 2 and 3

Port	Lowest 24 Slurry Flows	Highest 24 Slurry Flows
1	0.833	0.826
2	0.893	0.916
3	0.955	0.973
4	1.001	1.002
5	0.986	1.005

APPENDIX 4.4.0

MODIFIED DATA SET

INDIVIDUAL RESULTS OF FRACTIONAL BURNOUT

Oil Only

Run Number	Port 1	Port 2	Port 3
86	1.041	0.973	0.947
85	1.020	1.060	1.009
3	0.941	0.920	0.921
4	0.981	1.071	1.023
5	0.975	0.989	0.992
10	1.041	1.020	1.025
11	1.117	1.117	1.048
84	0.976	0.997	0.968
6	0.885	0.844	0.896
7	1.070	1.028	0.943
8	1.147	1.113	1.031
9	1.063	1.138	1.097
12	0.976	0.959	0.946
13	0.910	0.903	0.911
14	0.991	0.961	0.955
83	0.968	0.988	0.994

APPENDIX 4.4.1.

MODIFIED DATA SET
INDIVIDUAL RESULTS OF FRACTIONAL BURNOUT

COAL 1

Run Number	Port 1	Port 2	Port 3	Port 4	Port 5
75	0.818	0.831	0.883	0.941	0.936
74	0.830	0.889	0.890	0.956	0.978
73	0.798	0.906	0.967	1.006	1.030
72	0.841	0.897	0.958	1.008	1.018
55	0.924	0.909	0.945	1.007	1.004
54	0.815	0.920	0.949	1.046	1.082
56	0.831	0.949	1.010	1.010	1.010
71	0.796	0.933	0.997	1.013	1.026
46	0.797	0.950	0.963	1.059	0.958
47	0.829	0.903	0.980	1.015	0.955
48	0.804	0.855	0.863	0.879	0.813
49	0.862	0.989	1.045	1.025	0.998
51	0.857	0.880	0.981	1.001	1.005
50	0.841	0.913	0.973	1.050	1.094
52	0.891	0.953	1.012	1.013	1.017
53	0.815	0.939	0.983	0.948	0.919

APPENDIX 4.4.2.

MODIFIED DATA SET
INDIVIDUAL RESULTS OF FRACTIONAL BURNOUT

Coal 2

Run Number	Port 1	Port 2	Port 3	Port 4	Port 5
20	0.821	0.857	0.947	1.007	0.972
21	0.790	0.903	0.934	0.966	0.980
22	0.717	0.794	0.969	1.026	0.929
26	0.800	0.906	0.926	0.954	0.976
27	0.797	0.887	0.956	0.934	0.962
28	0.819	0.911	0.979	1.020	1.026
29	0.816	0.932	0.992	0.999	1.023
30	0.775	0.889	0.970	0.994	1.024
18	0.925	0.945	1.021	1.080	1.038
17	0.853	0.957	0.964	1.028	1.028
19	0.856	0.899	0.922	0.958	0.920
23	0.859	1.022	1.060	1.047	1.030
24	0.932	0.992	1.033	1.035	1.062
82	0.766	0.794	0.804	0.917	0.908
31	0.903	0.997	1.001	1.038	1.056
81	0.875	0.976	0.979	1.026	1.005

APPENDIX 4.4.3.

MODIFIED DATA SET
INDIVIDUAL RESULTS OF FRACTIONAL BURNOUT

COAL 3

Run Number	Port 1	Port 2	Port 3	Port 4	Port 5
64	0.825	0.849	0.967	1.027	1.074
63	0.829	0.885	0.982	1.021	1.017
66	0.779	0.964	0.967	0.995	0.991
65	0.761	0.845	0.930	0.971	0.967
67	0.856	0.897	0.986	1.043	1.040
68	0.805	0.892	0.932	0.965	0.990
69	0.812	0.907	0.993	1.018	1.028
70	0.795	0.893	0.966	0.966	0.914
58	0.816	0.800	0.927	0.982	0.929
57	0.871	0.935	1.044	1.112	1.088
60	0.844	0.899	0.984	1.041	1.013
59	0.795	0.853	0.928	0.929	0.947
62	0.794	0.811	0.900	0.966	0.966
61	0.782	0.811	0.916	0.976	0.961
79	0.909	0.922	0.966	1.013	1.015
80	0.904	0.976	1.028	1.043	1.057

APPENDIX 4.4.4.

MODIFIED DATA SET
INDIVIDUAL RESULTS OF FRACTIONAL BURNOUT

Coal 4

Run Number	Port 1	Port 2	Port 3	Port 4	Port 5
35	0.856	0.906	0.902	0.917	0.857
36	0.773	0.889	0.950	0.942	0.953
37	0.761	0.848	0.885	0.880	0.886
38	0.837	0.923	0.958	0.970	0.998
40	0.867	0.909	1.001	1.039	1.040
39	0.828	0.884	0.957	0.983	1.002
41	0.856	1.006	1.040	1.052	1.062
42	0.901	0.979	1.028	1.023	1.036
34	0.965	0.965	1.019	0.936	0.934
33	0.873	0.980	1.104	1.035	0.888
78	0.932	0.986	1.023	1.011	1.019
77	0.907	0.969	1.020	1.036	1.042
45	0.924	0.959	1.031	1.014	1.014
76	0.970	1.055	1.065	1.112	1.094
44	0.969	0.991	1.037	1.046	1.043
43	0.931	0.994	1.015	1.030	1.015

APPENDIX 4.5.0

MODIFIED DATA SET

MEAN RESULTS OF BURNOUT BY SLURRY TYPE

Port	Oil	Coal 1	Coal 2	Coal 3	Coal 4
1	1.006	0.834	0.831	0.823	0.884
2	1.005	0.914	0.916	0.884	0.953
3	0.982	0.962	0.966	0.963	1.002
4		0.999	1.002	1.004	1.002
5		0.990	0.996	1.000	0.995

APPENDIX 4.5.1.

MODIFIED DATA SET

MEAN RESULTS OF FRACTIONAL BURNOUT BY INPUT VARIABLE

OIL ONLY: TOTAL POPULATION 16 RUNS

Port	Air Preheat	
	750°C	1000°C
1	1.012	1.001
2	1.018	0.992
3	0.992	0.972
4		
5		

Port	Air Velocity	
	200 m/s	240m/s
1	1.018	0.994
2	1.018	0.992
3	0.983	0.980
4		
5		

Port	Air Oxygen Content	
	21%	26%
1	0.990	1.023
2	0.972	1.038
3	0.959	1.005
4		
5		

Port	Stoichiometric Ratio	
	0.8	0.9
1	1.009	1.004
2	0.985	1.025
3	0.967	0.996
4		
5		

APPENDIX 4.5.2.

MODIFIED DATA SET

MEAN RESULTS OF FRACTIONAL BURNOUT BY INPUT VARIABLE

ALL SLURRIES: TOTAL POPULATION 64 RUNS

Port	Air Preheat	
	750°C	1000°C
1	0.817	0.870
2	0.900	0.933
3	0.960	0.987
4	0.991	1.013
5	0.996	0.995

Port	Air Velocity	
	200 m/s	240m/s
1	0.832	0.855
2	0.906	0.927
3	0.965	0.982
4	0.993	1.011
5	0.975	1.016

Port	Air Oxygen Content	
	21%	26%
1	0.845	0.842
2	0.902	0.931
3	0.965	0.982
4	1.004	0.999
5	0.996	0.995

Port	Stoichiometric Ratio	
	0.8	0.9
1	0.851	0.835
2	0.911	0.922
3	0.972	0.975
4	0.999	1.004
5	0.990	1.001

APPENDIX 5

EFFICIENCY OF MATHEMATICAL MODEL

Type of Integration	Nominal No. of Iterations	Differential in Percentage Oxygen Prediction			Relative Run Time
		First Port	Fifth Port	Mean	
1	1000	0	0	0	10
	500	0.094	0.140	0.117	5
	400	0.135	0.204	0.170	4
	300	0.197	0.309	0.253	3
	200	0.303	0.495	0.399	2
	100	0.531	0.866	0.699	1
2	1000	-0.001	0	0	10
	500	0.093	0.140	0.117	5
	400	0.134	0.200	0.167	4
	300	0.195	0.309	0.252	3
	200	0.300	0.485	0.393	2
	100	0.524	0.894	0.709	1
3	1000	-0.018	-0.035	-0.027	13.0
	500	0.050	0.037	0.044	6.5
	400	0.079	0.069	0.074	5.2
	300	0.123	0.118	0.121	3.9
	200	0.198	0.204	0.201	2.6
	100	0.364	0.411	0.388	1.3
4	200	0.293	0.469	0.381	4.0
	150	0.373	0.618	0.500	3.0
	100	0.504	0.835	0.670	2.0
5	200	0.112	0.439	0.276	4.0
	150	0.196	0.587	0.392	3.0
	100	0.326	0.825	0.576	2.0
6	200	0.029	0.206	0.118	5.2
	150	0.094	0.279	0.187	3.9
	100	0.195	0.405	0.300	2.6

NOTE: RELATIVE RUN TIME = 1.0 Corresponds to a running time of 48 minutes on the "Pet" Microcomputer, 25 minutes on the Sirius Microcomputer in BASIC and 3.5 minutes on the Sirius Microcomputer in compiled BASIC. Speed on the PDP 11/45 Minicomputer varied between approximately 3mins and 11 mins depending on time sharing loading.

APPENDIX 6.0

PERCENTAGE ERROR OF MODEL AT FIRST FLAME TUNNEL PORT EFFECT OF VARYING NUMBERS OF MODEL ITERATIONS

	No. of Iterations	Rosin-Rammler Index	
		0.9	1.1
Coal 1	20	3.15	5.27
	30	3.10	5.23
	50	3.06	5.19
	100	3.03	5.16
	200	3.01	5.14
Coal 2	20	5.31	8.34
	30	5.27	8.30
	50	5.23	8.27
	100	5.20	8.25
	200	5.19	8.23
Coal 3	20	-2.12	-0.17
	30	-2.18	-0.22
	50	-2.24	-0.27
	100	-2.28	-0.31
	200	-2.31	-0.34
Coal 4	20	0.95	3.14
	30	0.91	3.11
	50	0.87	3.08
	100	0.85	3.06
	200	0.84	3.05

APPENDIX 6.1.0

FIRST PHASE OF OPTIMISATION OF MODEL
PERCENTAGE ERROR AT FIRST PORT FOR COAL No. 1

Mean Droplet Size (μ)	Rosin-Rammler Index					
	0.70	0.84	0.98	1.12	1.26	1.40
	No. of Overlaps = 3					
50	4.57	7.12	8.40	9.12	9.81	9.95
70	1.69	3.80	5.50	6.70	8.39	9.02
90	-1.88	0.16	1.90	3.92	5.17	6.95
110	-5.16	-3.43	-1.25	0.16	2.20	3.36
130	-8.16	-6.81	-4.90	-2.9	-1.77	-0.83
150	-10.88	-9.96	-8.40	-6.67	-5.83	-3.86
	No. of Overlaps = 4					
50	4.57	6.38	8.41	9.08	9.76	9.91
70	1.04	3.85	5.52	6.68	7.77	8.40
90	-1.68	0.32	2.01	3.38	5.22	6.14
110	-4.88	-3.17	-1.64	0.36	1.50	2.63
130	-7.80	-6.40	-5.17	-3.44	-2.35	-0.57
150	-10.46	-9.52	-8.01	-7.09	-5.44	-4.61
	No. of Overlaps = 5					
50	4.66	6.47	7.78	8.45	9.13	9.94
70	1.22	3.28	5.70	6.85	7.92	8.53
90	-2.14	0.60	2.30	3.80	4.87	5.80
110	-5.24	-2.74	-1.24	0.13	1.28	3.04
130	-7.36	-5.98	-4.67	-3.54	-1.82	-0.89
150	-9.96	-8.97	-8.01	-6.47	-5.64	-4.81
	No. of Overlaps = 6					
50	4.80	6.60	7.89	8.54	9.18	9.31
70	1.45	3.52	5.17	6.32	7.37	8.70
90	-1.82	0.18	1.88	4.18	5.24	6.14
110	-4.83	-3.04	-0.75	0.65	1.81	2.93
130	-7.59	-5.43	-4.07	-2.90	-1.78	-0.85
150	-10.10	-8.34	-7.32	-6.34	-5.48	-3.96
	No. of Overlaps = 7					
50	4.96	6.73	7.99	8.60	9.22	9.33
70	1.70	3.76	5.40	6.52	7.53	8.10
90	-1.48	0.54	2.24	3.73	4.77	5.66
110	-4.41	-2.58	-1.04	0.35	2.34	3.45
130	-7.08	-5.61	-4.24	-2.23	-1.10	-0.16
150	-9.53	-8.41	-6.59	-5.55	-4.65	-3.77
	No. of Overlaps = 8					
50	5.09	6.85	8.08	8.66	9.25	9.35
70	1.93	3.98	5.59	6.67	7.67	8.20
90	-1.15	0.87	2.56	4.03	5.04	5.90
110	-3.99	-2.14	-0.60	0.78	1.91	2.99
130	-6.58	-5.07	-3.68	-2.48	-1.36	0.46
150	-8.96	-7.78	-6.68	-5.64	-3.90	-3.01

APPENDIX 6.1.1.

FIRST PHASE OF OPTIMISATION OF MODEL
PERCENTAGE ERROR AT FIRST PORT FOR COAL NO. 2

Mean Droplet Size (μ)	Rosin-Rammler Index					
	0.70	0.84	0.98	1.12	1.26	1.40
	No. of Overlaps = 3					
50	7.63	9.61	11.79	12.54	13.28	13.46
70	3.71	6.73	8.55	9.85	11.05	12.36
90	0.67	2.78	4.61	6.77	8.11	9.14
110	-2.83	-1.09	0.53	2.68	3.93	6.07
130	-6.00	-4.71	-2.74	-1.54	0.54	1.53
150	-8.86	-8.04	-6.52	-5.58	-3.83	-2.93
	No. of Overlaps = 4					
50	7.69	9.62	11.03	11.79	13.22	13.40
70	3.90	6.06	8.61	9.86	11.02	11.71
90	0.20	3.05	4.82	6.26	7.55	9.19
110	-3.19	-0.70	0.88	2.31	4.18	5.36
130	-6.26	-4.20	-2.92	-1.10	0.02	0.96
150	-9.03	-7.44	-6.58	-5.02	-4.21	-2.43
	No. of Overlaps = 5					
50	7.84	9.73	11.12	11.86	12.58	12.77
70	4.18	6.31	8.04	9.28	11.19	11.85
90	0.60	2.62	5.20	6.62	7.88	8.85
110	-2.67	-0.16	1.41	2.83	4.01	5.16
130	-5.65	-3.55	-2.26	-1.11	-0.01	1.63
150	-8.36	-6.70	-5.81	-4.90	-3.40	-2.56
	No. of Overlaps = 6					
50	8.03	9.89	11.25	11.95	12.64	12.80
70	4.50	6.61	8.33	9.53	10.64	11.28
90	1.05	3.09	4.82	6.37	8.33	9.27
110	-2.11	-0.34	1.19	3.48	4.66	5.80
130	-5.00	-3.65	-1.48	-3.00	0.82	1.77
150	-7.62	-6.68	-4.91	-3.95	-3.10	-2.25
	No. of Overlaps = 7					
50	8.23	10.07	11.38	12.04	12.69	12.83
70	4.84	6.93	8.60	9.78	10.84	11.48
90	1.51	3.56	5.29	6.81	7.89	8.80
110	-1.54	0.27	1.82	3.23	4.40	5.52
130	-4.33	-2.91	-1.55	-0.37	1.69	2.64
150	-6.87	-5.84	-4.83	-2.96	-2.07	-1.19
	No. of Overlaps = 8					
50	8.41	10.21	11.49	12.11	12.73	12.84
70	5.14	7.21	8.86	9.99	11.01	11.58
90	1.94	3.98	5.69	7.19	8.23	9.11
110	-1.00	0.84	2.39	3.79	4.94	6.04
130	-3.69	-2.22	-0.83	0.37	1.49	2.43
150	-6.14	-5.03	-3.97	-2.95	-2.06	-1.19

APPENDIX 6.1.2.

FIRST PHASE OF OPTIMISATION OF MODEL
PERCENTAGE ERROR AT FIRST PORT FOR COAL NO. 3

Mean Droplet Size (μ)	Rosin-Rammler Index 0.70	0.84	0.98	1.12	1.26	1.40
	No. of Overlaps = 3					
50	-0.23	1.35	2.47	2.99	3.91	3.96
70	-3.27	-1.39	0.49	1.47	2.40	2.89
90	-6.32	-4.01	-2.46	-1.25	0.44	1.23
110	-9.19	-7.02	-5.60	-3.69	-2.66	-1.64
130	-11.49	-10.03	-8.10	-7.00	-5.97	-5.13
150	-13.97	-12.84	-11.22	-10.26	-9.45	-7.72
	No. of Overlaps = 4					
50	0.60	1.28	2.43	2.96	3.55	3.63
70	-3.38	-1.49	0.01	1.02	2.38	2.87
90	-6.41	-4.50	-2.52	-1.16	-0.22	0.59
110	-9.24	-7.07	-5.63	-4.37	-3.33	-1.63
130	-11.87	-10.03	-8.72	-7.63	-5.95	-5.11
150	-14.29	-12.79	-11.77	-10.21	-9.40	-8.61
	No. of Overlaps = 5					
50	-0.59	1.07	2.25	2.79	3.60	3.66
70	-3.64	-1.42	0.12	1.15	2.11	2.61
90	-6.38	-4.42	-2.82	-1.41	0.00	0.82
110	-9.18	-7.38	-5.91	-4.15	-3.06	-2.01
130	-11.77	-10.29	-8.50	-7.38	-6.31	-5.43
150	-14.16	-12.99	-11.53	-10.54	-9.70	-8.18
	No. of Overlaps = 6					
50	-0.52	1.16	2.34	2.86	3.41	3.46
70	-3.54	-1.56	0.00	1.04	2.27	2.74
90	-6.52	-4.24	-2.59	-1.16	-3.17	-2.10
130	-11.57	-10.02	-8.62	-7.43	-5.85	-4.93
150	-13.91	-12.69	-11.57	-10.08	-9.18	-8.30
	No. of Overlaps = 7					
50	0.42	1.27	2.43	2.92	3.45	3.49
70	-3.40	-1.40	0.16	1.17	2.11	2.57
90	-6.34	-4.31	-2.66	-1.23	0.27	0.87
110	-9.04	-7.16	-5.31	-3.39	-2.82	-1.76
130	-11.53	-9.68	-8.23	-7.02	-5.89	-4.97
150	-13.82	-12.29	-11.12	-10.03	-9.11	-8.22
	No. of Overlaps = 8					
50	-0.31	1.38	2.53	3.01	3.52	3.54
70	-3.25	-1.25	1.30	1.30	2.22	2.67
90	-6.13	-4.11	-2.46	-1.04	-0.09	0.70
110	-8.79	-6.89	-5.35	-3.99	-2.90	-1.85
130	-11.23	-10.63	-8.19	-6.98	-5.50	-4.58
150	-13.46	-12.17	-10.99	-9.57	-8.64	-7.74

APPENDIX 6.1.3.

FIRST PHASE OF OPTIMISATION

OVERALL PERCENTAGE ERROR OF MODEL AT FIRST PORT FOR COAL 4

Mean Droplet Size (μ)	Rosin-Rammler Index					
	0.70	0.84	0.98	1.12	1.26	1.40
	No. of overlaps = 3					
50	3.26	5.26	6.71	7.48	8.94	9.12
70	-0.67	1.56	4.20	5.50	6.71	7.42
90	-4.47	-2.39	0.28	1.79	3.14	4.80
110	-7.92	-5.39	-3.75	-2.26	-0.35	0.90
130	-11.01	-8.94	-7.61	-5.77	-4.57	-2.73
150	-13.78	-12.19	-11.29	-9.70	-8.01	-7.07
	No. of overlaps = 4					
50	3.34	5.28	6.68	7.44	8.18	8.38
70	-0.45	1.71	3.47	4.73	6.68	7.35
90	-4.14	-2.11	-0.34	1.95	3.23	4.23
110	-7.48	-5.82	-3.41	-1.97	-0.76	0.42
130	-10.50	-9.27	-7.16	-6.00	-4.87	-3.25
150	-13.21	-12.43	-10.75	-9.84	-8.35	-7.49
	No. of overlaps = 5					
50	3.50	5.38	6.75	7.48	8.20	8.39
70	-0.17	1.94	3.67	4.89	6.02	6.69
90	-3.72	-1.72	0.00	1.41	3.52	4.48
110	-6.907	-5.31	-3.77	-1.50	-0.32	0.83
130	-9.91	-8.66	-7.40	-5.40	-4.29	-3.36
150	-12.55	-11.74	-10.04	-9.13	-8.32	-7.48
	No. of overlaps = 6					
50	3.70	5.54	6.87	7.56	8.25	8.42
70	0.17	2.25	3.94	5.13	6.22	6.85
90	-3.26	-1.27	0.44	1.82	3.05	3.99
110	-6.40	-4.67	-3.18	-1.80	-0.64	1.40
130	-9.24	-7.95	-6.68	-5.55	-3.54	-2.60
150	-11.82	-10.94	-10.05	-9.14	-7.42	-6.57
	No. of overlaps = 7					
50	3.90	5.71	6.99	7.65	8.29	8.44
70	0.52	2.57	4.22	5.37	6.41	7.01
90	-2.78	-0.79	0.90	2.39	3.45	4.35
110	-5.81	-4.05	-2.55	-1.17	-0.03	-1.08
130	-8.56	-7.21	-5.90	-4.75	-3.65	-2.73
150	-11.05	-10.10	-9.14	-8.20	-7.35	-6.51
	No. of overlaps = 8					
50	4.10	5.86	7.10	7.72	8.33	8.46
70	0.85	2.87	4.48	5.58	6.59	7.14
90	-2.31	-0.33	1.33	2.79	3.81	4.67
110	-5.22	-3.45	-1.95	-0.59	0.54	1.61
130	-7.88	-6.48	-5.14	-3.98	-2.89	-1.98
150	-10.29	-9.25	-8.25	-7.27	-6.40	-5.56

APPENDIX 6.2.0

S.D. OF FIRST PHASE ERROR MATRIX FOR COAL NO. 1

Mean Droplet Size μ	Rosin Rammler Index			
	0.84	0.98	1.12	1.26
	No. of Overlaps = 4			
70	3.05	2.70	2.38	2.02
90	3.19	3.07	2.95	2.73
110	3.05	3.13	3.12	3.08
130	2.82	3.02	3.10	3.14
	No. of Overlaps = 5			
70	2.99	2.62	2.29	1.93
90	3.11	2.98	2.83	2.64
110	2.95	3.04	3.08	3.03
130	2.74	2.92	3.01	3.08
	No. of Overlaps = 6			
70	2.94	2.55	2.20	1.86
90	3.05	2.90	2.74	2.54
110	2.89	2.95	2.94	2.88
130	2.68	2.80	2.93	2.02
	No. of Overlaps = 7			
70	2.89	2.53	2.18	1.81
90	2.96	2.83	2.63	2.43
110	2.81	2.86	2.85	2.76
130	2.64	2.73	2.83	2.89

APPENDIX 6.2.1.

S.D. OF FIRST PHASE ERROR MATRIX FOR COAL NO. 2

Mean Droplet Size μ	Rosin Rammler Index 0.84	0.98	1.12	1.26
	No. of Overlaps = 4			
70	3.28	2.89	2.57	2.23
90	3.39	3.26	3.18	3.00
110	3.28	3.34	3.36	3.35
130	3.03	3.20	3.33	3.43
	No. of Overlaps = 5			
70	3.20	2.81	2.48	2.14
90	3.29	3.13	3.05	2.86
110	3.19	3.19	3.24	3.25
130	2.97	3.12	3.25	3.32
	No. of Overlaps = 6			
70	3.12	2.77	2.41	2.05
90	3.17	3.03	2.93	2.75
110	2.85	3.10	3.13	3.09
130	2.85	3.00	3.09	3.16
	No. of Overlaps = 7			
70	3.02	2.69	2.36	1.99
90	3.10	2.99	2.85	2.62
110	2.95	3.02	3.00	2.96
130	2.75	2.91	2.97	3.04

APPENDIX 6.2.2.

S.D. OF FIRST PHASE ERROR MATRIX FOR COAL NO. 3

Mean Droplet Size μ	Rosin Rammler Index			
	0.84	0.98	1.12	1.26
	No. of Overlaps = 4			
70	2.65	2.26	1.95	1.62
90	2.80	2.60	2.48	2.24
110	2.73	2.71	2.69	2.66
130	2.59	2.69	2.72	2.77
	No. of Overlaps = 5			
70	2.64	2.25	1.94	1.60
90	2.77	2.58	2.47	2.26
110	2.72	2.72	2.68	2.61
130	2.56	2.63	2.67	2.71
	No. of Overlaps = 6			
70	2.64	2.25	1.93	1.58
90	2.77	2.57	2.41	2.20
110	2.68	2.67	2.62	2.57
130	2.53	2.62	2.67	2.69
	No. of Overlaps = 7			
70	2.64	2.24	1.91	1.56
90	2.74	2.54	2.38	2.18
110	2.66	2.65	2.58	2.49
130	2.50	2.57	2.61	2.61

APPENDIX 6.2.3.

S.D. ERROR MATRIX FOR COAL NO. 3

Mean Droplet Size μ	Rosin Rammler Index			
	0.84	0.98	1.12	1.26
	No. of Overlaps = 4			
70	3.35	3.01	2.65	2.26
90	3.39	3.30	3.17	2.97
110	3.20	3.30	3.35	3.32
130	2.96	3.19	3.28	3.36
	No. of Overlaps = 5			
70	3.24	2.93	2.60	2.20
10	3.27	3.18	3.07	2.86
110	3.10	3.23	3.25	3.21
130	2.86	3.12	3.19	3.33
	No. of Overlaps = 6			
70	3.12	2.82	2.51	2.15
90	3.19	3.10	2.99	2.75
110	3.03	3.12	3.16	3.10
130	2.77	3.00	3.11	3.24
	No. of Overlaps = 7			
70	3.01	2.69	2.38	2.07
90	3.07	2.99	2.80	2.70
110	2.94	3.04	3.04	2.99
130	2.73	2.92	3.03	3.13

APPENDIX 6.3.0.

ORIGINAL DISTRIBUTION OF SLURRY AND FREE COAL

Distribution (A)			Distribution (B)		
Fraction Number	Proportion of Slurry	Proportion of Free Coal	Fraction Number	Proportion of Slurry	Proportion of Free Coal
0	0	0	0	0	0
1	0.016	0	1	0	0
2	0.024	0	2	0.017	0
3	0.040	0	3	0.048	0
4	0.057	0	4	0.089	0
5	0.070	0.016	5	0.112	0.017
6	0.075	0.025	6	0.108	0.027
7	0.076	0.035	7	0.092	0.043
8	0.072	0.038	8	0.070	0.052
9	0.065	0.034	9	0.050	0.052
10	0.055	0.026	10	0.034	0.044
11	0.046	0.018	11	0.029	0.032
12	0.038	0.012	12	0.015	0.020
13	0.030	0.013	13	0.010	0.011
14	0.043	0	14	0.017	0.017
15	0.065	0	15	0	0
TOTAL	0.775	0.225	TOTAL	0.686	0.314

APPENDIX 6.3.1.

DISTRIBUTION OF SLURRY AND FREE COAL AT THE FIRST PORT

Distribution (A)			Distribution (B)		
Fraction Number	Proportion of Slurry	Proportion of Free Coal	Fraction Number	Proportion of Slurry	Proportion of Free Coal
0	0	0	0	0	0
1	0.015	0	1	0	0
2	0.020	0	2	0.015	0
3	0.029	0	3	0.033	0
4	0.029	0	4	0.037	0
5	0.010	0.014	5	0.005	0.015
6	0	0.019	5	0	0.021
7	0	0.022	7	0	0.027
8	0	0.014	8	0	0.020
9	0	0.001	9	0	0.003
10	0		10	0	
11	0		11	0	
12	0		12	0	
13	0		13	0	
14	0		14	0	
15	0		15	0	
Total	0.103	0.070		0.090	0.086

APPENDIX 6.4.0.

SECOND PHASE OF OPTIMISATION

OVERALL PERCENTAGE ERROR OF THE MODEL FOR COAL 1, OVERLAP FIXED AT FOUR FRACTIONS

Mean Droplet Size (μ)	Rosin-Rammler Index						
	1.00	1.04	1.08	1.12	1.16	1.20	1.24
95	1.31	1.70	2.09	2.46	2.81	3.90	4.19
100	0.41	0.80	1.18	1.55	2.52	2.86	3.32
105	-0.56	-0.10	0.27	1.25	1.60	1.93	2.26
110	-1.47	-1.01	-0.02	0.32	0.67	1.00	1.31
115	-2.38	-2.00	-0.94	-0.60	-0.27	0.05	0.36
120	-3.28	-2.30	-1.94	-1.53	-1.21	-0.90	-0.60
125	-4.17	-3.21	-2.87	-2.54	-2.15	-1.86	-1.57

APPENDIX 6.4.1.

SECOND PHASE OF OPTIMISATION

OVERALL PERCENTAGE ERROR OF THE MODEL FOR COAL 2, OVERLAP FIXED AT SEVEN FRACTIONS

Mean Droplet Size (μ)	Rosin-Rammler Index						
	1.00	1.04	1.08	1.12	1.16	1.20	1.24
115	1.13	1.52	1.97	2.32	2.66	2.99	3.31
120	0.27	0.65	1.02	1.44	1.77	2.09	2.40
125	-0.58	-0.21	0.14	0.48	0.88	1.19	2.42
130	-1.42	-1.07	-0.73	-0.40	-0.01	1.21	1.51
135	-2.25	-1.92	-1.60	-1.29	-0.07	0.32	0.59
140	-3.07	-2.76	-2.46	-1.26	-0.96	-0.68	-0.31
145	-3.88	-3.59	-3.31	-2.13	-1.85	-1.58	-1.32

APPENDIX 6.4.2.

SECOND PHASE OF OPTIMISATION

OVERALL PERCENTAGE ERROR OF THE MODEL FOR COAL 3, OVERLAP FIXED AT SEVEN FRACTIONS

Mean Droplet Size (μ)	Rosin-Rammler Index						
	0.86	0.90	0.94	0.98	1.02	1.06	1.10
55	0.86	1.20	1.50	2.04	2.23	2.40	2.55
60	0.27	0.63	0.96	1.27	1.54	2.03	2.21
65	-0.52	0.04	0.39	0.72	1.02	1.29	1.82
70	-1.20	-0.76	-0.21	0.13	0.45	0.75	1.02
75	-1.89	-1.44	-1.02	-0.48	-0.15	0.16	0.45
80	-2.59	-2.13	-1.70	-1.30	-0.77	-0.45	-0.15
85	-3.29	-2.83	-2.40	-1.99	-1.60	-1.07	-0.77

APPENDIX 6.4.3 .

SECOND PHASE OF OPTIMISATION

PERCENTAGE ERROR OF THE MODEL FOR COAL 4, OVERLAP FIXED AT FIVE FRACTIONS

Mean Droplet Size (μ)	Rosin-Rammler Index						
	0.86	0.90	0.94	0.98	1.02	1.06	1.10
75	1.29	1.79	2.25	2.69	3.21	3.58	3.92
80	0.40	0.89	1.36	1.80	2.23	2.74	3.09
85	- 0.58	-0.01	0.45	0.90	1.32	1.73	2.23
90	- 1.49	-0.99	-0.46	-0.02	0.41	0.81	1.20
95	- 2.40	-1.91	-1.38	-0.94	-0.52	-0.12	0.27
100	- 3.30	-2.83	-2.37	-1.87	-1.46	-1.06	-0.68
105	- 4.19	-3.73	-3.30	-2.87	-2.39	-2.00	-1.63

APPENDIX 6.5.0.

THIRD PHASE OPTIMISATION

OVERALL PERCENTAGE ERROR OF THE MODEL FOR COAL 1

Internal Burning Index	Area Factor						
	4Π	13	16	19	22	25	28
0.05	0.95	0.92	0.85	1.03	1.17	1.28	1.37
0.09	0.95	0.92	0.85	1.03	1.17	1.28	1.37
0.13	0.95	0.92	0.85	1.03	1.17	1.28	1.37
0.17	0.95	0.92	0.85	1.03	1.17	1.28	1.37
0.21	0.95	0.92	0.85	1.03	1.17	1.28	1.37
0.25	0.95	0.92	0.85	1.03	1.17	1.28	1.37
0.29	0.95	0.92	0.85	1.03	1.17	1.28	1.37
0.33	0.96	0.92	0.85	1.03	1.17	1.28	1.37

APPENDIX 6.5.1.

THIRD PHASE OPTIMISATION

OVERALL PERCENTAGE ERROR OF THE MODEL FOR COAL 2

Internal Burning Index	Area Factor						
	4Π	13	16	19	22	25	28
0.05	0.99	0.95	0.71	0.56	0.67	0.80	0.91
0.09	0.99	0.95	0.71	0.56	0.67	0.80	0.91
0.13	0.99	0.95	0.71	0.56	0.67	0.80	0.91
0.17	0.99	0.95	0.71	0.56	0.67	0.80	0.91
0.21	0.99	0.95	0.71	0.56	0.67	0.80	0.91
0.25	0.99	0.95	0.71	0.56	0.67	0.80	0.91
0.29	0.99	0.95	0.71	0.56	0.67	0.80	0.91
0.33	0.99	0.95	0.71	0.56	0.67	0.80	0.91

APPENDIX 6.5.2.

THIRD PHASE OPTIMISATION

OVERALL PERCENTAGE ERROR OF THE MODEL FOR COAL 3

Internal Burning Index	Area Factor						
	4Π	13	16	19	22	25	28
0.05	1.92	1.85	1.44	1.16	0.95	1.09	1.36
0.09	1.92	1.85	1.44	1.16	0.95	1.09	1.36
0.13	1.92	1.85	1.44	1.16	0.95	1.09	1.36
0.17	1.92	1.85	1.44	1.16	0.95	1.09	1.36
0.21	1.92	1.85	1.44	1.16	0.95	1.09	1.36
0.25	1.92	1.85	1.44	1.16	0.95	1.09	1.36
0.29	1.92	1.85	1.44	1.16	0.95	1.09	1.36
0.33	1.92	1.85	1.44	1.16	0.95	1.09	1.36

APPENDIX 6.5.3.

THIRD PHASE OPTIMISATION

OVERALL PERCENTAGE ERROR OF THE MODEL FOR COAL 4

Internal Burning Index	Area Factor						
	4Π	13	16	19	22	25	28
0.05	1.11	1.08	0.92	0.88	0.97	1.06	1.12
0.09	1.11	1.08	0.92	0.88	0.97	1.06	1.12
0.13	1.11	1.08	0.92	0.88	0.97	1.06	1.12
0.17	1.11	1.08	0.92	0.88	0.97	1.06	1.12
0.21	1.11	1.08	0.92	0.88	0.97	1.06	1.13
0.25	1.11	1.08	0.92	0.88	0.97	1.06	1.13
0.29	1.11	1.08	0.92	0.88	0.97	1.06	1.13
0.33	1.11	1.08	0.92	0.88	0.97	1.06	1.13

APPENDIX 6.6.0.
FOURTH PHASE OF OPTIMISATION
OVERALL PERCENTAGE ERROR OF THE MODEL FOR COAL 1

Mean Droplet Size (μ)	Rosin-Rammler Index					
	0.70	0.84	0.98	1.12	1.26	1.40
	No. of overlaps = 3					
50	1.12	1.83	2.14	2.25	2.36	2.37
70	0.63	1.07	1.54	1.80	2.24	0.34
90	1.31	0.76	0.76	1.29	1.61	2.06
110	2.16	1.57	0.91	0.82	1.24	1.46
130	2.99	2.47	1.81	1.18	0.96	1.10
150	3.79	3.33	2.76	2.13	1.85	1.34
	No. of overlaps = 4					
50	1.11	1.58	2.12	2.22	2.34	2.35
70	0.85	1.06	1.51	1.77	2.03	2.13
90	1.29	0.76	0.75	1.08	1.58	1.78
110	2.11	1.54	1.08	0.81	1.03	1.25
130	2.92	2.42	1.96	1.41	1.09	1.08
150	3.69	3.25	2.69	2.34	1.81	1.55
	No. of overlaps = 5					
50	1.12	1.59	1.90	2.01	2.13	2.35
70	0.83	0.85	1.54	1.79	2.05	2.15
90	1.48	0.73	0.79	1.21	1.43	1.64
110	2.27	1.44	1.03	0.72	0.88	1.27
130	2.82	2.32	1.87	1.52	1.01	0.90
150	3.57	3.13	2.76	2.22	1.95	1.68
	No. of overlaps = 6					
50	1.15	1.62	1.93	2.03	2.14	2.15
70	0.81	0.90	1.35	1.60	1.86	2.18
90	1.43	0.90	0.62	1.27	1.50	1.70
110	2.18	1.59	0.95	0.72	0.92	1.14
130	2.94	2.20	1.74	1.39	1.06	0.89
150	3.65	2.99	2.61	2.26	1.98	1.51
	No. of overlaps = 7					
50	1.19	1.65	1.95	2.04	2.14	2.15
70	0.77	0.96	1.40	1.65	1.89	1.98
90	1.36	0.84	0.69	1.09	1.33	1.52
110	2.07	1.47	1.10	0.78	0.96	1.22
130	2.81	2.30	1.84	1.23	0.94	0.84
150	3.50	3.06	2.43	2.07	1.79	1.51
	No. of overlaps = 8					
50	1.22	1.67	1.96	2.05	2.15	2.16
70	0.74	1.01	1.44	1.68	1.91	1.99
90	1.29	0.78	0.75	1.15	1.38	1.57
110	1.96	1.37	1.02	0.71	0.77	1.03
130	2.68	2.17	1.70	1.35	1.07	0.89
150	3.35	2.90	2.51	2.16	1.61	1.33

APPENDIX 6.6.1.

FOURTH PHASE OF OPTIMISATION
OVERALL PERCENTAGE ERROR OF THE MODEL FOR COAL 2

Mean Droplet Size (μ)	Rosin-Rammler Index					
	0.70	0.84	0.98	1.12	1.26	1.40
	No. of overlaps = 3					
50	2.15	2.69	3.30	3.43	3.57	3.58
70	1.12	2.06	2.58	2.89	3.20	3.50
90	0.76	1.04	1.62	2.26	2.64	2.88
110	1.37	0.81	0.69	1.37	1.69	2.32
130	2.16	1.65	0.96	0.73	1.27	1.46
150	2.97	2.56	1.96	1.60	1.16	1.03
	No. of overlaps = 4					
50	2.16	2.69	3.04	3.18	3.55	3.57
70	1.16	1.82	2.58	2.88	3.17	3.30
90	0.97	1.09	1.65	2.06	2.42	2.87
110	1.53	0.74	0.72	1.18	1.71	2.05
130	2.28	1.53	1.05	0.74	1.11	1.32
150	3.06	2.41	2.04	1.47	1.21	1.05
	No. of overlaps = 5					
50	2.19	2.71	3.06	3.19	3.33	3.35
70	1.23	1.87	2.37	2.66	3.20	3.32
90	0.93	0.92	1.73	2.13	2.48	2.71
110	1.43	0.64	0.80	1.27	1.59	1.93
130	2.12	1.37	0.93	0.66	0.98	1.36
150	2.88	2.22	1.85	1.49	1.04	0.91
	No. of overlaps = 6					
50	2.24	2.75	3.09	3.21	3.33	3.35
70	1.31	1.95	2.43	2.71	2.99	3.11
90	0.88	1.03	1.57	2.03	2.58	2.80
110	1.34	0.75	0.66	1.39	1.72	2.06
130	1.98	1.49	0.79	0.70	1.05	1.27
150	2.69	2.28	1.63	1.27	0.99	0.81
	No. of overlaps = 7					
50	2.29	2.79	3.11	3.23	3.34	3.36
70	1.40	2.03	2.50	2.77	3.03	3.14
90	0.83	1.15	1.68	2.13	2.39	2.61
110	1.26	0.67	0.79	1.24	1.58	1.90
130	1.84	1.35	0.91	0.62	1.14	1.36
150	2.49	2.06	1.67	1.03	1.82	0.92
	No. of overlaps = 8					
50	2.34	2.82	3.14	3.24	3.35	3.36
70	1.48	2.10	2.56	2.82	3.07	3.16
90	0.77	1.26	1.78	2.22	2.47	2.68
110	1.17	0.60	0.93	1.37	1.71	2.03
130	1.70	1.20	0.77	0.63	0.96	1.20
150	2.29	1.85	1.45	1.12	0.89	0.76

APPENDIX 6.6.2.

FOURTH PHASE OF OPTIMISATION
OVERALL PERCENTAGE ERROR OF THE MODEL FOR COAL 3

Mean Droplet Size (μ)	Rosin-Rammler Index					
	0.70	0.84	0.98	1.12	1.26	1.40
	No. of overlaps = 3					
50	1.02	1.05	1.32	1.40	1.60	1.60
70	1.43	1.05	0.94	1.16	1.39	1.46
90	2.03	1.43	1.12	0.95	1.04	1.22
110	2.73	2.02	1.68	1.21	1.04	0.88
130	3.36	2.85	2.21	1.87	1.60	1.45
150	4.06	3.62	3.05	2.70	2.44	1.89
	No. of overlaps = 4					
50	1.08	1.04	1.32	1.39	1.49	1.49
70	1.44	1.06	0.90	1.03	1.38	1.45
90	2.04	1.55	1.12	0.90	0.86	1.04
110	2.73	2.02	1.68	1.39	1.21	0.88
130	3.46	2.83	2.39	2.05	1.59	1.45
150	4.14	3.59	3.21	2.68	2.41	2.15
	No. of overlaps = 5					
50	1.07	0.98	1.26	1.33	1.50	1.50
70	1.50	1.04	0.89	1.06	1.29	1.37
90	2.01	1.53	1.21	0.98	0.91	1.08
110	2.69	2.10	1.76	1.34	1.17	1.00
130	3.41	2.90	2.32	1.98	1.71	1.55
150	4.08	3.64	3.13	2.78	2.51	2.04
	No. of overlaps = 6					
50	1.05	1.00	1.27	1.35	1.43	1.43
70	1.47	1.09	0.95	1.01	1.32	1.39
90	2.05	1.49	1.17	0.95	0.88	1.01
110	2.71	2.03	1.70	1.40	1.23	1.07
130	3.33	2.81	2.35	2.01	1.62	1.46
150	3.99	3.54	3.14	2.65	2.37	2.10
	No. of overlaps = 7					
50	1.04	1.03	1.29	1.36	1.44	1.43
70	1.44	1.06	0.95	1.04	1.26	1.32
90	2.00	1.53	1.21	1.00	0.94	1.05
110	2.64	2.05	1.63	1.33	1.18	1.03
130	3.32	2.71	2.25	1.92	1.67	1.51
150	3.96	3.42	3.01	2.65	2.37	2.10
	No. of overlaps = 8					
50	1.03	1.05	1.31	1.37	1.44	1.44
70	1.41	1.04	0.95	1.07	1.28	1.34
90	1.96	1.49	1.18	0.98	0.94	0.99
110	2.57	1.99	1.67	1.37	1.23	1.08
130	3.24	2.71	2.25	1.94	1.59	1.44
150	3.86	3.39	2.99	2.53	2.25	1.98

APPENDIX 6.6.3.

FOURTH PHASE OF OPTIMISATION
OVERALL PERCENTAGE ERROR OF THE MODEL FOR COAL 4

Mean Droplet Size (μ)	Rosin-Rammler Index					
	0.70	0.84	0.98	1.12	1.26	1.40
	No. of overlaps = 3					
50	1.56	2.13	2.51	2.66	3.01	3.04
70	1.26	1.18	1.99	2.31	2.60	2.73
90	2.06	1.41	0.99	1.43	1.81	2.24
110	2.93	2.06	1.53	1.11	1.09	1.40
130	3.78	2.98	2.49	1.93	1.58	1.16
150	4.60	3.92	3.50	2.92	2.41	2.14
	No. of overlaps = 4					
50	1.59	2.14	2.50	2.65	2.80	2.83
70	1.23	1.23	1.75	2.06	2.60	2.73
90	1.98	1.35	0.89	1.47	1.84	2.08
110	2.82	2.23	1.46	1.05	0.97	1.25
130	3.64	3.11	2.37	2.00	1.66	1.24
150	4.43	4.02	3.35	2.98	2.51	2.24
	No. over overlaps = 5					
50	1.63	2.16	2.52	2.66	2.80	2.83
70	1.20	1.29	1.80	2.10	2.40	2.53
90	1.88	1.26	0.87	1.27	1.90	2.14
110	2.69	2.12	1.63	0.95	1.03	1.33
130	3.48	2.95	2.49	1.85	1.52	1.27
150	4.24	3.82	3.16	2.80	2.53	2.25
	No. of overlaps = 6					
50	1.69	2.20	2.55	2.68	2.81	2.84
70	1.18	1.37	1.86	2.15	2.44	2.56
90	1.77	1.21	0.97	1.37	1.72	1.95
110	2.56	1.94	1.50	1.11	0.87	1.46
130	3.31	2.77	2.30	1.95	1.34	1.10
150	4.03	3.60	3.22	2.87	2.31	2.04
	No. of overlaps = 7					
50	1.74	2.24	2.58	2.70	2.82	2.84
70	1.15	1.45	1.93	2.21	2.48	2.59
90	1.70	1.15	1.08	1.54	1.81	2.03
110	2.41	1.81	1.37	0.99	0.97	1.31
130	3.13	2.60	2.13	1.78	1.44	1.22
150	3.82	3.37	2.99	2.63	2.36	2.08
	No. of overlaps = 8					
50	1.79	2.28	2.60	2.71	2.82	2.84
70	1.12	1.53	1.99	2.25	2.51	2.61
90	1.62	1.10	1.19	1.63	1.89	2.10
110	2.28	1.67	1.25	0.87	1.10	1.42
130	2.96	2.43	1.96	1.62	1.30	1.08
150	3.63	3.13	2.75	2.40	2.13	1.85

APPENDIX 6.7.0.

S.D. OF FOURTH PHASE ERROR MATRIX OF COAL 1

Mean Droplet Size (μ)	Rosin-Rammler Index			
	0.84	0.98	1.12	1.26
	No. of overlaps = 4			
70	0.44	0.51	0.48	0.38
90	0.46	0.37	0.44	0.47
110	0.72	0.54	0.35	0.32
130	0.80	0.77	0.63	0.45
	No. of overlaps = 5			
70	0.41	0.48	0.46	0.35
90	0.45	0.36	0.42	0.45
110	0.70	0.52	0.36	0.30
130	0.78	0.74	0.63	0.48
	No. of overlaps = 6			
70	0.40	0.46	0.44	0.34
90	0.45	0.34	0.40	0.43
110	0.68	0.50	0.34	0.28
130	0.76	0.72	0.61	0.47
	No. of overlaps = 7			
70	0.40	0.46	0.45	0.34
90	0.42	0.33	0.39	0.42
110	0.66	0.48	0.33	0.27
130	0.74	0.69	0.59	0.45

APPENDIX 6.7.1.

S.D. OF FOURTH PHASE ERROR MATRIX OF COAL 2

Mean Droplet Size (μ)	Rosin-Rammler Index			
	0.84	0.98	1.12	1.26
	No. of overlaps = 4			
70	0.75	0.70	0.56	0.45
90	0.57	0.72	0.75	0.66
110	0.47	0.47	0.59	0.66
130	0.74	0.56	0.40	0.39
	No. of overlap = 5			
70	0.72	0.68	0.55	0.43
90	0.55	0.70	0.72	0.63
110	0.46	0.46	0.59	0.65
130	0.72	0.53	0.39	0.38
	No. of overlap = 6			
70	0.73	0.67	0.53	0.41
90	0.56	0.69	0.70	0.61
110	0.43	0.47	0.60	0.64
130	0.66	0.50	0.36	0.39
	No of overlap = 7			
70	0.72	0.65	0.52	0.40
90	0.58	0.70	0.69	0.59
110	0.40	0.48	0.60	0.65
130	0.60	0.46	0.35	0.41

APPENDIX 6.7.2.

S.D. OF FOURTH PHASE ERROR MATRIX OF COAL 3

Mean Droplet Size (μ)	Rosin-Rammler Index			
	0.84	0.98	1.12	1.26
	No. of overlaps = 4			
70	0.33	0.20	0.22	0.23
90	0.54	0.36	0.25	0.19
110	0.67	0.57	0.45	0.35
130	0.73	0.69	0.63	0.57
	No. of overlaps = 5			
70	0.33	0.20	0.21	0.22
90	0.54	0.37	0.26	0.19
110	0.66	0.57	0.47	0.36
130	0.72	0.67	0.61	0.55
	No. of overlaps = 6			
70	0.32	0.19	0.19	0.20
90	0.53	0.36	0.24	0.16
110	0.64	0.55	0.44	0.34
130	0.70	0.66	0.60	0.53
	No. of overlaps = 7			
70	0.31	0.18	0.18	0.20
90	0.51	0.35	0.23	0.16
110	0.63	0.53	0.43	0.33
130	0.69	0.64	0.57	0.50

APPENDIX 6.7.3.

S.D. OF FOURTH PHASE ERROR MATRIX OF COAL 4

Mean Droplet Size (μ)	Rosin-Rammler Index			
	0.84	0.98	1.12	1.26
	No. of overlaps = 4			
70	0.49	0.58	0.61	0.48
90	0.55	0.43	0.53	0.59
110	0.82	0.65	0.47	0.38
130	0.86	0.87	0.77	0.64
	No. of overlaps = 5			
70	0.49	0.58	0.60	0.47
90	0.52	0.41	0.52	0.58
110	0.79	0.64	0.47	0.38
130	0.82	0.83	0.76	0.64
	No. of overlaps = 6			
70	0.49	0.58	0.59	0.47
90	0.47	0.40	0.51	0.56
110	0.73	0.58	0.44	0.37
130	0.77	0.78	0.73	0.61
	No. of overlaps = 7			
70	0.49	0.57	0.55	0.45
90	0.42	0.40	0.52	0.57
110	0.67	0.51	0.39	0.36
130	0.75	0.75	0.69	0.57

APPENDIX 6.8.0.

FIFTH PHASE OF OPTIMISATION

OVERALL PERCENTAGE ERROR OF THE MODEL FOR COAL 1

Mean Droplet size (μ)	Rosin Rammler Index						
	0.875	0.910	0.945	0.980	1.015	1.050	1.085
75	0.82	0.93	1.03	1.19	1.26	1.33	1.40
80	0.64	0.74	0.85	0.95	1.04	1.18	1.25
85	0.61	0.58	0.68	0.77	0.86	0.95	1.34
90	0.82	0.67	0.60	0.61	0.94	1.02	1.10
95	0.97	0.88	0.74	0.73	0.79	0.87	0.95
100	1.13	0.81	0.72	0.64	0.71	0.77	0.83
105	1.29	0.97	0.88	0.80	0.67	0.68	0.74

APPENDIX 6.8.1.

FIFTH PHASE OF OPTIMISATION

OVERALL PERCENTAGE ERROR OF THE MODEL FOR COAL 2

Mean Droplet size (μ)	Rosin Rammler Index						
	0.735	0.770	0.805	0.840	0.875	0.910	0.945
95	0.90	0.77	0.60	0.67	0.81	1.22	1.38
100	1.02	0.88	0.69	0.60	0.84	0.98	1.11
105	1.15	1.01	0.89	0.71	0.63	0.76	0.89
110	1.29	1.16	1.03	0.65	0.50	0.55	0.67
115	1.47	1.34	1.22	0.83	0.67	0.58	0.52
120	1.65	1.52	1.40	1.02	0.91	0.75	0.67
125	1.83	1.70	1.32	1.20	1.09	0.92	0.84

APPENDIX 6.8.2.

FIFTH PHASE OF OPTIMISATION

OVERALL PERCENTAGE ERROR OF THE MODEL FOR COAL 3

Mean Droplet size (μ)	Rosin Rammler Index						
	1.155	1.190	1.225	1.260	1.295	1.330	1.365
75	1.03	1.08	1.12	1.25	1.27	1.29	1.31
80	0.92	0.97	1.01	1.06	1.10	1.23	1.25
85	0.89	0.89	0.90	0.95	0.99	1.03	1.07
90	0.93	0.91	0.88	0.89	0.89	0.92	0.96
95	1.01	0.98	0.96	0.93	0.91	0.89	0.89
100	1.16	1.12	1.03	1.01	0.98	0.96	0.94
105	1.25	1.21	1.18	1.08	1.06	1.04	1.02

APPENDIX 6.8.3.

FIFTH PHASE OF OPTIMISATION

OVERALL PERCENTAGE ERROR OF THE MODEL FOR COAL 4

Mean Droplet size (μ)	Rosin Rammler Index						
	1.155.	1.190	1.225	1.260	1.295	1.330	1.365
95	1.24	1.39	1.46	1.52	1.59	1.65	1.71
100	1.02	1.11	1.19	1.33	1.39	1.46	1.52
105	0.86	0.88	0.97	1.05	1.19	1.25	1.32
110	1.04	0.97	0.91	0.86	0.92	0.98	1.11
115	1.23	1.16	1.16	1.03	0.97	0.91	1.12
120	1.42	1.35	1.35	1.22	0.90	0.93	0.99
125	1.61	1.54	1.54	1.13	1.08	1.02	0.97

APPENDIX 6.9

SIXTH PHASE OF OPTIMISATION

OVERALL PERCENTAGE ERROR OF THE MODEL

COAL NO. 1

Area Factor	13	14	15	16	17	18	19
Percentage Error	0.83	0.72	0.64	0.58	0.68	0.76	0.85

COAL NO. 2

Area Factor	16	17	18	19	20	21	22
Percentage Error	0.65	0.60	0.54	0.50	0.48	0.53	0.58

COAL NO. 3

Area Factor	19	20	21	22	23	24	25
Percentage Error	1.15	1.05	0.96	0.88	0.88	0.98	1.08

COAL NO. 4

Area Factor	16	17	18	19	20	21	22
Percentage Error	0.98	0.93	0.89	0.86	0.83	0.87	0.90

APPENDIX 7.0.

ERROR DATA FOR FINALIZED MATHEMATICAL MODEL

COAL NO. 1

Condition (Nominal)	Average Percentage Error	Standard Deviation of Error
750°C Preheat	-0.28	4.74
1000°C Preheat	0.23	5.42
200 $m.s^{-1}$ velocity	2.28	5.99
240 $m.s^{-1}$ velocity	-2.33	3.98
21% Oxygen	0.20	4.92
26% Oxygen	-0.24	5.25
S. Ratio 0.8	1.40	6.22
S. Ratio 0.9	-1.45	3.61
Port 1	0.20	4.86
Port 2	0.88	4.88
Port 3	0.17	5.41
Port 4	-1.35	5.18
Overall for coal 1	-0.02	5.09

APPENDIX 7.1.

ERROR DATA FOR FINALIZED MATHEMATICAL MODEL

COAL NO. 2

Condition (Nominal)	Average Percentage Error	Standard Deviation of Error
750°C Preheat	1.61	5.03
1000°C Preheat	-1.64	6.96
200 $m.s^{-1}$ velocity	0.81	5.88
240 $m.s^{-1}$ velocity	-0.83	6.07
21% Oxygen	0.47	6.26
26% Oxygen	-0.50	5.89
S. Ratio 0.8	-0.33	6.23
S. Ratio 0.9	0.31	5.91
Port 1	-0.04	6.23
Port 2	0.86	7.21
Port 3	0.29	6.16
Port 4	-1.15	4.35
Overall for coal 2	-0.01	6.08

APPENDIX 7.2.

ERROR DATA FOR FINALIZED MATHEMATICAL MODEL

COAL NO. 3

Condition (Nominal)	Average Percentage Error	Standard Deviation of Error
750°C Preheat	-1.10	3.85
1000°C Preheat	0.66	6.77
200 $m.s^{-1}$ velocity	0.79	5.70
240 $m.s^{-1}$ velocity	-1.23	5.30
21% Oxygen	0.16	6.19
26% Oxygen	-0.60	4.72
S. Ratio 0.8	0.52	5.51
S. Ratio 0.9	-0.95	5.50
Port 1	-0.26	5.20
Port 2	3.24	7.21
Port 3	-1.02	4.24
Port 4	-2.83	4.91
Overall for coal 3	-0.22	5.50

APPENDIX 7.3.

ERROR DATA FOR FINALIZED MATHEMATICAL MODEL

COAL NO. 4

Condition (Nominal)	Average Percentage Error	Standard Deviation of Error
750°C Preheat	3.37	7.01
1000°C Preheat	-3.45	5.05
200 $m.s^{-1}$ velocity	3.08	7.00
240 $m.s^{-1}$ velocity	-3.16	5.07
21% Oxygen	0.35	6.08
26% Oxygen	-0.43	6.14
S. Ratio 0.8	0.93	6.61
S. Ratio 0.9	-1.00	5.57
Port 1	0.07	6.93
Port 2	1.01	5.69
Port 3	-1.03	5.79
Port 4	0.06	5.96
Overall for coal 4	-0.04	6.11

APPENDIX 8.0

COMPARISON OF EXPERIMENTAL RESULTS AND FINAL MODEL PREDICTIONS

COAL NO. 1

Units : Proportion Burnout

Run No.	Port 1		Port 2		Port 3		Port 4	
	Exp.	Pred.	Exp.	Pred.	Exp.	Pred.	Exp.	Pred.
75	0.818	0.837	0.831	0.927	0.883	0.969	0.941	0.988
74	0.830	0.823	0.889	0.911	0.890	0.954	0.956	0.978
73	0.798	0.844	0.906	0.930	0.967	0.970	1.006	0.988
72	0.841	0.827	0.897	0.911	0.958	0.953	1.008	0.977
55	0.924	0.811	0.909	0.908	0.945	0.956	1.007	0.981
54	0.815	0.797	0.920	0.892	0.949	0.941	1.046	0.968
56	0.831	0.823	0.949	0.915	1.010	0.960	1.010	0.983
71	0.796	0.806	0.933	0.896	0.997	0.945	1.013	0.971
46	0.797	0.864	0.950	0.940	0.963	0.977	1.059	0.993
47	0.829	0.848	0.903	0.925	0.980	0.963	1.015	0.983
48	0.804	0.869	0.855	0.944	0.863	0.979	0.879	0.995
49	0.862	0.854	0.989	0.932	1.045	0.968	1.025	0.986
51	0.857	0.844	0.880	0.929	0.981	0.969	1.001	0.988
50	0.841	0.828	0.913	0.914	0.973	0.956	1.050	0.979
52	0.891	0.847	0.953	0.931	1.012	0.971	1.013	0.989
53	0.815	0.830	0.939	0.914	0.983	0.956	0.948	0.979

APPENDIX 8.1.

COMPARISON OF EXPERIMENTAL RESULTS AND FINAL MODEL PREDICTIONS

COAL NO. 2

Run No.	Port 1		Port 2		Port 3		Port 4	
	Exp.	Pred.	Exp.	Pred.	Exp.	Pred.	Exp.	Pred.
20	0.821	0.831	0.857	0.927	0.947	0.972	1.007	0.993
21	0.790	0.818	0.903	0.915	0.934	0.962	0.966	0.987
22	0.717	0.836	0.794	0.926	0.969	0.970	1.026	0.992
26	0.800	0.821	0.906	0.913	0.926	0.959	0.954	0.985
27	0.797	0.807	0.887	0.910	0.956	0.961	0.934	0.986
28	0.819	0.796	0.911	0.897	0.979	0.950	1.020	0.980
29	0.816	0.813	0.932	0.909	0.992	0.959	0.999	0.985
30	0.775	0.798	0.889	0.895	0.970	0.947	0.994	0.978
18	0.925	0.856	0.945	0.939	1.021	0.979	1.080	0.995
17	0.853	0.843	0.957	0.930	0.964	0.972	1.028	0.993
19	0.856	0.859	0.899	0.941	0.922	0.979	0.958	0.995
23	0.859	0.846	1.022	0.931	1.060	0.974	1.047	0.994
24	0.932	0.837	0.992	0.927	1.033	0.972	1.035	0.993
82	0.766	0.821	0.794	0.914	0.804	0.961	0.971	0.986
31	0.903	0.837	0.997	0.926	1.001	0.970	1.038	0.992
81	0.875	0.823	0.976	0.914	0.979	0.961	1.026	0.986

APPENDIX 8.2.

COMPARISON OF EXPERIMENTAL RESULTS AND MODEL PREDICTIONS

COAL NO. 3

Run No.	Port 1		Port 2		Port 3		Port 4	
	Exp.	Pred.	Exp.	Pred.	Exp.	Pred.	Exp.	Pred.
64	0.825	0.818	0.849	0.913	0.967	0.959	1.027	0.982
63	0.829	0.804	0.885	0.897	0.982	0.941	1.021	0.964
66	0.779	0.830	0.964	0.920	0.967	0.962	0.995	0.983
65	0.761	0.812	0.845	0.900	0.930	0.943	0.971	0.964
67	0.856	0.791	0.897	0.895	0.986	0.946	1.043	0.971
68	0.805	0.778	0.892	0.877	0.932	0.926	0.965	0.954
69	0.812	0.809	0.907	0.906	0.993	0.954	1.018	0.979
70	0.795	0.791	0.893	0.886	0.966	0.933	0.966	0.959
58	0.816	0.852	0.800	0.931	0.827	0.969	0.982	0.987
57	0.871	0.836	0.935	0.914	1.045	0.953	1.112	0.974
60	0.844	0.861	0.899	0.940	0.984	0.975	1.042	0.991
59	0.795	0.842	0.853	0.920	0.928	0.958	0.929	0.978
62	0.794	0.828	0.811	0.918	0.900	0.961	0.966	0.983
61	0.782	0.811	0.811	0.900	0.916	0.943	0.976	0.965
79	0.909	0.835	0.922	0.925	0.966	0.966	1.013	0.985
80	0.904	0.817	0.975	0.905	1.028	0.948	1.043	0.969

APPENDIX 8.3

COMPARISON OF EXPERIMENTAL RESULTS AND MODEL PREDICTIONS

COAL NO. 4

Run No.	Port 1		Port 2		Port 3		Port 4	
	Exp.	Prod.	Exp.	Prod.	Exp.	Prod.	Exp.	Prod.
35	0.856	0.883	0.906	0.964	0.902	0.992	0.917	0.998
36	0.773	0.871	0.889	0.955	0.950	0.987	0.942	0.998
37	0.761	0.886	0.848	0.963	0.886	0.990	0.880	0.998
38	0.837	0.873	0.923	0.955	0.958	0.987	0.970	0.997
40	0.867	0.861	0.909	0.952	1.001	0.986	1.039	0.997
39	0.828	0.850	0.884	0.942	0.957	0.980	0.983	0.996
41	0.856	0.867	1.006	0.952	1.040	0.985	1.052	0.996
42	0.901	0.853	0.979	0.942	1.028	0.980	1.023	0.995
34	0.965	0.905	0.965	0.973	1.019	0.994	0.936	0.999
33	0.873	0.895	0.980	0.968	1.104	0.993	1.035	0.999
78	0.932	0.905	0.986	0.974	1.022	0.994	1.011	0.999
77	0.907	0.897	0.969	0.968	1.020	0.993	1.036	0.999
45	0.924	0.887	0.959	0.965	1.031	0.001	1.014	0.998
76	0.970	0.957	1.055	0.957	1.065	0.988	1.112	0.998
44	0.969	0.886	0.991	0.963	1.037	0.990	1.046	0.998
43	0.931	0.874	0.994	0.955	1.015	0.987	1.030	0.997